Ollscoil na hÉireann, Corcaigh

National University of Ireland, Cork

Development of electrochemical DNA-based biosensors for the detection of Shiga toxin-producing *E. coli* (STEC)

Thesis presented by

Luiza Adela Wasiewska

ORCID 0000-0002-9011-0814

for the degree of

Doctor of Philosophy

University College Cork

Tyndall National Institute

Head of School/Department: Dr Fatima Gunning

Supervisor(s): Dr Alan O'Riordan, Dr Geraldine Duffy and Dr Catherine M. Burgess

2022

Table of content

This is to certify that the work I am submitting is my own and has not been submitted for another degree, either at University College Cork or elsewhere. All external references and sources are clearly acknowledged and identified within the contents. I have read and understood the regulations of University College Cork concerning plagiarism and intellectual property.

Luiza Wasiewska

Abstract

Shiga toxin-producing *E. coli* (STEC) is a food-borne pathogen of significant public health concern, due to the severity of the illness it can cause including severe bloody diarrhoea and haemorrhagic uremic syndrome. A key pathogenicity factor is the ability to produce Shiga T Toxin 1 and 2, which are encoded by genes *stx1* or *stx2*. These genes are key targets in molecular-based assays to detect this group of pathogens. However, many of these assays, including real-time PCR approaches are considerably time-consuming and there is a need for a more rapid screening assay which could be used in agri-food settings. This publication-based thesis presents the development of DNA based electrochemical sensor as an alternative approach for the rapid detection of the *stx1* or *stx2* genes and explores the application of gold interdigitated micro electrodes (IDEs) for electrochemical pH control and redox molecule accumulation.

Firstly, a comprehensive literature review was undertaken regarding the current STEC detection approaches, challenges presented, and the opportunities for the development of electrochemical sensors to detect this group of pathogens. A detailed analysis of gene sequences used for targeting both general *E. coli* and STEC was performed and the recently developed electrochemical nucleic acid-based sensors were classified based on the electrode's material used and its modification. This literature review allowed the selection of the most promising approach for the development of the DNA sensor in this thesis.

Initial work focused on using reporter DNA tagged with silver nanoparticles that could subsequently be oxidised. The aim being that silver ions detected electrochemically could then be correlated to the DNA present in a sample. This began with the development of an electrochemical sensor for silver ions detection using

electrochemical pH control. In this approach, one interdigitated electrode (IDE) comb was used as a working electrode, while the other was used as a generator electrode that produced protons, subsequently decreasing the local pH. The combination of silver ions complexation with chloride and in-situ pH control resulted in a linear calibration range between 0.25 and 2 μM in tap water and a calculated limit of detection (LOD) of 106 nM without the need to add either acid or supporting electrolytes. However, even though the LOD of the silver ions detection sensor was satisfactory for their detection in tap water, it was not sufficiently sensitive for use with the DNA sensor. Therefore, the approach for DNA detection was changed, and the focus was moved to the use of methylene blue instead of silver nanoparticles.

In this work, a highly sensitive, label-free, electrochemical DNA-based sensor for the detection of the *stx1* gene was developed. Firstly, a working IDE was modified with gold nanoparticles and chitosan-gold nanocomposite allowing immobilisation of amine-modified probe DNA. Label-free electrochemical detection was undertaken using methylene blue as a redox molecule, which intercalated into the double-strand DNA. An accumulator IDE was used for the accumulation of methylene blue around the sensor IDE by applying an open circuit potential during the incubation. Reduction of methylene blue was recorded using square wave voltammetry. Using this label-free detection, a linear response was shown at concentrations ranging from 10^{-6} M to 10^{-16} for synthetic *stx1* target strands, with the lowest LOD of 10^{-16} M. Chromosomal DNA extracted from four different STEC *E. coli* strains was used to confirm the selectivity of the presented method.

Finally, a multiplex sensor for the simultaneous detection of two genes coding for toxin production, *stx1* and *stx2*, was developed. The LOD was further improved by three orders of magnitude, upon deposition of a thicker layer of gold nanoparticles and

re-optimisation of chitosan-gold nanocomposite deposition. The probes complementary to *stx1* and *stx2* were immobilised on the same chip allowing for multiplex detection. The modification of the surface has allowed for decreasing the LOD for both target genes to 10^{-19} M instead of 10^{-16} M. The multiplex sensor was validated by the detection of chromosomal DNA extracted from bacterial culture as well. Such a multiplex sensor, if combined with on-chip DNA extraction, could revolutionise the point-of-use detection of STEC as well as other pathogens for instance on-farm or in the food industry.

Acknowledgement

Even though I was supposed to start a job in Poland in a few days, I received an email from Kaye Burgess starting “Apologies for contacting you out of the blue like this.” which changed everything and a month later I packed my bags and moved to Ireland! Thank you so much for accepting me for this Teagasc Walsh Scholarship Programme (Ref: 2016024) which allowed me to grow as a scientist and as a person. Foremost, I would like to thank my supervisors, Alan O’Riordan from Tyndall National Institute in Cork and Kaye Burgess and Geraldine Duffy from Teagasc Food Research Center in Ashtown, Dublin. They have always been very supportive on my way and encouraged me to keep going when the road was challenging. I spent only one month in Teagasc in Dublin at the beginning of my PhD but I will always remember it as such a great time. Kaye and Geraldine made me feel very welcome to Ireland and even after this time they were always there if I needed their help. Working with Alan was a great experience, and even though sometimes we disagreed, he always encouraged me to do my best. I am truly impressed with his talent to contextualise research and telling a story and I am sure that each chapter in this thesis benefited from it. I am sure tha our paths will cross again in the future.

Aside from my supervisors, I would like to acknowledge Bernardo who gave me an introduction to electrochemistry, which at that time was only rocket science to me. His patience with explaining the basics brought me up to speed very quickly and was a base for future work. Afterwards, the role of my electrochemical guru laid on Ian who was invaluable for my work and understanding my complicated relationship with oxygen and chlorine. I owe a great thanks to these two lads without whom the silver paper would probably never happen.

My special thanks go to Fernando Diaz, a colleague and partner in crime from my second week in Tyndall. Even though we could barely communicate in English at the beginning, it didn't stop us from connecting immediately and becoming great friends. For the last 4.5 years, we shared the (messy) office, laboratory, lunches and coffees. My stay in Tyndall wouldn't be the same without you! I would also like to thank all my colleagues from the Nanotechnology group, especially the strong Impala fans! Pierre for all the help around the lab, laughs, Barcelona day and random songs that stuck to your head for a long time; Caoimhe for all the entertainment in the lab, teaching me a lot about Ireland (starting with the name 😉) and being a go-to Agresso person; Ian, again, for being a strong support in the lab and outside of it (read – Impala); Rob for all chats in the lab and the bottles to build my garden fence. Looking forward to the next BBQ in your garden! Han for all your effort with the chips and introducing us to your lovely doggos; Shane, the intern, for introducing Justin Timberlake Fridays together and developing a great music band; Benjy for the perfect week at the conference in Italy when you almost melted down from the heat; Colm for all the sarcasm, please make sure CH920 is doing fine when I am gone; Kathleen for bringing a great 99' vibe to the group, Yuqing for always putting a smile on my face, Tarun for bringing the good vibes; Vuslat for sharing long hours with me in the lab after the lockdown when there was hardly anyone around.

Special mention to Sofia, Eileen, Andrea B., Ryan, Alessandra, and Matteo from our sister group – LSI. I often felt like being part of their group, sharing the chemicals, equipment and lab space if needed but also the social moments. Also a special mention to the so-called "Italian table" which never had a limit on the number of people it would accommodate. At some point in Tyndall, everyone starts feeling a bit Italian. Somehow most of our Italian colleagues were called either Marco or Andrea which

makes it easier to say thanks to all of them with a special mention to Marco Sica and Marco Belcastro. Thank you for the discussions, lunches and coffees we shared.

Thanks to everyone involved in the Famelab competition. My PhD would never be the same without this great experience. It opened my eyes to different ways of communicating science, and allowed me to meet amazing people and simply have lots of fun (and stress) during the whole process. A special thanks to Andrea Pacheco who qualified together with me to the final starting a great friendship filled with train gossip. Looking forward to more gossip while picking up mushrooms in Poland.

A special thanks to my past and current flatmates at 13 The Avenue, Maeghan, Dave, Eugenia, Cathal, Kathi and Daniel, who were invaluable support during the whole process of doing my PhD. This was especially important since the beginning of the COVID pandemic when none of us could go home to see our families. I feel very lucky that I had people around me who I consider family. Together we did a great job in supporting the wine businesses which paid us back with surviving the lockdown! Special thanks to the local cats who visit us to get some food and cuddles.

My special thanks go to two men close to my heart - Dominick and Bear the bulldog. Dom has been such great support to me over the last two years that were especially challenging due to the COVID situation. He always supported me and made me feel good at my work even when I had doubts about it. He and his family also made me feel very welcome in Ireland (I mean Cork) which I can call my home now. Bear the bulldog came into our lives during the lockdown and I cannot imagine not having him in my life now. He could make me laugh in any situation. I also really enjoyed working from home with him even though sometimes a 25 kg dog sitting on my lap can be a slight challenge to see the screen of my computer.

Finally, a special thanks to my family in Poland. I am sure my parents would much prefer me to stay close to them in Poland, however, they always supported my decisions even though it meant being far away. They also visited me in each country I lived in so far. Thanks to my lovely sisters, Dominika and Natalia, who reported to me regularly about what was going on in Poland, and shared sessions of watching friends or musicals whenever I was back home. Thanks to Lukasz, my brother-in-law who did not protest whenever we were watching Friends or musicals when I was home. Thanks to my beautiful nieces, Zosia and Tosia, who always look forward to the time I go home which gives me a lot of joy.

Last but not least, special thanks to Justin Timberlake, whose music played in the laboratory every Friday made all experiments work. Without these productive Fridays with Justin, half of the results presented in this thesis would never be there.

“To the ones who dream…”

Chapter 1. Introduction

Under review in part in “Comprehensive Reviews in Food Science and Food Safety”

E. coli are a group of bacteria, which are a natural part of the intestinal flora of warm-blooded animals, including humans. Most *E. coli* are non-pathogenic and are essential for the normal function of a healthy intestine [1]. However, certain pathogenic types of *E. coli* can cause a broad range of symptoms such as stomach cramps, (bloody) diarrhoea, and urinary tract infections. Shiga toxin-producing *E. coli* (STEC), also called Verocytotoxin-producing *E. coli* (VTEC), is a group of one of major food-borne pathogens.

Detection of both, generic *E. coli*, as well as specific pathotypes, is of high importance in the context of food safety. Bacterial detection has advanced significantly in recent years and considerable efforts have been focused on the development of genetic-based techniques for the detection and characterization of key food-borne pathogens. These are based on the detection of a specific piece of genetic material (a specific sequence of nucleic acids i.e. DNA or RNA) that is unique to the target organism and as such, they are highly specific. Electrochemical DNA sensors offer advantages such as low cost, simplicity of use, and miniaturisation [2]. These characteristics make them especially attractive for application in the agri-food chain. A simple detection technique could allow real-time pathogen detection by non-specialized users to detect contamination quickly, decreasing infection rates and subsequently decreasing economic and environmental losses in case the final food product contamination is detected.

This chapter provides a detailed description of *E. coli* types with a particular focus on STEC, a description of the traditional methods used for its detection as well as a critical review of all aspects of the development of electrochemical DNA sensors for the detection of STEC and general *E. coli* reported since 2010. First, the probe sequence selection is discussed in the context of specificity, with a focus on STEC

virulence factors. This is followed by the most common techniques of probe DNA attachment to the working electrode. Subsequently, the performance of selected DNA sensors is reviewed for detection of *E. coli* and STEC including those classified based on the surface, the electrode material, its modification, and size (micro, nano). In the end, the potential application of sensors to detect naturally contaminated samples is assessed and future perspectives and challenges are discussed.

1.1. *E. coli* and Shiga toxin-producing *E. coli* (STEC)

It is estimated that every year 600 million people worldwide become ill because of contaminated food resulting in over 420,000 deaths due to 31 identified hazards worldwide of which 11 are diarrhoeal disease agents [3]. The pathogens which have caused most of the food-borne illnesses in the European Union in 2018 were: *Salmonella* spp., *Campylobacter jejuni*, *Escherichia coli*, *Yersinia* and *Listeria monocytogenes* [4].

1.1.1. General information

E. coli are a group of bacteria, which are a natural part of the intestinal flora of warm-blooded animals, including humans. Most *E. coli* are not pathogenic, in fact, they are essential for a normal function of a healthy intestine [1]. However, certain pathogenic types of *E. coli* can cause a broad range of symptoms such as stomach cramps, (bloody) diarrhoea, and urinary tract infections. *E. coli* strains associated with human infections are classified into six pathotypes, based on their virulence factors and modes of infection: Enterotoxigenic *E. coli* (ETEC), Enteropathogenic *E. coli* (EPEC), Enterohemorrhagic *E. coli* (EHEC), Enteroaggregative *E. coli* (EAEC), Enteroinvasive *E. coli* (EIEC) and Diffusely Adherent *E. coli* (DAEC) [5].

Shiga toxin-producing *E. coli* (STEC), also called Verocytotoxin-producing *E. coli* (VTEC), is classified within the EHEC pathotype. STEC is a group of one of the major food-borne pathogens. The virulence of STEC is associated mainly with the production of two cytotoxins: *stx1* and *stx2*, with which the mode of action involves inhibition of protein synthesis in the target cell [6]. Abdominal cramps, (bloody) diarrhoea and in some cases fever and vomiting are the most common symptoms of STEC infection. Most often, the patients would completely recover within a maximum of ten days, however, in severe cases, the infection may lead to the development of haemolytic uremic syndrome (HUS) which is a life-threatening disease [7]. Although the prevalence of STEC infections is significantly lower compared with some other food-borne pathogens (ex. *Salmonella* spp., *Campylobacter* spp.), it remains a high risk to public health due to its low infection dose, its ability to survive in various environments, and the highly severe consequences of the infections compared to other food-borne pathogens [8].

1.1.2. Source of infections and outbreaks

STEC infections are generally associated with the consumption of contaminated food and water [9]. Undercooked beef meat, raw milk, unpasteurised apple juice, raw vegetables and sprouts are the most common foods which are very often linked to outbreaks or sporadic cases [10-13]. Cattle have been considered to be the main reservoir of STEC associated with human infections because the bacteria is found in the gut of healthy cattle [14]. Therefore, the contamination may happen once the raw meat gets in contact with the faeces during the slaughtering process. Recent studies suggest that some animals can shed a very high concentration of bacteria, ($>10^4$ CFU/g faeces) and have been labelled super-shedders [15]. It was estimated that super-shedders may be responsible for up to 95% of STEC cases even though they represent

a small portion of a herd [15]. Therefore, the determination of the existence of super-shedders on farms may have an enormous impact on decreasing the probability of food contamination.

In 1982, STEC was recognised as a human pathogen for the first time after two reported outbreaks of hemorrhagic colitis in Oregon and Michigan, USA, which affected at least 47 people[16]. Since then several outbreaks took place in the world including the biggest one, which originated in Germany in 2011 due to the consumption of sprouts contaminated with *E. coli* O104:H4, previously not considered as dangerous for human health [17, 18]. Furthermore, there have been 8,161 confirmed cases of STEC infections reported in the European Union in 2018 based on the recent report of EFSA and the European Centre for Disease Prevention and Control (CDC) [4]. The highest incidence rate was observed in Ireland, followed by Sweden, Malta and Denmark (20, 8.8, 8.6, 8.4 cases per 100 000 people, respectively) [4]. The total number of reported cases of all STEC infections between 2014 and 2018 increased significantly.

Similar to previous years, the highest occurrence of STEC outbreaks was associated with the serotype O157 (34.5%) followed by O26, O103, O91, O146, O145, and O128 (16.6%, 4.7%, 3.8%, 3.5, 3.1% and 2.1% respectively). In addition, almost 10% of isolated strains were non-typeable so their O serotype could not be defined [4]. *E. coli* O157 has been considered the most dangerous strain of STEC and therefore the most attention has been placed on its detection in the food chain [19]. Karmali et al. [20] have classified it in group A because it is most often associated with outbreaks, severe consequences of the infections and a common connection with HUS development. However, the percentage contribution of the serogroup O157 to the overall burden of diseases in the European Union has decreased in recent years (46.3%, 34.5% in years

2014 and 2018 respectively). This may be the result of the increased awareness of non-O157 serotypes-originated-infections [6].

1.1.3. Virulence factors

Karmali et al. [20] have classified STEC strains into 5 seropathotypes (A, B, C, D and E) which are based on the existence of certain strains in cases of human infections, outbreaks and the frequency of HUS development. According to that classification, group A consisted of the most dangerous strains (O157 strains) and group E was composed of strains that do not pose any risk to human health. However, The European Food Safety Agency (EFSA) has issued a revaluation of that classification due to its insufficient accuracy towards STEC pathogenicity since it does not include all possible pathogenic STEC strains and proposed an alternative approach based on the molecular virulence factors [21].

The virulence factors of STEC are still not fully understood because of the complexity of the infection process, requiring the expression of several genes. The main known factor causing disease is the production of toxins which are mostly encoded by two genes - *stx1* and *stx2*, furthermore it is known that several subtypes of these genes exist. Another gene that was typically associated with the potential of human infection is known as *eae* and it is responsible for intimin production, a protein allowing bacterial attachment to gut epithelial cells. Based on the epidemiological data, the strains responsible for most severe symptoms contained *stx2* alone or in combination with *eae*, *stx1* or all 3 of them [4, 22]. The report from EFSA related to the STEC pathogenicity (2013) has advised including the additional virulence-associated genes into the list: "*aai*C" is responsible for protein secretion and "*agg*R" is a plasmid-encoded regulator [21]. However, recently (2020) EFSA has reported that any strain

which contains any subtype or combination of different *stx* genes subtypes may cause a severe illness [23]. Due to the existence of the infection reports in the absence of the *eae* gene, which was found in the majority of the infection-causing strains, the *eae* gene has not been considered anymore as an essential virulence factor that causes severe infection. The last alteration on the 2013 EFSA report is the removal of the *aaiC* and *aggR* genes from the routine screening procedures since there have been no reported outbreaks related to those strains since the outbreak in 2011 [23].

The following section will focus on reviewing the common pathogens detection methods and their applications in particular for *E. coli* and STEC. The techniques commonly used in the food safety area will be described, including their limitation for a real-time application for on-farm detection and routine tests in the food industry.

1.2. Traditional methods for pathogens detection in the food chain and *E. coli* perspective

The most effective way to reduce the incidence of food-borne zoonosis is the early detection of pathogens along the food chain. However, this is highly challenging since available detection methods are time-consuming, laborious and not cost-effective. As a result, products are usually tested at the end of the production process and if found contaminated often the whole batch of food has to be discarded. There are three types of conventional pathogens detection methods used every day in the food industry; culture, immunological and molecular methods. The key advantages and disadvantages of these traditional detection techniques are summarised in Table 1.1.

Table 1.1. Summary of traditional methods for pathogens detection

Method of detection	Time to get results	Advantages	Disadvantages	Ref.
Traditional microbiological methods	2-6 days	- Sensitive - Specific - Only viable organisms detected	- Laborious - Require special culture media and conditions - Results interpretation can be subjective - Some organisms cannot be cultured	[24]
Immunological methods (ex. ELISA)	Up to 24 hours	- Faster than culture-based - Simple to perform - A large number of samples at the same time - Can be automated	- Enrichment required - Possible false-positive results - Requires specialist expensive equipment	[25, 26]
Molecular methods (ex. PCR, qPCR)	Few hours	- Rapid - Sensitive - Accurate - Identification of non-cultivable organisms	- Laborious - Requires specialist expensive equipment	[27]

There are two major reasons to highlight the significance of *E. coli* detection for food safety. Firstly, *E. coli* is a very important indicator organism for faecal contamination, in particular for drinking water. Since *E. coli* is present in high numbers in mammalian faeces while it is very sensitive to environmental conditions, its presence in water suggests its contamination with faeces. Thus, the determination of the strain is not necessary, as faecal contamination in water is a great health risk [28]. The second reason for the detection of *E. coli* is the identification of STEC in food products to inactivate the bacteria or discard the infected food product. It is usually done in foods

that are most often associated with infections (beef, sprouts) and animal faeces to control STEC spread [4]. In the European Union, testing for STEC in foods is only required for sprouts. These requirements are included in the Commission Regulation (EU) No.209/2013 amending Regulation (EC) No.2073/2005 which was added after the big outbreak which happened in 2011. The regulation involves testing for six main serogroups (O157, O26, O103, O111, O145, and O104:H4). Even though there is no legal requirement for testing other foodstuffs for STEC, some food businesses operators may do it as a part of their food safety management system. They may also be required to include testing when exporting outside of European Union. This would be particularly relevant for the businesses producing raw beef, foods made from raw milk and fresh vegetables [29].

1.2.1. Traditional culture methods

Culture methods are the oldest and still one of the most commonly used techniques for microbial identification. These methods rely on creating controlled growth conditions including nutrient composition, temperature, pH, gas concentration (mostly oxygen), and humidity which will favour only specific pathogens to grow. They usually consist of three steps: enrichment of target pathogen from food sample, plating on selective or differential agar plates and finally confirmation of results using a series of morphological, biochemical and serological tests [30]. Although these methods are highly sensitive, selective, and relatively cheap, they are highly laborious and time-consuming. Getting results from traditional culture methods can take several days or even weeks.

Multiple tube fermentation (MFT), plate count enumeration and membrane filter method (MF) are well-established traditional methods for sensitive detection of *E. coli*

in water even though these techniques provide results in several days [31]. The detection of STEC O157 is well established and it is based on the inability to ferment sorbitol within the first 24 hours [32]. Plating STEC O157 into sorbitol-containing agar causes *E. coli* O157 to grow as colourless colonies, while other *E. coli* colonies show a pink colour. Thus, selected colourless O157 colonies may be re-grown on a non-selective media and subjected to further confirmation tests [33]. This method is time-consuming and requires visual selection of the colonies, which is a subjective process. In addition, its primary focus is the detection of O157 serotype only, while it can still lead to false-negative results due to the occurrence of sorbitol fermenting *E. coli* O157, which have already been reported in some outbreaks [34]. Detection of non-O157 *E. coli* using traditional culture methods is more challenging because of high variations in phenotypic and biochemical characteristics between different serotypes. Chromogenic media have been developed that allow the detection of six main STEC serogroups. The media are based on β-galactosidase activity, selection of carbohydrate sources and other components which cause colonies' colour change [35, 36].

1.2.2. Immunological techniques

Immunological techniques utilise highly specific antibody-antigen interactions for the detection of the target pathogen. The most widely used immunological method is enzyme-linked immunosorbent assay (ELISA) which is a multiple-step process used for the detection of host biomarkers, such as antibodies, antigens or glycoproteins. There are four distinct types of ELISA and the sandwich ELISA is the most common method for bacterial detection. First, the surface is modified with the capture antibody which has a high affinity to the target bacteria surface antigens. When the sample is introduced to the modified surface, the target pathogen is recognised and attached to

the capture antibodies due to the affinity reaction while the rest is washed away. This step is followed by the treatment of the surface with an enzyme-tagged capture antibody which is specific to the surface antigen of a pathogen. Finally, the detection is accomplished with the addition of a substrate that reacts with the detection antibody-linked enzyme, resulting in a colour change in the sample proportional to the concentration of bacteria in the sample. Other immunological techniques include enzyme-linked fluorescent assay (ELFA), enzyme immunoassay (EIA) and flow injection immunoassay, which work similarly to sandwich ELISA [37].

The major advantage of immunological techniques is that it takes up to 24 hours to get results compared to the other methods, such as culturing, which takes up to several days. In addition, the immunological assay is usually less complex and laborious and allows high throughput processing, therefore it allows the development of commercial immune-based detection systems. For instance, VIDAS® is an automated immune analyser based on ELFA technology, which can perform up to 30 tests simultaneously in 5 independent sections. The results are recorded in real-time. However, this equipment is expensive and requires a laboratory setup. Therefore, it is not suitable for real-time on-farm detection or in the food industry. The major drawback of the immunological methods is the non-specific binding of the non-target antigens which causes false-positive results [38]. Finally, the antibodies are selective for the antigens which can be present on viable and non-viable cells, therefore the result may be positive even though it contains dead bacteria only [39].

Recognition of *E. coli* in the immunological method is typically based on targeting the O antigen at the bacterial membrane. There are several commercially available antibodies for the detection of *E. coli* including polyclonal antibodies, which can detect several serotypes at the same time and monoclonal antibodies which are specific

for the detection of, for example only *E. coli* O157 [26]. The antibodies can also be used for the detection of toxins produced by STEC [40, 41]. Among several immunological-based detection methods for *E coli* and STEC, ELISA is the most commonly used [26]. Paper-based ELISA is a promising, low-cost tool for allowing its use at distinct steps of food production by non-specialised personnel [42]. However, the sensitivity of this method is still not sufficient for point-of-use detection of bacteria if no enrichment step is used [43]. Immunoseparation based on the use of the magnetic beads modified with antibodies specific to the target pathogen is commonly applied for recovering specific targets from food samples or bacterial culture. It was shown that combining enrichment and immunoseparation can significantly increase the sensitivity of *E. coli* O157 detection [44].

1.2.3. Molecular techniques for bacteria detection

Molecular methods for pathogen detection are based on two key types of nucleic acids: deoxyribonucleic acid (DNA) and ribonucleic acid (RNA) previously extracted from cells/samples. The most common molecular technique is polymerase chain reaction (PCR), where specific genes are rapidly multiplied millions of times and afterwards visualised with, for instance, an agarose gel [45]. PCR relies on the use of Taq polymerase, a thermostable enzyme that enables the synthesis of a new DNA strand complementary to the template strand [46]. Briefly, the double-stranded DNA is de-hybridized by applying a high temperature. Afterwards, two primers are added; one forward and one reverse. They are short single-strand DNA fragments complementary to the opposite sides of a target DNA strand, which are desired to be multiplied. Taq polymerase, added in the following step with a mix of single nucleotides (A, T, G and C), begins the synthesis of the new strand between the region where primers are attached. These steps are repeated several times, resulting in exponential amplification

of a few million DNA copies. Therefore, it is possible to detect even a small amount of DNA [47]. PCR application towards pathogens provides several advantages such as high sensitivity (95-100 %) and accuracy (100%) [48, 49]. Furthermore, by using PCR it is possible to detect non-cultivable or slow-growing organisms. On the other hand, the equipment needed to undertake the PCR such as a thermal cycler, agar gel diffusion tray as well as some chemicals and reagents, may be costly and it requires highly trained personnel to perform the experiments [49]. Therefore, it is not feasible to use PCR for a point-of-use detection on-farm or in the food industry.

Another type of PCR is multiplex PCR, where several targets are multiplied in a single experiment. It comprises several primer sets in a single PCR mixture and therefore various reactions can occur simultaneously [50]. When optimised properly, multiplex PCR can significantly reduce the cost and time of the detection process [51]. While the traditional PCR is a qualitative method identifying either presence or absence of a certain gene, real-time PCR or qPCR is its quantitative version which is achieved using fluorescence [52]. There are two methods of detection in qPCR: using a non-specific fluorescent dye that intercalates between any kind of double-strand DNA, or with a set of fluorescently labelled primers complementary to the target sequence, allowing signal detection only if the specific hybridisation took place [53].

PCR is a well-established method for the detection of *E. coli* in food samples and water [54, 55]. Identification of general *E. coli* is commonly studied based on the *uid*A gene, coding for ß-glucuronidase enzyme production, which is specific for most *E. coli* strains [56]. Another possibility is to use 16s rRNA which is more suitable for the detection of only viable cells, it is, however, less stable compared to DNA making its handling challenging [57]. STEC detection is typically based on three genes associated with its virulence: *stx1* and *stx2* coding toxin production and *eae* coding intimin

secretion [58]. With a growing need for multiple virulence genes detection, multiplex PCR techniques are preferred. For STEC detection, multiplex PCR allows quick detection of O157 likewise non-O157 serotypes for which there is still a lack of traditional methods [59-61]. Conventional PCR is a relatively quick detection technique, however, it still requires the preparation of agarose gel, which is laborious and can lead to false-positive results when contaminated. Real-time PCR allows avoiding this step while quantifying DNA in the sample. Some protocols for detection of STEC with real-time PCR allowed limit of detection as low as 1–10 CFU/mL after enrichment [62, 63].

1.2.4. ISO detection methods for STEC and their limitations

In practice, the traditional culture methods are often used in combination with immunological or molecular methods to obtain the most accurate and rapid results. For instance, an internationally recognised horizontal method which includes the traditional culture methods combined with PCR was developed by an International Organization for Standardization (ISO), ISO/TS 13136:2012, for the detection of STEC and recognition of 6 main serotypes (O157, O111, O26, O103, O145 and O104:H4) [64]. Briefly, the enrichment is applied to multiply the potentially present STEC and this is followed by PCR to detect *stx* genes. If *stx* genes are not present, no further actions are necessary and the sample is negative for STEC. If *stx* genes are detected, another PCR is carried out to determine the occurrence of the other genes connected to STEC virulence such as *eae* or a gene responsible to determine O antigen. The next step is the culture isolation from presumably STEC positive enrichment medium by plating it into selective agars. Determining the O antigen in the previous step could help in the selection of the selective agar based on the serogroup or

introduce an immunoseparation using specific antibodies to isolate certain strains. The last step is the confirmation of STEC presence and identification of serogroups based on the assessment of the colonies [65].

Another ISO method, ISO 16654:2001, describes the method of *E. coli* O157 detection in food and animal feed, recommended for being used in the EU and outside of the EU [66]. It relies on its unique biochemical and serological characteristics. Similar to the previously described ISO method, it comprises a combination of enrichment culture methods, immunoseparation and PCR. The first step is enrichment in a selective medium- a soy broth containing tryptone and novobiocin- which favours the growth of *E. coli* O157 over the other gram-negative bacteria. This is followed by the second enrichment step in a non-selective media where *E. coli* O157 is extracted by immunoseparation using magnetic beads coated with the antibodies specific for the O157 antigen. Afterwards, the magnetic beads are plated into chromogenic agar media which are specifically designed to differentiate *E. coli* O157 from non-O157 based on their colour. In the end, the confirmation tests are performed for isolated colonies, including the indole formation test, agglutination test and PCR to confirm the presence of the *stx* genes [67].

The ISO methods for STEC detection are the current detection tests for *E. coli* and STEC however, there is an urgent need for the development of rapid and more reliable methods. Avoiding the enrichment and culture methods is the greatest desire since they are highly laborious and time-consuming. Currently, using a combination of the most suitable methods decreases the disadvantages of a single method. For example, the enrichment media including novobiocin and acriflavine support the growth of *E. coli* O157 while they inhibit the growth of the other STEC. Moreover, stressed or slightly damaged cells may not grow and lead to false-negative results if only culture

methods are used. Furthermore, excluding the enrichment step may result in an insufficient sample material for DNA detection using PCR. This would lead to a false-negative result. In addition, *stx* genes may be detected in the sample where no STEC was confirmed using the culture methods. This could imply either the presence of bacteriophages containing the *stx* gene, dead cells or non-cultivable bacteria. False-positive and false-positive results could be the outcome. Therefore, biosensors may be considered highly promising tools to overcome the limitations of the traditional methods for the detection of *E. coli* and STEC. Their definition, distinct types and applications for *E. coli* and STEC detection are summarised in the following sections.

1.3. Electrochemical biosensors

A biosensor is an analytical device converting a biological response into a measurable signal which is then read and quantified by a transducer [68]. They are typically used to detect and quantify a specific analyte such as bacteria [69], viruses [70], heavy metals [71]or allergens [72]. Recently they have been gaining much attention due to their advantages over the traditional detection methods, such as rapid measurements, portable size, and simplicity of use [73]. A biosensor consists of two major components - a biologically active receptor and a transducer which is schematically summarised in Fig. 1.1. The role of the biorecognition element is to recognize the target analyte and the most common receptors are antibodies [74], enzymes [75], nucleic acids [76], aptamers [77], or bacteriophages [78]. After the analyte's recognition, a transducer transforms the event into a measurable signal. Based on the applied transducer, biosensors are classified into three types: optical [79], electrochemical [80] and electromechanical (mass-based) biosensors [81]. This work focuses on the development of an electrochemical biosensor, therefore, the focus of

the further review will be on electrochemistry. Electrochemical biosensors are analytical devices that convert a biological response into an electrical signal [82, 83]. They are in high demand to provide rapid, point-of-care detection of pathogens like bacteria or viruses especially since the beginning of the COVID-19 pandemic [84, 85]. Their advantages over different detection techniques are high sensitivity, simplicity of use, relatively low cost, and suitability for miniaturisation [86, 87].

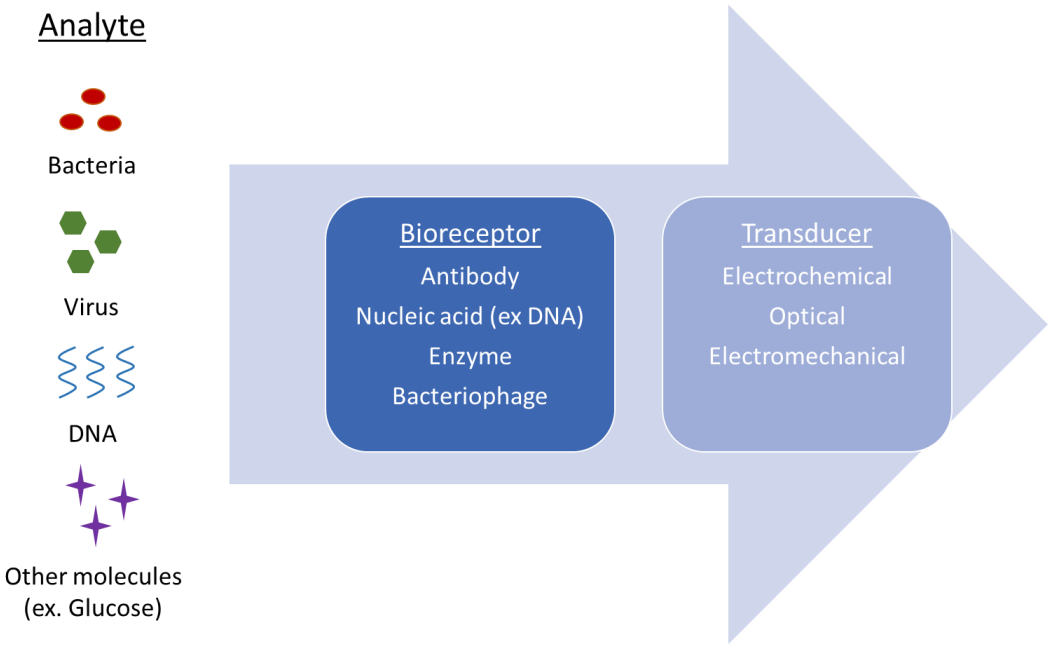

Fig. 1.1. A representative image of the biosensor construction components

1.3.1. The basic theory of electrochemistry

From a food safety perspective, electrochemical sensors may allow real-time pathogen detection at each step of food production processes and *in situ* in food plants or the field in primary production. Electrochemistry is a study in the field of physical chemistry regarding the movement of the electrons between the electrodes (electronic conductor) and electrolyte (ionic conductor). A large part of electrochemistry deals with the chemical reactions caused by imposing electrical signals (voltages or

currents) and using chemical reactions for electrical energy production. The key principle used in electrochemistry is a redox reaction, which is based on oxidation (losing electrons) and reduction (gaining electrons) which can be described using a simple equation. In brief, when the oxidised species (O) accepts the electron (e^-) it becomes reduced (R) and the reaction is reversible if the reduced species can lose the electron with relative ease, see Eq 1.

$$O + ne^- \rightleftharpoons R \qquad \text{(Eq.1.1)}$$

Reversibility is one of the key concepts in electrochemistry and an electrochemical reaction is considered reversible if reversing the current through the cell causes the species to return to its original state, without the formation of side products. A reaction is considered irreversible if reversing the current does not result in the formation of the original species, or if the rate associated with the reverse reaction is too low. This can happen if the product of the forward reaction is no longer soluble in the sample matrix (i.e. precipitation), or if a gas is produced.

One of the fundamental equations used in electrochemistry is the Nernst equation. A system that follows the Nernst equation or its derived form is considered to be reversible. The Nernst equation explains the potential of an electrochemical cell containing a reversible system and it is only valid at the electrode's surface.

$$E = E^0 - \frac{RT}{nF} \ln\left(\frac{Ox}{Red}\right) \qquad \text{(Eq. 1.2)}$$

Where E is the electrode's potential [V], E^0 is a standard reduction potential of Ox/Red couple [V], R is a gas constant ($8.315\ \frac{J}{K\ x\ mol}$), T is the temperature [K], and C_x is a concentration of the respective specie at the electrode [$\frac{mol}{L}$].

There are two types of currents in electrochemistry, Faradaic and non-faradaic. The faradaic currents are all the currents that are created through the redox reactions (oxidation or reduction), named as they obey Faraday's law. All other currents occurring at the electrode, which are part of the solution's conductivity and capacitive charging, are called non-faradaic and they follow Ohm's law.

1.3.2. Electrochemical cell

A typical electrochemical cell applied for sensor development comprises three electrodes – working, counter and reference electrodes that are placed in the same solution. In this setup, the potential of the working electrode is measured between the working electrode and the reference electrode, while the current flows between the working electrode and counter electrode.

1.3.2.1. Working electrode

A working electrode is an electrode at which the electrochemical reaction occurs and is the part of the electrochemical cell which typically has the most focus. Its shape, size and material have a huge influence on the outcome of the experiment and therefore it is critical for consideration in experiment design. The most commonly used materials are gold, platinum, carbon or mercury, due to their high electrical conductivity. In this research, all work was done using gold microelectrode arrays. The advantages of using gold electrodes are their high conductivity and ability for functionalisation. The disadvantage is its easy oxidation at positive potential, hydrogen evolution at the negative potential and high cost of fabrication.

In addition, using the microelectrode arrays offers additional advantages for electrochemical sensing including their ability to quickly achieve steady-state currents, having low capacity of the electrical double layer, high signal-to-noise ratio

and allowing for a small amount of sample and supporting electrolyte [88, 89]. A microelectrode can be defined as an electrode with critical dimensions of the micron or submicron scale while macro electrodes typically have a critical dimension of 1mm or larger.

1.3.2.2. Reference electrode

A reference electrode is an electrode with a known and stable potential. A good reference electrode should remain a constant composition, undependably of the experiment's length, providing a stable potential at the working electrode. In addition, it should be non-polarisable so the potential would not change depending on the current flow as well as the reaction should be reversible and the potential should be calculated based on the Nernst equation. The Standard Hydrogen Electrode (SHE) is the standard reference electrode and all standard reduction potentials are referred to it. SHE potential is assigned as 0.0000 V at all temperatures. It typically comprises platinized platinum foil or any other material catalysing hydrogen. Another type of commonly used reference electrode, also used in this research, is an Ag/AgCl electrode. It comprises a silver wire (Ag) coated with a layer of silver chloride (AgCl) immersed in a solution of KCl or AgCl. Its half-reaction is as follows:

$$AgCl_{(s)} + e^- \rightleftharpoons Ag_{(s)} + Cl^- \text{ , } E°_{Ag/AgCl} = 0.222 \text{ V vs NHE (25°C)} \qquad \text{(Eq. 1.3)}$$

It was used in this research to obtain a stable potential during the electrodeposition. In other experiments, a pseudo-reference platinum on-chip reference electrode was used. On such solid-state reference electrodes, the developed potential will be solely due to the solution's composition. This can, therefore, cause potential shifts after any changes to the solution of the cell. Using such a reference electrode is generally accepted if it is employed using redox species with a well-defined potential, such as ferrocene. In

the work presented in this thesis, this kind of reference electrode was applied for methylene blue.

1.3.2.3. Counter electrode

A counter electrode also called an auxiliary electrode, is essential in the two as well as the three-electrode electrochemical cell to complete the electrical circuit. Its main purpose is to provide a pathway for the current flow to decrease the current flown through the reference electrode. The most commonly used material for the counter electrode is platinum due to its non-corrosion and the speed of current transfer. Other materials can be used as well, such as carbon, gold or copper. In this research, a gold on-chip counter electrode was used.

1.3.3. Electrochemical methods for biosensors development

1.3.3.1. Chronoamperometry

In chronoamperometry, a fixed potential is applied to the electrode and the corresponding current related to the redox reaction (oxidation or reduction) at the interface is measured for a fixed amount of time. Typically, the current magnitude corresponds to the concentration of a measured redox species, therefore it found wide applications in sensors development [90]. For instance, it can be applied to the electrodeposition of metal nanoparticles and polymers or for the detection of metals from a solution. In both cases, an optimal potential at which the species of interest gets oxidised or reduced is applied to the electrode causing its electrodeposition. Other applications of amperometric sensors are immunosensors and enzymatic sensors.

1.3.3.2. Cyclic voltammetry (CV)

CV is a very popular technique for studying the reduction and oxidation of redox species. It is based on cycling the potential in a positive and subsequently in a negative

direction (or vice versa) and recording the current response, see Fig. 1.2 (A). The corresponding voltammogram or cyclic voltammogram represents the recorded current against applied potential, see Fig. 1.2 (B). The scan rate in CV controls the speed at which the potential is scanned. The faster the scan rate, the lower the diffusion layer around the electrode, which leads to higher currents. Studying CV at an increased scan rate can give much information about the reaction happening at the electrode. CV allows assessing if the reaction at the electrode is reversible based on the ratio of the peak currents potential and by applying the Nernst equation. The reaction is fully reversible in the peak potential separation is 0.059 V at 25 °C [91].

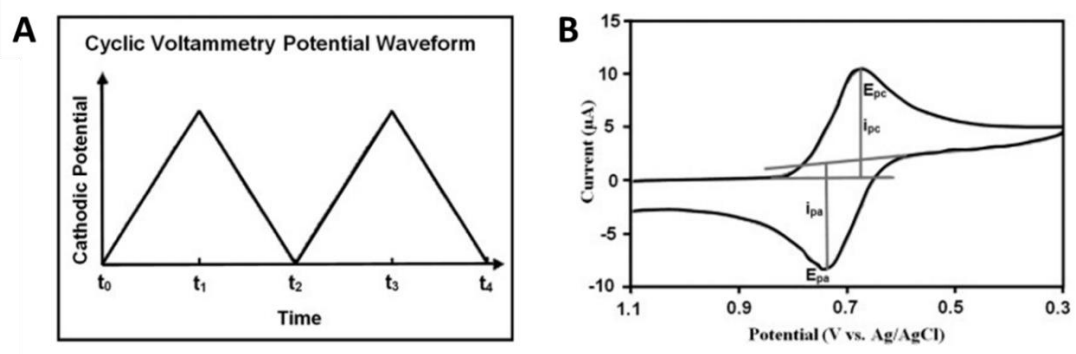

Fig. 1.2 (A) Typical CV potential waveform. (B) Typical cyclic voltammogram. E_{pc} and E_{pa} are the cathodic and anodic peak potentials, and I_{pc} and I_{pa} are the cathodic and anodic peak currents, respectively [92].

1.3.3.3. Square Wave voltammetry (SWV)

SWV is a type of pulse voltammetry technique that is the fastest and extremely sensitive and it was used as a detection technique throughout this research. The limits of detection using SWV are comparable to the chromatography and spectroscopic techniques [93]. During the SWV measurement, a potential is swept across the electrode in a series of forward and reverse pulses from an initial to the final potential, see. The length of the forward step is determined by an amplitude, the reverse step by subtracting the increment from the amplitude and the measurement speed can be

modified with the square wave frequency, see Fig. 1.3 (A). The outcome of the SWV experiment is a current obtained by subtraction of the experimentally measured forward and reverse currents, plotted versus the applied potential. The forward and reverse currents are measured at the end of the forward step and reverse steps, respectively, and their different results in a higher peak since the two currents have an opposite sign, see Fig. 1.3 (B) [94]. This corresponds to the faradaic current which effectively gets amplified. The charging current on the other hand has the same polarity during forward and background scans, thus it gets reduced after the subtraction. ΔI is therefore directly correlated to the concentration of an electroactive molecule around the electrode surface [95, 96]. This big advantage of SWV of background currents being significantly reduced and the corresponding peak currents relating to faradaic currents leads to the high sensitivity of this method.

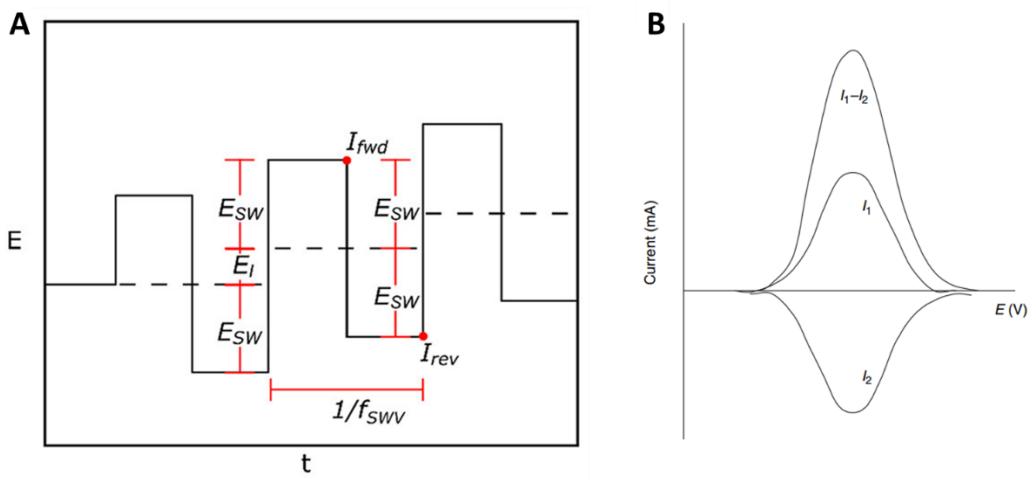

Fig. 1.3 (A) SWV potential pulse sequence, where E_{SW} is the amplitude, f_{SWV} is the square wave frequency, E_I is the increment, and I_{fwd} and I_{rev} are the end of pulse sampling points for the forward and reverse currents, respectively [95]. (B)

Electrical-current signal in square-wave voltammetry, resulting in a peak-shaped curve obtained by I1–I2 [94].

1.3.3.4. Differential pulse voltammetry (DPV)

DPV is another type of pulse voltammetry similar to SWV. In this case, the short pulses with limited amplitude are superimposed on a linear ramp potential. The base potential, where no faradaic reaction occurs is applied and it is swept in a positive or negative direction using pulses with equal increments. The current in this technique is measured at the beginning and the end of each pulse [97]. The biggest advantage of DPV, same as SWV is that the corresponding peak currents relate to the faradaic currents representing the redox reaction and the background currents are significantly reduced. This leads to the high sensitivity of these methods.

The research presented in this thesis used some of the presented electrochemical techniques. Amperometry and SWV voltammetry were used for the detection of silver ions in chapter 2 while SWV was used for DNA detection in chapters 3 and 4. In addition, more techniques for DNA detection are presented in the following section of the literature review summarising the DNA sensors for *E. coli* and STEC detection.

1.4. Electrochemical nucleic acid-based sensors for detection of *E. coli* and Shiga toxin-producing *E. coli* (STEC) – Review of the recent developments

Designing a sensitive and robust electrochemical nucleic acid-based biosensor typically requires the following three main steps:

a) Selection of specific probe sequence and its robust attachment to the electrode

b) Hybridisation with a target nucleic acid

c) Hybridisation detection using a label or label-free electrochemical method.

Robust attachment of probe DNA to the surface of a working electrode is a crucial step in the development of DNA sensors allowing good reactivity, access of a target to the probe, and good stability of the sensor. At the same time, the conductivity of the electrode has to be considered allowing a low limit of detection. Therefore, several strategies have been developed by the researchers to improve the sensing performance of the DNA sensors such as the integration of nanostructures, or polymers and miniaturisation of the system.

In this section, new aspects of nucleic acid-based electrochemical sensors for the detection of generic *E. coli* and Shiga toxin-producing *E. coli* (STEC) developed since 2010 were reviewed. First, issues related to probe sequence selection for generic *E. coli* and STEC detection are discussed and the three fundamental immobilisation techniques such as adsorption, covalent bonding and avidin-biotin interaction are explained. This is followed by a review of nucleic acid-based electrochemical sensors reported for detection of generic *E. coli* and STEC since 2010. These are grouped into different categories based on the most commonly used electrode materials (gold, ITO and screen printed) and magnetic particles. Finally, future trends in the development

of commercial nucleic acid-based biosensors and their potential application to agri-food samples are discussed.

1.4.1. Probe sequence selection for selective detection

Molecular detection of microorganisms targets specific regions of selected genes and their length and sequence will depend on the desired level of specificity (species, virulence, or other factors) [98]. A gene is a fragment of DNA or RNA which contributed to a single phenotype or function which may consist of hundreds or thousands of nucleotides. The selection of a probe sequence for specific target recognition is the first step in the development of an electrochemical nucleic acid-based sensor which will have a huge influence on its specificity [99]. This could also affect the affinity of redox molecules, often used in electrochemical detection, towards DNA. For example, methylene blue has a high affinity toward guanine, therefore the higher amount of guanine bases on the probe DNA, the higher the signal from methylene blue will be recorded [100]. Therefore, the probe sequence could also influence the intensity of an electrochemical signal of the sensor. This section will critically review the types of nucleic acid and target genes most commonly used in nucleic acid-based sensors for the detection of general *E. coli* and STEC that were summarised in Table 1.2.

DNA is typically more stable compared to RNA and it can persist for several days after a cell's death, depending on the environment [101]. For example, researchers have detected DNA in stream water after 25 days or in the soil after 70 days [102]. On the other hand, RNA can be damaged easily and its half-life for *E. coli* has been reported as 5 minutes [103]. In this context, detection based on RNA is considered to

be more suitable for detecting viable cells. However, with RNA being more prone to damage, its extraction and storage before testing are much more challenging [104].

Table 1.2 Summary of target nucleic acids used for specific identification of generic E. coli and STEC using electrochemical sensors.

E. coli / STEC	Target nucleic acid	Target gene	Biological function	References
E. coli				
	RNA	16 rRNA	Species-specific sequence	[105-108] [109-112]
	DNA	*uid*A	Production of enzyme - beta-D-glucuronidase	[113-116]
STEC				
	RNA	16S rRNA	Strain-specific sequence	[117]
	DNA	*stx1*/*stx2*	Shiga toxin production	[118, 119]
	DNA	*eae*	Intimin production	[120-124]
	DNA	*rfb*E	O-antigen synthesis for O157 serotype	[125]
	DNA	z3276	Pilus assembly protein	[126]

The main challenge in nucleic acid-based specific detection of generic *E. coli* is its close genetic relationship with *Shigella* spp., another common pathogen that belongs to the same family *Enterobacteriaceae*. It was estimated that their nucleotide similarity varies between 80 and 90% and they are usually differentiated based on their biochemical characteristics. This makes the selection of truly unique and specific primers for *E. coli* detection a real challenge to avoid a non-specific detection of microorganisms not related to faecal contamination [57].

The majority of nucleic acid-based sensors for the detection of generic *E. coli* have targeted recognition based on RNA, more specifically the 16S ribosomal RNA (rRNA) region [106, 108, 109]. 16 rRNA is a part of the 30S subunit of prokaryotic ribosome

containing a highly conserved region within the same group of microorganisms due to its low rate of evolution. In the past, studying 16S rRNA has facilitated the discovery and classification of several uncultivable bacteria [127]. Due to its unique sequence, it also allows differentiation of specific groups of bacteria, However, using 16 rRNA is unacceptable to differentiate between *E. coli* and *Shigella* spp. because of >99% sequence similarity [128]. Therefore, the sensors developed based on 16S rRNA detection could not be considered specific for *E. coli.*

The electrochemical sensors developed for the detection of generic *E. coli* based on DNA recognition have typically focused on targeting the *uid*A gene responsible for the ß-glucuronidase enzyme [113-115]. The enzyme catalase breaking of the glycosidic bond was claimed to be specific for *E. coli.* However, targeting only this gene will fail again to differentiate *E. coli* from *Shigella* spp. The solution to that problem could be the development of a sensor targeting at least two different genes. For instance, Pavlovic et al. [129] developed a duplex PCR to answer this limitation. In their work, in addition to the *uidA* gene, detection of the *lacY* gene coding for lactose permease was performed. It was shown that the *uidA* gene was present in all strains tested, *E. coli* and *Shigella* spp. while *lacY* was specific only to *E. coli*. Such a combination of detecting multiple genes would be beneficial for the future of sensor development.

Detection of STEC among the non-pathogenic strains is another challenge because the infection involves the expression of several genes. A need for the revaluation of STEC virulence factors has especially become evident after the big outbreak in Germany in 2011 caused by enteroaggregative hemorrhagic *E. coli* (EAHEC) O104:H4 which acquired a gene coding for toxin production (*stx2*) from a bacteriophage [130]. Based on extensive research on STEC pathogenicity in the last years, it was concluded that

all *E. coli* strains containing at least one *stx* gene coding for toxin production may cause human infection [23, 131, 132]. The nucleic acid-based detection should thereof focus on the genes coding for toxin production. Several subtypes of each gene exist; having any subtype of *stx* in a genome or a combination may be pathogenic. Some studies have shown the use of the *stx* gene as a target for STEC detection [118, 119]. Another gene commonly used in the development of STEC-specific DNA sensors is the *eae* gene [120-124]. The gene *eaeA* is responsible for intimin production and it has been considered a virulence factor for STEC. A recent study has however concluded that containing this gene is not essential for causing a severe illness. Epidemiological research showed that even though the majority of STEC strains from samples contained the *eaeA* gene, not all of them contained this gene. It was found that STEC could use alternative means of attachment to mucous cells without intimin. Moreover, there are known strains which contained *eaeA* gene and either did not cause any infection or only a mild one. Therefore, it was concluded that the *eaeA* gene alone cannot be a virulence factor for the detection of STEC [23]. More accurate virulence factors for STEC recognition are two groups of genes - *stx1* and *stx2*, which encode Shiga toxin production. Less often, different virulence factors were used. For example, in the work of Minaei et al. [125], the *rfb*E gene was used for the detection of STEC O157. STEC O157 is considered the most pathogenic strain of *E. coli*, however, in recent years the non-O157 serotypes are reported in a growing amount of STEC outbreaks. Therefore, an ideal STEC detection technique should include all serotypes which could potentially cause an infection. Another virulence gene was chosen by Deshmukh et al. [126]. In their sensor, STEC O157 was detected using the z3276 gene which is known for encoding a unique putative fimbrial protein allowing the adhesion to the host cell. In this case, however, also only STEC O157 was targeted.

In summary, choosing the right nucleic acid sequence is crucial for selectivity and specificity in bacterial detection. The majority of electrochemical sensors developed for the detection of *E. coli* and STEC to date focused on the detection of a single DNA gene or 16 rRNA sequence. Based on the research, using the selected sequences fails to be specific for the detection of *E. coli* and STEC. This problem could be solved by including additional genes in the detection assay to confirm the specificity, such as *lacY* gene in addition to *uidA* for the detection of *E. coli* or *stx1* and *stx2* genes in addition to *eaeA* gene for STEC. This shows the need for the development of multiplex sensors allowing the detection of multiple genes.

1.4.2. Probe attachment methods

1.4.2.1. Adsorption

Adsorption is the simplest method for probe attachment in which negatively charged phosphate groups of DNA strands are directly attracted to positively charged groups at the modified working electrode [133]. The visual representation of this attachment technique can be found in Fig. 1.4. Typically, the electrode is modified with a positively charged polymer, such as chitosan, poly-L-lysine, polypyrrole or polyaniline [134]. The key advantage of the adsorption is its simplicity, however, it can be unstable which may result in the DNA desorbing from the electrode [135]. In addition, the probe orientation may be random, which will negatively affect the efficiency and reproducibility of a sensor [136].

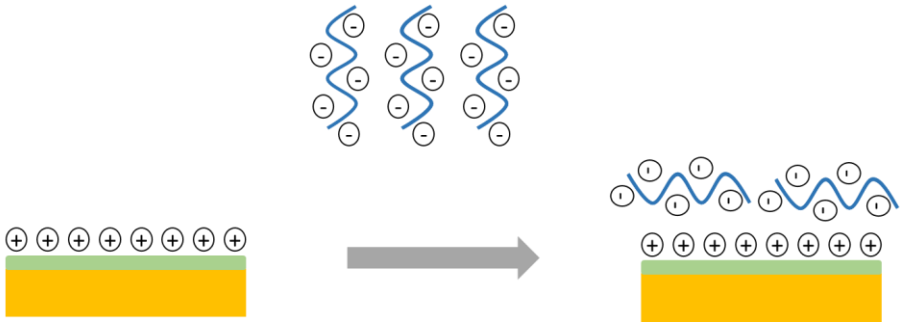

Fig. 1.4 Scheme presenting DNA attachment to the working electrode using adsorption

1.4.2.2. Covalent bond

Covalent bonding is the most frequently used for DNA attachment because of its high stability, compared to adsorption [134]. It also provides the flexibility of the probe structure allowing for its conformation to change when the hybridisation takes place [137]. Chemisorption and covalent attachment are two dominant types of covalent bonding.

Chemisorption is similar to adsorption, however, it involves a chemical reaction and electron transfer between a molecule or an atom and a surface, resulting in a stronger bond [138]. Probe DNA modified with thiols on one end is most often used, see Fig. 1.5. Thiols can react with several surface materials such as gold, silver, platinum or copper with gold being the most commonly used [139, 140]. DNA attachment via thiols is still one of the most popular ways of immobilisation used in electrochemical sensor development [105, 113]. The biggest advantage is its simplicity as it needs only an incubation process similarly to absorption but the bond is much stronger and the DNA orientation is more suitable for optimal hybridisation [134].

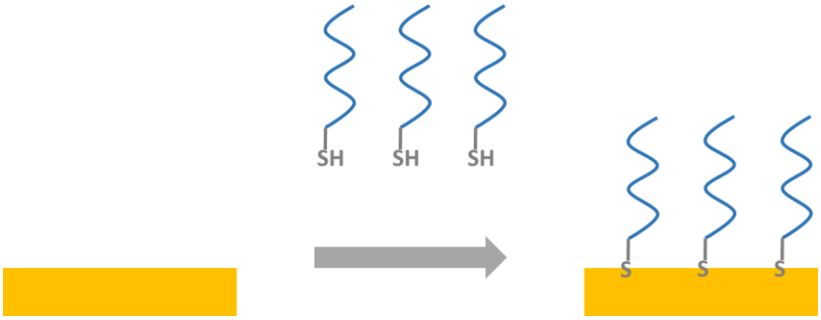

Fig. 1.5 Scheme presenting DNA attachment to the working electrode using chemisorption

Covalent attachment is another type of covalent binding, often used in the development of DNA sensors. Typically, a probe DNA modified with a primary amine group creates a bond with one of the functional groups presented in Fig. 1.6, such as the carboxyl group, aldehyde group, sulfonic group, epoxy group or isothiocyanate group [134]. Typically, an additional linker molecule is needed to immobilise the amine-modified probe to these functional groups. For instance, the attachment using carboxyl groups requires first incubation in a mixture of 1-ethyl-3-(-3-dimethylaminopropyl) carbodiimide hydrochloride (EDC) and N-hydroxysuccinimide (NHS). EDC transform the carboxyl group into O-acylisourea intermediate which can be easily replaced with a primary amine group, therefore allowing the probe to attach. NHS is commonly used in combination with EDC to improve the efficiency of the coupling and to create amine-reactive, dry-stable intermediates [136]. A commonly used alternative is modifying a surface rich in amine groups with glutaraldehyde to obtain the aldehyde groups which can subsequently be used for amine-modified probe immobilisation [141].

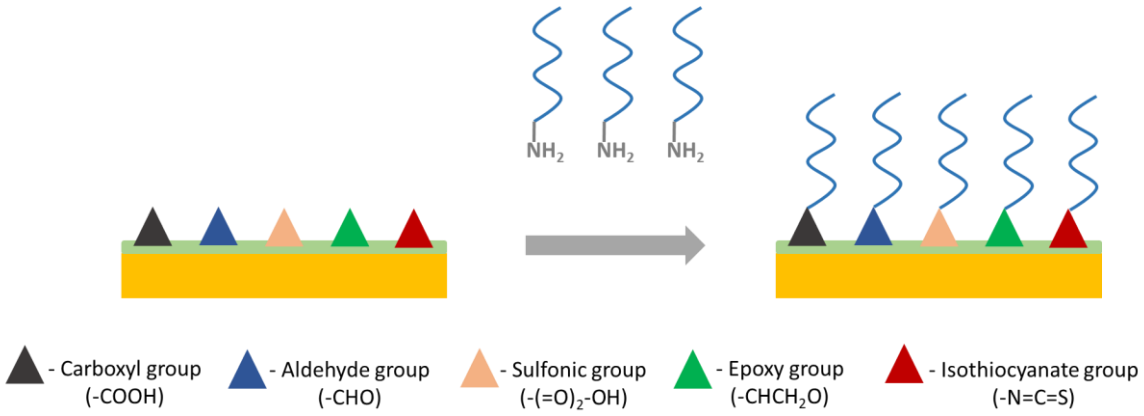

Fig. 1.6 Scheme presenting DNA attachment to the working electrode using a covalent attachment with examples of different functional groups

1.4.2.3. Avidin – biotin interaction

Another commonly used method for probe attachment is avidin-biotin interaction. It is the strongest, non-covalent interaction between a protein and ligand [142]. The interaction is created rapidly and once formed it is resistant to changes in pH, temperature and the use of various solvents or denaturation agents [143]. These characteristics make it suitable for sensor development, and one example of its application is the binding of oligonucleotides to the electrode [144]. Typically, probe DNA modified with biotin is immobilised on the electrode surface modified with Avidin or its derivatives such as Streptavidin or Neutravidin, see Fig. 1.7.

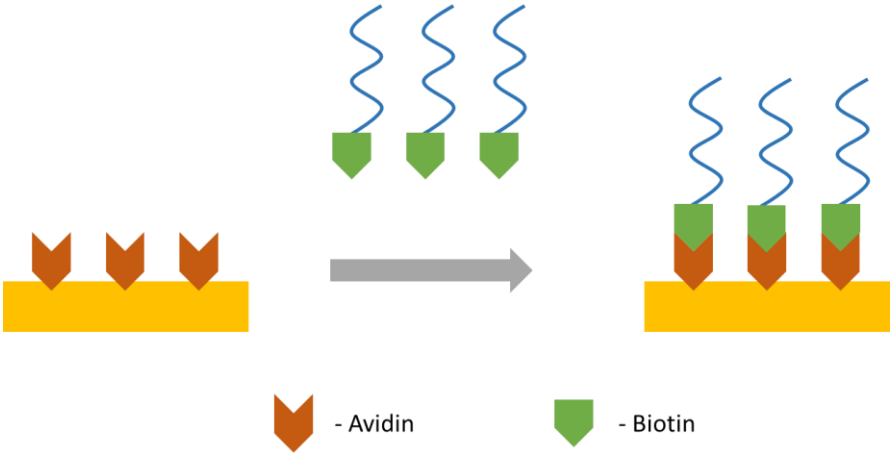

Fig. 1.7 Scheme presenting DNA attachment to the working electrode using avidin-biotin interaction

1.4.3. Nucleic acid-based sensors for detection of *E. coli* and STEC

The main parameters of reviewed electrochemical sensors for the nucleic acid-based sensors for the detection of generic *E. coli* and STEC developed since 2010 are summarised in Table 1.3. These sensors and described in more detail in the following part.

Table 1.3 Summary of nucleic acid-based sensors for detection of generic E. coli and STEC since 2010.

Category	Nucleic acid target	Electrode + modification (attachment)	Technique	Linear range	LOD	Assay time (*not full)	Sample volume [mL]	Complex samples	Ref.
Gold electrodes	16s rRNA	Au + thiols (covalent)	EIS	10^{-6} - 10^{-9} M	1.6 x 10^{-8} M	1 hour*	0.05	PCR product	[145]
	16s rRNA	Au + thiols (covalent)	Amp	-	10^{-12} M 2.5x10^{4} CFU/mL	1.5 hour	0.004	Bacterial culture	[146]
	16s rRNA	Au + thiols (Covalent)	Amp	-	2x10^{3} CFU/mL or (1 CFU/mL)	5 hours (7 hours)	0.01	Meat samples	[147]
	lacZ gene	Au + thiols (covalent)	ACV	10^{-11} – 10^{-8} M	3 x 10^{-14} M	60 min*	1	Milk, beer, tap water, peanut milk	[148]
	16s rRNA	Au + thiols (covalent)	Amp	-	10^{-15} M 250 CFU/mL	<1 hour	0.004	Bacterial culture	[149]
	16s rRNA	SPGE + AuNPs	Amp	2.5x10^{-14} – 1x10^{-9} M	2.5x10^{-14} M 3x10^{6} CFU/mL	30 min	0.01	human serum and urine samples	[150]
	uidA gene	Au + thiols (Covalent)	Amp	-	10^{-15} M	< 3 hours	0.1	PCR product	[151]
	DNA sequence reported	Au + polyA	Amp	10-^{14} to 10^{-8} M	5x10^{-15} M	<3 hours	0.15	PCR products	[152]
	16s rRNA	Au + mesoporous silica thin films	CV	5x10^{-9} – 7x10^{-7} M	2.5 x 10^{-14} M	1 hour	0.01	Bacterial culture	[153]

	16s rRNA	Au + cystine nanoflowers (Covalent)	EIS	10^{-15} - 10^{-6} M	10^{-15} M	20 min*	NI	Bacterial culture	[154]
	16s rRNA	Au + microstructural cystine (Covalent)	EIS	10^{-14} - 10^{-6} M	10^{-14} M	1.5 hour	NI	Bacterial culture	[155]
	16s rRNA	Au + FNAB + ODT covalent	DPV	0.5×10^{-18} – 1×10^{-6} M	0.5×10^{-18} M	60 s*	0.5	Bacterial culture	[156]
	16s rRNA	Au	CV	-	$3x10^{-16}$ M	>1 hour	0.1	Bacterial culture	[109]
	*rfb*E	Au	EIS	10^{-13} – 10^{-6} M	$9.1x10^{-14}$ M	1 hour	NI	PCR product, Bacterial culture	[125]
ITO	*z3276* gene	ITO + APTES (covalent)	EIS	$6.3x10^{-16}$ – 3.2×10^{-14} M	2 CFU/mL	<1 hour	0.7	Bacterial culture	[126]
	16s rRNA	ITO + PLGA + IONPs (covalent)	EIS	10^{-13} to 10^{-6} M	8.7×10^{-14} M	30 min*	NI	Bacterial culture	[157]
	16s rRNA	ITO + GOx + NiF + chitosan (covalent)	DPV	10^{-16} – 10^{-6} M	10^{-16} M	<1 hour	NI	Bacterial culture	[107]
	16s rRNA	ITO + ZnO + cGNF	EIS	10^{-16} to 10^{-6} M	10^{-16} M	1 hour 15 min	NI	Bacterial culture	[158]
	16s rRNA	ITO + GOx/AuNPs + PPY	DPV	10^{-15} to 10^{-6} M	10^{-15} M	<1 hour	NI	Bacterial culture	[159]

Carbon and graphite based electrodes	DNA sequence reported	SPCE + Ag	DPV	10^{-19} M to 10^{-10} M 10 - 10^{6} CFU/mL	5.6x10^{-19} M 17 CFU/mL	<1.5 hour	0.02	Bacterial culture	[160]
	yaiO gene	SPCE + AuNPs (covalent)	EIS	10^{-15} - 10^{-7} M	10^{-15} M	< 1 hour	0.01	Bacterial culture	Rabti et al 2021
	stx gene	SPE + PtNPs + chitosan (adsorption)	EIS	10^{-12} – 10^{-4} M	3.6x10^{-14} M	<2 hours	NI	Surface water (PCR product)	[161]
	16s rRNA	SPCE + hollow silica NPs	DPV	1×10^{-18} – 1×10^{-8} M	8.17×10^{-20} M	<1.5 hour	0.3	River water samples	[112]
	DNA sequence reported	SPE + AuNPs + HSMs (Covalent)	EIS	10^{-16} to 10^{-11} M	1.95x10^{-21} M	<1.5 hour	0.3	River water samples	[162]
	*eae*A gene	GCE + GOx + AuNPs + thiols (Covalent)	DPV	2x10^{-11} – 5x10^{-8} M	10^{-11} M	< 2 hours*	1.5	Synthetic stool samples	[121]
	DNA sequence reported	GCE + MWCNTs-Chi-Bi	DPV	1.94×10^{-13} - 2.01×10^{-14}	1.97 × 10^{-14} M	<4 h	NI	Beef meat	[163]
	16s rRNA	PGE + MWCNT (Covalent)	DPV	5.5x10^{-8} - 9x10^{-8} M	1.7x10^{-8} M	<3 hours	NI	PCR product	[106]
Magnetic MPs and NPs	DNA sequence reported	SA-magnetic beads	DPV	3x10^{-17} – 3x10^{-10} M	3x10^{-17} M	3 hours*	0.002	Milk and peach juice	[164]
	*eae*A gene	streptAv-MPs	Amp	-	5.9x10^{-12} M	<4 hours	NI	PCR product	[120]
	*stx*1 gene	MMP + AuNPs	DPV	-	5 CFU/mL	<4 hours	0.2	Bacterial culture	[119]

	DNA sequence reported	MNPs (Fe_2O_3@Au)	Amp	$1x10^3$ – $5x10^5$ CFU/mL	$5x10^2$/ 5 CFU/mL	<2/<5 hours	0.125	River water	[165]
	*eae*A gene	Silica MP m-GEC	Amp	-	$2.6x10^{-9}$ M	<3 hours	0.08	PCR	[166]
	*eae*A gene	Silica MP M-GEC	Amp	$5x10^{-10}$ – $2x10^{-8}$ M	$5 x10^{-10}$ M	<3 hours	0.08	PCR product	[167]
	*uid*A gene	CMB + alginic acid	DPV	$1x10^{-9}$ – $7x10^{-9}$ M; $1x10^2$-$2x10^3$ CFU	$3x10^{-10}$ M; 50 CFU/mL	2 hours	0.3	PCR product, chromosomal DNA, water samples	[115]
	16s rRNA	CeO_2	DPV	2 - $10x10^{-8}$ M	$2x10^{-8}$ M	<2 hours	0.15	Human serum	[168]

IDE – interdigitated electrode, MPTS - (3-mercaptopropyl)-trimethoxysilane, GOx – graphene oxide, HSMs - hollow silica microspheres, SA – Streptavidin-coated, CMB – cobalt magnetic beads, streptAv-MPs - streptavidin-magnetic particles, MNPs – magnetic nanoparticles, MMP – magnetic micro particles, CMB – cobalt magnetic beads, streptAv-MPs – Streptavidin-coated magnetic particles, ZnO – Zinc oxide, cGNF - carboxylated graphene nanoflakes, Cx-GNF - carboxylated graphene nanoflakes, PPY – polypyrrole, PyBA - 1-pyrenebutyric acid, NiF - nickel ferrite, TiO_2 – titanium dioxide, FNAB - 1-fluoro-2-nitro-4-azidobenzene; ODT - octadecanethiol; m-GEC - magneto-graphite epoxy composite; IONPs - iron oxide nanoparticles; PLGA - cationic poly(lactic-co-glycolic acid); NI – no information

1.4.3.1. Gold electrodes

Gold electrodes are the most commonly employed in nucleic acid-based electrochemical sensor development. The reason for that could be their good biocompatibility, high conductivity and stability [169]. They are especially attractive for sensors based on nucleic recognition because the thiol-modified probes can be easily immobilised on the surface using chemisorption [134]. For instance, Yang et al. [145] developed a simple biosensor for the detection of STEC O157:H7 based on gold electrodes fabricated on waste newspaper. The thiol-modified probe DNA was immobilised onto the gold electrode and label-free detection of STEC O157:H7 was undertaken using EIS. The authors achieved an LOD of 1.6 x 10^{-8} M and confirmed the selectivity of the sensor with a PCR product from STEC and *Salmonella*. Walter et al. [146] have also used thiols to immobilise a probe DNA complementary to 16s rRNA sequence of *E. coli* on an array of 16 gold electrodes. The enzymatic detection was done based on a sandwich-type assay achieving an LOD of 10^{-12} M. That accounted for 2.5x10^{4} CFU/mL with an assay taking one and a half hours without the need for DNA amplification. Li et al. [148] developed a sensor for the detection of *lacZ* gene sequence of *E. coli* using reporter DNA tagged with MB. The probe DNA was immobilized using thiols, similar to previous studies, and the signal was detected using ACV. The authors achieved an LOD of 3x10^{-14} M and validated their sensors using real samples such as milk, beer, tap water, and peanut milk, showing its dependency on pH and ionic strength. These samples, however, were only spiked with the synthetic DNA to test if the matrix affects the sensors efficiency without using the DNA extracted from bacterial cells. The sensor was regenerated six times after hybridisation in milk samples by simply rinsing it with DI water for 60 seconds which is a promising result for the continuous monitoring. In the study of Heidenreich et al.

[147], an electrochemical chip-based sensor was developed for detection of 16S rRNA specific for general *E. coli*. Each chip contained 8 gold electrodes of which 4 were treated with a $Ag/AgCl_2$ solution for use as reference electrodes, and the other 4 were modified with thiolated probe DNA for use as working electrodes. The detection was based on a sandwich assay, explained in Fig. 1.8, using esterase 2 (EST2) enzyme-modified oligonucleotide as a reporter. In brief, if the target RNA was present in the sample and hybridised to a probe, the enzyme-modified reporter could bind to its other side. Subsequently, a substrate *p*-aminophenyl butyrate was introduced onto the sensor that hydrolysed into *p*-aminophenol if the enzyme-tagged reporter was present. This reaction was recorded using amperometry with a corresponding current correlating to the concentration of target DNA. The sensor was tested using naturally contaminated meat samples and compared results with traditional plating methods. Using this technique 2000 CFU/mL were detected in a 5-hour long assay that was effectively lowered to 1 CFU/mL if the assay time was increased to 7 hours. The relatively long time of the assay compared to other techniques was caused by several hours long enrichment to increase the number of target bacteria in the sample.

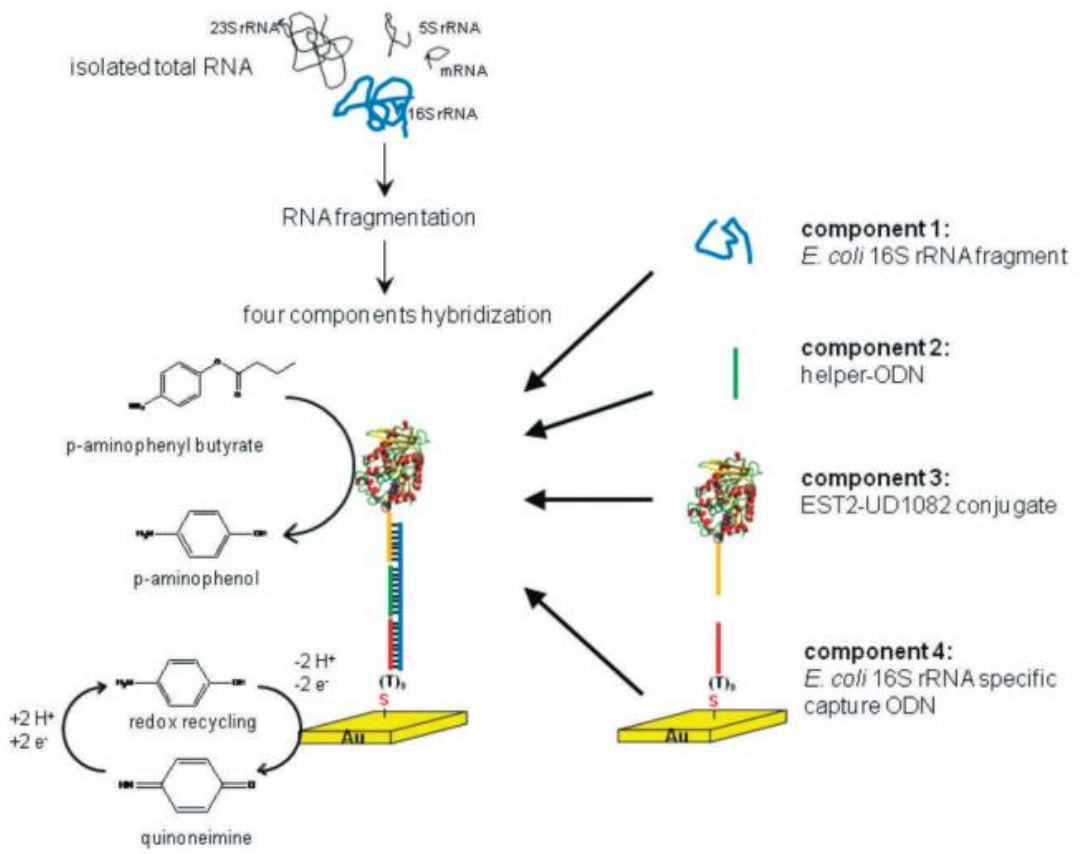

Fig. 1.8 Electrochemical biochip detection of E. coli 16S rRNA using four-component sandwich hybridization (Reprinted with permission from Heidenreich et al. [147]. Copyright 2010 International Association for Food Protection).

The unreacted surface of a gold electrode modified with thiolated probe DNA needs to be blocked to avoid the non-specific binding and typically 6-mercapto-1-hexanol (MCH) is used. Wu et al. [149] showed that the LOD of a sensor could be improved by using α,ω-alkanedithiol dithiothreitol (DTT) in addition to MCH. Such modification decreased the background noise and limited the non-specific binding. Authors used common enzymatic detection with reported DNA tagged with an enzyme, horse radish peroxide (HRP). HRP catalysed the reduction of hydrogen peroxide, which in the presence of 3,3′,5,5′-tetramethylbenzidine (TMB), a co-substrate, generated a quantitative electrochemical current detected using amperometry. The current magnitude was positively proportional to the concentration

of the target DNA present in the sample. The authors achieved an LOD of 10^{-15} M corresponding to 250 CFU/mL in less than one hour, including the DNA extraction. In the work of Kuralay et al. [150], a similar approach was utilised but in this case, hexanedithiol (HDT) in addition to MCH was used to backfill the unreacted gold surface. The authors report a tenfold improvement in the signal-to-noise ratio for the detection of 10^{-9} M target strand. Using enzymatic detection, they achieved an LOD of $2.5x10^{-14}$ M that corresponded to $3x10^{6}$ CFU/mL and used human serum and urine samples for validation. These two works of Wu et al. [149] and Kuralay et al. [150] highlight the difficulty in comparison between the articles using molar and CFU/mL units. Even though 16s rRNA was used in both works, and the LOD in molar units was similar (10^{-15} M and $2.5x10^{-14}$ M) it corresponded to very different values in CFU/mL (250 and $3x10^{6}$).

Another way of improving the sensitivity of gold electrode-based nucleic acid sensor was proposed by Wen et al. [151] who immobilized a novel 3D probe DNA nanostructure via thiols, see Fig. 1.9. The nanostructure comprised of four DNA strands specifically designed to form a 3D structure allowing an upright probe orientation to avoid surface steric hindrance effect without its overcrowding. The detection was studied by using a sandwich method where, after 3D probe hybridisation with the target, the reporter strand tagged with HRP enzyme was introduced and the detection was achieved using amperometry, as described above. The developed sensor had an LOD of 10^{-15} M with the synthetic DNA and it was applied to detect PCR amplicons of *E. coli* genomic DNA to assess its selectivity.

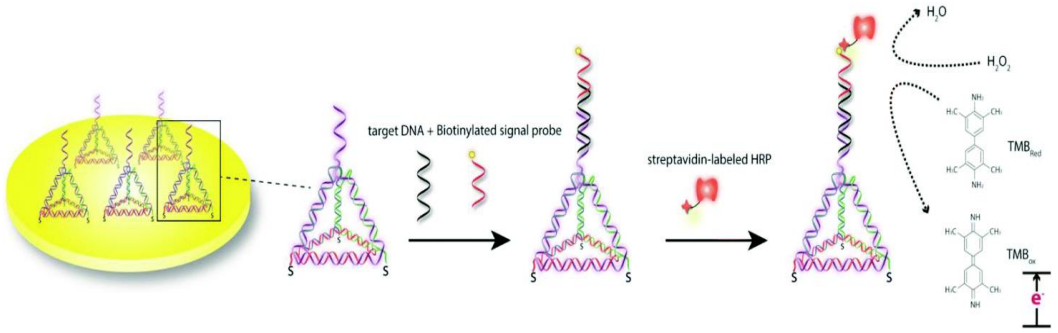

Fig. 1.9 Scheme for the DNA tetrahedral nanostructure-based "sandwich-type" biosensing strategy for electrochemical DNA analysis (Reprinted with permission from Wen et al. [151]. Copyright 2016 The Royal Society of Chemistry).

An alternative to using thiolated probe DNA probes, the gold electrode can also be modified with molecules containing the sulphur groups and other functional groups such as cystine. Pandey et al. [155] and Pandey et al. [154] used gold electrodes modified with self-assembled cystine structures for a subsequent covalent attachment of amine-modified probe DNA complementary to *E. coli*, see Fig. 1.10. The label-free detection in both studies was undertaken using EIS and sensors achieved an LOD of 10^{-14} M and 10^{-15} M, respectively. The specificity of the presented sensors was confirmed with chromosomal DNA extracted from a selection of overnight bacteria cultures including *E. coli*, *Salmonella typhimurium*, *Neisseria meningitides*, and *Klebsiella pneumonia*. The detection was achieved in ~1.5 hours, including the DNA extraction. The use of cystine increased the complexity of sensor development compared to bare gold due to the long time required for microstructures synthesis (9-12 h). However, using such nanostructures has increased the sensitivity of the sensor compared to bare gold macro electrodes.

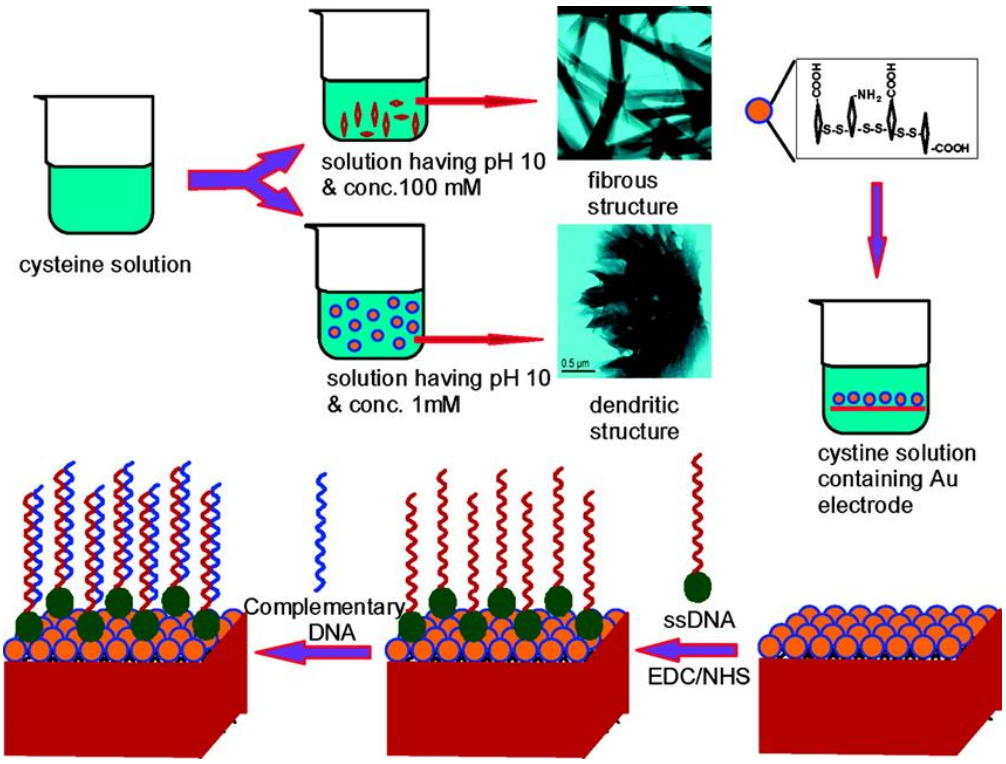

Fig. 1.10 Schematic showing the preparation and fabrication of microcystine and ssDNA/denCys/Au bioelectrode (Reprinted with permission from Pandey et al. [155]. Copyright 2011 Chemical Society).

Another strategy was employed by Pandey et al. [156] where a gold electrode was modified with SAM of octadecanethiol (ODT) subsequently forming a covalent bond with 1-fluoro-2-nitro-4-azidobenzene (FNAB) under UV irradiation. An amine-modified probe DNA was also covalently attached to the modified surface by binding to the thermally activated fluoro group on FNAB, as shown in Fig. 1.11. Methylene blue (MB) was used as a redox-active molecule known to interact with ssDNA and dsDNA. The authors achieved a very high sensitivity with an LOD of 0.5×10^{-18} M and a wide linear range between 10^{-18} and 10^{-6} M after only 60 s hybridisation. The sensor could be reused up to 10 times after dipping it into a tris-HCl buffer for 3 minutes at 100°C. The excellent selectivity of the sensor was confirmed using DNA extracted from *E. coli* and non-*E. coli*. The full assay including the DNA extraction

was done in less than 1 hour which in a combination with high sensitivity was shown as a promising method for POC testing.

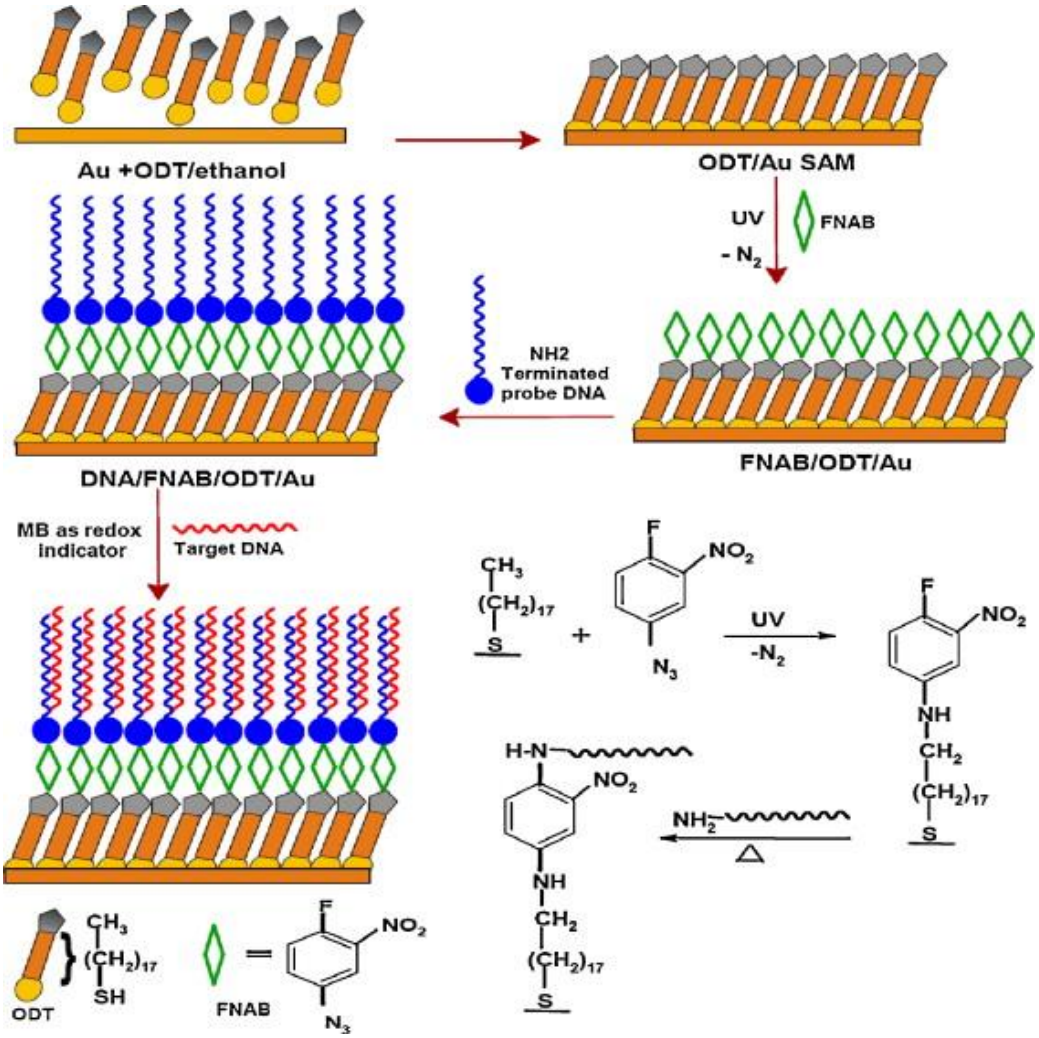

Fig. 1.11 Schematic showing the fabrication of DNA/FNAB/ODT/Au bioelectrode (Reprinted with permission from Pandey et al [156]. Copyright 2011 Elsevier B. V.)

An alternative probe DNA attachment approach was used by Li et al 2018 who used poly-adenine (poly-A) blocks instead of thiols. This immobilisation method has been previously reported by other authors offering advantages to the thiolated DNA such as lower cost, faster immobilisation and an easier way to control probe density by testing the different lengths of poly-A blocks [170]. A different length of poly-adenine blocks was tested with 30 adenine blocks chosen as most optimal. The enzymatic

detection using HRP tagged reporter probe achieved an LOD of $5x10^{-15}$ M. The assay was performed in less than 3 hours, including the PCR amplification. Saadaoui et al. [153] modified the gold electrode with mesoporous silica thin films that offer larger surface area and hydroxyl group content for biomolecules attachment. The heptylamine-phosphoramidite moiet modified probe, complementary to the 16s rRNA sequence of *E. coli* was immobilised on top of the modified electrode and the detection was done using CV in 5 mM Fe^{-3}/Fe^{-4}. This method achieved an LOD of 2.5 x 10^{-14} M and tests were done with RNA extracted from the *E. coli* bacterial culture in around one hour, including the RNA extraction.

Decreasing the area of working electrode to micro/nano scale offers several advantages to the electroanalytical performance of the sensor such as enhanced signal-to-noise ratio [171-173]. The double layer around the micro/nano electrode has a lower capacitance and smaller time constant that allow the signal to be measured more rapidly and with less destruction to the sensor [174]. As the electrode dimensions are smaller than its diffusion layer, the mass transport increases and therefore its sensitivity also increases [174]. Smaller size electrodes also allow the fabrication of multiple electrodes at high density, opening the door for multiplex sensing using single miniaturised devices enabling their commercialisation [175]. In the work of Zimdars et al. [109] an array comprised of 32 individually addressable, gold microelectrodes was developed for the detection of native 16S rRNA fragments of *E. coli* and synthetic DNA targets of pathogens responsible for urinary tract infections. The thiol-modified DNA capture probes were immobilised at the electrode using a micro-spotter and the hybridization was detected using an intercalator - biotinylated proflavine derivative. The presented sensor allowed detection of $6x10^{-8}$ M of synthetic DNA strands and $3x10^{-14}$ M of native 16S rRNA stands extracted from bacterial cells. In the study

reported by Minaei et al. [125] two sizes of gold electrodes (2 mm diameter and nanoelectrode (no size stated)) were selected for the development of sensors for the detection of the *rfb*E gene from STEC O157 : H7. However, only the data from the nanoelectrode were presented. It was modified with a layer of gold NPs followed by an attachment of thiol-modified probe DNA. Using EIS as a label-free detection technique, the sensor exhibited linear response between $1x10^{-6}$ M and $1x10^{-13}$ M with the LOD of $9.1x10^{-14}$ M of synthetic DNA. It was therefore, comparable to the microelectrode. The sensor was as well validated using chromosomal DNA extracted from *E. coli* O157:H7 and it showed a great selectivity towards *E. coli* O157:H7 among other bacteria species tested (*Vibrio cholerae* O1 (Ogawa) and *Shigella flexneri*) in a one hour long assay including DNA extraction.

1.4.3.2. Indium tin oxide (ITO) based electrodes

ITO has been a popular material for biosensors development due to its high conductivity, wide electrochemical window and ease of modification [176]. To compensate for their poor electrocatalytic properties, they usually are modified with catalytically active metals for the development of biosensors [176]. The modification is also needed for the attachment of biomolecules, such as probe DNA. For instance, Deshmukh et al. [126] modified the ITO chip with Aminopropyltrimethoxysilane (APTES) creating amine groups on the surface allowing for covalent attachment of amine-modified probe DNA using glutaraldehyde as a linker. The label-free detection of z3276 gene from STEC O157:H7 was recorded using EIS. The authors used chromosomal DNA for the detection and achieved a linear range between $6.3x10^{-16}$ – 3.2×10^{-14} M and an LOD 2 CFU/mL in potable water samples in less than one hour including DNA extraction. Two *E. coli* strains negative for the z3276 gene and Bacillus subtilis were used to confirm the specificity of the developed sensor. In the

work of Pandey et al. [157] schematically summarised in Fig. 1.12, an ITO electrode was modified with iron oxide nanoparticles (IONPs) encapsulated into cationic poly(lactic-co-glycolic acid) (PLGA). The modified electrode was employed to immobilise the amine-modified probe DNA complementary to *E. coli* using a covalent attachment. The authors achieved a label-free detection using EIS in a linear range between 10^{-13} and 10^{-6} M and an LOD of 8.7×10^{-14} M using synthetic strands. The sensor was also applied to the detection of bacterial DNA extracted from *E. coli* and five other bacterial cultures, however, the protocol of DNA extraction was not described and therefore the total time of assay, aside from a 30-minute hybridisation step, could not be estimated.

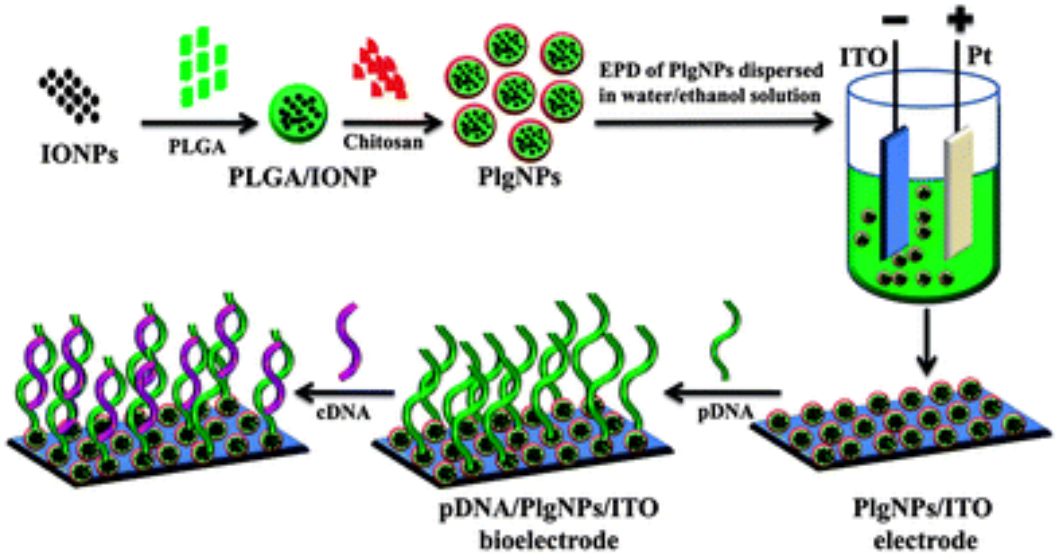

Fig. 1.12 Schematic illustration for the preparation of PlgNPs, EPD of PlgNPs onto ITO electrode and its application for electrochemical detection of E. coli. (Reprinted with permission from Pandey et al [157]. Copyright 2013 The Royal Society of Chemistry).

Jaiswal et al. [158] demonstrated the use of a composite including carboxylated graphene nanoflakes (c-GNF) and aminopropyltrimethoxysilane-functionalized zinc oxide nanorods (APTMS-ZnO) electrophoretically deposited onto the surface of an

ITO coated glass substrate. The developed APTMS-ZnO/c-GNF composite matrix, rich in amine groups, was deployed for the covalent attachment of amine-modified probe DNA for the detection of STEC O157:H7. The authors have successfully shown that the developed impedimetric genosensor exhibited a linear range from 10^{-16} to 10^{-6} M with an LOD of 10^{-16} M. The selectivity of the developed sensor was confirmed using overnight bacterial culture of *E. coli*, *Salmonella Typhimurium*, *Neisseria meningitides* and *Klebsiella pneumonia* achieving detection in around one hour and 15 minutes including the DNA extraction. Tiwari et al. [159] reported a modification of ITO-coated glass substrate with a combination of graphene oxide, gold nanoparticles, and pyrrole. This electrode was used as a matrix for covalent immobilization of amine-modified probe DNA to develop a genosensor for *E. coli*. The electrochemical response of the sensor was studied using methylene blue as a redox indicator. The authors demonstrated an LOD of $1x10^{-15}$ M and a linear range from $1x10^{-15}$ to $1x10^{-6}$ M using synthetic DNA target after only 60 s hybridisation. To validate the sensor's real-life application, it was incubated with the DNA extracted from *E. coli*, *K. pneumonia*, *Neisseria meningitides* and *S. typhimurium* showing a great selectivity in less than one hour, including the DNA extraction. In another study by Tiwari et al. [107], an ITO electrode was modified with a nanocomposite comprising chitosan, graphene oxide and nickel ferrite nanoparticles for the detection of 16s rDNA specific to general *E. coli.* The graphene oxide and nickel ferrite offered a high conductivity and less resistance to mass transfer while chitosan acted as an immobilisation matrix for probe DNA attachment. The detection was undertaken using MB as a redox-active molecule as well, and using the presented technique the authors showed a linear response between 10^{-16} and 10^{-6} M of synthetic DNA and an

LOD of 10^{-16} M. Similar to the previous study, the bacterial cultures were used to confirm the specificity of the sensor.

1.4.3.3. Carbon-based electrodes

Another commonly used material in the reviewed studies was carbon. Screen printed electrodes (SPE) are types of electrodes fabricated using different types of inks on various substrates such as plastics or ceramics. Their big advantage is a low cost and therefore, SPE is often used as disposable sensors [177]. Carbon is the most commonly used ink and it can be additionally altered with other metals, polymers or enzymes, depending on the application. For instance, Widaningrum et al. [160] immobilised a peptide nucleic acid (PNA) probe onto the SPCE by applying -0.5 V potential to the working electrode for 300 seconds. PNA is a synthetic polymer similar to DNA and RNA used as an alternative to oligonucleotides. It binds to the complementary DNA or RNA with high affinity and specificity resulting in more stable complexes compared to natural nucleic acids while being more resistant to high temperature, proteases, and nucleases [178, 179]. The authors detected a DNA sequence from *E. coli* using a sandwich assay with a reporter DNA tagged with latex spheres and biobarcode DNA, see Fig. 1.13. This barcode DNA was used to attract positively charged silver ions to its negatively charged phosphate groups and effectively, these silver ions, dissolved with nitric acid, were detected using DPV. Using the sandwich assay platform, the authors achieved a very low LOD of 5.6×10^{-19} M corresponding to 17 CFU/mL and good discrimination against *Salmonella* without the need for DNA amplification. The full assay, including DNA extraction, took less than 1.5 hours making it a promising method for POC testing.

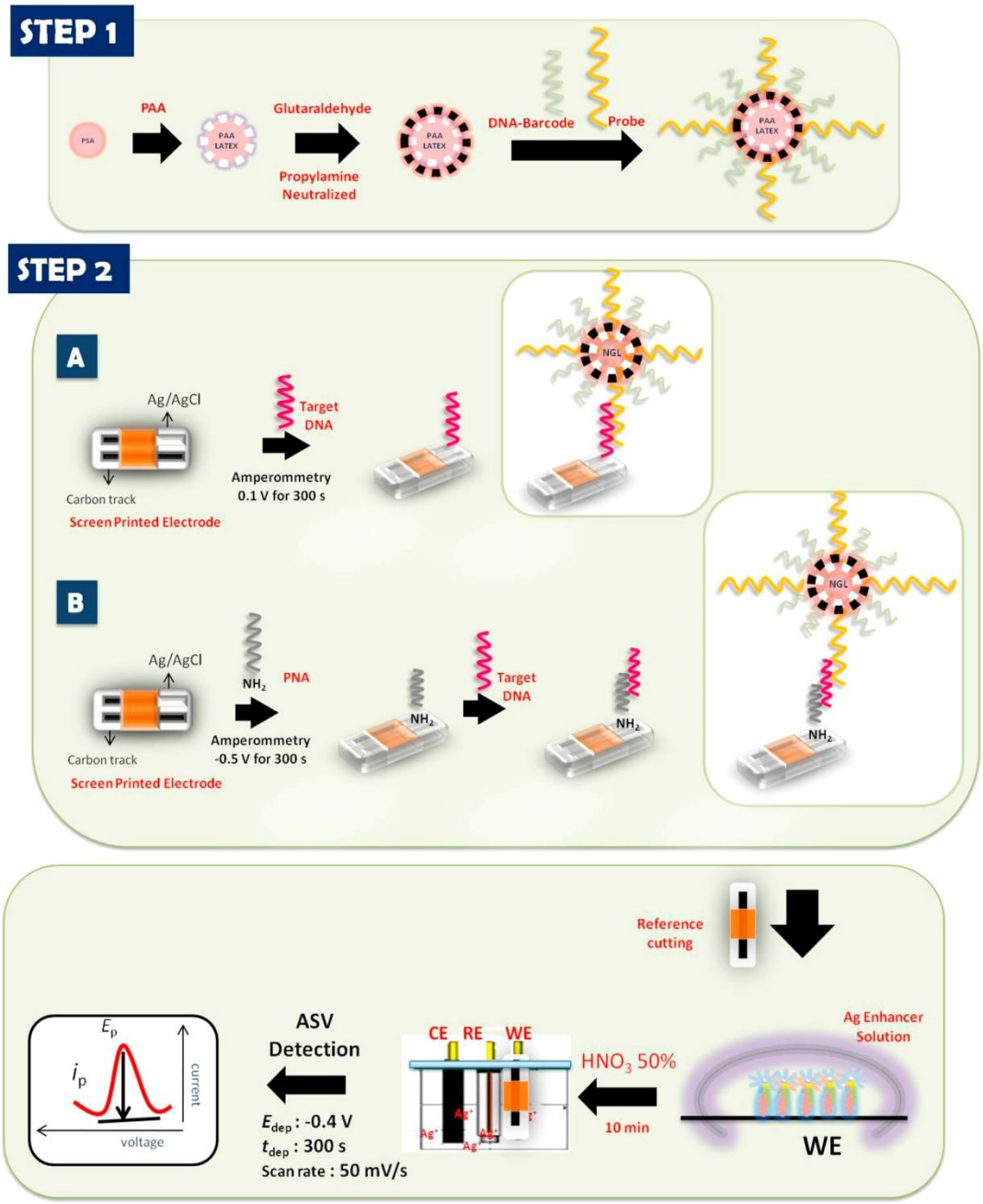

Fig. 1.13 Schematic representation of biobarcode construction (Step 1) followed by DNA assay using direct (Step 2 A) or sandwich (Step 2 B) hybridization. (Reprinted with permission from Widaningrum et al [160]. Copyright 2017 Elsevier B. V.).

Rabti et al. [180] developed a sensor for the detection of *E. coli* using carbon SPE modified with electrodeposited AuNPs and the thiol-modified probe DNA was immobilised using chemisorption. The hybridisation was detected after only 5 minutes using EIS to achieve an LOD of 10^{-15} M and using synthetic DNA. The method was

also validated using the genomic DNA and digested DNA using restriction enzymes extracted from *E. coli* strains isolated from camel calves. The sensor showed a good response after hybridisation treated and untreated DNA while DNA digestion added another 4 hours to otherwise less than one-hour long assay.

The SPCE could also be modified with different types of polymers, such as chitosan, for the attachment of the biomolecules. Kashish et al. [161] modified SPCE with chitosan and platinum NPs composite. The probe complementary to the *stx* gene was immobilised onto the electrode using absorption based on the negatively charged phosphate groups of the DNA being directly attracted by the positively charged groups of chitosan. The hybridization was detected using EIS with the charge increasing after DNA hybridisation. Using this technique, an LOD was 3.6×10^{-14} M was achieved using a synthetic target. The sensor's validation was done using different concentrations of PCR amplified target DNA dispersed in surface water and a buffer. The full assay was estimated to be around two hours, however, the DNA extraction time was not mentioned. Similar results obtained in both matrixes suggest that the surface water did not affect the sensor's specificity, however, PCR amplification was required.

Hollow silica is a type of inorganic material that has attracted attention for sensor development due to its large surface, good biocompatibility, and thermal stability. In the work of Ariffin et al. [112] an SPCE was modified with AuNPs and hollow silica spheres rich in amine groups. They were used as a base for immobilization of amine-modified probe DNA for detection of *E. coli* using glutaraldehyde as a linker. Hybridization was detected with DPV using anthraquinone-2-sulfonic acid monohydrate salt (AQMS), a redox-active molecule that intercalates between dsDNA. The developed sensor achieved a very low LOD of 8.17×10^{-20} M using synthetic strand

and was validated using real water samples. Without the need for DNA amplification, the results confirmed with culture methods were obtained in around 1.5 hours. Ariffin et al. [162] also used the hollow silica microspheres to modify the SPCE for the detection of *E. coli*. In this work, EIS instead of DPV was used for the measurements and an LOD was further decreased to $1.95x10^{-21}$ M with a synthetic strand. Finally, tests in river water, similar to the previous work were undertaken and the results were obtained in 1.5 hours.

A glassy carbon electrode (GCE) is fabricated by controlled pyrolysis of selected polymer resins. It combines ceramic and glassy characteristics next to the ones of graphite. Li et al. [121] used GCE modified with a layer of graphene oxide and AuNPs for the immobilisation of thiol-modified probe DNA complementary to the *eae* gene. The detection was done using a "sandwich" assay utilizing a hemin/G-quadruplex, an HRP-mimicking enzyme. In brief, the reporter probe labelled with HRP-mimicking enzyme was attached to the specially developed nanocomposite comprising graphene oxide (GOx), thionine (THI), and AuNPs coated silicon oxide ($Au@SiO_2$); see Fig. 1.14, employed for signal amplification. The target DNA was detected using DPV and an LOD of $1x10^{-11}$ M using synthetic DNA was achieved in less than two hours. The sensor was validated using synthetic stool samples spiked with known amounts of synthetic DNA showing recovery between 95% and 104.8%. The real bacterial samples were, however, not used in this study. Abdalhai et al. [163] tagged the reported DNA with cadmium sulphide nanoparticles (CdSNPs). The target DNA hybridised to the probe DNA with one side while the other side could hybridise with the reported DNA. The CdSNPs were subsequently oxidised using nitric acid into cadmium ions that were consequently detected using DPV with a GCE modified with MWCNT, chitosan and bismuth. The authors achieved an LOD of 1.97×10^{-14} M

using PCR amplified target DNA of *E. coli* O157:H7. The whole assay, including DNA extraction, PCR and detection took around four hours which was relatively long compared to the other assays.

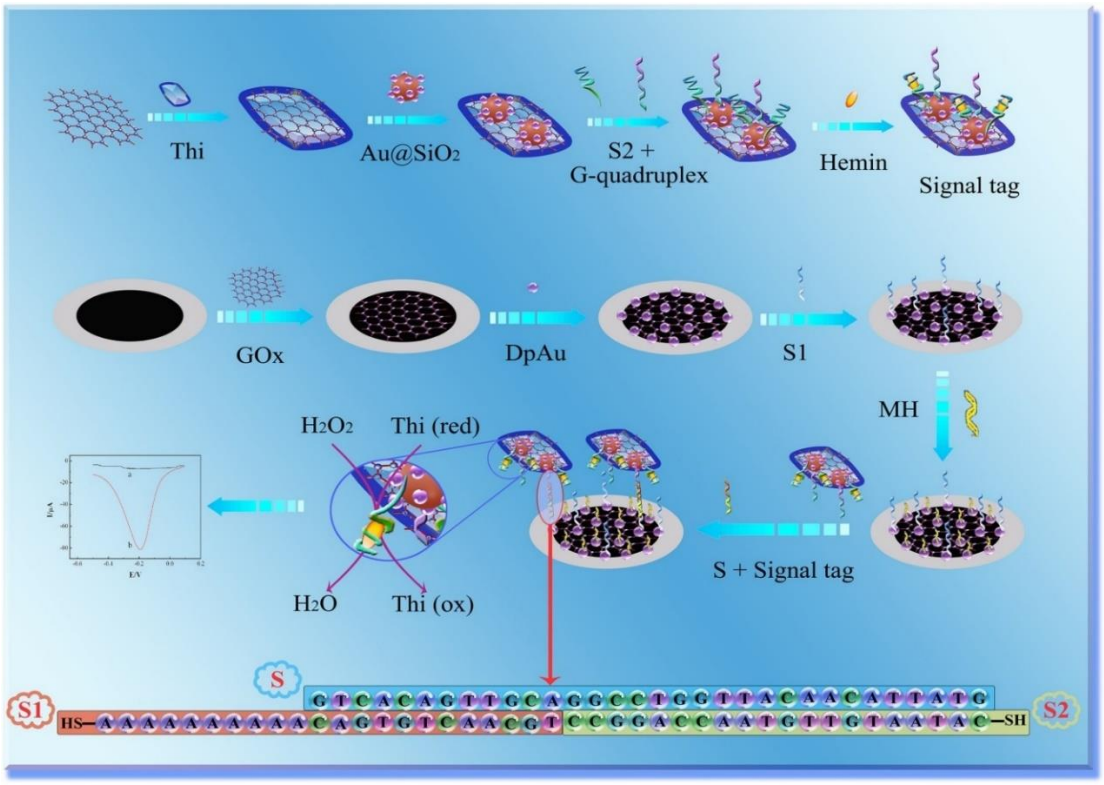

Fig. 1.14 Schematic diagram of the preparation of GOx–Thi–Au@SiO2 nanocomposites and fabrication and detection of the DNA sensor (Reprinted with permission from Li et al. [121] Copyright 2014 Elsevier B.V.).

The sensor developed by Ozkan-Ariksoysal et al. [106] involved wrapping the DNA probe around the multi-wall carbon nanotubes (MWCNTs) and their attachment to the pencil graphite electrode (PGE) facilitated with chitosan. The detection was undertaken using the guanine oxidation signal around 1 V studied by DPV. In this work, PCR amplified DNA strands from *E. coli* and other bacteria were used to confirm the sensor's selectivity. An LOD of only 1.7×10^{-8} M was achieved, with the whole assay taking less than three hours, including DNA extraction and PCR amplification.

1.4.3.4. Magnetic particles

Magnetic particles (MPs), in sizes ranging from nano to micro, have gained much attention in the development of sensors due to their physical properties. Their high surface area allows the immobilisation of the biorecognition molecules at a high density, limiting the background noise. In addition, they allow for sample enrichment and separation under the magnetic field, making them a perfect candidate for rapidly detecting low numbers of pathogens in complex samples [181]. They can be either integrated into the transducer or dispersed in the sample and subsequently get attracted using the magnetic field onto the electrode surface [182]. A "sandwich" method for the detection of *E. coli*, based on magnetic NPs was developed by Li et al. [165]. In their work, the NPs comprised of iron oxide coated with gold (Fe_2O_3@Au). The thiol-modified capture probe was attached to the NPs followed by hybridization of the complementary target DNA, with the reporter strand labelled with HRP. The magnetic nanoparticles were separated from the solution using a magnet and resuspended in citrate-phosphate buffer mixed with H_2O_2 and TMB. The enzyme reduced H_2O_2 and the current was recorded with amperometry, similar to the previously described procedure by Wen et al. [151]. Using the magnetic NPs, the authors have shown an LOD of $1x10^{-13}$ M using synthetic DNA strand and 500 CFU/mL using bacterial culture, without the need for nucleic acid amplification step in less than two hours, including DNA extraction. In addition, if the hybridization time was increased to 4 hours (instead of 40 minutes), the LOD was further decreased to 5 CFU/mL. This, however, increased the length of the full assay to around 5 hours. The developed sensor was applied to the detection of *E. coli* in river water and 100 CFU/mL were detected in around four hours. Zhang et al. [164] developed a dual DNA walkers strategy for the detection of STEC O157. A DNA walker is defined as a type of nucleic

acid nanomachines able to move along a well-designed track comprised of DNA building blocks. They are synthesised to mimic the natural DNA walkers like myosin, dynein or kinesin [183]. Fig. 1.15 presented the scheme summarising steps of the development of the sensor. First, hybridisation of target DNA was done using magnetic beads and the detection was subsequently done at the gold-modified electrodes using DPV. The authors were able to detect synthetic DNA in a range of $3x10^{-17}$ M and $3x10^{-10}$ M in three hours using synthetic DNA. To confirm the applicability of the developed sensor in the agri-food chain, the sensor was used in peach juice and milk samples. The food samples were inoculated with synthetic DNA to a final concentration of 0.3 nM and similar results were shown to the ones obtained with PBS buffer. The real bacterial samples were, however, not used indicating that the whole assay time would be longer than three hours if DNA extraction/amplification time was included.

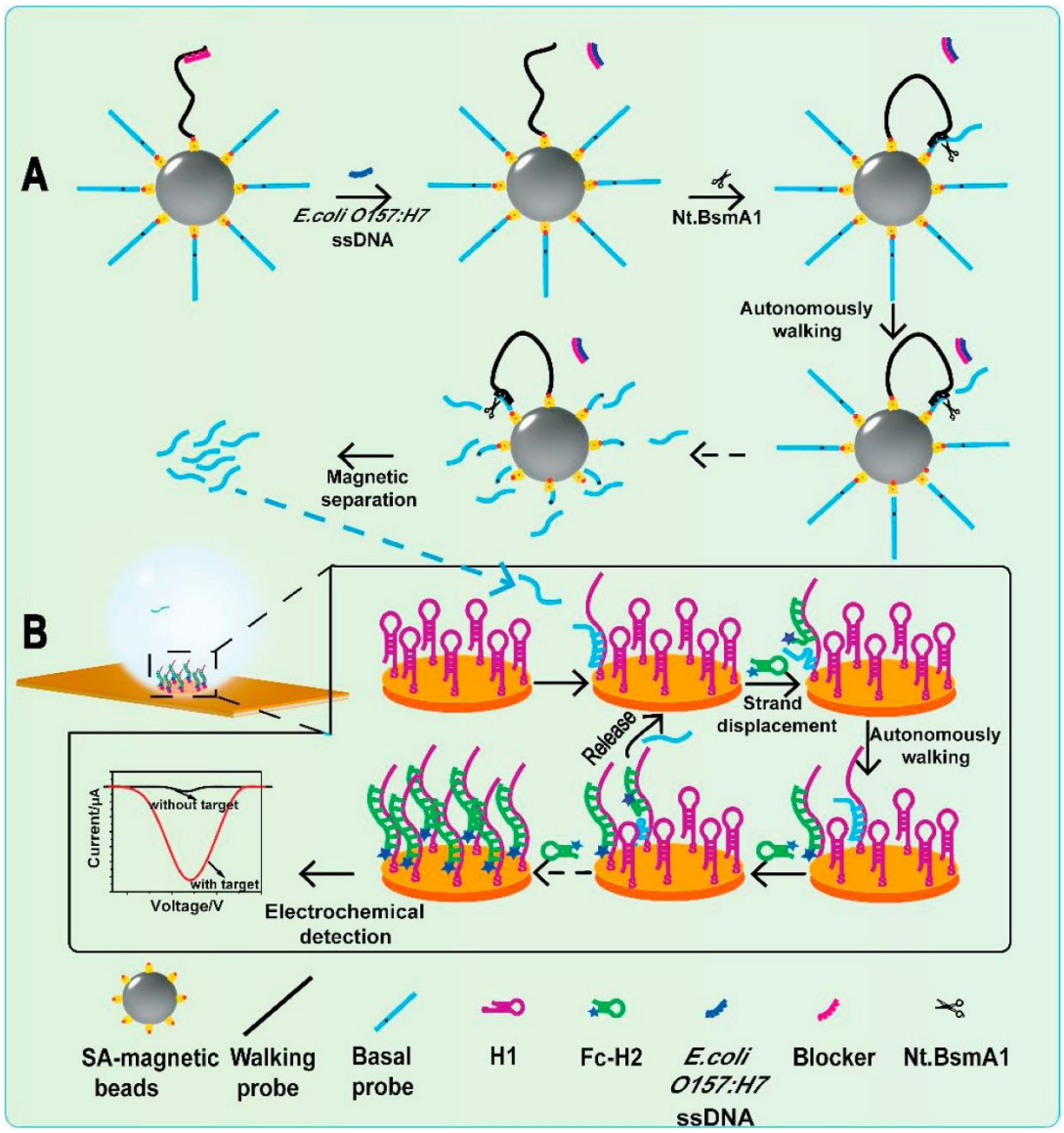

Fig. 1.15 Schematic illustration of the superwettable electrochemical sensor based on a dual-DNA walker strategy for sensitive DNA detection (Reprinted with permission from [164]. Copyright 2020 Elsevier B.V.).

Magnetic microparticles (MMPs) were also employed in the work of [119] who developed a genosensor for the detection of the *stx*1 gene from STEC without the need for PCR amplification. In parallel to electrochemical detection, three optical methods based on different fluorescent dyes were presented and compared. The electrochemical detection was based on a "sandwich assay" in which the probe DNA was attached to the MMPs via amide bond and the reporter probe was tagged with

AuNPs. After hybridization with the target DNA and the reporter DNA, the MMPs are separated from the solution and transferred onto the screen-printed carbon electrode (SPCE) where the AuNPs are dissolved with hydrochloric acid and the gold ions were electrochemically detected using DPV. The electrochemical method outperformed the fluorescent method achieving a limit of detection of 5 CFU/mL, compared to $5x10^4$ CFU/mL achieved by the most sensitive of fluorescent methods. The full assay, including DNA extraction from bacterial cultures, took around four hours. Geng et al. [115] used alginic-coated cobalt magnetic beads for the detection of *E. coli* in water, see Fig. 1.16. First, the amine-modified probe DNA was attached to the magnetic beads via an amide bond. Afterwards, the modified beads were incubated with the target DNA and separated using a magnet. The hybridization was detected using daunomycin, a redox-active molecule typically used as an anti-cancer drug, which intercalates between double-stranded DNA. The DPV signal from the molecule decreased with an increased concentration of target DNA due to slower diffusion of the trapped molecule to the electrode. The authors reported LOD using synthetic DNA strands, PCR amplicons as well as chromosomal DNA extracted directly from *E. coli* cells that was $3x10^{-10}$ M, 0.5 ng/µL and 50 CFU/mL, respectively. The whole assay using bacterial cells without the amplification was done in less than 2 hours.

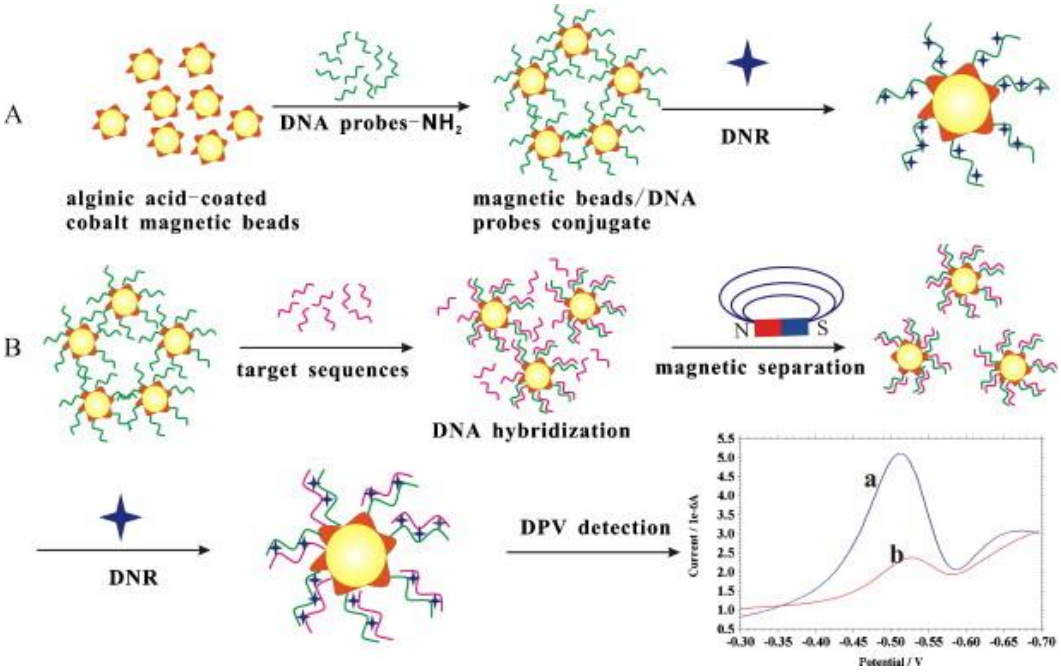

Fig. 1.16 Schematic representation of DNA hybridization detection based on the electrochemical sensor (Reprinted with permission from Geng et al. [115]. Copyright 2011 Elsevier B.V.).

Ben Aissa et al. [120] have compared two techniques, electrochemical and lateral flow, for the detection of *E. coli* and *Salmonella*. The electrochemical detection began with amplification of specific genes for both pathogens using quadruple PCR where the amplicons were simultaneously tagged with biotin (BIO) for the attachment and fluorescein (FLU) or digoxigenin (DIG) for the detection. Subsequently, the modified PCR amplicons were immobilised to streptavidin-magnetic particles using the biotin modification while FLU/DIG modification was used for specific attachment of HRP tagged reporter antibodies. The complexes were later separated using a magnet and detection was done using amperometry in the presence of H_2O_2 and hydroquinone. Using electrochemical detection, the authors achieved a limit of detection of 5.9×10^{-12} M using PCR amplicons in less than four hours including the DNA extraction and amplification. The electrochemical technique was shown to be much more sensitive compared to lateral flow detection. Brandão et al. [166] and Liébana et al. [167] used

silica magnetic particles and the magneto electrode (m-GEC) for the detection of the three most common food-borne pathogens, including STEC. The first step of the method was PCR amplification of target genes using one primer from the set tagged with a label, which was digoxigenin for STEC. The tagged amplicons were afterwards immobilised on the magnetic particles through electrostatic forces and hydrogen bond formation and labelled with HRP enzyme using HRP tagged antibodies. Subsequently, the magnetic particles were captured using m-GEC electrodes and amperometric detection was performed. Using this method, Brandão et al. [166] and Liébana et al. [167] detected $2.6x10^{-9}$ M and $5x10^{-10}$ M of PCR amplified target, respectively, in around three hours including all steps.

Another approach was used in the work of Kim et al. [168] where cerium oxide NPs (CeO_2NPs), instead of magnetic particles, were used to develop a simple assay without the need for probe immobilisation shown in Fig. 1.17. The CeO_2NPs are known to catalyse the oxidation reaction very quickly and were used to oxidise TMB in this work. The oxidised TMB would be further reduced at the gold electrode using DPV generating a high current of around 0.47 V. The target DNA, if present, is adsorbed to the surface of CeO_2NPs because of the electrostatic interaction causing their aggregation. In addition, the DNA interacted with positively charged oxidised TMB. As a result of these interactions, the electron transfer and therefore the cathodic current was significantly lower if the target DNA was present in the sample. The authors achieved an LOD of $2x10^{-8}$ M using this technique which suggests that the sensor is not very sensitive compared to the other studies. Another disadvantage is a lack of specificity of the methods if a complex sample and no PCR amplification was used. The estimated time for the full assay is less than 2 hours, with the detection around 6 minutes, one hour for PCR amplification and the DNA extraction time was not stated.

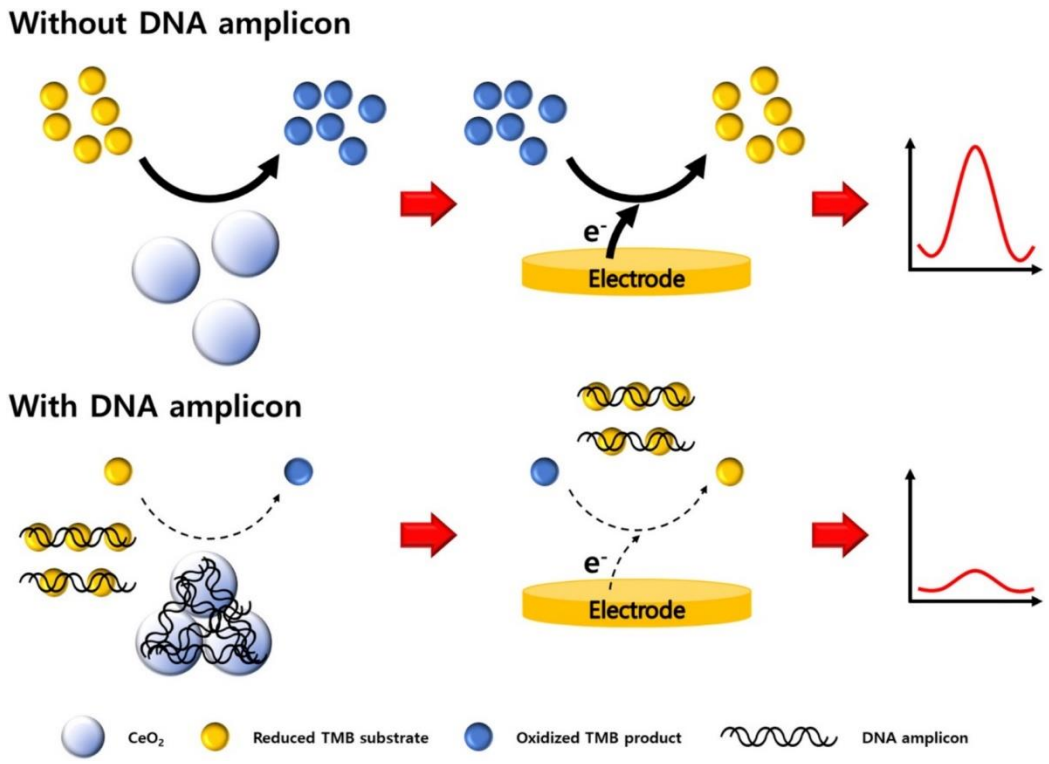

Fig. 1.17 Schematic illustration of the label-free, electrochemical DNA detection based on the target-induced inhibition against the oxidase-mimicking activity of CeO2 (Reprinted with permission from Kim et al [168]. Copyright 2018 Elsevier B. V.).

In summary, several electrochemical DNA-based sensors for the detection of general *E. coli* and STEC were developed since 2010. The authors typically applied gold, ITO or carbon electrodes or magnetic nanoparticles with gold electrodes found to be the most commonly used. This could be due to their high conductivity as well as an easy to immobilise thiols modified probe DNA. They can be either unmodified or modified with a mix of polymers and nanomaterials. Carbon-based electrodes were also a popular choice which was found to achieve the highest limit of detection among the collected literature. The magnetic nano/microparticles-based sensing methods did not achieve as low limits of detection compared to the solid state sensors and typically required more steps and therefore longer time-to-results. They may find a great application when working with high volume, complex samples common in the agri-food industry. However, they would need to be tested in higher volume samples that

were typically only between 100 and 200 µL in the collected literature. Finally, the ITO-based sensors also achieved good limits of detection, although they typically required complex and laborious modifications which limit their use in point-of-use detection.

This selection highlighted how crucial the selection of electrode material, electrode modification, as well as detection technique, is for the sensitivity and selectivity of the developed sensor. The proof-of-concept is usually done with synthetic DNA strands, but the real-life application should be done with real bacterial samples. The following section is going to summarise the approach for testing DNA sensors with real samples.

1.4.4. Application of nucleic acid-based sensors in naturally contaminated samples

A considerable challenge in the development of DNA sensors is proving their ability to perform robustly with naturally contaminated samples with adequate specificity and limit of detection. The following section will explore the state of the art on how the confirmation of field application for different *E. coli* detection sensors were carried out. As a proof-of-concept, synthetic DNA is usually employed in the development phase. Typically, the results with a complementary strand, a strand with few mismatched nucleotides (up to three) and a non-complementary have been reported. However, this does not reflect the potential performance of the sensor to work in very complex matrixes such as samples from the agri-food chain including food products or environmental samples. Other authors have proven the sensor works using chromosomal DNA [76]. Typically, after the DNA extraction, the DNA is denatured at a high temperature and rapidly cooled down. In addition, the DNA can be broken into smaller fragments using sonication.

The challenges associated with naturally contaminated samples compared to the laboratory environment include a low number of cells and available target DNA, interference from DNA from other cells, and the food or sample matrix. Common ways to increase the amount of target DNA is to either use enrichment to increase the number of target bacterial cells in the sample or to use PCR and multiply the target gene after DNA extraction from the bacterial culture [113, 120] or real samples [106, 118]. These steps, however, require a professional laboratory and cannot be performed for example on a farm.

Another limitation in using nucleic acid-based sensors is the need for DNA extraction. It is usually made in laboratories by highly trained personnel. Being able to do the whole detection for example at the farm, we need quick and easy methods which could be performed by anyone with minimal training. The miniaturisation of the electrochemical cell onto a single chip and integration with the microfluidics is gaining a lot of attention recently since such devices may provide a simple detection platform for target analyte or multiplexed detection of the species with very small sample applications [184]. Combining such sensing platforms with necessary electronics for the development of an automated device is the overall aim to allow on-site detection. Microfluidic chips can be designed to couple with several functions for high-throughput and automated analysis of bacterial targets.

Another limitation in the detection based on nucleic acids is a low number of target genes in a complex sample and therefore a need for amplification. PCR and real-time PCR are the most commonly used technique, however, it requires high-precision thermal cycler equipment and reagents that can be expensive and require laboratory settings. Recently, a portable PCR has been introduced which is a cheaper version of PCR that can be performed outside of the laboratory, the issues related to non-specific

amplifications if contaminated, likely for the application outside of the sterile laboratory conditions, may however remain [185, 186]. Therefore its application in point-of-use detection is limited. The alternative that gets a lot of attention in recent years is the use of isothermal amplification techniques such as loop-mediated isothermal amplification (LAMP), recombinase polymerase amplification (RPA), and helicase dependent amplification (HAD), or rolling circle amplification (RCA) [186]. The isothermal amplification methods use enzymatic DNA denaturation instead of high temperature like in PCR. Therefore, a simple device which can hold a constant temperature is sufficient for primer annealing and extension, instead of a sophisticated thermal cycler [187]. Especially LAMP found wide applications in molecular diagnostics because of its high efficacy and specificity while offering a simple and quick amplification method under isothermal conditions [188-190]. It has been developed by Notomi et al. [185] who showed in their work that this method can create up to 10^9 copies of target DNA in less than an hour and is less prone to non-specific amplification compared to PCR.

1.5. Conclusions

E. coli are a group of bacteria with high significance in food safety and a lot of effort is placed on the development of rapid methods for its point-of-use detection that could be applied on the farm or in the food industry. There are both, pathogenic and non-pathogenic *E. coli* and since the outbreak in 2011 in Germany with STEC, researchers have pointed out that DNA-based detection is most suitable to distinguish the pathogenic strains. Electrochemical DNA sensors have received considerable attention in pathogens detection due to their simplicity of use, relatively low cost, and suitability for miniaturisation. Several DNA sensors for the detection of generic *E. coli* and STEC have been developed to date.

Selecting the right target gene sequence is the first step to consider when developing a nucleic acid-based sensor. It is especially crucial for STEC detection to selectively distinguish the pathogenic strains from the non-pathogenic ones. For general *E. coli*, usually, 16s rRNA is most often used since it contains valuable information for distinguishing the species. Alternatively, a gene *uid*A gene responsible for the ß-glucuronidase enzyme is used. Specific detection of STEC is however more complicated. Several researchers have focused on the gene coding for intimin production (*eae*A) however the most recent research is pointing towards targeting genes coding for toxin production (*stx1* or *stx2*) to screen for all strains which may be able to cause disease.

Another important factor to be considered when developing an electrochemical DNA sensor is the material of the electrode and its modification. In this chapter, we have explored different ways of designing the biosensor and it was shown that the most often used materials for attachment of DNA probe include gold, graphene oxide or

carbon, and chitosan. A combination of these materials with different nanoparticles, nanomaterials, or magnetic particles has shown excellent limits of detection reaching attomolar concentration. Device miniaturisation is another way to achieve a lower limit of detection due to a lower signal-to-noise ratio. Such devices have a chance as well to be integrated into fully automated devices in the future. Even though such low limits of detection are commonly achieved, the focus should be placed on the use of such devices in complex matrices.

Usually, the selectivity of a sensor is shown by using non-target or mismatched synthetic strands or chromosomal DNA extracted from target and non-target bacterial cultures. However, this doesn't show if the detection will be selective in a complex sample such as food or faeces, which is important for food safety applications. In traditional methods, typically an enrichment step or a PCR amplification would be introduced to increase the concentration of a target. Such a step is undesirable for point-of-use detection because it increases its complexity and requires highly trained personnel and laboratory equipment. This issue could be addressed with the development of fully integrated microfluidics devices incorporating DNA extraction and isothermal amplification such as LAMP.

1.6. Thesis scope

The main objective of the presented thesis was to develop electrochemical sensors for the detection of STEC using the silicon-based chips developed previously in the Nanotechnology group in Tyndall. To achieve this objective, the work comprised of three aims:

1. Develop a chemical sensor for the detection of silver ions in tap water using electrochemical pH control.

2. Develop surface chemistry for probe DNA attachment and electrochemical method for the detection of *stx1* gene from STEC.

3. Develop a multiplex sensor for the detection of *stx1* and *stx2* genes from STEC.

This is a publication-based thesis that was divided into five chapters. The first four chapters are prepared for publication and have either already been published or submitted for publication. The last, 5th chapter summarises the thesis and sets the future perspective for the work described.

Chapter 1 summarises the state of the art regarding all the relevant topics included in the thesis. First, the relevance of Shiga toxin-producing *E. coli* (STEC) is highlighted and the traditional methods for its detection are described. Subsequently, the need for the development of rapid detection methods is highlighted and how the electrochemical sensors could answer that need. Finally, the review summarising STEC virulence factors and DNA sensors for the detection of generic *E. coli* and STEC since 2010 are described. First, the sequences of the genes used as recognition probes were discussed and compared to the most recent research regarding *E. coli* detection and STEC virulence factors. Subsequently, different probe DNA attachment

techniques were described and the detection approaches were categorised based on the electrode's materials (gold, carbon), their modifications (chitosan, nanoparticles) and miniaturisation (micro/nanoelectrodes, micro/nano magnetic particles) and discussed. Finally, we have critically looked at the real samples application on developed biosensors including some examples of fully integrated devices for DNA detection including DNA extraction.

In Chapter 2 the development of an electrochemical sensor for silver ions detection in tap water using anodic sweep voltammetry with in-situ pH control was reported. This was an outcome of the original approach to detect the DNA using a reporter strand tagged with silver nanoparticles which would effectively get oxidised and the concentration of silver ions would be correlated to the concentration of target DNA in a sample. The in-situ pH control, enabled by closely spaced interdigitated electrode arrays (IDEs), allowed the pH of a test solution to be tailored to pH 3 (experimentally determined as the optimal pH). Using this approach, an initial proof-of-concept study for silver detection in sodium acetate was undertaken where 1.25 V was applied during deposition (to compensate for oxygen production) and 1.65 V during stripping. For the final application in tap water, 1.65 V was applied to a protonator electrode for both deposition and stripping of silver. The combination of the complexation of silver ions with chloride and in-situ pH control resulted in a linear calibration range between 0.25 and 2 μM in tap water and a calculated limit of detection of 106 nM without the need to add acid or supporting electrolytes. Even though the approach of using silver nanoparticles for DNA detection has been modified due to not satisfactory LOD achieved, the technique used in this chapter – square wave voltammetry, was later applied for the detection of DNA hybridisation in Chapters 3 and 4. In addition, the IDEs used in this chapter to generate the protons to modify the solution's pH were

applied in the following chapters for an accumulation of methylene blue, which was chosen as an alternative molecule for DNA detection.

In Chapter 3 we report the development of a highly sensitive, label-free, electrochemical DNA sensor for detection of the *stx1* gene using the IDEs on fully integrated silicon chips. Each IDE comprised a working IDE, used for DNA probe immobilisation and an accumulator IDE used for accumulation of methylene blue. First, the working IDE was modified with gold nanoparticles (AuNPs) and chitosan gold nanocomposite. Afterwards, amine-modified probe DNA was immobilised on the chitosan-modified electrode using glutaraldehyde as a linker. The label-free electrochemical detection was undertaken using methylene blue as a redox molecule that intercalated into the double-strand DNA after applying an open potential circuit at the generator IDEs. The reduction of methylene blue was recorded using SWV. Using this label-free detection, we have achieved a linear response between 10^{-16} and 10^{-6} M synthetic target strand with the lowest measured limit of detection of 10^{-16} M after 20 minutes of hybridisation time. The chromosomal DNA extracted from four different *E. coli* strains (two *stx1* positives and two *stx1* negatives), and two non-*E. coli* (*Listeria monocytogenes*, and *Bacillus cereus*) was used to confirm the selectivity of the presented method. This novel on-chip biosensor for the detection of VTEC has the potential to be used in point-of-use detection, for example, on the farm.

In Chapter 4 the conditions for surface modification developed in chapter 3 were re-optimised, the layer of AuNPs was increased and the chitosan was electrodeposited at a different potential. In addition, the second probe DNA was introduced and a multiplex sensor for the detection of *stx1* and *stx2* was developed. These modifications caused an improvement in sensitivity by three orders of magnitude and an LOD of 10^{-19} M was achieved. The chromosomal DNA extracted from bacterial cultures was

tested on this multiplex sensor, demonstrating its ability for selective detection of two main virulence genes on a single chip. This highly sensitive sensor for the detection of multiple genes is a stepping stone for the development of a point-of-use device for STEC detection on the farm or in the food industry.

The electrochemical sensors offer a huge advantage over the traditional techniques used for pathogens detection. This work presents the advances in the development of chemical sensors and biosensors using DNA as a biorecognition element. Chapter 5 summarises the key findings and presents the perspective for the future to improve such devices offering the possibility to use them in point-of-use settings.

1.7. References

1. N.A. Campbell and J.B. Reece, *Biology: International Edition*. 2002, San Fransisco, Boston New York: Pearson Education, Inc, publishing as ….
2. X. Hai, Y. Li, C. Zhu, W. Song, J. Cao, and S. Bi, *DNA-based label-free electrochemical biosensors: from principles to applications.* TrAC Trends in Analytical Chemistry, 2020: p. 116098.
3. W.H. Organization, *WHO estimates of the global burden of foodborne diseases: foodborne disease burden epidemiology reference group 2007-2015*. 2015: World Health Organization.
4. EFSA and ECDC, *The European Union One Health 2018 Zoonoses Report.* EFSA Journal, 2019. **17**(12): p. e05926.
5. A. Clements, J.C. Young, N. Constantinou, and G. Frankel, *Infection strategies of enteric pathogenic Escherichia coli.* Gut microbes, 2012. **3**(2): p. 71-87.
6. K.A. Bettelheim, *The non-O157 Shiga-toxigenic (verocytotoxigenic) Escherichia coli; under-rated pathogens.* Critical reviews in microbiology, 2007. **33**(1): p. 67-87.
7. WHO. *E. coli key facts.* 2018 7.02.2018 [cited 2020 02.03]; Available from: https://www.who.int/news-room/fact-sheets/detail/e-coli.
8. J.Y. Lim, J.W. Yoon, and C.J. Hovde, *A brief overview of Escherichia coli O157: H7 and its plasmid O157.* Journal of microbiology and biotechnology, 2010. **20**(1): p. 5.
9. E. De Boer and A.E. Heuvelink, *Foods as vehicles of VTEC infection.* Verocytotoxigenic *E. coli*, 2001: p. 181-200.
10. G. Willshaw, J. Thirlwell, A. Jones, S. Parry, R. Salmon, and M. Hickey, *Vero cytotoxin-producing Escherichia coli O157 in beefburgers linked to an outbreak*

of diarrhoea, haemorrhagic colitis and haemolytic uraemic syndrome in Britain. Letters in Applied Microbiology, 1994. **19**(5): p. 304-307.

11. A. Liptakova, L. Siegfried, J. Rosocha, L. Podracka, E. Bogyiova, and D. Kotulova, *A family outbreak of haemolytic uraemic syndrome and haemorrhagic colitis caused by verocytotoxigenic Escherichia coli O157 from unpasteurised cow's milk in Slovakia.* Clinical microbiology and infection, 2004. **10**(6): p. 576-578.
12. D.L. Woodward, C.G. Clark, R.A. Caldeira, R. Ahmed, and F.G. Rodgers, *Verotoxigenic Escherichia coli (VTEC): a major public health threat in Canada.* Canadian Journal of Infectious Diseases and Medical Microbiology, 2002. **13**(5): p. 321-330.
13. L.A. King, F. Nogareda, F.-X. Weill, P. Mariani-Kurkdjian, E. Loukiadis, G. Gault, et al., *Outbreak of Shiga toxin–producing Escherichia coli O104: H4 associated with organic fenugreek sprouts, France, June 2011.* Clinical Infectious Diseases, 2012. **54**(11): p. 1588-1594.
14. J. Blanco, M. Blanco, J.E. Blanco, A. Mora, M.P. Alonso, E.A. Gonzalez, et al., *Epidemiology of verocytotoxigenic Escherichia coli (VTEC) in ruminants.* Verocytotoxigenic Escherichia coli, 2001: p. 113-148.
15. S.W. Naylor, D.L. Gally, and J.C. Low, *Enterohaemorrhagic E. coli in veterinary medicine.* International journal of medical microbiology, 2005. **295**(6-7): p. 419-441.
16. J. Wells, B. Davis, I. Wachsmuth, L. Riley, R. Remis, R. Sokolow, et al., *Laboratory investigation of hemorrhagic colitis outbreaks associated with a rare Escherichia coli serotype.* Journal of clinical microbiology, 1983. **18**(3): p. 512-520.

17. R. Burger, *EHEC O104: H4 in Germany 2011: Large outbreak of bloody diarrhea and haemolytic uraemic syndrome by shiga toxin-producing E. coli via contaminated food.* 2012.

18. H. Karch, E. Denamur, U. Dobrindt, B.B. Finlay, R. Hengge, L. Johannes, et al., *The enemy within us: lessons from the 2011 European Escherichia coli O104: H4 outbreak.* EMBO molecular medicine, 2012. **4**(9): p. 841-848.

19. H. Pennington, *Escherichia coli O157.* The Lancet, 2010. **376**(9750): p. 1428-1435.

20. M.A. Karmali, M. Mascarenhas, S. Shen, K. Ziebell, S. Johnson, R. Reid-Smith, et al., *Association of genomic O island 122 of Escherichia coli EDL 933 with verocytotoxin-producing Escherichia coli seropathotypes that are linked to epidemic and/or serious disease.* Journal of clinical microbiology, 2003. **41**(11): p. 4930-4940.

21. EFSA Panel on Biological Hazards, *Scientific Opinion on VTEC-seropathotype and scientific criteria regarding pathogenicity assessment.* EFSA Journal, 2013. **11**(4): p. 3138.

22. B. Soborg, S. Lassen, L. Muller, T. Jensen, S. Ethelberg, K. Mølbak, et al., *A verocytotoxin-producing E. coli outbreak with a surprisingly high risk of haemolytic uraemic syndrome, Denmark, September-October 2012.* Eurosurveillance, 2013. **18**(2): p. 20350.

23. EFSA Panel on Biological Hazards, *Pathogenicity assessment of Shiga toxin-producing Escherichia coli (STEC) and the public health risk posed by contamination of food with STEC.* EFSA Journal, 2020. **18**(1): p. e05967.

24. J.W.-F. Law, N.-S. Ab Mutalib, K.-G. Chan, and L.-H. Lee, *Rapid methods for the detection of foodborne bacterial pathogens: principles, applications, advantages and limitations.* Frontiers in microbiology, 2015. **5**: p. 770.

25. L. Zeng, L. Wang, and J. Hu, *Current and Emerging Technologies for Rapid Detection of Pathogens.* Biosensing Technologies for the Detection of Pathogens: A Prospective Way for Rapid Analysis, 2018: p. 5.

26. C.A. Baker, P.M. Rubinelli, S.H. Park, and S.C. Ricke, *Immuno-based detection of Shiga toxin-producing pathogenic Escherichia coli in food–A review on current approaches and potential strategies for optimization.* Critical reviews in microbiology, 2016. **42**(4): p. 656-675.

27. L. Váradi, J.L. Luo, D.E. Hibbs, J.D. Perry, R.J. Anderson, S. Orenga, et al., *Methods for the detection and identification of pathogenic bacteria: past, present, and future.* Chemical Society Reviews, 2017. **46**(16): p. 4818-4832.

28. S. Edberg, E. Rice, R. Karlin, and M. Allen, *Escherichia coli: the best biological drinking water indicator for public health protection.* Journal of applied microbiology, 2000. **88**(S1): p. 106S-116S.

29. FSAI, *Advice on Shiga toxin-producing Escherichia coli (STEC) detection in food*, 2019, https://www.fsai.ie/publications/STEC_Report/

30. P. Fratamico, A. Gehring, J. Karns, and J. van Kessel, *Detecting pathogens in cattle and meat*, in *Improving the Safety of Fresh Meat*. 2005, Elsevier. p. 24-55.

31. M. Nurliyana, M. Sahdan, K. Wibowo, A. Muslihati, H. Saim, S. Ahmad, et al. *The detection method of Escherichia coli in water resources: A review*. in *Journal of Physics: Conference Series*. 2018. IOP Publishing.

32. J. Farmer and B.R. Davis, *H7 antiserum-sorbitol fermentation medium: a single tube screening medium for detecting Escherichia coli O157: H7 associated with hemorrhagic colitis.* Journal of Clinical Microbiology, 1985. **22**(4): p. 620-625.

33. S.B. March and S. Ratnam, *Sorbitol-MacConkey medium for detection of Escherichia coli O157: H7 associated with hemorrhagic colitis.* Journal of clinical microbiology, 1986. **23**(5): p. 869-872.

34. A. Ammon, L.R. Petersen, and H. Karch, *A Large Outbreak of Hemolytic Uremic Syndrome Caused by an Unusual Sorbitol-Fermenting Strain of Escherichia coli O157: H—.* The Journal of infectious diseases, 1999. **179**(5): p. 1274-1277.

35. B. Possé, L. De Zutter, M. Heyndrickx, and L. Herman, *Novel differential and confirmation plating media for Shiga toxin-producing Escherichia coli serotypes O26, O103, O111, O145 and sorbitol-positive and-negative O157.* FEMS microbiology letters, 2008. **282**(1): p. 124-131.

36. N. Kalchayanand, T.M. Arthur, J.M. Bosilevac, J.E. Wells, and T.L. Wheeler, *Chromogenic agar medium for detection and isolation of Escherichia coli serogroups O26, O45, O103, O111, O121, and O145 from fresh beef and cattle feces.* Journal of food protection, 2013. **76**(2): p. 192-199.

37. I.A. Darwish, *Immunoassay methods and their applications in pharmaceutical analysis: basic methodology and recent advances.* International journal of biomedical science: IJBS, 2006. **2**(3): p. 217.

38. R.L. Atmar, *Immunological detection and characterization*, in *Viral Infections of Humans*. 2014, Springer. p. 47-62.

39. R. Kfir and B. Genthe, *Advantages and disadvantages of the use of immunodetection techniques for the enumeration of microorganisms and toxins in water*. Water Science and Technology, 1993. **27**(3-4): p. 243-252.

40. M. Cavaiuolo, S. Paramithiotis, E.H. Drosinos, and A. Ferrante, *Development and optimization of an ELISA based method to detect Listeria monocytogenes and Escherichia coli O157 in fresh vegetables.* Analytical Methods, 2013. **5**(18): p. 4622-4627.

41. J. Willford, K. Mills, and L.D. Goodridge, *Evaluation of three commercially available enzyme-linked immunosorbent assay kits for detection of Shiga toxin.* Journal of food protection, 2009. **72**(4): p. 741-747.

42. C.-M. Shih, C.-L. Chang, M.-Y. Hsu, J.-Y. Lin, C.-M. Kuan, H.-K. Wang, et al., *Paper-based ELISA to rapidly detect Escherichia coli.* Talanta, 2015. **145**: p. 2-5.

43. R.P. Johnson, R.J. Durham, S.T. Johnson, L.A. Macdonald, S.R. Jeffrey, and B.T. Butman, *Detection of Escherichia coli O157: H7 in meat by an enzyme-linked immunosorbent assay, EHEC-Tek.* Appl. Environ. Microbiol., 1995. **61**(1): p. 386-388.

44. D. Wright, P. Chapman, and C. Siddons, *Immunomagnetic separation as a sensitive method for isolating Escherichia coli O157 from food samples.* Epidemiology & Infection, 1994. **113**(1): p. 31-39.

45. J.M. Bartlett and D. Stirling, *A short history of the polymerase chain reaction*, in *PCR protocols*. 2003, Springer. p. 3-6.

46. G. Schochetman, C.-Y. Ou, and W.K. Jones, *Polymerase chain reaction.* The Journal of infectious diseases, 1988. **158**(6): p. 1154-1157.

47. L. Garibyan and N. Avashia, *Research techniques made simple: polymerase chain reaction (PCR).* The Journal of investigative dermatology, 2013. **133**(3): p. e6.

48. R.A. Masake, P.A. Majiwa, S.K. Moloo, J.M. Makau, J.T. Njuguna, M. Maina, et al., *Sensitive and Specific Detection ofTrypanosoma vivaxUsing the Polymerase Chain Reaction.* Experimental parasitology, 1997. **85**(2): p. 193-205.

49. M.T. Rahman, M.S. Uddin, R. Sultana, A. Moue, and M. Setu, *Polymerase chain reaction (PCR): a short review.* Anwer Khan Modern Medical College Journal, 2013. **4**(1): p. 30-36.

50. M.C. Edwards and R.A. Gibbs, *Multiplex PCR: advantages, development, and applications.* Genome Research, 1994. **3**(4): p. S65-S75.

51. P. Markoulatos, N. Siafakas, and M. Moncany, *Multiplex polymerase chain reaction: a practical approach.* Journal of clinical laboratory analysis, 2002. **16**(1): p. 47-51.

52. M. Ricchi, C. Bertasio, M.B. Boniotti, N. Vicari, S. Russo, M. Tilola, et al., *Comparison among the quantification of bacterial pathogens by qPCR, dPCR, and cultural methods.* Frontiers in microbiology, 2017. **8**: p. 1174.

53. N. Martínez, M.C. Martín, A. Herrero, M. Fernández, M.A. Alvarez, and V. Ladero, *qPCR as a powerful tool for microbial food spoilage quantification: Significance for food quality.* Trends in Food Science & Technology, 2011. **22**(7): p. 367-376.

54. R. Meyer, J. Lüthy, and U. Candrian, *Direct detection by polymerase chain reaction (PCR) of Escherichia coli in water and soft cheese and identification*

of enterotoxigenic strains. Letters in applied microbiology, 1991. **13**(6): p. 268-271.

55. R.F. Wang, W.W. Cao, and C. Cerniglia, *A universal protocol for PCR detection of 13 species of foodborne pathogens in foods.* Journal of applied microbiology, 1997. **83**(6): p. 727-736.

56. A.F. Maheux, F.J. Picard, M. Boissinot, L. Bissonnette, S. Paradis, and M.G. Bergeron, *Analytical comparison of nine PCR primer sets designed to detect the presence of Escherichia coli/Shigella in water samples.* Water research, 2009. **43**(12): p. 3019-3028.

57. D.I. Walker, J. McQuillan, M. Taiwo, R. Parks, C.A. Stenton, H. Morgan, et al., *A highly specific Escherichia coli qPCR and its comparison with existing methods for environmental waters.* Water research, 2017. **126**: p. 101-110.

58. J. Holland, L. Louie, A. Simor, and M. Louie, *PCR detection of Escherichia coli O157: H7 directly from stools: evaluation of commercial extraction methods for purifying fecal DNA.* Journal of clinical microbiology, 2000. **38**(11): p. 4108-4113.

59. G. Wang, C.G. Clark, and F.G. Rodgers, *Detection in Escherichia coli of the genes encoding the major virulence factors, the genes defining the O157: H7 serotype, and components of the type 2 Shiga toxin family by multiplex PCR.* Journal of clinical microbiology, 2002. **40**(10): p. 3613-3619.

60. A.W. Paton and J.C. Paton, *Direct detection and characterization of Shiga toxigenic Escherichia coli by multiplex PCR for stx1, stx2, eae, ehxA, and saa.* Journal of clinical microbiology, 2002. **40**(1): p. 271-274.

61. M. Louie, S. Read, A. Simor, J. Holland, L. Louie, K. Ziebell, et al., *Application of multiplex PCR for detection of non-O157 verocytotoxin-producing*

Escherichia coli in bloody stools: identification of serogroups O26 and O111. Journal of clinical microbiology, 1998. **36**(11): p. 3375-3377.

62. A.A. Bhagwat, *Simultaneous detection of Escherichia coli O157: H7, Listeria monocytogenes and Salmonella strains by real-time PCR.* International journal of food microbiology, 2003. **84**(2): p. 217-224.
63. E. Omiccioli, G. Amagliani, G. Brandi, and M. Magnani, *A new platform for Real-Time PCR detection of Salmonella spp., Listeria monocytogenes and Escherichia coli O157 in milk.* Food microbiology, 2009. **26**(6): p. 615-622.
64. C. Ferreri, F. Galati, L. Grande, A. Maugliani, V. Michelacci, F. Minelli, et al., *The proficiency testing program of the European Union Reference Laboratory for E. coli.* Accreditation and Quality Assurance, 2015. **20**(5): p. 381-385.
65. I.T. 13136:2012, *Microbiology of Food and Animal Feed-Real-time Polymerase Chain Reaction (PCR)-Based Method for the Detection of Food-borne Pathogens-Horizontal Method for the Detection of Shiga Toxin-producing Escherichia Coli (STEC) and the Determination of O157, O111, O26, O103 and O145 Serogroups*, 2012, ISO: https://www.iso.org/standard/53328.html
66. R. Tozzoli, A. Maugliani, V. Michelacci, F. Minelli, A. Caprioli, and S. Morabito, *Validation on milk and sprouts of EN ISO 16654: 2001-Microbiology of food and animal feeding stuffs-Horizontal method for the detection of Escherichia coli O157.* International journal of food microbiology, 2019. **288**: p. 53-57.
67. I. 16654:2001/Amd.1, *Microbiology of Food and Animal Feeding Stuffs — Horizontal Method for the Detection of Escherichia coli O157 AMENDMENT 1: Annex B: Result of Interlaboratory Studies*, 2017, https://www.iso.org/standard/64704.html

68. D.G. Buerk, *Biosensors: Theory and applications*. 2014: Crc Press.

69. Y. Wang, Z. Ye, and Y. Ying, *New trends in impedimetric biosensors for the detection of foodborne pathogenic bacteria.* Sensors, 2012. **12**(3): p. 3449-3471.

70. C.-Y. Yao and W.-L. Fu, *Biosensors for hepatitis B virus detection.* World Journal of Gastroenterology: WJG, 2014. **20**(35): p. 12485.

71. N. Verma and M. Singh, *Biosensors for heavy metals.* Biometals, 2005. **18**(2): p. 121-129.

72. R.C. Alves, M.F. Barroso, M.B. González-García, M.B.P. Oliveira, and C. Delerue-Matos, *New trends in food allergens detection: toward biosensing strategies.* Critical reviews in food science and nutrition, 2016. **56**(14): p. 2304-2319.

73. P. Mehrotra, *Biosensors and their applications–A review.* Journal of oral biology and craniofacial research, 2016. **6**(2): p. 153-159.

74. E.B. Aydın, M. Aydın, and M.K. Sezgintürk, *Electrochemical immunosensor based on chitosan/conductive carbon black composite modified disposable ITO electrode: An analytical platform for p53 detection.* Biosensors and Bioelectronics, 2018. **121**: p. 80-89.

75. E. Povedano, F.H. Cincotto, C. Parrado, P. Díez, A. Sánchez, T.C. Canevari, et al., *Decoration of reduced graphene oxide with rhodium nanoparticles for the design of a sensitive electrochemical enzyme biosensor for 17β-estradiol.* Biosensors and Bioelectronics, 2017. **89**: p. 343-351.

76. H.A.M. Faria and V. Zucolotto, *Label-free electrochemical DNA biosensor for zika virus identification.* Biosensors and Bioelectronics, 2019. **131**: p. 149-155.

77. Y. Li, Y. Bu, F. Jiang, X. Dai, and J.-P. Ao, *Fabrication of ultra-sensitive photoelectrochemical aptamer biosensor: Based on semiconductor/DNA*

interfacial multifunctional reconciliation via 2D-C3N4. Biosensors and Bioelectronics, 2020. **150**: p. 111903.

78. K. Nakama, M. Sedki, and A. Mulchandani, *Label-free chemiresistor biosensor based on reduced graphene oxide and M13 bacteriophage for detection of coliforms.* Analytica Chimica Acta, 2021. **1150**: p. 338232.
79. P. Damborský, J. Švitel, and J. Katrlík, *Optical biosensors.* Essays in biochemistry, 2016. **60**(1): p. 91-100.
80. E.O. Blair and D.K. Corrigan, *A review of microfabricated electrochemical biosensors for DNA detection.* Biosensors and Bioelectronics, 2019. **134**: p. 57-67.
81. G. Caluori, J. Pribyl, M. Pesl, S. Jelinkova, V. Rotrekl, P. Skladal, et al., *Non-invasive electromechanical cell-based biosensors for improved investigation of 3D cardiac models.* Biosensors and Bioelectronics, 2019. **124**: p. 129-135.
82. I. Seymour, B. O'Sullivan, P. Lovera, J.F. Rohan, and A. O'Riordan, *Electrochemical detection of free-chlorine in Water samples facilitated by in-situ pH control using interdigitated microelectrodes.* Sensors and Actuators B: Chemical, 2020. **325**: p. 128774.
83. R. Daly, T. Narayan, H. Shao, A. O'Riordan, and P. Lovera, *Platinum-Based Interdigitated Micro-Electrode Arrays for Reagent-Free Detection of Copper.* Sensors, 2021. **21**(10): p. 3544.
84. N. Gupta, S. Augustine, T. Narayan, A. O'Riordan, A. Das, D. Kumar, et al., *Point-of-Care PCR Assays for COVID-19 Detection.* Biosensors, 2021. **11**(5): p. 141.

85. C. Hwang, N. Park, E.S. Kim, M. Kim, S.D. Kim, S. Park, et al., *Ultra-fast and recyclable DNA biosensor for point-of-care detection of SARS-CoV-2 (COVID-19).* Biosensors and Bioelectronics, 2021. **185**: p. 113177.

86. K. Dawson, A.l. Wahl, R. Murphy, and A. O'Riordan, *Electroanalysis at single gold nanowire electrodes.* The Journal of Physical Chemistry C, 2012. **116**(27): p. 14665-14673.

87. A. Murphy, I. Seymour, J. Rohan, A. O'Riordan, and I. O'Connell, *Portable Data Acquisition System for Nano and Ultra-Micro Scale Electrochemical Sensors.* IEEE Sensors Journal, 2020. **21**(3): p. 3210-3215.

88. C. Barrett, K. Dawson, C. O'Mahony, and A. O'Riordan, *Development of low cost rapid fabrication of sharp polymer microneedles for in vivo glucose biosensing applications.* ECS Journal of Solid State Science and Technology, 2015. **4**(10): p. S3053.

89. P. Tomčík, *Microelectrode arrays with overlapped diffusion layers as electroanalytical detectors: theory and basic applications.* Sensors, 2013. **13**(10): p. 13659-13684.

90. S.B. Adeloju, *Amperometry*, in *Enclyclopedia of Analytical Science*. 2005, Elsevier. p. 70-79.

91. N. Elgrishi, K.J. Rountree, B.D. McCarthy, E.S. Rountree, T.T. Eisenhart, and J.L. Dempsey, *A practical beginner's guide to cyclic voltammetry.* Journal of chemical education, 2018. **95**(2): p. 197-206.

92. J. Zhang, J. Wu, H. Zhang, and J. Zhang, *PEM fuel cell testing and diagnosis*. 2013: Newnes.

93. O. de Oliveira Jr, L. Ferreira, G. Marystela, F. de Lima Leite, and A.L. Da Róz, *Nanoscience and its Applications*. 2016: William Andrew.

94. P. Westbroek, G. Priniotakis, and P. Kiekens, *Analytical electrochemistry in textiles*. 2005: Elsevier.

95. S.J. Cobb and J.V. Macpherson, *Enhancing square wave voltammetry measurements via electrochemical analysis of the non-faradaic potential window.* Analytical chemistry, 2019. **91**(12): p. 7935-7942.

96. R. Franklin, S. Martin, T. Strong, and R. Brown, *Chemical and Biological Systems: Chemical Sensing Systems for Liquids.* 2016.

97. F. Simões and M. Xavier, *Nanoscience and its Applications*. 2017, Elsevier BV Amsterdam, The Netherlands:.

98. E. de Boer and R.R. Beumer, *Methodology for detection and typing of foodborne microorganisms.* International journal of food microbiology, 1999. **50**(1-2): p. 119-130.

99. M. Ermini, S. Scarano, R. Bini, M. Banchelli, D. Berti, M. Mascini, et al., *A rational approach in probe design for nucleic acid-based biosensing.* Biosensors and Bioelectronics, 2011. **26**(12): p. 4785-4790.

100. W. Yang, M. Ozsoz, D.B. Hibbert, and J.J. Gooding, *Evidence for the direct interaction between methylene blue and guanine bases using DNA-modified carbon paste electrodes.* Electroanalysis: An International Journal Devoted to Fundamental and Practical Aspects of Electroanalysis, 2002. **14**(18): p. 1299-1302.

101. M.E. Cristescu, *Can environmental RNA revolutionize biodiversity science?* Trends in ecology & evolution, 2019. **34**(8): p. 694-697.

102. R. Li, H.M. Tun, M. Jahan, Z. Zhang, A. Kumar, W.D. Fernando, et al., *Comparison of DNA-, PMA-, and RNA-based 16S rRNA Illumina sequencing for detection of live bacteria in water.* Scientific reports, 2017. **7**(1): p. 1-11.

103. D.W. Selinger, R.M. Saxena, K.J. Cheung, G.M. Church, and C. Rosenow, *Global RNA half-life analysis in Escherichia coli reveals positional patterns of transcript degradation.* Genome research, 2003. **13**(2): p. 216-223.

104. S. Saleh-Lakha, M. Miller, R.G. Campbell, K. Schneider, P. Elahimanesh, M.M. Hart, et al., *Microbial gene expression in soil: methods, applications and challenges.* Journal of microbiological methods, 2005. **63**(1): p. 1-19.

105. J.L. Zhang, J.J. Wang, X.Q. Zhang, and F.J. He, *Rapid detection of Escherichia coli based on 16S rDNA nanogap network electrochemical biosensor.* Biosensors & Bioelectronics, 2018. **118**: p. 9-15.

106. D. Ozkan-Ariksoysal, Y.U. Kayran, F.F. Yilmaz, A.A. Ciucu, I.G. David, V. David, et al., *DNA-wrapped multi-walled carbon nanotube modified electrochemical biosensor for the detection of Escherichia coli from real samples.* Talanta, 2017. **166**: p. 27-35.

107. I. Tiwari, M. Singh, C.M. Pandey, and G. Sumana, *Electrochemical detection of a pathogenic Escherichia coli specific DNA sequence based on a graphene oxide–chitosan composite decorated with nickel ferrite nanoparticles.* RSC Advances, 2015. **5**(82): p. 67115-67124.

108. N. Paniel and J. Baudart, *Colorimetric and electrochemical genosensors for the detection of Escherichia coli DNA without amplification in seawater.* Talanta, 2013. **115**: p. 133-142.

109. A. Zimdars, M. Gebala, G. Hartwich, S. Neugebauer, and W. Schuhmann, *Electrochemical detection of synthetic DNA and native 16S rRNA fragments on a microarray using a biotinylated intercalator as coupling site for an enzyme label.* Talanta, 2015. **143**: p. 19-26.

110. U. Kim, A. Ravikumar, J. Seubert, and S. Figueira. *Detection of bacterial pathogens through microfluidic DNA sensors and mobile interface toward rapid, affordable, and point-of-care water monitoring*. in *2013 IEEE Point-of-Care Healthcare Technologies (PHT)*. 2013. IEEE.

111. K. Yamanaka, T. Ikeuchi, M. Saito, N. Nagatani, and E. Tamiya, *Electrochemical detection of specific DNA and respiratory activity of Escherichia coli.* Electrochimica acta, 2012. **82**: p. 132-136.

112. E.Y. Ariffin, Y.H. Lee, D. Futra, L.L. Tan, N.H. Abd Karim, N.N.N. Ibrahim, et al., *An ultrasensitive hollow-silica-based biosensor for pathogenic Escherichia coli DNA detection.* Analytical and Bioanalytical Chemistry, 2018. **410**(9): p. 2363-2375.

113. Y. Wen, L. Wang, L. Xu, L. Li, S. Ren, C. Cao, et al., *Electrochemical detection of PCR amplicons of Escherichia coli genome based on DNA nanostructural probes and polyHRP enzyme.* Analyst, 2016. **141**(18): p. 5304-5310.

114. G. Liu, R.J. Lao, L. Xu, Q. Xu, L.Y. Li, M. Zhang, et al., *Detection of Single-Nucleotide Polymorphism on uidA Gene of Escherichia coli by a Multiplexed Electrochemical DNA Biosensor with Oligonucleotide-Incorporated Nonfouling Surface.* Sensors, 2011. **11**(8): p. 8018-8027.

115. P. Geng, X.A. Zhang, Y.Q. Teng, Y. Fu, L.L. Xu, M. Xu, et al., *A DNA sequence-specific electrochemical biosensor based on alginic acid-coated cobalt magnetic beads for the detection of E. coli.* Biosensors & Bioelectronics, 2011. **26**(7): p. 3325-3330.

116. M.I. Rodriguez and E.C. Alocilja, *Embedded DNA-polypyrrole biosensor for rapid detection of Escherichia coli.* IEEE sensors journal, 2005. **5**(4): p. 733-736.

117. P.U. Arumugam, E. Yu, R. Riviere, and M. Meyyappan, *Vertically aligned carbon nanofiber electrode arrays for nucleic acid detection.* Chemical Physics Letters, 2010. **499**(4-6): p. 241-246.

118. S. Bansal, A. Jyoti, K. Mahato, P. Chandra, and R. Prakash, *Highly Sensitive in vitro Biosensor for Enterotoxigenic Escherichia coli Detection Based on ssDNA Anchored on PtNPs-Chitosan Nanocomposite.* Electroanalysis, 2017. **29**(11): p. 2665-2671.

119. M.J. Anderson, H.R. Miller, and E.C. Alocilja, *PCR-less DNA co-polymerization detection of Shiga like toxin 1 (stx1) in Escherichia coli O157: H7.* Biosensors and Bioelectronics, 2013. **42**: p. 581-585.

120. A. Ben Aissa, J. Jara, R. Sebastián, A. Vallribera, S. Campoy, and M. Pividori, *Comparing nucleic acid lateral flow and electrochemical genosensing for the simultaneous detection of foodborne pathogens.* Biosensors and Bioelectronics, 2017. **88**: p. 265-272.

121. Y. Li, J. Deng, L.C. Fang, K.K. Yu, H. Huang, L.L. Jiang, et al., *A novel electrochemical DNA biosensor based on HRP-mimicking hemin/G-quadruplex wrapped GOx nanocomposites as tag for detection of Escherichia coli O157:H7.* Biosensors & Bioelectronics, 2015. **63**: p. 1-6.

122. N. Zainudin, A.R.M. Hairul, M.M. Yusoff, L.L. Tan, and K.F. Chong, *Impedimetric graphene-based biosensor for the detection of Escherichia coli DNA.* Analytical Methods, 2014. **6**(19): p. 7935-7941.

123. L.J. Wang, Q.J. Liu, Z.Y. Hu, Y.F. Zhang, C.S. Wu, M. Yang, et al., *A novel electrochemical biosensor based on dynamic polymerase-extending hybridization for E.coli O157:H7 DNA detection.* Talanta, 2009. **78**(3): p. 647-652.

124. J. Berganza, G. Olabarria, R. García, D. Verdoy, A. Rebollo, and S. Arana, *DNA microdevice for electrochemical detection of Escherichia coli 0157: H7 molecular markers.* Biosensors and Bioelectronics, 2007. **22**(9-10): p. 2132-2137.

125. M.E. Minaei, M. Saadati, M. Najafi, and H. Honari, *Label-free, PCR-free DNA Hybridization Detection of Escherichia coli O157:H7 Based on Electrochemical Nanobiosensor.* Electroanalysis, 2016. **28**(10): p. 2582-2589.

126. R. Deshmukh, A.K. Prusty, U. Roy, and S. Bhand, *A capacitive DNA sensor for sensitive detection of Escherichia coli O157:H7 in potable water based on the z3276 genetic marker: fabrication and analytical performance.* Analyst, 2020. **145**(6): p. 2267-2278.

127. P. Woo, S. Lau, J. Teng, H. Tse, and K.-Y. Yuen, *Then and now: use of 16S rDNA gene sequencing for bacterial identification and discovery of novel bacteria in clinical microbiology laboratories.* Clinical Microbiology and Infection, 2008. **14**(10): p. 908-934.

128. N.D. Ragupathi, D.M. Sethuvel, F. Inbanathan, and B. Veeraraghavan, *Accurate differentiation of Escherichia coli and Shigella serogroups: challenges and strategies.* New microbes and new infections, 2018. **21**: p. 58-62.

129. M. Pavlovic, A. Luze, R. Konrad, A. Berger, A. Sing, U. Busch, et al., *Development of a duplex real-time PCR for differentiation between E. coli and Shigella spp.* Journal of applied microbiology, 2011. **110**(5): p. 1245-1251.

130. L. Beutin and A. Martin, *Outbreak of Shiga toxin–producing Escherichia coli (STEC) O104: H4 infection in Germany causes a paradigm shift with regard to human pathogenicity of STEC strains.* Journal of food protection, 2012. **75**(2): p. 408-418.

131. V.S. Castro, R.C.T. Carvalho, C.A. Conte-Junior, and E.E.S. Figuiredo, *Shiga-toxin producing Escherichia coli: pathogenicity, supershedding, diagnostic methods, occurrence, and foodborne outbreaks.* Comprehensive Reviews in Food Science and Food Safety, 2017. **16**(6): p. 1269-1280.

132. L. Rodríguez-Rubio, N. Haarmann, M. Schwidder, M. Muniesa, and H. Schmidt, *Bacteriophages of Shiga toxin-producing Escherichia coli and their contribution to pathogenicity.* Pathogens, 2021. **10**(4): p. 404.

133. M.I. Pividori and S. Alegret, *DNA adsorption on carbonaceous materials.* Immobilisation of DNA on Chips I, 2005: p. 1-36.

134. J.I.A. Rashid and N.A. Yusof, *The strategies of DNA immobilization and hybridization detection mechanism in the construction of electrochemical DNA sensor: A review.* Sensing and bio-sensing research, 2017. **16**: p. 19-31.

135. B. Liu and J. Liu, *DNA adsorption by indium tin oxide nanoparticles.* Langmuir, 2015. **31**(1): p. 371-377.

136. A. Lopez and J. Liu, *Covalent and noncovalent functionalization of graphene oxide with DNA for smart sensing.* Advanced Intelligent Systems, 2020. **2**(11): p. 2000123.

137. E. Huang, F. Zhou, and L. Deng, *Studies of surface coverage and orientation of DNA molecules immobilized onto preformed alkanethiol self-assembled monolayers.* Langmuir, 2000. **16**(7): p. 3272-3280.

138. D. Jambrec, F. Conzuelo, B. Zhao, and W. Schuhmann, *Potential-pulse assisted thiol chemisorption minimizes non-specific adsorptions in DNA assays.* Electrochimica Acta, 2018. **276**: p. 233-239.

139. Y. Xue, X. Li, H. Li, and W. Zhang, *Quantifying thiol–gold interactions towards the efficient strength control.* Nature communications, 2014. **5**(1): p. 1-9.

140. F. Lucarelli, G. Marrazza, A.P. Turner, and M. Mascini, *Carbon and gold electrodes as electrochemical transducers for DNA hybridisation sensors.* Biosensors and Bioelectronics, 2004. **19**(6): p. 515-530.

141. A. Singh, G. Sinsinbar, M. Choudhary, V. Kumar, R. Pasricha, H. Verma, et al., *Graphene oxide-chitosan nanocomposite based electrochemical DNA biosensor for detection of typhoid.* Sensors and Actuators B: Chemical, 2013. **185**: p. 675-684.

142. Q. Sun, H. Tian, H. Qu, D. Sun, Z. Chen, L. Duan, et al., *Discrimination between streptavidin and avidin with fluorescent affinity-based probes.* Analyst, 2015. **140**(13): p. 4648-4653.

143. S. Ke, J.C. Wright, and G.S. Kwon, *Intermolecular interaction of avidin and PEGylated biotin.* Bioconjugate chemistry, 2007. **18**(6): p. 2109-2114.

144. Q. Lv, Y. Wang, C. Su, T. Lakshmipriya, S.C. Gopinath, K. Pandian, et al., *Human papilloma virus DNA-biomarker analysis for cervical cancer: signal enhancement by gold nanoparticle-coupled tetravalent streptavidin-biotin strategy.* International journal of biological macromolecules, 2019. **134**: p. 354-360.

145. M. Yang, S.W. Jeong, S.J. Chang, K.H. Kim, M. Jang, C.H. Kim, et al., *Flexible and Disposable Sensing Platforms Based on Newspaper.* Acs Applied Materials & Interfaces, 2016. **8**(51): p. 34978-34984.

146. A. Walter, J. Wu, G.-U. Flechsig, D.A. Haake, and J. Wang, *Redox cycling amplified electrochemical detection of DNA hybridization: Application to pathogen E. coli bacterial RNA.* Analytica chimica acta, 2011. **689**(1): p. 29-33.

147. B. Heidenreich, C. Poehlmann, M. Sprinzl, and M. Gareis, *Detection of Escherichia coli in meat with an electrochemical biochip.* Journal of food protection, 2010. **73**(11): p. 2025-2033.

148. F. Li, Z. Yu, H. Qu, G. Zhang, H. Yan, X. Liu, et al., *A highly sensitive and specific electrochemical sensing method for robust detection of Escherichia coli lac Z gene sequence.* Biosensors and Bioelectronics, 2015. **68**: p. 78-82.

149. J. Wu, S. Campuzano, C. Halford, D.A. Haake, and J. Wang, *Ternary surface monolayers for ultrasensitive (zeptomole) amperometric detection of nucleic acid hybridization without signal amplification.* Analytical chemistry, 2010. **82**(21): p. 8830-8837.

150. F. Kuralay, S. Campuzano, D.A. Haake, and J. Wang, *Highly sensitive disposable nucleic acid biosensors for direct bioelectronic detection in raw biological samples.* Talanta, 2011. **85**(3): p. 1330-1337.

151. Y. Wen, L. Wang, L. Xu, L. Li, S. Ren, C. Cao, et al., *Electrochemical detection of PCR amplicons of Escherichia coli genome based on DNA nanostructural probes and polyHRP enzyme.* Analyst, 2016. **141**(18): p. 5304-5310.

152. L. Li, L. Wang, Q. Xu, L. Xu, W. Liang, Y. Li, et al., *Bacterial Analysis Using an Electrochemical DNA Biosensor with Poly-Adenine-Mediated DNA Self-Assembly.* Acs Applied Materials & Interfaces, 2018. **10**(8): p. 6895-6903.

153. M. Saadaoui, I. Fernández, G. Luna, P. Díez, S. Campuzano, N. Raouafi, et al., *Label-free electrochemical genosensor based on mesoporous silica thin film.* Analytical and bioanalytical chemistry, 2016. **408**(26): p. 7321-7327.

154. C.M. Pandey, I. Tiwari, and G. Sumana, *Hierarchical cystine flower based electrochemical genosensor for detection of Escherichia coli O157:H7.* Rsc Advances, 2014. **4**(59): p. 31047-31055.

155. C.M. Pandey, G. Sumana, and B.D. Malhotra, *Microstructured Cystine Dendrites-Based Impedimetric Sensor for Nucleic Acid Detection.* Biomacromolecules, 2011. **12**(8): p. 2925-2932.

156. C.M. Pandey, R. Singh, G. Sumana, M. Pandey, and B. Malhotra, *Electrochemical genosensor based on modified octadecanethiol self-assembled monolayer for Escherichia coli detection.* Sensors and Actuators B: Chemical, 2011. **151**(2): p. 333-340.

157. C.M. Pandey, A. Sharma, G. Sumana, I. Tiwari, and B.D. Malhotra, *Cationic poly (lactic-co-glycolic acid) iron oxide microspheres for nucleic acid detection.* Nanoscale, 2013. **5**(9): p. 3800-3807.

158. N. Jaiswal, C.M. Pandey, S. Solanki, I. Tiwari, and B.D. Malhotra, *An impedimetric biosensor based on electrophoretically assembled ZnO nanorods and carboxylated graphene nanoflakes on an indium tin oxide electrode for detection of the DNA of Escherichia coli O157:H7.* Microchimica Acta, 2020. **187**(1).

159. I. Tiwari, M. Gupta, C.M. Pandey, and V. Mishra, *Gold nanoparticle decorated graphene sheet-polypyrrole based nanocomposite: its synthesis, characterization and genosensing application.* Dalton Transactions, 2015. **44**(35): p. 15557-15566.

160. T. Widaningrum, E. Widyastuti, F.W. Pratiwi, A.I.F. Fatimah, P. Rijiravanich, M. Somasundrum, et al., *Sub-attomolar electrochemical measurement of DNA hybridization based on the detection of high coverage biobarcode latex labels at PNA-modified screen printed electrodes.* Talanta, 2017. **167**: p. 14-20.

161. Kashish, S. Bansal, A. Jyoti, K. Mahato, P. Chandra, and R. Prakash, *Highly Sensitive in vitro Biosensor for Enterotoxigenic Escherichia coli Detection*

Based on ssDNA Anchored on PtNPs-Chitosan Nanocomposite. Electroanalysis, 2017. **29**(11): p. 2665-2671.

162. E.Y. Ariffin, L.Y. Heng, L.L. Tan, N.H. Abd Karim, and S.A. Hasbullah, *A Highly Sensitive Impedimetric DNA Biosensor Based on Hollow Silica Microspheres for Label-Free Determination of E. coli.* Sensors, 2020. **20**(5).
163. M.H. Abdalhai, A.n.M. Fernandes, X. Xia, A. Musa, J. Ji, and X. Sun, *Electrochemical genosensor to detect pathogenic bacteria (Escherichia coli O157: H7) as applied in real food samples (fresh beef) to improve food safety and quality control.* Journal of agricultural and food chemistry, 2015. **63**(20): p. 5017-5025.
164. X.Y. Zhang, T.T. Wu, Y.M. Yang, Y.Q. Wen, S.T. Wang, and L.P. Xu, *Superwettable electrochemical biosensor based on a dual-DNA walker strategy for sensitive E. coli O157: H7 DNA detection.* Sensors and Actuators B-Chemical, 2020. **321**.
165. K. Li, Y.J. Lai, W. Zhang, and L.T. Jin, *Fe2O3@Au core/shell nanoparticle-based electrochemical DNA biosensor for Escherichia coli detection.* Talanta, 2011. **84**(3): p. 607-613.
166. D. Brandão, S. Liébana, S. Campoy, M.P. Cortés, S. Alegret, and M.I. Pividori, *Simultaneous electrochemical magneto genosensing of foodborne bacteria based on triple-tagging multiplex amplification.* Biosensors and Bioelectronics, 2015. **74**: p. 652-659.
167. S. Liébana, D. Brandão, P. Cortés, S. Campoy, S. Alegret, and M.I. Pividori, *Electrochemical genosensing of Salmonella, Listeria and Escherichia coli on silica magnetic particles.* Analytica Chimica Acta, 2016. **904**: p. 1-9.

168. H.Y. Kim, J.K. Ahn, M.I. Kim, K.S. Park, and H.G. Park, *Rapid and label-free, electrochemical DNA detection utilizing the oxidase-mimicking activity of cerium oxide nanoparticles.* Electrochemistry Communications, 2019. **99**: p. 5-10.

169. J. van der Zalm, S. Chen, W. Huang, and A. Chen, *recent advances in the development of nanoporous Au for sensing applications.* Journal of The Electrochemical Society, 2020. **167**(3): p. 037532.

170. H. Jiang, E.M. Materon, M.D.P.T. Sotomayor, and J. Liu, *Fast assembly of non-thiolated DNA on gold surface at lower pH.* Journal of colloid and interface science, 2013. **411**: p. 92-97.

171. V.B. Juska, A. Walcarius, and M.E. Pemble, *Cu Nanodendrite Foams on Integrated Band Array Electrodes for the Nonenzymatic Detection of Glucose.* ACS Applied Nano Materials, 2019.

172. A. Tarasov, D.W. Gray, M.-Y. Tsai, N. Shields, A. Montrose, N. Creedon, et al., *A potentiometric biosensor for rapid on-site disease diagnostics.* Biosensors and Bioelectronics, 2016. **79**: p. 669-678.

173. L.A. Wasiewska, I. Seymour, B. Patella, R. Inguanta, C.M. Burgess, G. Duffy, et al., *Reagent free electrochemical-based detection of silver ions at interdigitated microelectrodes using in-situ pH control.* Sensors and Actuators B: Chemical, 2021. **333**: p. 129531.

174. Y. Liu, X. Li, J. Chen, and C. Yuan, *Micro/Nano Electrode Array Sensors: Advances in Fabrication and Emerging Applications in Bioanalysis.* Frontiers in Chemistry, 2020: p. 1102.

175. A. Wahl, K. Dawson, J. MacHale, S. Barry, A.J. Quinn, and A. O'Riordan, *Gold nanowire electrodes in array: simulation study and experiments.* Faraday discussions, 2013. **164**: p. 377-390.

176. M. Seo, S.Y. Yeon, J. Yun, and T.D. Chung, *Nanoporous ITO implemented bipolar electrode sensor for enhanced electrochemiluminescence.* Electrochimica Acta, 2019. **314**: p. 89-95.

177. O.D. Renedo, M. Alonso-Lomillo, and M.A. Martínez, *Recent developments in the field of screen-printed electrodes and their related applications.* Talanta, 2007. **73**(2): p. 202-219.

178. V. Menchise, G. De Simone, T. Tedeschi, R. Corradini, S. Sforza, R. Marchelli, et al., *Insights into peptide nucleic acid (PNA) structural features: The crystal structure of a d-lysine-based chiral PNA–DNA duplex.* Proceedings of the National Academy of Sciences, 2003. **100**(21): p. 12021-12026.

179. H. Shi, F. Yang, W. Li, W. Zhao, K. Nie, B. Dong, et al., *A review: Fabrications, detections and applications of peptide nucleic acids (PNAs) microarray.* Biosensors and Bioelectronics, 2015. **66**: p. 481-489.

180. A. Rabti, R. Zayani, M. Meftah, I. Salhi, and N. Raouafi, *Impedimetric DNA E-biosensor for multiplexed sensing of Escherichia coli and its virulent f17 strains.* Microchimica Acta, 2020. **187**(11).

181. Y. Xianyu, Q. Wang, and Y. Chen, *Magnetic particles-enabled biosensors for point-of-care testing.* TrAC Trends in Analytical Chemistry, 2018. **106**: p. 213-224.

182. T.A. Rocha-Santos, *Sensors and biosensors based on magnetic nanoparticles.* TrAC Trends in Analytical Chemistry, 2014. **62**: p. 28-36.

183. S.D. Mason, Y. Tang, Y. Li, X. Xie, and F. Li, *Emerging bioanalytical applications of DNA walkers.* TrAC Trends in Analytical Chemistry, 2018. **107**: p. 212-221.

184. K. Hsieh, B.S. Ferguson, M. Eisenstein, K.W. Plaxco, and H.T. Soh, *Integrated Electrochemical Microsystems for Genetic Detection of Pathogens at the Point of Care.* Accounts of Chemical Research, 2015. **48**(4): p. 911-920.

185. T. Notomi, H. Okayama, H. Masubuchi, T. Yonekawa, K. Watanabe, N. Amino, et al., *Loop-mediated isothermal amplification of DNA.* Nucleic acids research, 2000. **28**(12): p. e63-e63.

186. H.Y. Lau and J.R. Botella, *Advanced DNA-based point-of-care diagnostic methods for plant diseases detection.* Frontiers in plant science, 2017. **8**: p. 2016.

187. A. Rani, V.B. Ravindran, A. Surapaneni, N. Mantri, and A.S. Ball, *Trends in point-of-care diagnosis for Escherichia coli O157: H7 in food and water.* International Journal of Food Microbiology, 2021. **349**: p. 109233.

188. X. Fang, Y. Liu, J. Kong, and X. Jiang, *Loop-Mediated Isothermal Amplification Integrated on Microfluidic Chips for Point-of-Care Quantitative Detection of Pathogens.* Analytical Chemistry, 2010. **82**(7): p. 3002-3006.

189. H. Zhang, Y. Xu, Z. Fohlerova, H. Chang, C. Iliescu, and P. Neuzil, *LAMP-on-a-chip: Revising microfluidic platforms for loop-mediated DNA amplification.* TrAC Trends in Analytical Chemistry, 2019. **113**: p. 44-53.

190. C.-H. Wang, K.-Y. Lien, T.-Y. Wang, T.-Y. Chen, and G.-B. Lee, *An integrated microfluidic loop-mediated-isothermal-amplification system for rapid sample pre-treatment and detection of viruses.* Biosensors and Bioelectronics, 2011. **26**(5): p. 2045-2052.

Chapter 2. Reagent free electrochemical-based detection of silver ions at interdigitated microelectrodes using in-situ pH control.

Published in “Sensors and Actuators B: Chemical”

DOI 10.1016/j.snb.2021.129531

2.1. Introduction

Silver nanoparticles, due to their antimicrobial effect and physical properties, have become ubiquitous in a wide variety of products ranging from electronic & medical devices, textiles, cosmetics through to home disinfectants [1]. Their increased use in consumer products has, however, resulted in their unwanted release into the environment, particularly into water sources [2]. It is purported that the antimicrobial activity of silver nanoparticles involves the slow release of silver ions into the solution, which is the most toxic form of silver [3]. Silver toxicity to aquatic life has been well documented, while bioaccumulation in humans may lead to a disease called argyria [4]. Despite the lack of robust data on silver toxicity in humans, the World Health Organisation (WHO) [5] have suggested 0.1 mg/L (~ 0.93 µM) as the upper limit for silver in drinking water. Accordingly, in recent Drinking Water Standards and Health Advisories Tables, the United States Environmental Protection Agency (EPA) [6] have proposed the same permissible (0.1 mg/L) concentration of silver in drinking water. There is therefore a need, on health grounds, for rapid methods to monitor silver concentrations in drinking water.

Several instrumental and non-instrumental methods for the detection of silver in aqueous solutions have been described to date. These include atomic absorbance spectroscopy [7], colorimetric [8], fluorescent [9], and electrochemical methods [10]. Recently, much attention has focused on electrochemistry as a detection technique, due to its low cost, suitability to device miniaturization & portability, as well as simplicity of use, crucial for point-of-use application [11, 12, 13, 14]. One of the most often used electrochemical technique for silver detection is anodic sweep voltammetry (ASV) which comprises two major steps - pre-concentration of the metal at an electrode followed by its oxidation by sweeping the potential around its oxidation

potential. Several authors have developed sensors for silver detection with ASV using a wide range modified and non-modified of electrode materials, such as boron-doped diamond [15], gallium nitrate [16], graphite felt [17] or carbon paste [18]. Typically, carbon paste or glassy carbon electrodes modified with a variety of different ligands, such as N,N0-bis(2-hydroxybenzylidene)-2,20(aminophenylthio) ethane [19]; CNT and (E)-4-(2-hydroxyethylimino) pentan-2-one (EHPO) [20]; phenylthiourea-functionalized high ordered nanoporous silica gel [21] or 8-Mercaptoquinoline [22], offered very low limits of detection, which addresses one of the major challenge in development of sensor for silver detection. However, the modification of the electrodes is laborious, of variable quality and reproducibility, and may be expensive. The application of nano- and micro-electrodes for electrochemical analysis has offered significant advantages such as increased signal-to-noise ratio, higher current density and therefore higher sensitivity without the need for electrode's modification [23, 24]. For instance, the study conducted by Sidambaram and Colleran [25] applied gold and platinum nanoelectrodes for the detection of silver ions. However, they have conducted their experiments in chloride-free buffer stating that the presence of chloride ions greatly affects reproducibility of the sensor.

Another challenge in development of silver sensor is a typical need for pH modification before the measurements. The pH of a sample solution is one of the crucial parameters in metal detection using ASV and its optimisation during deposition, and stripping is one of the first steps in sensor development [26, 27, 28]. The optimal concentration of H^+ ions can delay side reactions, e.g., a metal's complexation with other species and thus increase the availability of the metal for electrodeposition and consequently, the final measured signal [29]. However, in many deployment scenarios for real-time silver detection, pH adjustment of a solution prior

to a measurement remains unfeasible. The optimal pH for silver detection is strongly affected by electrode material composition, type of ligand, modification process, and the supporting electrolyte and has been reported by other authors to vary between pH 1.1 [30] and 9.5 [19, 31]; depending on the parameters used. Tap water pH typically varies between 6.5 and 8.5, and thus prior to detection in these samples, reagents such as nitric acid [21] or acetic acid [32] are usually added. Ideally, an electrochemical-based sensor for tap water should allow for detection within this pH range without manual adjustment. Mineral acids are usually used to adjust the pH. However, more recently, an electrochemical based in-situ pH adjustment method, using a boron-doped ring disc electrode system, was demonstrated for the detection of mercury in water [29]. This approach was based on electrochemically driven decomposition of water achieved by applying a sufficiently high oxidising potential to the ring electrode. During this process, hydrogen ions were anodically produced at the ring electrode which diffused to and caused acidification of the solution near the 'sensing' disk electrode.

In the current study, we extended this approach by developing solid-state sensors on silicon chip substrates that incorporated interdigitated microelectrodes for the detection of silver ions in sodium acetate and tap water. Each sensor comprised two interdigitated electrodes arrays (IDAs) and in our approach, the platinum protonator IDA was used to electro-generate H^+ ions while the gold working IDA was used to detect the silver (I) ions. By applying a constant potential to a pronator IDA, the in-situ pH surrounding an electrode could be easily tailored within a range of pH 2–10. The optimisation of the technique and the proof-of-concept experiments were performed in sodium acetate while the final application was done in tap water.

2.2. Material and methods

2.2.1. Reagents

Sodium acetate, silver nitrate, nitric acid, ferrocenecarboxylic acid, and PBS tablets were obtained from Sigma Aldrich, Ireland. Hydrogen dinitrosulphatoplatinate(II) (DNS) platinum plating solution was obtained from Johnston Matthey chemical products. 50 mL stock solution of 20 mM silver nitrate was prepared by diluting it with ultra-pure Milli-Q water (18.2 MΩ.cm, Milli-Q) which was stored in a fridge at 4ºC. Silver samples were made by diluting the stock solution with the selected electrolyte (sodium acetate or tap water) before each measurement. Sodium acetate was prepared by diluting it to the desired concentration (0.01 M) with ultra-pure Milli-Q water (18.2 MΩ.cm, Milli-Q). If needed, 1 M nitric acid was added drop-wise until the desired pH was obtained. Tap water used for the experiments was not treated prior to use.

2.2.2. Apparatus

All the electrochemical measurements were undertaken using a CHI 920 potentiostat with a bipotentiostat function. A three electrode configuration was used for the silver detection in acidified solutions where gold interdigitated microband electrode (working IDA) was employed as a working electrode, gold on-chip wire as a counter electrode, and an external Ag/AgCl as a reference electrode. An additional platinum protonator interdigitated electrode (protonator IDA) was used in a four electrode configuration in the experiments employing in-situ electrochemical pH control.

2.2.3. Silicon chips fabrication

Interdigitated electrodes array (IDA) at silicon chips were designed and fabricated for silver detection. Fabrication of the chips was similar to those described by Wahl et al.

[23]. Briefly, gold microband electrodes were fabricated on four-inch silicon wafer substrates bearing a ~300 nm layer of thermally grown silicon dioxide; see Fig. S2.1. IDAs were first fabricated using a combination of optical lithography, metal evaporation (Ti 5 nm /Au 50 nm Temescal FC-2000 E-beam evaporator) and lift-off techniques to yield well-defined, stacked metallic (Ti/Au) microband (1 µm width, 50 nm height, 80 µm length) structures. Each chip comprised six independent sensors. A second optical lithographic and metal deposition (Ti 10 nm/Au 100 nm) process was then undertaken to define a MicroSD pin-out, interconnection tracks, as well as counter electrodes (500 µm wide x 10 mm long). In this work, an on-chip microSD style electrical pin-out was included to permit facile electrical connection to external electronics. In this manner, chips could be easily swapped in and out with the potentiostat, enabling rapid analysis of multiple samples. A custom-built cell was designed and fabricated so that when screwed together, the microSD primary contact pads protruded out of the holder to allow connection with a PCB mounted microSD port. As platinum is known to catalyse water electrolysis, following fabrication, platinum was electrodeposited on a protonator IDA to promote proton flux production at lower over-potentials. The platinum deposition was undertaken by immersing a chip with an electrical connection made to one interdigitated comb in the commercial DNS plating solution and applying -0.5 V (vs Ag/AgCl) for five seconds.

2.2.4. Electrode characterisation

Following fabrication, optical microscopy was employed to identify any obvious defects or faults, with faulty chips being discarded. Chips were cleaned by immersion and sonication for ten minutes, first in ethanol, then in de-ionized water, and dried in a flow of nitrogen. The electrochemical characterisation was undertaken in a Faraday cage using a CHI 920 potentiostat. Cyclic voltammograms (CV) were performed from

0 V to 0.6 V at 50 mV/s in 1 mM ferrocene carboxylic acid (FCA). Generator–collector scans, where the protonator IDA were held at 0 V and the working IDA swept as above, were also undertaken. All electrochemical characterisation measurements were recorded versus an Ag/AgCl external reference electrode.

2.2.5. Silver detection method in acidic media

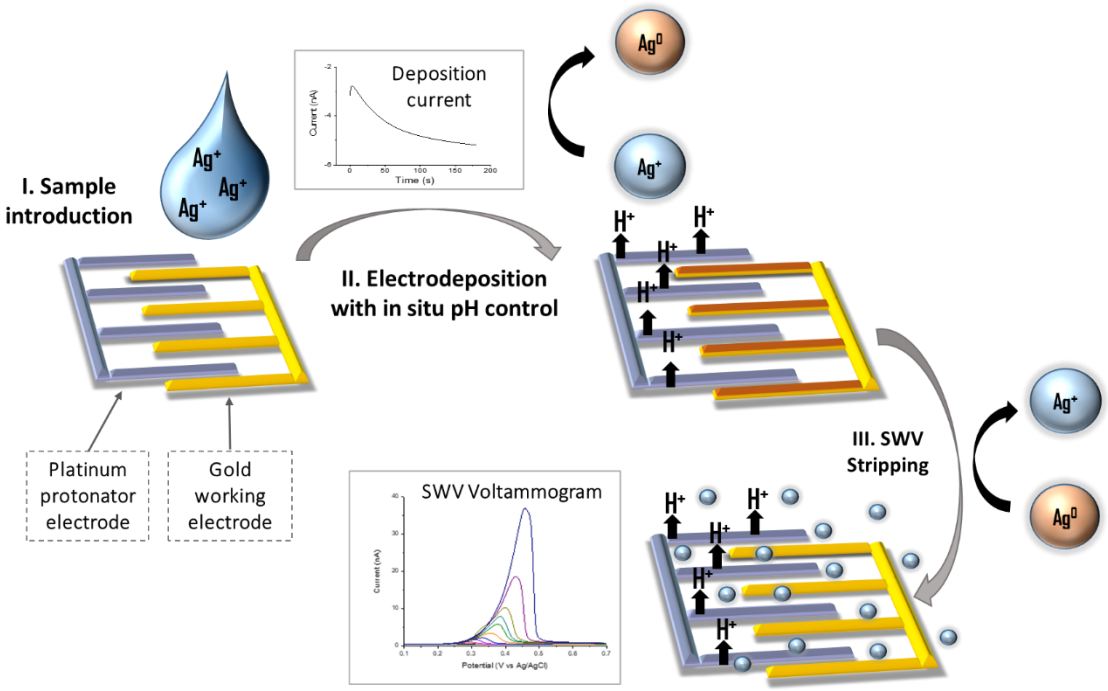

Fig. 2.1 Scheme showing the silver detection process on an interdigitated microband electrode.

Electrochemical detection of silver was undertaken as shown schematically in Fig. 2.1. (i) First, 500 µL of test solution was introduced onto a sensor chip. (ii) Silver ions were then electrodeposited to form bulk silver on the surface of gold working IDA according to equation 1.

$$Ag^{+} + e^{-} \rightarrow Ag^{0} \qquad (2.1.)$$

(iii) Finally, square wave stripping voltammetry (SWV) was used to strip the silver from the underlying gold working IDA (see equation 2), with the corresponding

oxidation peak height current proportional to a concentration of silver pre-deposited on a sensor.

$$Ag^0 - e^- \rightarrow Ag^+ \quad (2.2)$$

In brief, the method comprised the following steps: a) A 500 µL aliquot of 0.01 M sodium acetate, pH 3, containing the desired concentration of silver nitrate diluted from a stock solution, was pipetted into the sample well. (b) A bias of -0.2 V (vs Ag/AgCl) was applied for 3-5 minutes to a working IDA to reduce and deposit the silver ions. c) The silver was stripped from the electrode by using SWV undertaken in a positive direction between -0.2 and 0.8 V (vs Ag/AgCl) at the following conditions: frequency 15 Hz, increment potential 0.004 V, amplitude 0.025 V, and the silver stripping peak was recorded at ~0.3 V (vs Ag/AgCl). d) Following the measurement, the electrode was potientio-dynamically cleaned by replacing the sample with 0.01 M sodium acetate solution and applying the potential of 0.5 V for 150 s, which is a slightly more oxidative potential than observed for silver stripping in sodium acetate. e) SWV was again recorded between -0.2 and 0.8 V in blank, sodium acetate solution to confirm that all the silver was oxidised from the electrode to prevent carry over from previous experiments.

2.2.6. Silver detection method using in-situ pH control

For the silver detection using in-situ electrochemical pH control, the same conditions for deposition and stripping as described above were applied, except that pH of sodium acetate and tap water was not chemically adjusted before (both remained at pH ~7.5). Instead, a constant oxidising potential was applied to the protonator IDA, to produce protons (H^+ ions) according to equation 3, thus tailoring the pH in the vicinity of the sensor IDA.

$$2H_2O \rightarrow O_2 + 4H^+ + 4e^- \quad (2.3)$$

During deposition (step b) 1.25 V (vs Ag/AgCl) or 1.65 V (vs Ag/AgCl) was simultaneously applied at the protonator IDA when the measurements were done in 0.01 M sodium acetate and tap water, respectively. During stripping (step c) 1.65 V (vs Ag/AgCl) was applied to the protonator IDA in 0.01 M sodium acetate and tap water. The oxidation peak was recorded at ~0.3 V for measurements in sodium acetate while ~0.2 V for measurements in tap water.

2.3. Results and discussion

2.3.1. Sensor Characterisation.

Each chip contained six sensors, comprising two separate microband IDAs, and a gold counter electrode shown in Fig. 2.2 (A) while a platinum pseudo reference electrode was also fabricated on-chip, an eternal Ag/AgCl electrode was used in this work for better stability. A microSD pin-out was implemented to allow facile and rapid interconnection with external instrumentation. Each sensor comprised two fully passivated IDAs; the protonator IDA comprised 14 tines while the working IDA comprised 13 tines. The electrochemically active dimensions of each IDA tine were 50 nm high, 1 µm wide, and 45 µm long (defined by the width of the passivation window opening) while the gap between the tines in the neighbouring IDAs was 2 µm. The underlying titanium in the electrode metal stack formed a native oxide layer, when immersed in solution, and was thus electrochemically passivated. Fig. 2.2 (B) shows a sensor chip in a chip holder, prior to insertion into a PCB mounted microSD connector. The well in the centre has a volume of ~500 µL, sealed onto the chip using an o-ring, and aligned over the on-chip sensor electrodes. As part of the well, there was a space for the external reference electrode, allowing it to maintain in the solution during measurements.

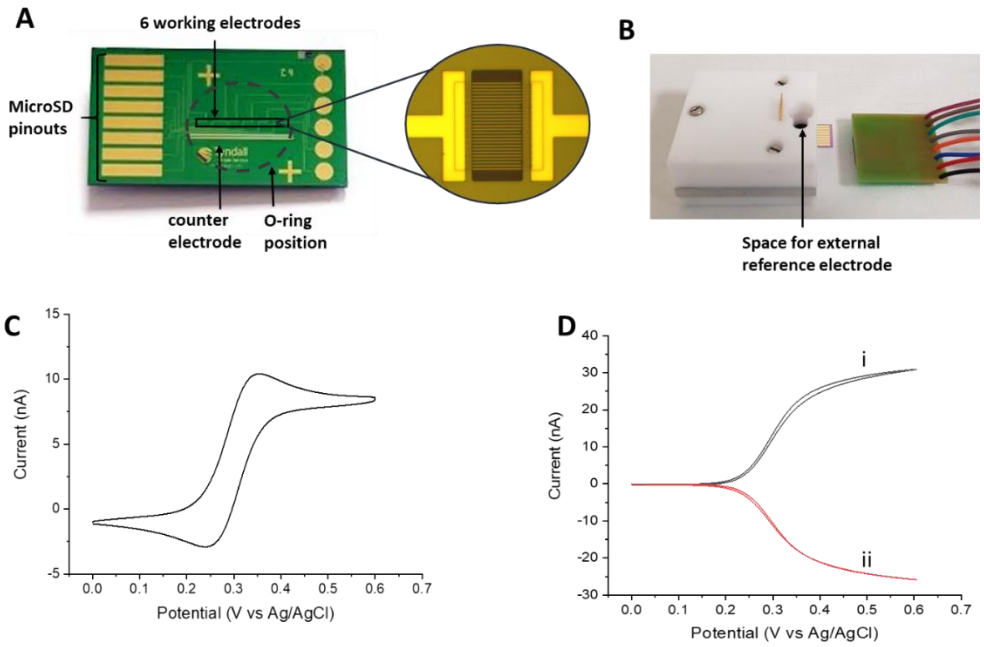

Fig. 2.2 (A) Picture of a fully integrated silicon sensor chip and optical micrograph of a sensor electrode comprising two interdigitated electrode arrays. The central dark rectangle region is the passivation window opening. (B) Electrochemical cell with sensor chip and a PCB microSD connector. (C) Typical cyclic voltammogram in 1 mM FCA in 10 mM PBS measured at an interdigitated electrode comb. (D) CVs at the generator and collector IDAs of 1 mM FCA in 10 mM PBS at a scan rate of 50 mV/s. The generator IDA (i) was cycled between 0 V and 0.6 V (vs Ag/AgCl) while the collector IDA (ii) was held at 0 V.

In Fig. 2.2 (C), a typical CV voltammogram obtained using a pristine cleaned gold working IDA is shown. The observed voltammogram exhibited a diffusion-limited behaviour consistent with a large microelectrode which arose from the radial diffusion profiles surrounding individual tines of an IDA overlapping, thus resulting in an overall time-dependent behaviour [23]. Sensors were then characterised in Generator-Collector mode and a typical voltammogram is presented in Fig. 2.2 (D). In this approach, the generator IDA first oxidised FCA to FCA^+ species which then diffused across the gap to the collector electrode where it was subsequently reduced back to FCA; establishing redox cycling resulting in higher measured currents. As a result of

redox cycling, the Generator–Collector voltammograms exhibited a quasi-steady-state, time independent behaviour typically associated with ultra-microelectrodes [33]. The collection efficiency of the sensor, which is a ratio of the collector to the generator currents, was determined to be ~84%. This thus suggested that 84% of protons, produced at a protonator IDA, would diffuse to the working IDA, and tailor the pH as desired.

2.3.2. Silver detection optimisation and performance in acidic media

The influence of the solution pH on silver deposition was evaluated by varying the buffer pH between pH 2 and pH 4.5. 1 µM $AgNO_3$ dissolved in 10 mM sodium acetate at different pH was electrodeposited at a working IDA at -0.2 V for 3 minutes. Following deposition, the silver was then stripped using SWV and the peak current was recorded. In Fig. 2.3 (A), representative stripping current peak heights measured for silver stripping at different pH are presented. The measurements were undertaken in duplicate for each pH, and the average values with standard deviation were plotted. Decreasing the pH from 4.5 led to a change in the measured stripping current with the maximum stripping peak current found to be between pH 2.5 and 3.0; pH 3 was thus selected as the pH of choice for further experiments as the most optimal pH for silver detection. The corresponding deposition currents are presented in Fig. S2.2 (A) with a change in deposition current magnitude observed with different pH. Following pH optimisation, the influence of reduction potential on the peak height was evaluated and optimised. A series of silver electro-reduction voltages were assessed by first electro-depositing silver at a selected voltage, followed by a SWV where the peak current was measured. Electro-reduction was undertaken in the voltage range of -0.1 V and -0.5 V. It can be seen in Fig. 2.3 (B), a maximum peak current was observed when using a

reduction potential of -0.2 V. Higher currents were measured at more cathodic potentials, this increase arose from the superimposition of an oxygen reduction signal onto the electrodeposition current; see Fig. S2.2 (B). To this end, -0.2 V was selected as the optimal for silver detection and used in further studies.

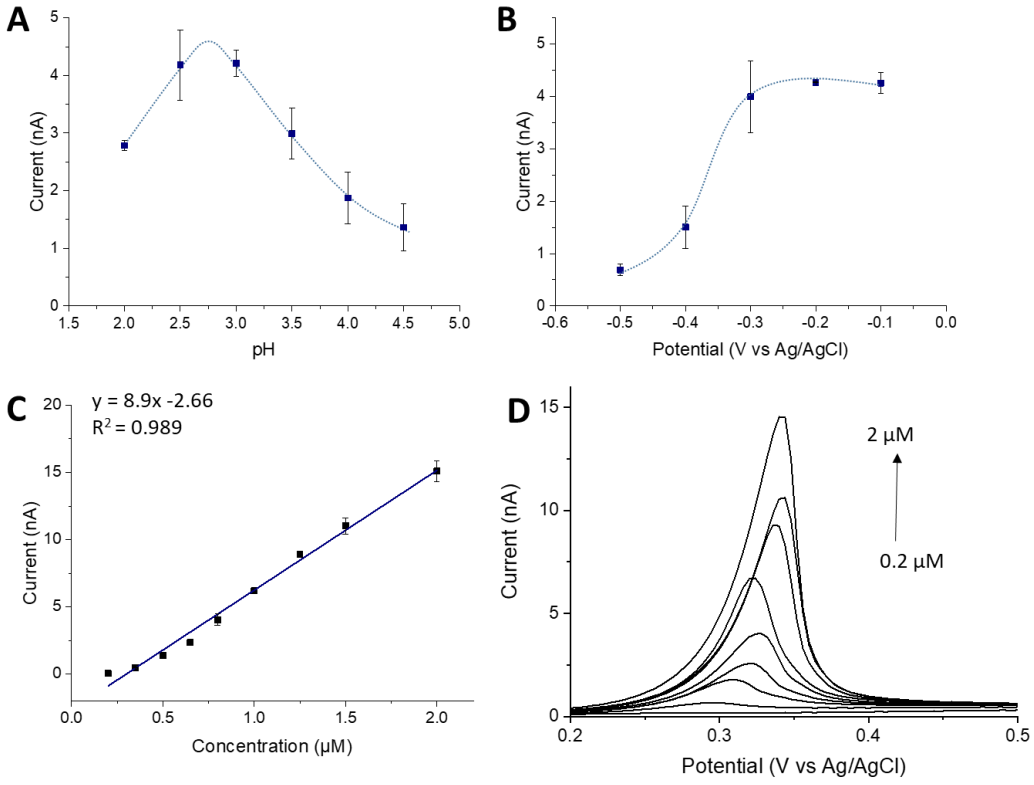

Fig. 2.3 (A) Influence of the pH of the solution on measured stripping current (peak height) for 1 µM of $AgNO_3$ in 10 mM sodium acetate when -0.2 V was applied for 3 minutes. The dotted line is a guide for the eye only. (B) Influence of deposition potential on measured stripping current (peak height) for 1 µM of $AgNO_3$ in 10 mM sodium acetate, pH 3, when the deposition was done for 3 minutes. The dotted line is a guide for the eye only. (C) Linear calibration curve corresponding to silver ions detection in 0.01 M sodium acetate, pH 3 for a gold working IDA. Deposition time: 4 minutes at -0.2 V. (D) Corresponding stripping peaks.

The deposition time used for silver ion deposition depended on the expected concentration of silver in the solution. In theory, the longer the deposition time, the lower the limit of detection for silver detection can be achieved. However, this must

be offset and balanced by an electrode potentially becoming saturated at higher silver concentrations. A series of deposition times were explored. Fig. 2.3 (C) shows the calibration line for silver in 10 mM sodium acetate, pH 3, when the deposition was 4 minutes while the Fig. 2.3 (D) shows the corresponding stripping peaks. The linear region was recorded between 0.2 - 2 µM. Increasing the deposition time to 5 minutes decreased the detection concentration to 0.1 µM. However, the response became nonlinear above 1 µM, consistent with an electrode becoming saturated. As a result, the calibration line with 5 minutes deposition time was between 0.1 - 1 µM; see Fig. S2.3.

2.3.3. In-situ electrochemical pH control: potential selection

As discussed previously, the pH of the solution greatly influenced the silver deposition process. Electro-generated in-situ pH control was explored to eliminate the requirement of sample acidification prior to the analysis. First, the potential to be applied at the protonator IDA had to be optimised. It is known that when undertaking cyclic voltammetry at a gold electrode, the positions of the gold oxide and reduction peaks vary, depending on the solution's pH [34]. In this manner, the voltage at which the gold oxide reduction peak maximum occurs may be used as an indicative measure of the pH of the solution at a sensor. To confirm this, cyclic voltammetry in 10 mM sodium acetate in the voltage range of 0.2 to 1.2 V was performed at pH 3 and pH 7.5 (the selected pH for silver detection and the pH of sodium acetate without acidification, respectively). The CVs are presented in Fig. 2.4 (A). At pH 7.5 the gold oxide reduction peak maximum was observed at 0.55 V. On the addition of nitric acid to acidify the sodium acetate buffer to pH 3, the gold oxide reduction peak moved anodically to 0.76 V, as expected. The decrease in the measured reduction peak area

arose from a limited amount of gold oxide formed due to the narrow potential window used; as the gold oxidation process would also have shifted to higher anodic voltages at this lower pH value.

Fig. 2.4 (B) shows a portion of cyclic voltammograms recorded at the working IDA in 10 mM sodium acetate solution when different potentials (1.55 to 1.7 V) were applied to the protonator IDA. On increasing the protonator potential, the gold oxide reduction peak was observed to move to higher anodic voltages consistent with a decrease in pH. In these experiments, an applied potential of 1.65 V yielded a maximum gold reduction peak at 0.76 V; which was the same location as data recorded in acidified sodium acetate pH 3; shown by the dashed line in Fig. 2.4 (B). Although the acetate buffer has a solution pH of 7.5 in the bulk away from the electrode, the local in-situ pH in the vicinity of the electrode was electrochemically tailored to pH 3.0 using this approach. Thus an applied voltage of 1.65 V was selected as the protonator voltage of choice.

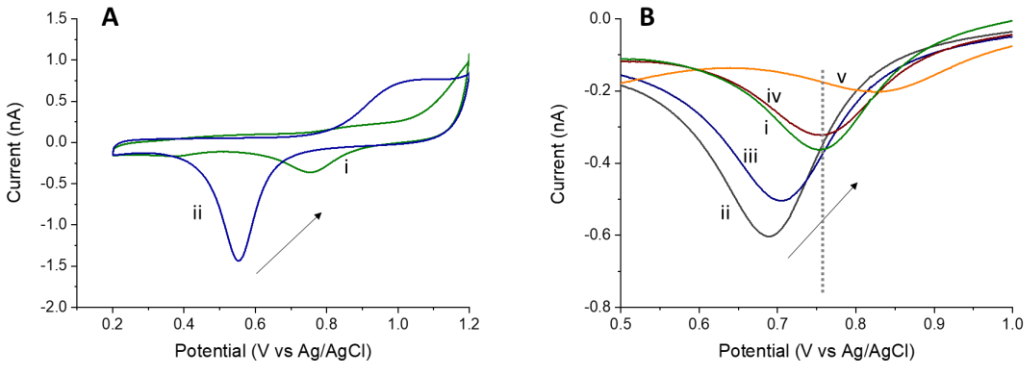

Fig. 2.4 (A) Cyclic voltammograms recorded in 10 mM sodium acetate at i) pH 3 and ii) 7.5 (B) Selected regions of the cycling voltammogram recorded in different solutions of 10 mM sodium acetate showing the gold oxide reduction peak at i) pH 3 when acidified with nitric acid and at pH 7.5 and also when applying potentials ii) 1.55; iii) 1.6; iv) 1.65V; v) 1.7 V to the protonator IDA. The dashed line shows the location of the gold oxide reduction peak maximum when 1.65 V was applied to the

protonator occurring at the same position as when the solution was acidified to pH 3 with nitric acid.

2.3.4. Silver detection using in-situ pH control in acetate buffer

The initial experiments to assess and optimise in-situ pH control were undertaken in 10 mM sodium acetate, as described previously. However, as shown in Fig. 2.5 (A), when 1.65 V was applied to a protonator IDA and a cathodic potential of -0.2 V was applied to the working IDA (during silver electrodeposition), the stripping peak for silver was significantly lower when compared to the stripping peak obtained using chemically acidified silver solutions. In addition, the measured current during deposition was significantly higher when using pH control (~ -40 nA at 100 s) compared to the deposition current in chemically acidified sodium acetate (~ -0.6 nA at 100 s); see Fig. S2.4. To explain this observation, we believe that this discrepancy may have arisen from competitive parallel electrochemical processes occurring at the sensors electrode in sodium acetate: namely silver electrodeposition and direct oxygen reduction. To explore this further, CVs were undertaken in 0.01 M sodium acetate using pristine gold working IDAs both with and without the protonator IDA biased at +1.65 V. The corresponding voltammograms are presented in Fig. S2.5 (A). A significant increase in anodic current was observed at ~ 1.2 V without the pH control and ~ 1.5 V when in-situ pH control (i.e., biasing the protonator) was applied. This current increase corresponds to the formation of a gold oxide layer at the gold working IDA, which is in accordance with the observation of Burke and Nugent [34]. This suggests that setting the protonator IDA to 1.65 V during silver detection could lead to the production of a significant amount of molecular oxygen. This argument is strongly supported by the significant current increase corresponding to gold oxide

reduction at potential ~ 0.6 V when pH control was applied. The cyclic voltammogram in sodium acetate, with applied pH control, also exhibits an increase of cathodic current starting around -0.2 V corresponding to the potential at which the oxygen begins to be reduced in the acidic conditions [35]. Consequently, applying a bias of 1.65 V to the protonator IDA results in the generation of molecular oxygen which diffuses to and is reduced at a working IDA biased at -0.2 V. This can explain the observed increase in the magnitude of deposition current (Fig. S2.4). Concerning analyte mass transfer transport, diffusion of silver ions to a working IDA is diffusion limited, as shown in Fig. 2.2 (C). However, diffusion of oxygen, generated along the entire length of a protonator IDA, to a sensing IDA will be radial in nature and will thus be more efficient. These competitive processes may thus result in the lower concentrations of silver deposited at the working IDA when in-situ pH control was used compared to the chemically modified solution.

Consequently, a trade-off was required between the applied protonator voltages versus the associated molecular oxygen formation. To this end, 1 µM $AgNO_3$ dissolved in 10 mM sodium acetate at pH 7.5 was deposited at the working IDA while different potentials, varying from 1.15 V to 1.65 V, were applied to the protonator IDA during deposition, followed by SWV, see Fig. 2.5 (A). It was observed that 1.25 V applied during deposition yielded the maximum stripping peak current and thus was selected for further experiments. The potential applied to a protonator IDA during stripping of silver electrodeposited at the working IDA was also optimised. It can be seen in Fig. 2.5 (B) that resetting the protonator voltage back to 1.65 V during SWV resulted in the highest stripping peak. This further supports the hypothesis that molecular oxygen formation was an interferent during deposition but not during the stripping process

due to the more anodic applied anodic potentials (too positive to enable oxygen reduction).

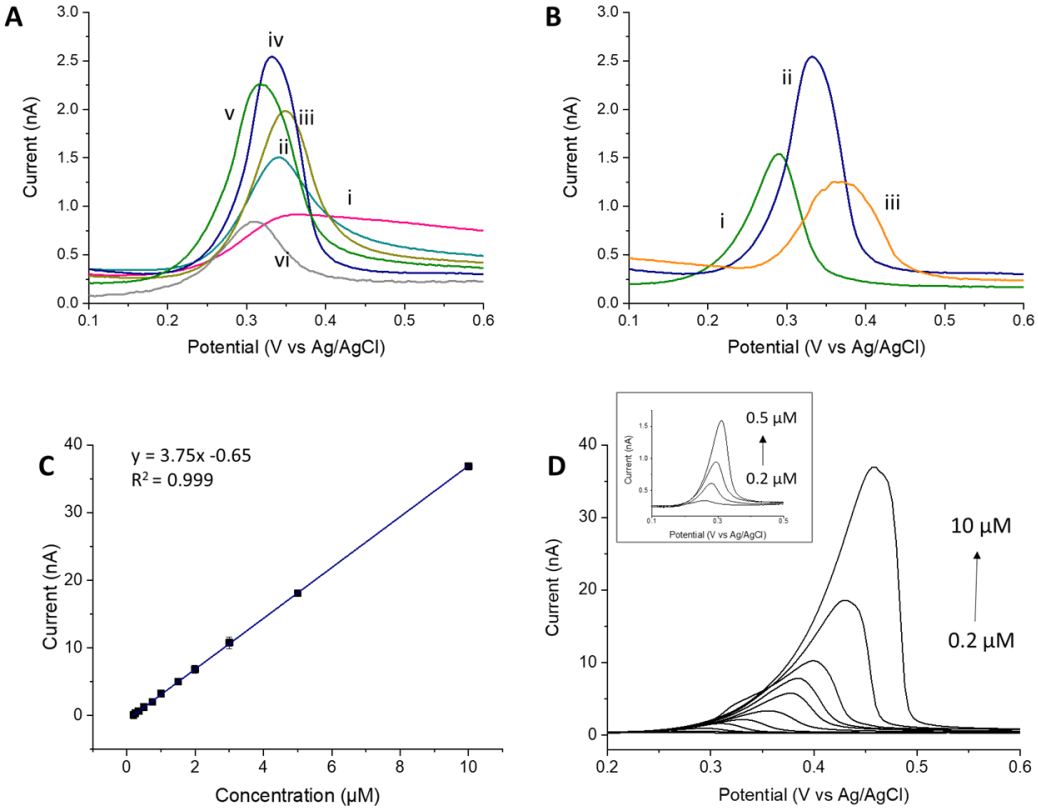

Fig. 2.5 Square Wave Voltammograms for 1 µM of AgNO3 in 10 mM sodium acetate pH 7.5 when (A) i) 1.65 V; ii) 1.45 V; iii) 1.35 V; iv) 1.25 V v) 1.15 V and vi) no potential was applied to protonator IDA during silver deposition, while 1.65 V was applied during stripping (B) 1.25 V was applied to the protonator IDA during deposition while i) 1.55 V; ii) 1.65 V and iii) 1.75 V was applied during stripping. (C) Linear calibration curve corresponding to silver ions detection using pH control. The measurements were done in 10 mM sodium acetate pH 7.5 with 1.25 V applied at protonator IDA during deposition and 1.65 V during stripping. Deposition time: 3 minutes at -0.2 V. (D) Corresponding stripping peaks. Inset: Stripping peaks for the lowest concentrations.

A silver detection calibration was then undertaken in the concentration range from 0.2 to 10 µM (10 mM sodium acetate, deposition time: three minutes) using the in-situ electro-generated pH control method and the resulting plot is presented in Fig. 2.5 (C).

The data points represent the mean value of three replicate measurements, with the error bars representing one standard deviation. The calibration curve exhibited excellent linearity with R^2 of 0.999 and a wide linear dynamic range of 0.2–10 µM with the lowest limit of detection (LOD) of 13 nM, calculated using the equation:

$$LOD = 3.3 \times SD \div s \quad (2.4).$$

Where SD is the standard deviation of the blank solution and s is the slope. These results highlight the suitability of the proposed approach for the electrochemical detection of silver using in-situ pH control. Fig. 2.5 (D) shows the corresponding stripping voltammograms for the different concentrations and a clear anodic shift of the stripping peak with increased concentration of silver was noted. Fig. 2.5 (D): inset shows the stripping peaks in the lowest concentrations (0.2–0.5 µM) for their better evaluation. A similar potential shift in detection of silver ions was reported in a previous study [16] and it can be explained with the Nernst equation where, with increased concentration of Ag ions, the equilibrium potential of Ag/Ag+ increase. The potential was stable for triplicate measurements at the same concentration, see Fig. S2.6.

2.3.5. Silver detection using in-situ pH control in tap water

Having shown a proof of concept of silver detection using in-situ pH control in sodium acetate buffer as described above, the developed method was applied and optimised for potable tap water. Typically, the pH of drinking water varies between 6.5 to 8.5 [36] and may need to be adjusted and optimised before silver detection, i.e., pH 3. A CV was undertaken in tap water with 1.65 V applied to the protonator IDA; see Fig. S2.7. It was observed that oxygen reduction in tap water requires a more cathodic

potential (~ -0.5 V) compared to sodium acetate (~ -0.2 V) which suggested that the competitive process, described above, should not significantly interfere with silver deposition. To this end, in-situ pH control was undertaken by applying the desired 1.65 V to the protonator during both the silver deposition and stripping steps.

Tap water was spiked with 1 µM $AgNO_3$ as silver was not present at detectable levels in water in our lab, which was confirmed with water analysis. No additional supporting electrolyte was added to the test to verify that the sensor could be used for real time tap water detection. Fig. 2.6 (A) shows the square wave voltammograms in tap water, both with and without pH control. We note that the silver stripping peaks shifted to more cathodic values, and the peaks became higher and sharper when compared to measurements undertaken in sodium acetate buffer (the silver stripping peaks measured in sodium acetate with and without pH control are included in Fig. 2.6 (A) for comparison). The cathodic shift and change in the voltammetric profile can likely be attributed to the presence of chloride ions due to the disinfection of tap water with chlorine. Therefore, the stripping peak in tap water corresponded to an $AgCl^-$ complex, instead of Ag^+ ion as detected in sodium acetate, following the mechanism previously described by Saterlay et al. [30]. In their work the process of a peak sharpening upon complexation of silver with chloride was used for its beneficial analytical applications, with KCl added to the sample after optimisation, following the equations:

$$Ag_{(s)} + Cl^- \leftrightarrow AgCl_{(s)} + e^- \quad (2.5)$$

$$AgCl_{(s)} + Cl^- \leftrightarrow AgCl^-_{2(aq)} \quad (2.6)$$

$$AgCl^-_{2(aq)} \rightarrow bulk\ solution \quad (2.7)$$

In this work, chlorine was naturally present in excess in tap water due to the chlorination, which is a water disinfection process the most commonly used in Ireland

and worldwide [37, 38]. These results show that the pH control approach works for both silver ions and silver complexes. Thus, no additional reagent had to be added to enhance silver detection. Regardless of the form of chlorine used (gaseous chlorine, calcium hypochlorite or sodium hypochlorite), a combination of hypochlorous acid (HOCl) and hypochlorite ion (OCl^-) will be present in tap water as "free available chlorine" at levels between 0.2 g/L and 1 mg/L to assure the safety of water [5, 39].

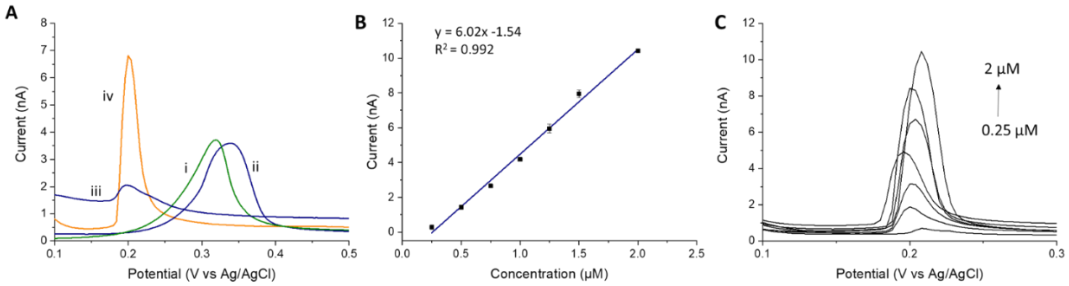

Fig. 2.6 (A) Square Wave Voltammograms of 1 µM AgNO3 in i) 10 mM sodium acetate pH 3; ii) 10 mM sodium acetate at pH 7.5 when pH control was applied (1.25 V at the protonator IDA during deposition and 1.65 V during stripping); iii) tap water at pH 7; iv) tap water when pH was applied (1.65 V at the protonator IDA during deposition and stripping). Conditions for the experiment were: deposition at -0.2 V for 3 minutes. (B) Linear calibration curve corresponding to silver ions detection in tap water. Conditions for the experiment were: deposition at -0.2 V for 2 minutes, 1.65 V at protonator IDA during deposition, and stripping. (C) Corresponding stripping peaks.

Since the measured silver species changed from an Ag^+ ion to AgCl complex, an additional calibration line was established for tap water. First it was observed that a deposition time of three minutes (as used previously) resulted in an electrode becoming saturated with silver chloride at concentrations above 1 µM of $AgNO_3$. For this reason, the deposition time was reduced to two minutes. This resulted in both a wider linear dynamic range and provided a faster time to result. A linear calibration plot for silver detection in tap water, using in-situ electro-generated pH control, was found between 0.25 and 2 µM, see Fig. 2.6 (B) and the LOD was found to be 106 nM.

The data points represent the mean value of three replicate measurements, with the error bars representing 1 standard deviation. The calibration curve exhibited excellent linearity with R^2 of 0.992. The corresponding stripping peaks are presented on Fig. 2.6 (C) and it is important to highlight that the peak did not move with increased Ag^+ concentration as expected According to Nernst equation, the peak potential depends just on chloride concentration [40, 41]. Considering that in our experiments chloride concentration is constant, the peak potential remains in the same position. This confirm confirms our thesis that the reaction detected in tap water is the oxidation of silver to silver chloride.

Table 2.1 Comparison of silver detection studies using anodic sweep voltammetry

Electrode	Linear Range µM	Sensitivity mA μM^{-1} cm^{-2}	LOD nM	Solution pH	Real samples	Ref
NBHAE-MCPE	0.0046 - 1.85	1.787	0.85	9.5	X-ray films, Water samples	[19]
NanoAg-MWCNTs-MCPE	0.0005 - 0.28	4.97	0.12	5 2 (real samples)	Tap, river, ground water	[42]
GCE-ABP	0.05 - 1	0.548	25	5.2	Tap, river water	[32]
GaN MPE	0.092 - 9.27	0.113	30.6	5.2	Tap water	[16]
Au-SC	0.0005 - 1000	0.0000465	0.02	-	Tap, river water	[43]
BDD	0.01 - 0.08	8.778 0.00877 with SO_4^{2-}	0.2	5.2	Soap water	[15]
GCE-TCA	0.05 - 3	0.0167	10	4.5	Tap, Lake, Synthesized water	[44]
Pt-PTH	0.649 - 9.27	0.282	556	5	Wastewat	[45]
CPE-2-HBBH	0.0000093 - 0.00037	0.863	0.0093	5.5 1 (real samples)	River Water	[18]
Au-IDA (sodium acetate)	**0.2 - 10**	**0.641**	**13**	**7.5**	**Tap water**	**This Work**
Au-IDA (tap water)	**0.25 - 2**	**1.029**	**106**	**7.5**		

NBHAE: N,N0-bis(2-hydroxybenzylidene)-2,20(amino-phenylthio)ethane, **MCPE**: modified carbon paste electrode, **NanoAg**: nanosized silver IIP, **MWCNTs**: multi-walled carbon nanotubes, **GCE**: Glassy Carbon Electrode, **ABP**: (2-Aminoethyl)-4,4'-

Bipyridine, **MPE**: Micropillar electrode, **SC**: Single Cytosine, **BDD**: Boron Doped Diamond, **TCA**: 4tertbutyl1(ethoxycarbonylmethoxy)thiacalixarene, **CPE**: Carbon Paste Electrode, **PTH**: polythiophene, **CPE**: Carbon Paste Electrode, **2-HBBH**: 2-hydroxybenzaldehyde benzoylhydrazone, **HA**: heptylsulfonic acid, **IDA**: interdigitated microelectrode array

Table 2.1 summarises other studies describing detection of silver ions in aqueous samples using ASV. Although several authors have reported electrochemical approaches for silver detection in tap water, most of these reports had to (i) first acidify the solution using an acid [10, 18] and/or (ii) add additional electrolyte before performing the measurements [19, 20] to obtain optimal pH for silver detection, see Table 2.1. To the best of our knowledge, none of these papers have reported silver detection using in-situ pH control. Moreover, our sensor exhibited excellent sensitivity comparable to other authors. We believe that the LOD could be further increased if the electrode modification/ increased time of deposition. The limitation of the presented study is a need for the optimisation of the potential applied to the generator electrode, depending on the matrix of the sample as the potential at which the oxygen is reduced may vary. Our results have suggested that silver detection efficiency was improved with the chloride ions present in tap water. Based on Saterlay et al. [30] the intensity of the AgCl peak will depend on the concentration of chloride in the water, which they have shown by undertaking measurements with different concentrations of KCl. This suggests that the concentration of chlorine in the tap water could be another limiting factor for the presented technique. Based on WHO guidelines, chlorine is present in most disinfected tap water at a concentration between 0.2 mg/L and 1 mg/L [5]. This means there should be a sufficient amount of chlorine present to allow the detection of the target silver concentrations (0.1 mg/L). Using this approach and the sensors developed herein, silver detection may be undertaken in previously

chlorinated tap water without the addition of electrolyte, acid, or base when a prior calibration is done. If insufficient concentration of chlorine was present (<0.1 mg/L) in solution, the additional chloride salt may need to be added.

2.4. Conclusions

We present an easy and quick technique that employs interdigitated electrodes for silver detection in sodium acetate and tap water using an electro generated in-situ pH control method. Silver detection was undertaken using square wave voltammetry at a working IDA with simultaneous production of hydrogen ions at a protonator IDA which allowed the pH to be tailored in the vicinity of the sensor. In addition, the complexation of the silver ions with chlorine present in tap water enabled more sensitive detection and faster time-to-result with no addition of electrolytes. The sensors have the potential to be directly deployed for real time detection in water utility systems as well as in estuarine or marine waters, without the need for preconditioning of a sample. There might be a need for adding chloride salt prior to measurement if other than chlorination disinfection process was used as well as optimising the potential applied at the protonator IDA according to the sample matrix.

2.5. References

1. G. Oberdörster, V. Stone, and K. Donaldson, *Toxicology of nanoparticles: a historical perspective.* Nanotoxicology, 2007. **1**(1): p. 2-25.
2. R. Behra, L. Sigg, M.J. Clift, F. Herzog, M. Minghetti, B. Johnston, et al., *Bioavailability of silver nanoparticles and ions: from a chemical and biochemical perspective.* Journal of the Royal Society Interface, 2013. **10**(87): p. 20130396.
3. S.-j. Yu, Y.-g. Yin, and J.-f. Liu, *Silver nanoparticles in the environment.* Environmental Science: Processes & Impacts, 2013. **15**(1): p. 78-92.
4. K.D. Rosenman, A. Moss, and S. Kon, *Argyria: clinical implications of exposure to silver nitrate and silver oxide.* Journal of occupational medicine.: official publication of the Industrial Medical Association, 1979. **21**(6): p. 430-435.
5. WHO, *Guidelines for drinking-water quality, 4th edition, incorporating the 1st addendum*, 2017, World Health Organization: Geneva, 564, https://www.who.int/publications/i/item/9789241549950
6. US EPA, *2018 Edition of the Drinking Water Standards and Health Advisories Tables* 2018, United States Environmental Protection Agency Washington, DC, https://www.epa.gov/sites/production/files/2018-03/documents/dwtable2018.pdf
7. M. Karimi, S. Mohammadi, A. Mohadesi, A. Hatefi-Mehrjardi, M. Mazloum-Ardakani, L.S. Korani, et al., *Determination of silver (I) by flame atomic absorption spectrometry after separation/preconcentration using modified magnetite nanoparticles.* Scientia Iranica, 2011. **18**(3): p. 790-796.

8. Z. Gao, G.G. Liu, H. Ye, R. Rauschendorfer, D. Tang, and X. Xia, *Facile colorimetric detection of silver ions with picomolar sensitivity.* Analytical chemistry, 2017. **89**(6): p. 3622-3629.
9. T. Anand, G. Sivaraman, P. Anandh, D. Chellappa, and S. Govindarajan, *Colorimetric and turn-on fluorescence detection of Ag (I) ion.* Tetrahedron Letters, 2014. **55**(3): p. 671-675.
10. A. Afkhami, A. Shirzadmehr, T. Madrakian, and H. Bagheri, *New nano-composite potentiometric sensor composed of graphene nanosheets/thionine/molecular wire for nanomolar detection of silver ion in various real samples.* Talanta, 2015. **131**: p. 548-555.
11. A. Waheed, M. Mansha, and N. Ullah, *Nanomaterials-based electrochemical detection of heavy metals in water: current status, challenges and future direction.* TrAC Trends in Analytical Chemistry, 2018. **105**: p. 37-51.
12. C. Barrett, K. Dawson, C. O'Mahony, and A. O'Riordan, *Development of low cost rapid fabrication of sharp polymer microneedles for in vivo glucose biosensing applications.* ECS Journal of Solid State Science and Technology, 2015. **4**(10): p. S3053-S3058.
13. K. Dawson, A. Wahl, S. Barry, C. Barrett, N. Sassiat, A.J. Quinn, et al., *Fully integrated on-chip nano-electrochemical devices for electroanalytical applications.* Electrochimica Acta, 2014. **115**: p. 239-246.
14. B. Patella, R. Inguanta, S. Piazza, and C. Sunseri, *Nanowire ordered arrays for electrochemical sensing of H2O2.* Chemical Engineering Transactions, 2016. **47**: p. 19-24.
15. E. Culková, Z. Lukáčová-Chomisteková, R. Bellová, D. Melicherčíková, J. Durdiak, M. Rievaj, et al., *Voltammetric detection of silver in commercial*

products on boron doped diamond electrode: stripping at lowered potential in the presence of thiosulfate ions. Monatshefte für Chemie-Chemical Monthly, 2020: p. 1-9.

16. Q. Liu, J. Li, W. Yang, X. Zhang, C. Zhang, C. Labbé, et al., *Simultaneous detection of trace Ag (I) and Cu (II) ions using homoepitaxially grown GaN micropillar electrode.* Analytica Chimica Acta, 2020. **1100**: p. 22-30.
17. T.J. Davies, *Anodic stripping voltammetry with graphite felt electrodes for the trace analysis of silver.* Analyst, 2016. **141**(15): p. 4742-4748.
18. H. El-Mai, E. Espada-Bellido, M. Stitou, M. García-Vargas, and M.D. Galindo-Riaño, *Determination of ultra-trace amounts of silver in water by differential pulse anodic stripping voltammetry using a new modified carbon paste electrode.* Talanta, 2016. **151**: p. 14-22.
19. H.H. Nadiki, M.A. Taher, H. Ashkenani, and I. Sheikhshoai, *Fabrication of a new multi-walled carbon nanotube paste electrode for stripping voltammetric determination of Ag (I).* Analyst, 2012. **137**(10): p. 2431-2436.
20. S. Jahandari, M.A. Taher, H. Fazelirad, and I. Sheikhshoai, *Anodic stripping voltammetry of silver (I) using a carbon paste electrode modified with multi-walled carbon nanotubes.* Microchimica Acta, 2013. **180**(5-6): p. 347-354.
21. M. Javanbakht, F. Divsar, A. Badiei, F. Fatollahi, Y. Khaniani, M.R. Ganjali, et al., *Determination of picomolar silver concentrations by differential pulse anodic stripping voltammetry at a carbon paste electrode modified with phenylthiourea-functionalized high ordered nanoporous silica gel.* Electrochimica acta, 2009. **54**(23): p. 5381-5386.
22. S.X. Guo and S.B. Khoo, *Highly selective and sensitive determination of silver (I) at a poly (8-mercaptoquinoline) film modified glassy carbon electrode.*

Electroanalysis: An International Journal Devoted to Fundamental and Practical Aspects of Electroanalysis, 1999. **11**(12): p. 891-898.

23. A. Wahl, S. Barry, K. Dawson, J. MacHale, A. Quinn, and A. O'Riordan, *Electroanalysis at ultramicro and nanoscale electrodes: a comparative study.* Journal of The Electrochemical Society, 2014. **161**(2): p. B3055-B3060.
24. K. Dawson, A.l. Wahl, R. Murphy, and A. O'Riordan, *Electroanalysis at single gold nanowire electrodes.* The Journal of Physical Chemistry C, 2012. **116**(27): p. 14665-14673.
25. P. Sidambaram and J. Colleran, *Nanomole Silver Detection in Chloride-Free Phosphate Buffer Using Platinum and Gold Micro- and Nanoelectrodes.* Journal of the Electrochemical Society, 2019. **166**(6): p. B532-B541.
26. Y. Zhang, G.M. Zeng, L. Tang, J. Chen, Y. Zhu, X.X. He, et al., *Electrochemical sensor based on electrodeposited graphene-Au modified electrode and nanoAu carrier amplified signal strategy for attomolar mercury detection.* Analytical chemistry, 2015. **87**(2): p. 989-996.
27. A. Zeng, E. Liu, S. Tan, S. Zhang, and J. Gao, *Stripping Voltammetric Analysis of Heavy Metals at Nitrogen Doped Diamond-Like Carbon Film Electrodes.* Electroanalysis: An International Journal Devoted to Fundamental and Practical Aspects of Electroanalysis, 2002. **14**(18): p. 1294-1298.
28. B. Patella, C. Sunseri, and R. Inguanta, *Nanostructured based electrochemical sensors.* Journal of nanoscience and nanotechnology, 2019. **19**(6): p. 3459-3470.
29. T.L. Read, E. Bitziou, M.B. Joseph, and J.V. Macpherson, *In situ control of local pH using a boron doped diamond ring disk electrode: optimizing heavy metal (mercury) detection.* Analytical chemistry, 2014. **86**(1): p. 367-371.

30. A.J. Saterlay, F. Marken, J.S. Foord, and R.G. Compton, *Sonoelectrochemical investigation of silver analysis at a highly boron-doped diamond electrode.* Talanta, 2000. **53**(2): p. 403-415.

31. A. Mohadesi and M.A. Taher, *Stripping voltammetric determination of silver (I) at carbon paste electrode modified with 3-amino-2-mercapto quinazolin-4 (3H)-one.* Talanta, 2007. **71**(2): p. 615-619.

32. M.-C. Radulescu, A. Chira, M. Radulescu, B. Bucur, M.P. Bucur, and G.L. Radu, *Determination of silver (i) by differential pulse voltammetry using a glassy carbon electrode modified with synthesized N-(2-Aminoethyl)-4, 4'-Bipyridine.* Sensors, 2010. **10**(12): p. 11340-11351.

33. A.J. Wahl, I.P. Seymour, M. Moore, P. Lovera, A. O'Riordan, and J.F. Rohan, *Diffusion profile simulations and enhanced iron sensing in generator-collector mode at interdigitated nanowire electrode arrays.* Electrochimica Acta, 2018. **277**: p. 235-243.

34. L. Burke and P. Nugent, *The electrochemistry of gold: I the redox behaviour of the metal in aqueous media.* Gold Bulletin, 1997. **30**(2): p. 43-53.

35. N. Alexeyeva, T. Laaksonen, K. Kontturi, F. Mirkhalaf, D.J. Schiffrin, and K. Tammeveski, *Oxygen reduction on gold nanoparticle/multi-walled carbon nanotubes modified glassy carbon electrodes in acid solution.* Electrochemistry communications, 2006. **8**(9): p. 1475-1480.

36. WHO, *pH in Drinking-water. Revised background document for development of WHO Guidelines for Drinking-water Quality* 2007, World Health Organization: https://www.who.int/water_sanitation_health/dwq/chemicals/ph_revised_2007_clean_version.pdf

37. J.G. Jacangelo and R.R. Trussell, *International report: Water and wastewater disinfection-trends, issues and practices.* Water science and technology: water supply, 2002. **2**(3): p. 147-157.

38. EPA Ireland, *The Provision and Quality of Drinking Water in Ireland. A Report for the Year 2010*, 2011, Environmental Protection Agency: Wexford, 126, https://www.epa.ie/pubs/reports/water/drinking/drinkingwaterreport2010.html

39. I. Seymour, B. O'Sullivan, P. Lovera, J.F. Rohan, and A. O'Riordan, *Electrochemical detection of free-chlorine in Water samples facilitated by in-situ pH control using interdigitated microelectrodes.* Sensors and Actuators B: Chemical, 2020. **325**: p. 128774.

40. F. Pargar, H. Kolev, D.A. Koleva, and K. van Breugel, *Potentiometric response of Ag/AgCl chloride sensors in model alkaline medium.* Advances in Materials Science and Engineering, 2018. **2018**.

41. D. Tao, L. Jiang, and M. Jin, *A Method of Preparation of Ag/AgCl Chloride Selective Electrode.* Journal of Wuhan University of Technology-Mater. Sci. Ed., 2018. **33**(4): p. 767-771.

42. R. Zhiani, M. Ghanei-Motlag, and I. Razavipanah, *Selective voltammetric sensor for nanomolar detection of silver ions using carbon paste electrode modified with novel nanosized Ag (I)-imprinted polymer.* Journal of Molecular Liquids, 2016. **219**: p. 554-560.

43. J.H. Kim, K.B. Kim, J.S. Park, and N. Min, *Single cytosine-based electrochemical biosensor for low-cost detection of silver ions.* Sensors and Actuators B: Chemical, 2017. **245**: p. 741-746.

44. F. Wang, C. Xin, Y. Wu, Y. Gao, and B. Ye, *Anodic stripping voltammetric determination of silver (I) in water using a 4-tert-butyl-1*

(ethoxycarbonylmethoxy) thiacalix [4] arene modified glassy carbon electrode. Journal of Analytical Chemistry, 2011. **66**(1): p. 60-65.

45. H. Zejli, J.H.-H. de Cisneros, I. Naranjo-Rodriguez, and K. Temsamani, *Stripping voltammetry of silver ions at polythiophene-modified platinum electrodes.* Talanta, 2007. **71**(4): p. 1594-1598.

2.6. Supporting information

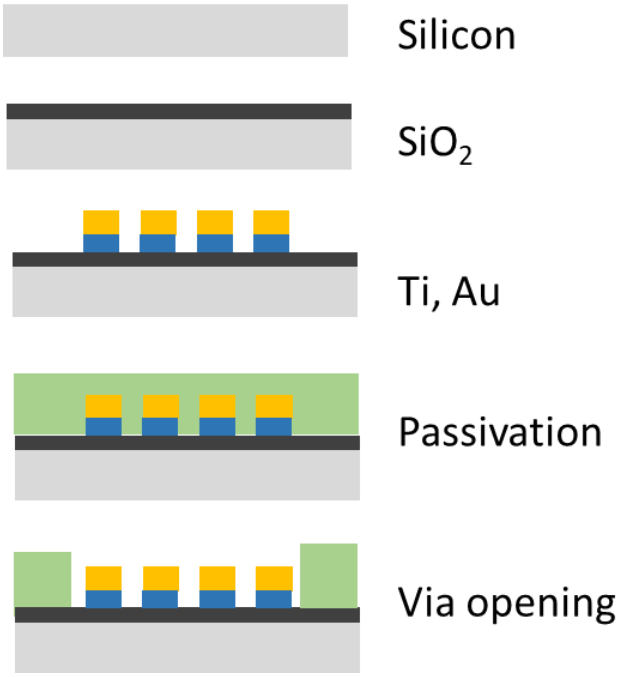

Fig. S2.1 Schematic of the fabrication steps employed in sensor fabrication.

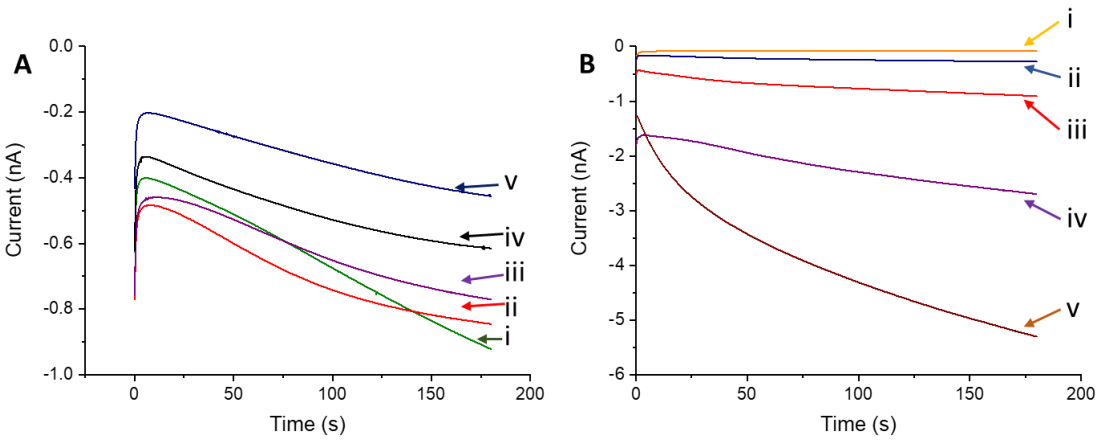

Fig. S2.2 (A) Influence of different pH of a solution on corresponding silver deposition currents recorded for 1 µM of AgNO3 in 10 mM sodium acetate, deposited at -0.2 V for 3 minutes at i) pH 2; ii) pH 3; iii) pH 3.5; iv) pH 4; v) pH 4.5 (B) Influence of different potential applied during silver deposition on corresponding currents recorded for 1 µM of AgNO3 in 10 mM sodium acetate, pH 3, deposited for 3 minutes at i) -0.1 V; ii) -0.2 V; iii) -0.3 V; iv) -0.4 V; v) -0.5 V.

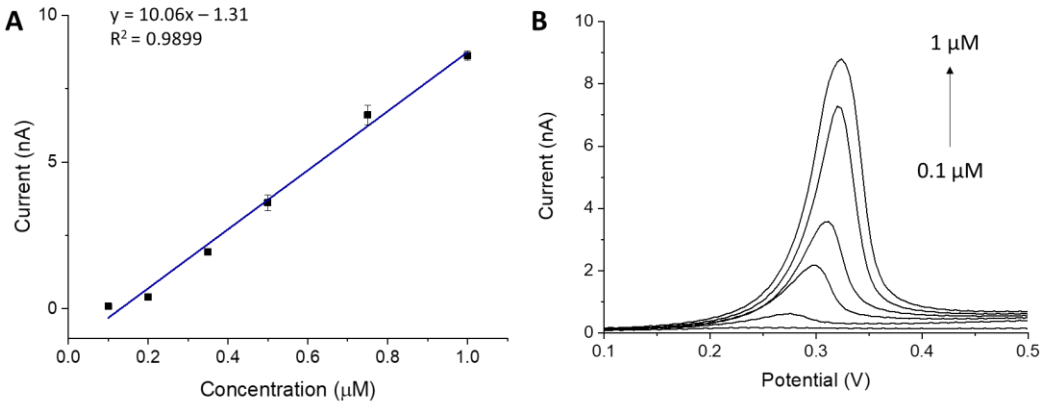

Fig. S2.3 (A) Linear calibration curve corresponding to silver ions detection in 0.01 M sodium acetate, pH 3 for an unmodified gold working IDA. Deposition time: 5 minutes at -0.2 V. (B) Corresponding stripping peaks.

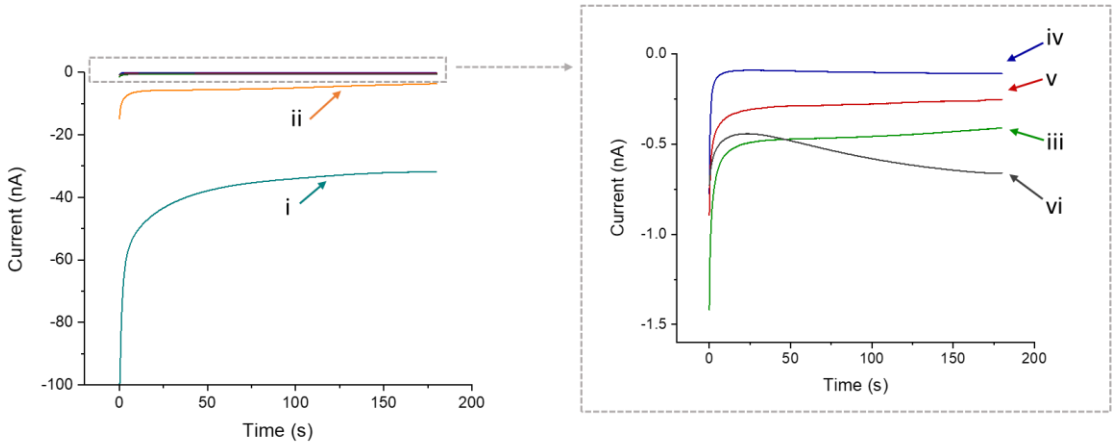

Fig. S2.4 Influence of potential applied to the protonator IDA during deposition of 1 µM AgNO3 in 10 mM sodium acetate, pH 7.5 at -0.2 V for 3 minutes on corresponding current when i) 1.65 V; ii) 1.45 V; iii) 1.35 V; iv) 1.25 V; v) no potential; was applied; while v) current during deposition of 1 µM of AgNO3 in 10 mM sodium acetate, pH 3 at -0.2 V for 3 minutes.

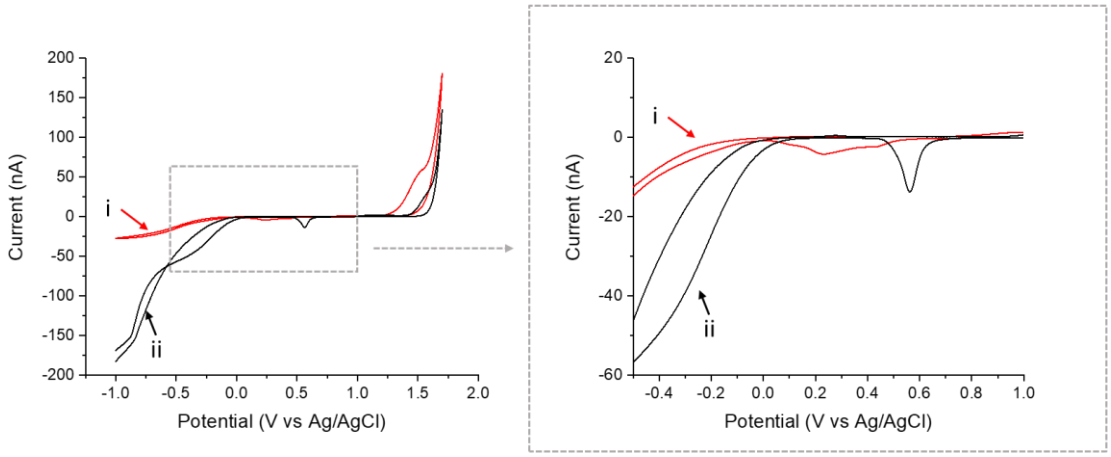

Fig. S2.5 Cyclic voltammograms recorded in i) 10 mM sodium acetate, pH 7.5 and ii) 10 mM sodium acetate, pH 7.5 with 1.65 V applied at the protonator electrode.

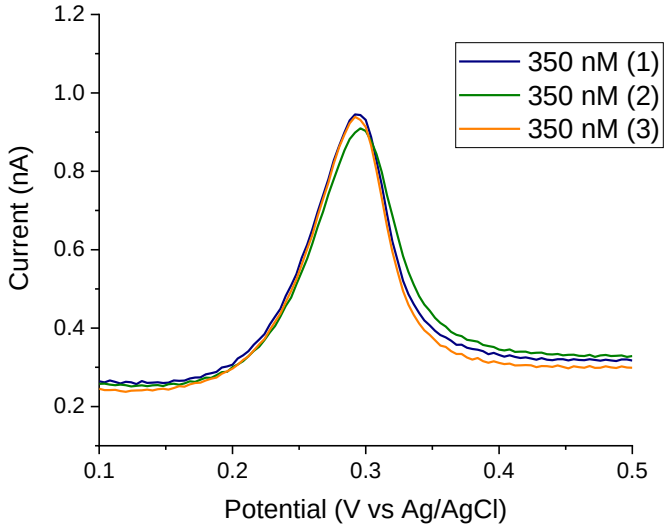

Fig. S2.6 Square Wave Voltammograms for three separate measurements of 350 nM AgNO3 in sodium acetate using in-situ pH control. The measurements were done in 10 mM sodium acetate pH 7.5 with 1.25 V applied at protonator IDA during deposition and 1.65 V during stripping. Deposition time: 3 minutes at -0.2 V.

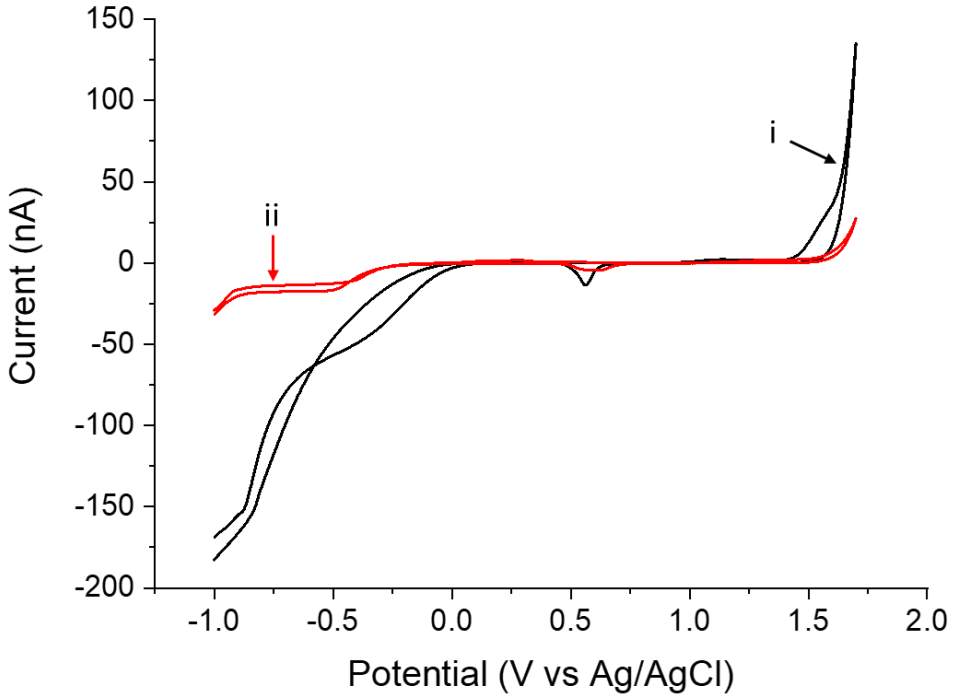

Fig. S2.7 Cyclic voltammograms recorded in i) 10 mM sodium acetate, pH 7.5 with 1.65 V applied at the protonator electrode and ii) tap water with 1.65 V applied at the protonator electrode.

Chapter 3. Highly sensitive electrochemical sensor for the detection of Shiga toxin-producing *E. coli* using interdigitated micro-electrodes selectively modified with a chitosan-gold nanocomposite

Published in “Electrochimica acta”

DOI 10.1016/j.electacta.2022.140748

3.1. Introduction

Shiga toxin-producing *E. coli* (STEC) is a food-borne pathogen of a great public health concern, which can cause severe illness including haemolytic uremic syndrome (HUS), that may even lead to death [1]. Cattle are known to be their main reservoir, and the most typical source of infection is via the consumption of contaminated undercooked beef meat [2, 3]. Since most *E. coli* are harmless and a part of healthy gut flora in humans and animals, specific detection of STEC is crucial for preventing infections. Since the big multi-national STEC O104 outbreak in Germany in 2011, plus an increasingly wide range of STEC serogroups linked to human illness, the targets for detection have shifted off from serogroup-based approaches towards targeting the genes coding for Shiga toxin production (*stx1* or *stx2*); which are major virulence factors of STEC [4, 5]. The foremost common technique for DNA-based detection is polymerase chain reaction (PCR), in which the specific target sequence from the DNA extracted from the organism is amplified, significantly increasing the sensitivity of the method. Especially real-time PCR (qPCR) found a large application in pathogens during which the number of amplified DNA at a particular time is monitored using fluorescent probes [6]. This approach offers significant advantages like high sensitivity and selectivity, however, it is time-consuming and requires highly trained staff to perform experiments, making it unsuitable for point-of-use detection [7, 8].

A potential alternative is to employ solid-state electrochemical DNA biosensors, comprising a probe DNA as a recognition element and a transducer, which provides a measurable signal following a DNA hybridisation event [9]. Their advantages over traditional techniques include the speed in obtaining results, simplicity of use, and suitability for miniaturisation and portability [10]. The key aspects to consider when

developing DNA-based electrochemical biosensors are (i) sensor miniaturisation [11] (ii) requirements for robust probe attachment [12], and (iii) detection methods with low complexity [13], all of which have enormous impacts on the ultimate performance and use. Miniaturised electrochemical sensors (<10 μm diameter) benefit from enhanced analyte mass transport, reduced background noise, and high current densities making them an ideal choice for point-of-use sensors.

Interdigitated microelectrodes (IDEs), comprising two comb-like closely spaced electrodes which are individually electrically connected, have found several applications in point-of-use sensing [14]. For instance, they have recently been applied for the detection of a variety of heavy metal species in water where one comb was used as a working electrode and the other as a generator electrode, allowing electrochemical modification of local pH for improving sensing efficacy [15, 16]. They have also been applied to DNA detection where the probe DNA was either immobilised on both IDEs [17] or the silicon surface between them [18-20]. Typically, the DNA hybridisation was detected using conductance measured between the two IDEs or impedance, when IDEs were used. Selective modification of only one IDE could enable using the other IDE for other function that sensing as well as using other techniques for DNA detection, such as linear sweep voltammetry. It is a straightforward electrochemical technique that has been applied for DNA detection using redox-active molecules, such as methylene blue (MB) [21], anthraqinone-2-sulfonic acid monohydrate sodium salt (AQMS) [22] or daunomycin (DNR) [23]. These molecules have different interaction mechanisms to single-stranded (ssDNA) and double-strand DNA (dsDNA). The advantages of such an approach include the short time needed to obtain results and the simplicity of the system.

The attachment of probe DNA in a stable and robust manner remains a key challenge in electrochemical sensor development [12]. In this regard, chitosan, a natural polymer, has gained a lot of attention as it is rich in amine groups, thereby allowing subsequent covalent attachment of a range of biomolecules [24]. It has been widely used in the development of DNA-based biosensors, where typically the probe DNA modified with an amine group is attached to the polymer using glutaraldehyde as a linker [21, 25]. Since it is a non-conductive polymer, several researchers have combined it with other conductive 0D, 1D, and 2D materials [26], [27], [28], [29] to enhance the electrical conductivity and therefore the sensitivity of detection. For instance, Singh et al. [21] modified the surface of indium tin oxide (ITO) electrode with graphene oxide-chitosan nanocomposite for the detection of the target DNA of *Salmonella typhi* achieving a linear detection between 10 fM and 50 nM and a limit of detection (LOD) of 10 fM. In the work of Bansal et al. [30], the surface of the screen-printed electrode (SPE) was modified with chitosan and platinum nanoparticles nanocomposite to establish a LOD of 360 pM. These modifications, however, can be complex, e.g., require several steps, and high temperatures, thus increasing the complexity of sensor development [31, 32]. In contrast, Du et al. [33], developed a simple, one-step co-electrodeposition technique for chitosan with simultaneous deposition of gold nanoparticles on large 2 mm diameter electrodes. Their technique was applied for glucose detection and no biomolecule attachment was tested in their work.

In this work, gold IDEs fabricated on silicon chips were used for the development of a voltammetric sensor allowing highly sensitive detection of the STEC virulence gene, *stx1*. The sensor IDE was specifically modified with Cht-Au nanocomposite and probe DNA leaving the other IDE (accumulator IDE) unmodified, confirmed with optical

and fluorescent microscopy. This accumulator IDE was then used to pre-concentrate a redox probe, MB, around the sensor IDE by applying open circuit potential (OCP), enhancing the hybridisation signal and increasing sensitivity. To the best of our knowledge, interdigitated electrodes have never been utilised to enhance molecule accumulation for DNA detection. By this approach, we have managed to achieve highly sensitive detection of 100 aM and detection of chromosomal DNA without the amplification step. This non-complex method of electrode modification and DNA detection has the potential to be applied to multiplex detection of different DNA strands in the future.

3.2. Materials and methods

3.2.1. Chemicals

Chitosan (>75% deacetylated), gold(III) chloride trihydrate (HAuCl4 x 3H2O, ≥99.9% trace metal basis), N,N-Dimethylformamide (DMF, 99.8%), KCl (≥99%), PBS, sodium acetate (≥99%), glutaraldehyde (50 wt. % in H2O), atto565 NHS ester, HEPES (≥99.5% titration), were obtained from Sigma Aldrich, Ireland. All solutions were prepared by diluting with ultra-pure Milli-Q water (18.2 MΩ.cm, Milli-Q). All synthetic oligonucleotides were obtained from Sigma Aldrich Ireland in a dried form. Upon arrival, they were diluted with sterile DI water to 100 µM and stored at -20°C. Before use, they were diluted in 0.1 M PBS buffer to the desired concentration. The probe sequence for *stx1* detection was selected based on ISO/TS 13136:2012 standard. The probe was modified with an amine group at the 5' end, enabling covalent attachment to the electrode. For fluorescent confirmation, the target sequence was modified on the 5' end with Atto565 fluorescent dye. The sequences used in this work are detailed in Table 3.1.

Table 3.1 Summary of DNA sequences used in this work

Name	Sequence
stx1 probe	5' NH_2 (C6) CTG GAT GAT CTC AGT GGG CGT TCT TAT GTAA 3'
stx1 target	5' TTAC ATA AGA ACG CCC ACT GAG ATC ATC CAG 3'
stx1 target + Atto565	5' [Atto 565] TTAC ATA AGA ACG CCC ACT GAG ATC ATC CAG 3'
Non-target	5' CCGA TGC TAC GTC AAT GTA ACT GAT TGA GCT 3'
Non-target + Atto565	5' [Atto 565] GGA GCA GTT TCA GAC AGT GCC TGA CGA 3'

Chitosan stock solution (0.2%) was prepared by dissolving 0.1 g of chitosan in 50 mL DI water containing 1% acetic acid. The solution was stirred overnight and filtered using filter paper to remove undissolved polymer. The final pH of the stock solution was ~3. Two gold ions stock solutions were prepared and stored at 4°C. The first stock solution, used for AuNPs electrodeposition, contained 1000 ppm $HAuCl_4$ dissolved in 0.01 M sodium acetate, pH 3, while the other stock solution, used for Cht-Au nanocomposite electrodeposition, contained 1000 ppm of $HAuCl_4$ dissolved in DI water.

3.2.2. Apparatus

All voltametric measurements were undertaken using a CHI920 potentiostat while electrochemical impedance measurements (EIS) were undertaken using a Multi AutoLab M101. A three-electrode electrochemical setup was used for modification of one comb of a gold IDE (used as the working electrode), an on-chip gold counter electrode and an external Ag/AgCl reference electrode (IJ Cambria Scientific, 1 M KCl). A modified four-electrode setup was employed for DNA detection: a modified gold IDE was used as a sensor, an unmodified gold IDE was used as an accumulator and on-chip gold and platinum as counter and pseudo reference electrodes, respectively.

White light optical microscopy images and fluorescent microscopy images of the non-modified and modified IDEs were acquired using an Axioskop II (Carl Zeiss Ltd.) microscope equipped with a halogen lamp and a charge-coupled detector camera (CCD; Coolsnap CF, Photometrics). The surface morphology and compositional analysis of AuNPs and Cht-Au modified IDEs were performed using a field emission

scanning electron microscope (FEI QUANTA 650 HRSEM) with energy-dispersive X-ray spectroscopy (EDX Oxford Instruments INCA energy system).

3.2.3. Chips fabrication

IDEs with 10 µm gaps were fabricated on silicon chip substrates. Each silicon chip comprised six sensors containing two IDEs, a gold counter electrode, and a platinum pseudo-reference electrode. Gold contact pads and interconnection metallisation on two sides of the chip allowed electrical connection to both IDEs. The method of chip fabrication was described previously [32, 33]. In brief, four-inch silicon wafer substrates bearing a ~300 nm layer of thermally grown silicon dioxide were used. IDEs were first fabricated using optical lithography, metal evaporation (Ti 10 nm /Au 150 nm Temescal FC-2000 E-beam evaporator) and lift-off techniques to yield well-defined, stacked metallic (Ti/Au) microband (1 µm width, 50 nm height, 45 µm length) structures. Each chip comprised six independent sensors. A second optical lithographic and metal deposition (Ti 10 nm/Ni 70 nm/Au 200 nm) process was then undertaken to define a MicroSD pin-out, interconnection tracks, as well as counter electrodes (500 µm wide x 10 mm long). Finally, a passivation SiN_X layer was deposited on the chip by PECVD, with windows opened in this layer directly above the working, reference and counter electrodes. The windows defined the length of the working electrode to be 45 µm. In this work, an on-chip microSD style electrical pin-out was included to permit a facile electrical connection to external electronics. In this manner, chips could be easily swapped in and out with the potentiostat, enabling rapid analysis of multiple samples. A custom-built cell was designed and fabricated so that when screwed together, the microSD primary contact pads protruded out of the holder to allow connection with a PCB mounted microSD port.

3.2.4. DNA sensor development

Prior to electrode modification, silicon chips were cleaned by sonicating in ethanol and DI water, for ten minutes each. Once clean, the chip was dried in a stream of nitrogen, placed in a chip holder and connected to the potentiostat using either an SD connector or probe pins. The scheme presenting steps of DNA sensor development is shown in Fig. 3.1. Each sensor IDE was modified with gold nanoparticles, electrodeposited by applying -0.2 V for 60 s in 500 µL of 400 ppm $HAuCl_4$ dissolved in 10 mM sodium acetate, pH 3. Subsequently, Cht-Au nanocomposite was electrodeposited on top of the pre-AuNPs modified IDE. The solution was prepared by diluting chitosan from a stock solution (0.2%) to 0.04% (v/v) with DI water containing 1% acetic acid. Afterwards, 1 M NaOH was added to the solution to increase its final pH to ~pH 5. Gold ions from a (DI water) stock solution were added to chitosan just before the deposition to achieve a final concentration of 50 ppm $HAuCl_4$. The Cht-Au solution was mixed using a vortex and 500 µL was added to the sample well. A voltage of -1.5 V was applied for 15 seconds to each electrode. Subsequently, the modified chip was immersed in 0.01 M PBS buffer, pH 7, for 10 minutes to increase the stability of the layer, washed thoroughly with DI water and dried in a stream of nitrogen. The electrodes were then immersed in 0.2% (v/v) glutaraldehyde for 2 hours. Afterwards, a 50 µL droplet of 0.5 µM amine-modified probe ssDNA was deposited on top of an electrode, incubated for 2 hours, then the unattached probe was removed with DI water.

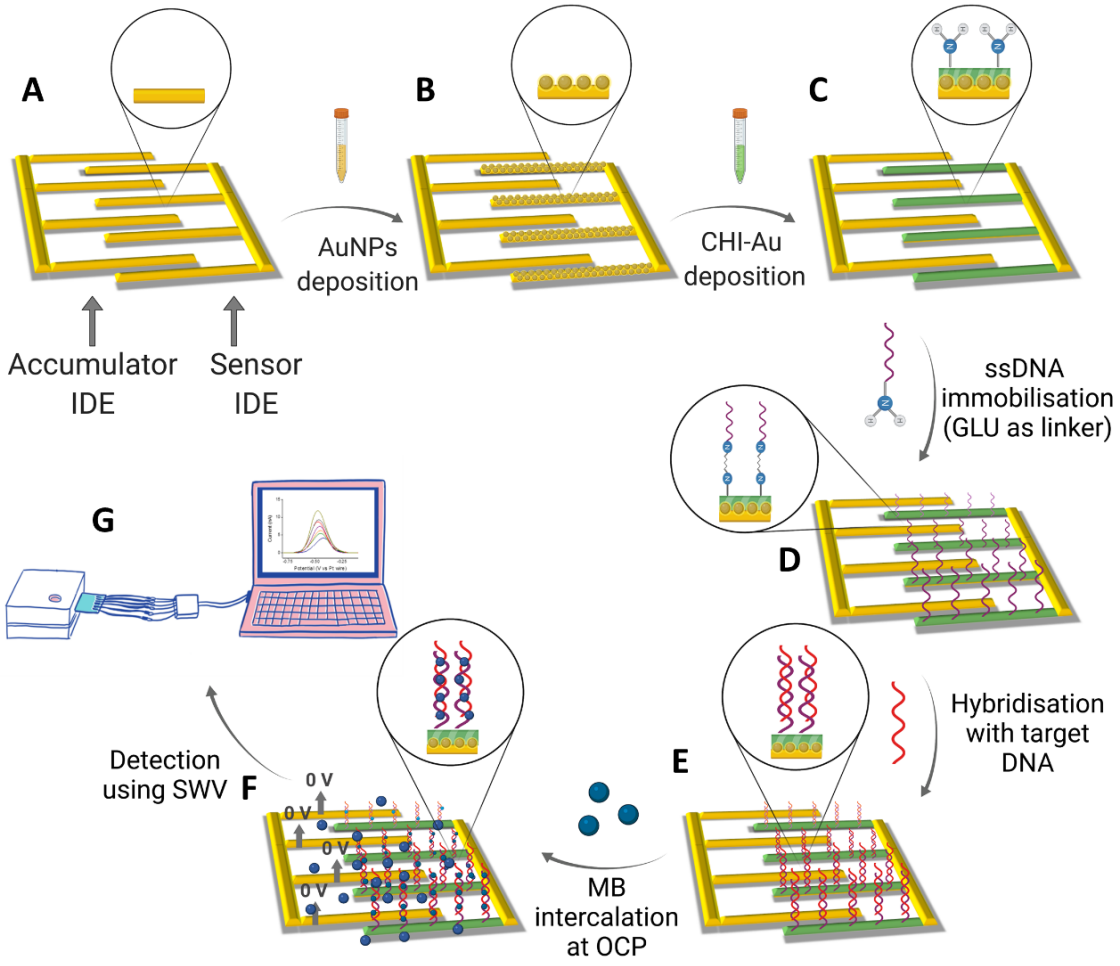

Fig. 3.1 Scheme showing the sensor IDE modification and DNA detection with methylene blue accumulated using the accumulator IDE (Created with BioRender.com). (A) Gold IDEs comprising sensor and accumulator IDE. (B) Modification of the sensor IDE with a layer of AuNPs (C) Further modification of sensor IDE with Cht-Au nanocomposite. (D) Surface activation with 0.02 % (v/v) glutaraldehyde and subsequent immobilisation of amine-terminated 5' ssDNA complementary to the stx1 gene. (E) Hybridisation with a complementary target DNA. (F) The label-free electrochemical detection using MB as a redox-active molecule accumulated at OCP applied to the accumulator IDE. (G) Direct reduction of MB, using SWV, to detect DNA hybridisation.

3.2.5. Fluorescence characterisation

To confirm a uniform electrodeposited chitosan layer, modified electrodes were immersed in a fluorescently labelled succinimidyl ester (Atto565-NHS ester) which is

known to bind to the primary amine groups. First, 0.5 mg Atto565-NHS ester was reconstituted in 500 uL DMF. Then, 50 µL of this solution was diluted in 30 mL of PBS buffer. Chips with chitosan modified electrodes were immersed in this mixture and incubated for 30 minutes at room temperature. After this time, chips were removed, washed with DI water to remove the unattached dye and dried in a stream of nitrogen. Fluorescent microscopy was then used to confirm that the target DNA hybridised with the probe DNA and that no unspecific binding took place. Two different DNA strands, target and non-target, tagged with Atto565 were employed. AuNPs/CHI-Au/ssDNA modified sensor IDEs were incubated for 30 minutes with either 10 nM target DNA or non-target DNA both DNA strands were tagged with Atto565. Afterwards, chips were washed with DI water, dried under nitrogen and characterised using fluorescent microscopy.

3.2.6. Hybridisation detection and methylene blue accumulation using open circuit potential

Square wave voltammetry (SWV) using methylene blue as a redox molecule was employed for hybridisation detection. Methylene blue is well known to interact with single and double-strand DNA based using different modes of action. After hybridisation, a chip was immersed in 50 µM methylene blue in HEPES buffer (20 mM HEPES, 10 mM KCl, pH 7) for 10 minutes, with an applied OCP for the first five minutes to accumulate the MB. After this time, MB was washed away with HEPES buffer followed by SWV recorded between 0 and -0.8 V versus on the platinum pseudo reference electrode (frequency 75 Hz, pulse amplitude 75 mV, increment 15 mV)

3.2.7. Culture preparation and target DNA extraction

DNA was extracted from four *E. coli* strains, Listeria monocytogenes and Bacillus cereus. Two *E. coli* strains contained the *stx1* gene (O157 - ATCC35150 and O103) while the other two strains did not contain this gene (O157 - NCTC12900 and O91 - 09_A_15_1_1). Briefly, the cultures were grown up from culture collection stocks (Teagasc Food Research Centre Ashtown) which were stored on protective beads at -80°C. A single bead of each isolate was streaked on Tryptone Soy Agar (Oxoid, Fisher Scientific Ireland) and incubated overnight at 37 °C. An isolated colony was then placed in Tryptone Soy Broth and incubated overnight at 37 °C. DNA was extracted from the overnight culture using a Qiagen DNeasy Blood and Tissue kit (Qiagen, Manchester, UK), and in accordance with the manufacturer's instructions. The DNA concentration was measured using a Qubit dsDNA BR Assay Kit (Thermo Fisher Scientific, Ireland) on a Qubit 4.0 fluorometer.

Before electrochemical measurements, DNA samples were diluted 5 times in 0.1 M PBS buffer, pH 7.2, and heated to 95 °C for 5 minutes to denature dsDNA. Subsequently, the samples were cooled down on ice and incubated on prepared sensors for 30 minutes at room temperature followed by electrochemical measurements.

3.3. Results

3.3.1. Characterisation of modified electrodes

Fig. 3.2 (A) presents a picture of the silicon chip. In this work, an external Ag/AgCl reference electrode was used during the deposition of AuNPs and Cht-Au nanocomposite, while the on-chip pseudo-reference electrode was used for DNA detection. Fig. 3.2 (B) shows a silicon chip in a chip holder. Chitosan was electrodeposited at sensor IDE in presence of Au ions, similar to Du et al. [33]. To find the optimal potential for cathodic deposition of chitosan, cyclic voltammetry (CV) in Cht-Au solution (0.04 % chitosan, 50 ppm Au) at pH ~5 was undertaken. The potential was cycled between 0 V and -2 V, see Fig. 3.2 (C), and it was found that the cathodic current increased significantly around -1.4 V suggesting the commencement of hydrogen evolution and therefore an increase in pH around the electrode. The observed current remained stable (plateaued) until -1.8 V whereon it started increasing rapidly at more cathodic applied voltages. Consequently, based on CV data, the potential range of interest for Cht-Au deposition was found to be between -1.4 and -1.8 V. To confirm this, multiple electrodepositions were undertaken in the potential of -1.2 V, and -2 V and visualised under optical microscopy. Fig. S3.1 shows that a defined polymer layer was electrodeposited at sensor IDEs for potentials of -1.4, -1.5 and -1.6, which supports the results based on CV. At -1.2 V the pH change was not sufficient for chitosan deposition at the electrode while at greater than -1.8 V the hydrogen evolution was so rapid that the polymer deposited around the electrode instead of specifically at an array. Following these experiments, a potential of -1.5 V was selected as optimal for chitosan deposition.

CV in 5 mM $Fe(CN)_6^{3-}/Fe(CN)_6^{4-}$ in 0.1 M KCl as supporting electrolyte (scan rate 100 mV/s) were undertaken to characterise the different gold surfaces of a pristine IDE

and post modified IDEs. In addition, the electrodeposition of a gold nanoparticle layer onto gold electrodes was explored to increase surface roughness prior to Cht-Au deposition. Fig. 3.2. (D) presents CV for (i) unmodified gold, (ii) Cht-Au, (iii) AuNPs, and (iv) AuNPs/Cht-Au. For pristine gold electrodes, a well-defined voltammogram exhibited typical characteristics for the $Fe(CN)_6^{3-}/Fe(CN)_6^{4-}$ redox couple with a peak oxidation current of ~25 nA and low hysteresis was observed. Following electrodeposition of a Cht-Au complex at the unmodified electrode, a significant decrease in the magnitude of the redox currents for the $Fe(CN)_6^{3-}/Fe(CN)_6^{4-}$ redox couple was observed (~3 nA). This suggests a Cht-Au layer deposited effectively onto the electrode surface and that this layer had a lower conductivity and thus partially insulated the surface of the electrode; due to the lack of conduction pathways from the underlying electrode to the modified layer. We attribute the lack of these pathways to the smoothness of the evaporated gold of the electrode. An increase in $Fe(CN)_6^{3-}/Fe(CN)_6^{4-}$ current magnitudes, compared to the pristine gold electrodes (~50 nA), were observed for IDE electrodes first modified with an Au-NP layer, which may be attributed to an increase in surface area. A Cht-Au layer was then deposited onto these modified electrodes and characterised by CV and electrochemical impedance spectroscopy (EIS). From the CV data, it was observed that (unlike the unmodified electrodes) the addition of the Cht-Au layer, resulted in a slight increase in the $Fe(CN)_6^{3-}/Fe(CN)_6^{4-}$ current magnitudes and also decreased the separation between the oxidation and reduction peaks, suggesting a successful deposition of this layer. The CV results are supported by the EIS data presented in Fig. 3.2 (E) where a decrease in impedance was observed from 12.2 MΩ at unmodified IDE to 5 MΩ following modification of the underlying AuNPs layer, due to the increased surface area and 5.5 MΩ following deposition of a subsequent Cht-Au layer.

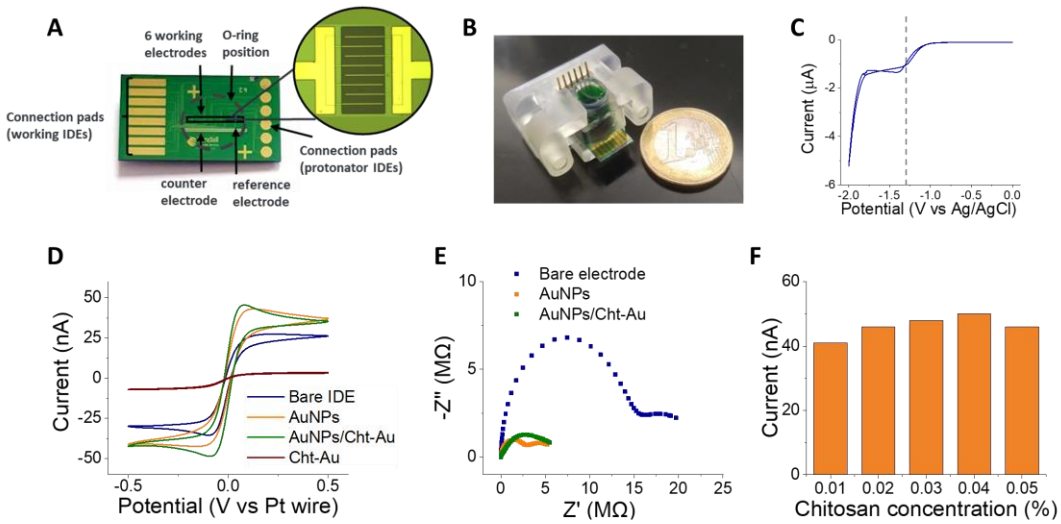

Fig. 3.2 (A) Picture of a fully integrated silicon chip and an optical image of IDE. (B) Silicon chip in a chip holder. (C) Cyclic voltammogram at the unmodified sensor IDE in 0.04 % chitosan, 50 ppm Au pH 5. (D) Cyclic voltammograms in 5 mM Fe(CN)63−/Fe(CN)64−, 0.1 M KCl at (i) unmodified IDE and after deposition of (ii) 0.4% chitosan with 50 ppm HAuCl4 (Cht-Au), (iii) AuNPs, and (iv) AuNPs/Cht-Au. (E) Impedance measurements in 5 mM Fe(CN)63−/Fe(CN)64−, 0.1 M KCl at (i) unmodified IDE and after deposition of (ii) AuNPs and (iii) AuNPs/Cht-Au. (F) Oxidation peak current of CV in 5 mM Fe(CN)63−/Fe(CN)64−, 0.1 M KCl at IDE modified with ChtAu nanocomposite where the concentration of CHI varied between 0.01% and 0.05%.

The effect of varying the Cht concentrations within the Cht-Au complex was also investigated at IDEs pre-modified with AuNPs, see Fig. 3.2 (F). Cht-Au complexes were deposited at -1.5 V for 15 seconds with the CHI concentrations varying between 0.01% and 0.05%. It was found that the conductivity of the electrode increased with the increasing chitosan concentration reaching a maximum at 0.04% of chitosan and decreasing thereafter. This suggests that, with increasing chitosan concentration in a solution, the Cht enables the formation of more gold nanoparticles at an electrode, which results in an increase in electrode conductivity. However, at higher Cht concentrations, the Cht: Au ratio becomes unfavourable, thereby decreasing the conductivity of the electrode. Fig. S3.2 shows the electrochemical characterisation of

AuNPs/Cht-Au IDE in 5 mM $Fe(CN)_6^{3-}/Fe(CN)_6^{4-}$ redox couple at different scan rates (10 mV-200 mV). As expected, the peak currents increased with an increased scan rate, suggesting that the redox reaction is diffusion-controlled [36, 37]. The inset shows linear relationships of the anodic and cathodic peak currents as a function of the square root of scan rate which indicates that the diffusional profiles of individual micro bands overlap and the electrode behaves like a larger microelectrode.

Following electrode optimisation as described above, an optical and electron microscopy characterisation study was undertaken in Fig. 3.3 and Fig. S3.3. Fig. 3.3 (A) shows an optical image of a sensor following modification of one IDE (dark bands) with AuNPs. It can be seen that the modification only occurred at a sensor IDE while the accumulator IDE remained unmodified. Fig. 3.3 (B) shows an SEM image of the AuNPs modified sensor IDE and an inset at higher magnification. Two different nanostructure morphologies were observed, round nanoparticles on the length of the electrode and bigger clusters at the electrode edges. The size of the round NPs varied between ~30 nm and ~90 nm (see Fig. S3.3. (A)) while larger dendritic particles, ~500 nm, were observed at the band edges. These larger particles arose from the high electric fields, present at the boundary discontinuities occurring at the interface between the top surface and sidewalls of the bands, enhancing gold deposition. Fig. 3.3 (C) shows an optical image of a microelectrode, with a sensor IDE following AuNPs/CHI-Au modification. A defined green coloured layer can be seen around each band in the sensor IDE, compared to the electrode modified with just AuNPs only (Fig. 3.3 (A)). This green layer is attributed to the chitosan and suggests that the polymer was deposited on top of the IDE. The SEM image in Fig. 3.3 (D) shows the gold nanostructures of the AuNP modification. At higher magnification (inset) a thin layer can be seen around the Au nanostructures, indicated by the arrows, which can be

attributed to the chitosan. This suggests that using 50 ppm Au in a chitosan solution did not cause additional deposition of AuNPs, but facilitated polymer deposition. Optical and SEM images for an IDE modified with Cht-Au only (i.e., with the AuNP layer suppressed) are presented in Fig. S3.3 (B). The optical image shows a green-coloured layer, indicative of chitosan, around the bands in the sensor IDE while under high-resolution SEM, a thin layer, similar to the inset of Fig. 3.3 (D), at the electrode edges, can be observed. EDX analysis of IDEs electrodes modified with AuNPs and AuNPs/Cht-Au modified was undertaken as it is well known that chitosan is rich in amine functional groups. Consequently, EDX can be used to confirm the presence of nitrogen on the surface of a modified electrode. Nitrogen was not present on the electrode modified with AuNPs only (negative values in the table; inset), Fig. 3.3 (E), while it was present on the electrode modified with AuNPs/CHI-Au, (positive 3.43% in the table, inset), Fig. 3.3 (F).

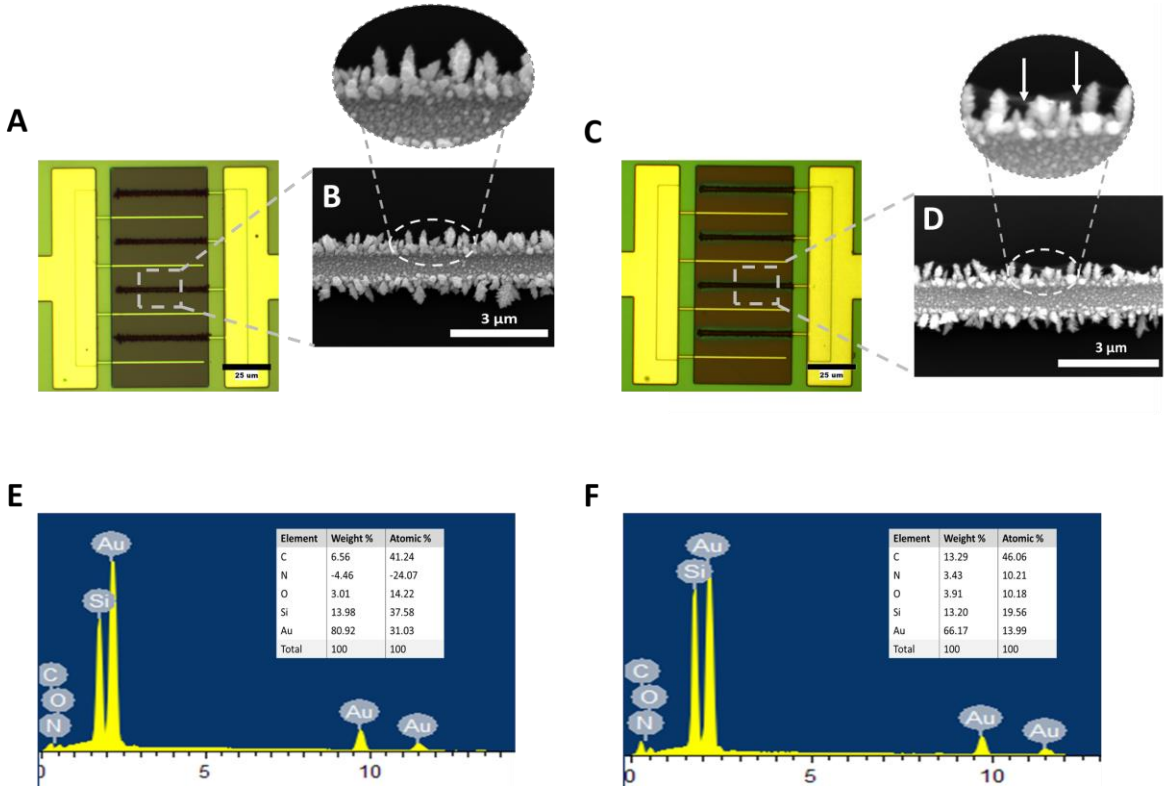

Fig. 3.3 (A) optical image of the AuNPs modified IDE. (B) SEM image of the AuNPs surface. (C) optical image of the AuNPs/Cht-Au modified IDE. (D) SEM image of the AuNPs/Cht-Au surface. (E) EDX spectrum of the AuNPs modified IDE. (F) EDX spectrum of the AuNPs/Cht-Au modified IDE.

3.3.2. Confirmation of sensor functionality using fluorescence

Following EDX confirmation of the presence of nitrogen at an AuNPs/Cht-Au modified sensor IDE surface, Atto565 NHS ester (a fluorescent dye modified to bind to primary amine groups) was used to confirm the presence of amine groups on the AuNPs/Cht-Au modified IDE and visualise their distribution along the electrode; similar to Wu et al. [38]. Subsequently, Atto565 modified DNA complementary and non-complementary strands were used to visualise DNA binding to probe ssDNA.

Fig. 3.4 (A) presents a fluorescent image of AuNPs/Cht-Au IDE following 30 min incubation with Atto565 NHS ester. The observed uniform fluorescent signal strongly suggests that the amine groups are equally distributed along the whole length of the modified sensor IDE. In addition, the high intensity suggests the amine groups are quite dense. By contrast, the lack of fluorescence from the unmodified accumulator IDE confirms the selective deposition of the polymer matrix at the sensor IDE only. Fig. 3.4 (B) presents a fluorescent image of an AuNPs/Cht-Au modified IDE in the absence of Atto565 NHS ester dye confirming that the chitosan layer is not autofluorescent and the fluorescence in Fig. 3.4 (A) was attributed to the functionalised amine groups. Similarly, fluorescence experiments were performed at Cht-Au and Cht only modified IDEs and incubated in Atto565 for 30 mins. Fluorescence was not observed at Cht only modified electrode indicating that chitosan did not deposit onto a pristine gold electrode, see Fig. S3.4 (A). By contrast, a uniform fluorescent signal was observed for the Cht-Au modified electrode, see Fig. S3.4 (B),

however, the signal intensity was significantly reduced compared to electrodes with an underlying AuNPs layer presented in Fig. 3.4 (A). This suggests that the underlying AuNPs layer, below the Cht-Au layer, is essential not only to increase the conductivity of the chitosan film but also to increase the concentration of amine groups.

Subsequently, ssDNA was immobilised at AuNPs/Cht-Au IDEs using 0.2% glutaraldehyde as a linker molecule. Atto565 modified target (10 nM) DNA was introduced onto an electrode and incubated for 30 minutes. Following hybridisation, unattached DNA was washed away and fluorescent microscopy was used to confirm specific hybridisation of the complementary DNA occurred. Fig. 3.4 (C) presents a fluorescent image following incubation with complementary DNA strands. The observed fluorescence exhibited high intensity and was uniformly distributed across the electrode confirming successful hybridisation. Fig. 3.4 (D) presents a fluorescent image following incubation with Atto565 modified non-complementary DNA strands. The lack of a fluorescent signal indicates that non-specific binding did not occur.

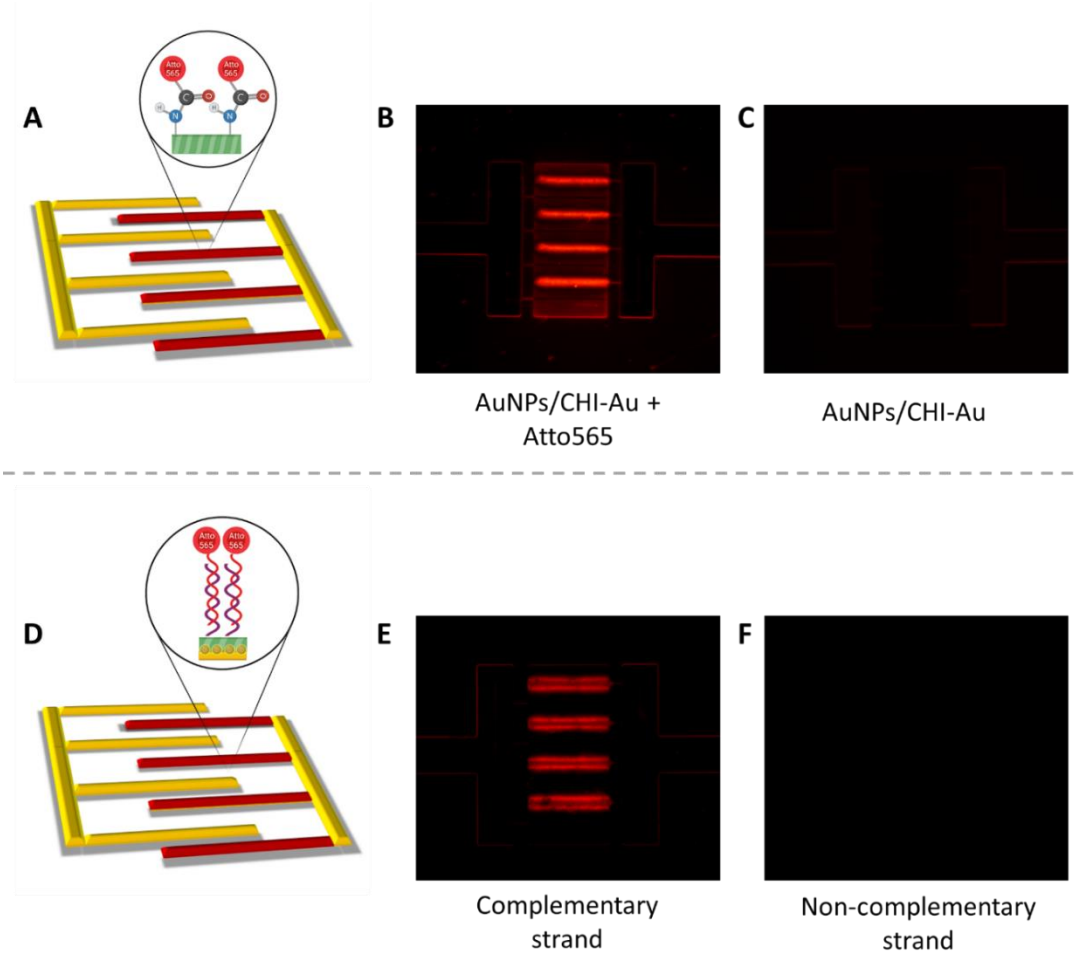

Fig. 3.4 (A) Image under the fluorescent microscope showing the AuNPs/Cht-Au modified sensor IDE after incubation with atto565 NHS ester dissolved in 0.01 M PBS. (B) Image under the fluorescent microscope showing AuNPs/Cht-Au modified sensor IDE without the fluorescent dye – negative sample. (C) Image under fluorescent microscopy showing an AuNPSs/CHI-Au/ssDNA modified sensor IDE after incubation with 10 nM DNA strand complementary DNA strand, tagged with atto565 (D) Image under the fluorescent microscopy showing AuNPSs/CHI-Au/ssDNA modified sensor IDE after incubation with 10 nM DNA strand non-complementary to stx1 gene tagged with atto565.

3.3.3. Electrochemical-based DNA detection using methylene blue

Methylene blue (MB), a redox-active molecule, is known to interact with DNA and the difference in its affinity towards ssDNA and dsDNA has been commonly exploited

in the development of electrochemical biosensors [39-41]. The molecule can (i) bind directly to guanine bases [42], (ii) is electrostatically attracted to the negatively charged phosphate backbone of DNA [43], or (iii) intercalate between dsDNA [44, 45]. The mechanisms at which it will interact with DNA can be influenced by the experimental parameters used. In this work, we focused on enhancing MB intercalation between dsDNA and detecting DNA hybridisation based on an increased SWV signal compared to ssDNA. One parameter that was shown to affect MB to dsDNA binding efficiency is the ionic strength of the solution [43]. Kara et al. [46] have suggested that the concentration of Cl^- ions can influence the efficiency of MB intercalation between dsDNA. In their work, the MB intercalation between dsDNA was preferred over the other type of MB interactions at 10 mM NaCl. In this work, DNA detection was undertaken using 50 μM MB dissolved in 0.02 M HEPES buffer with 10 mM KCl and an accumulation step to achieve the highest efficiency of intercalation.

The electrochemical detection of DNA in this work was undertaken by accumulating MB at a DNA-modified electrode followed by its reduction to leukomethylene blue recorded with SWV. An OCP [47] commonly used for the accumulation of methylene blue in DNA sensor development [46] was applied to an accumulator electrode as described above. Fig. 3.5 (A) and Fig. 3.5 (B) show square wave voltammograms before and after exposure to 50 nM of complementary DNA, with and without applying OCP to the accumulator IDE, respectively. In both cases, the accumulation was done by incubating the chip for 10 minutes in 50 μM MB dissolved in 0.02 M HEPES and 0.01 M KCl (pH 7).

The peak increase for dsDNA (50 nM) over ssDNA, without applying an OCP, was 2.28 nA equivalent to a ~50% increase in the measured signal. When an OCP was

applied to an accumulator IDE, it was observed that the ssDNA peak current had a similar magnitude compared to the static accumulation. By contrast, a significant increase in peak current on the binding of complementary dsDNA (50 nM) was observed with a Δ peak height current (between ssDNA and dsDNA) increased to 5.05 nA, over a 100% increase. This suggests that applying an OCP (measured to be 8 mV, see Fig. S3.5) increases the efficiency of MB intercalation between dsDNA without affecting its interaction with ssDNA.

In Fig. 3.2 (D) we have previously shown that electrodeposition of AuNPs as a first layer significantly increased the conductivity of the modified sensor IDE. We further evaluated how AuNPs affected DNA detection using MB. Fig. 3.5 (C) summarises peak current height before (orange) and after (green) hybridisation with complementary strand when the electrode was not modified and modified (400 ppm) with the first layer of AuNPs. It was found that the difference between ssDNA and dsDNA was hard to distinguish without the layer of AuNPs. This is in agreement with Fig. 3.2 (D) where the conductivity of the electrode decreased after Cht-Au modification. However, in the presence of the underlying AuNPs layer, a significant increase in MB measured current was observed between ssDNA and dsDNA, again confirming the need for this layer.

Finally, the effect of ssDNA concentration immobilised at AuNPs/Cht-Au modified sensors IDE on the MB reduction signal was assessed. Fig. S3.6 presents the peak height increase observed after dsDNA (50 nM) binding with different concentrations of immobilised ssDNA (i) 0.25 μM, (ii) 0.5 μM, (iii) 1 μM and (iv) 1.5 μM, respectively. The best response was achieved when 0.5 μM probe concentration was used. This suggests that with 0.25 μM there was not enough probe ssDNA attached to the surface, while at higher concentrations 1 μM and 1.5 μM the probe density was

too high to achieve optimal hybridisation due to steric hindrance. Fig. 3.5 (D) presents square wave voltammograms after incubation of a sensor with 50 nM of (i) target DNA, (ii) non-complementary strand and (iii) a DNA strand containing 3 base mismatches. An increase in current magnitude was not observed for the non-complementary or mismatched strands. However, a significant increase was observed for the complementary strand, confirming the specificity of the developed biosensor.

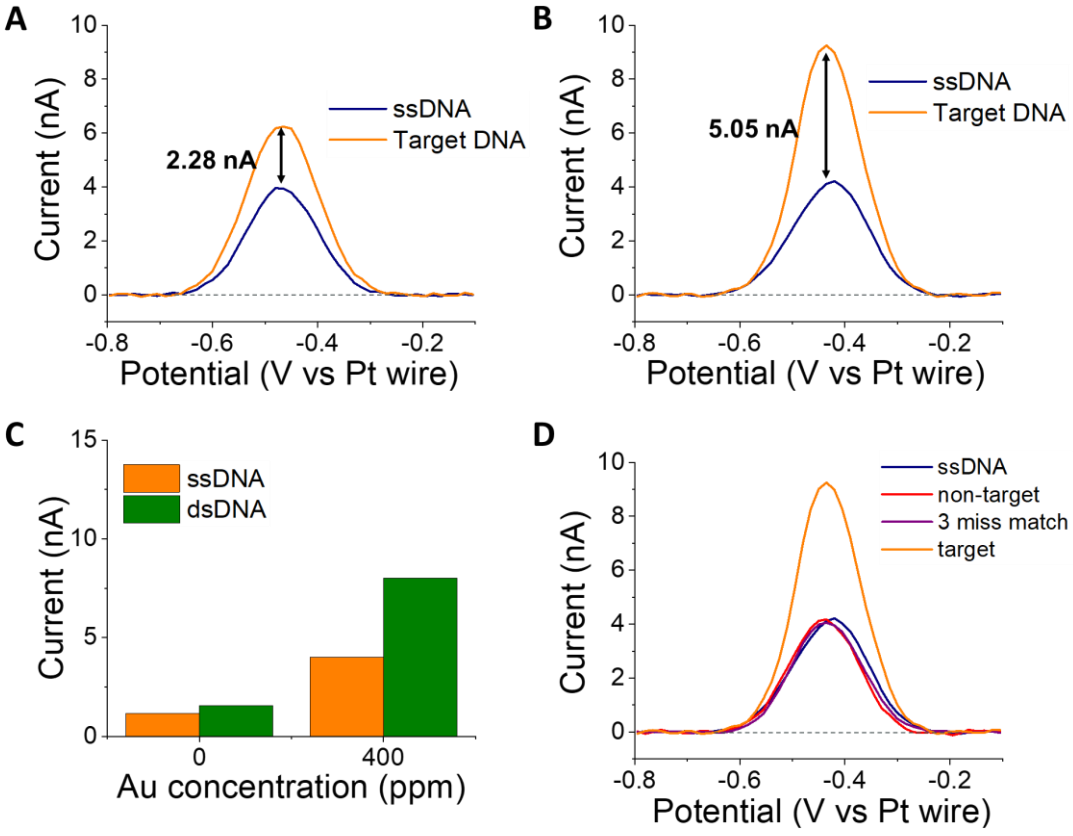

Fig. 3.5 (A) Square wave voltammograms before and after exposure to 50 nM complementary DNA strand after 10 min of static accumulation (no OCP) at 50 µM MB in 0.02 M HEPES and 0.01 M KCl, pH 7. (B) Square wave voltammograms before and after exposure to 50 nM complementary DNA strand when OCP was applied to accumulator IDE for 5 minutes followed by 5 minutes of a static accumulation. (C) Peak current heights before and after exposure to 50 nM complementary DNA strand at sensor IDE modified with Cht-Au layer deposited for 20 s with (i) no underlying AuNPs and (ii) underlying AuNPs. (D) Square wave voltammograms before and after

exposure to 50 nM (i) complementary DNA strand, (ii) non-complementary strand, (iii) 3 bases miss-matched strand.

To find the limit of detection and establish a calibration curve, the AuNPs/Cht-Au/ssDNA modified IDEs were incubated for 20 minutes with a series of DNA concentrations diluted with 0.1 M PBS buffer. The peak height was found to increase linearly between 100 aM and 1 µM of target DNA. Fig. 3.6 (A) shows the calibration curve where the difference between dsDNA and ssDNA peak height current was plotted against the logarithm of DNA concentration. All data points represent an average value of four measurements (from different sensors) and a standard deviation for each point. The calibration line showed excellent linearity, with a correlation coefficient of R^2=0.995. The lowest measured concertation, and thus experimentally established limit of detection, was observed to be 100 aM. Fig. 3.6 (B) presents square wave voltammograms for each concentration. The baseline was normalised to allow better visualisation. The reproducibility of the sensor was calculated for 1 pM concentration and the relative standard deviation (RSD%) was 10.61% and 3.98% between the electrodes on a single chip (n=5) and the electrodes on different chips, respectively.

To evaluate the specificity of the developed sensor in complex samples, chromosomal DNA extracted from different strains of *E. coli, viz, stx1* positive (O103 and O157) and *stx1* negative (O91 and 12900) and non-*E. coli* (*Listeria monocytogenes* and *Bacillus cereus*) was tested. After the extraction, the DNA was diluted 5 times with the PBS buffer, heated to 95°C for 5 mins and immediately cooled on ice for 60 s. The samples were then incubated on a sensor for 30 minutes. Fig. 3.6 (C) presents combined square wave voltammograms from different sensors following incubation with the chromosomal DNA. It can be seen that only DNA extracted from *E. coli*

containing the *stx1* gene (O103 and O157) resulted in an increase in the signal, further demonstrating the selectivity of the sensor to complex samples. The signal from the O103 strain was higher than O157, suggesting that it either contained more *stx1* gene or it was more readily available to hybridise with the sensor. Fig. 3.6 (D) summarises the difference in peak height current after detection using chromosomal DNA samples (Fig. 3.6 (C)). Each data point represents the average value of three measurements from different sensors.

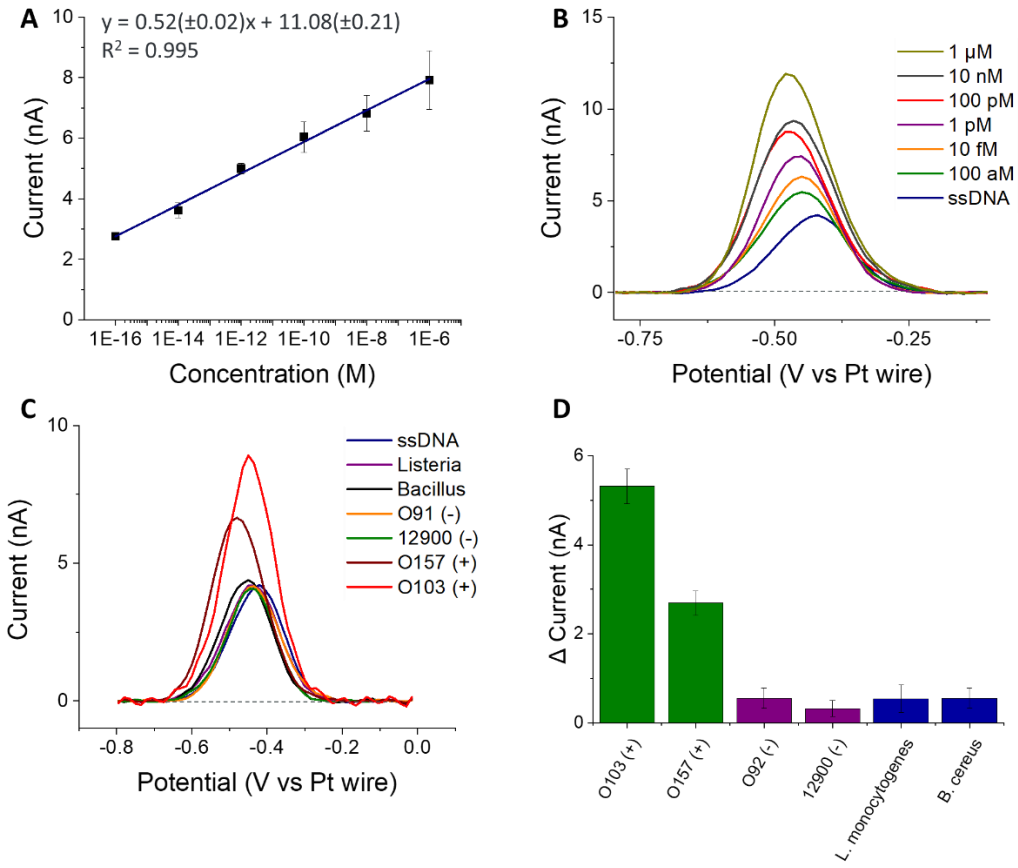

Fig. 3.6 (A) Calibration line representing the difference between peak height current of dsDNA and ssDNA plotted against the logarithm of the target DNA concentration. (B) Square wave voltammograms corresponding to each concentration of the calibration curve. SWV parameters were frequency 75 Hz, and pulse amplitude 75 mV. The baseline was corrected for a better visual analysis of the voltammograms (C) Square wave voltammograms for detection of the chromosomal DNA. The baseline was corrected to enable a better visual analysis of the voltammograms. (D) Δ peak

current heigh between MB response at ssDNA and after incubation with chromosomal DNA.

Table 3.2 summarises the main parameters of the sensor developed in this work and similar DNA-based electrochemical biosensors for bacteria detection. It was found that our sensor exhibited very high sensitivity and wide linear range compared to other authors, which could be attributed to the micro size of the electrode, increasing the electrode's conductivity using nanoparticles and MB accumulation using OCP. Several authors used MB as a redox-active molecule in their work, however, only in our work IDEs were used for its more efficient accumulation. Another commonly used technique for DNA detection was EIS, which did not achieve such low LOD. Nanomaterials were used by other authors as well, they, however, often required several hours (between 20 and 60 h) of preparation and a heating process. For instance, Tiwari et al. [25] modified ITO electrodes with a composite comprised of chitosan, graphene oxide and nickel ferrite. Even though these nanomaterials allowed a high sensitivity, similarly to this work, the electrode's modification method was laborious and required around three days to synthesise the graphene oxide-nickel ferrite composite and some steps done at high temperature (50°C and 180°C). Using the technique developed in this work the electrode is modified in less than two minutes with the nanoparticles electrodeposited at room temperature. These aspects are crucial for the feasibility of using such a method for point-of-use detection.

Table 3.2 Comparison of main parameters of electrochemical DNA-based biosensors for bacteria detection

Target organism	Electrode + modification	Approx. modif. time	Technique & redox molecule	Linear range [M]	LOD [M]	Complex matrix	Ref.
S. Typhi	ITO + GO-Cht	~ 20 h	DPV, MB	10^{-14} – $5x10^{-8}$	10^{-14}	Serum	[21]
STEC	ITO + GO + NiF + Cht	>60 h	DPV, MB	10^{-16} – 10^{-6}	10^{-16}	Chromosomal DNA	[25]
E. coli	SPCE + AuNPs	6 min.	EIS, Fe^{2+}/Fe^{3+}	10^{-15} - 10^{-7}	10^{-15}	Chromosomal DNA	[48]
STEC	SPE + PtNPs + Cht	~ 8 h	EIS, Fe^{2+}/Fe^{3+}	10^{-12} – 10^{-4}	3.6x 10^{-14}	Surface water	[30]
STEC O157	AuE	N/A	EIS, Fe^{2+}/Fe^{3+}	10^{-13} – 10^{-6}	9.1x 10^{-14}	PCR product, chromosomal DNA	[49]
E. coli	AuE + cystine nanoflowers	~ 25 h	EIS, Fe^{2+}/Fe^{3+}	10^{-15} - 10^{-6}	10^{-15}	Chromosomal DNA	[50]
STEC	**AuE + AuNPs + Cht-Au**	**<2 min.**	**SWV, MB**	**10^{-16} – 10^{-6}**	**10^{-16}**	**Chromosomal DNA**	**This work**

GO – graphene oxine, **NiF** – Nickel ferrite, **SPCE** – screen-printed carbon electrode, **AuE** – gold electrode, **DPV** – differential pulse voltammetry

3.4. Conclusions

In this work, we presented a highly sensitive, on-chip, DNA-based sensor for detection of the *stx1* gene from STEC, using gold IDEs enabled by the pre-concertation of MB at the sensor. The facile method for the specific modification of the sensor IDE with Cht-Au nanocomposite was achieved without affecting the accumulator IDE, which was confirmed using fluorescent techniques. It was demonstrated that deposition of solely a layer of chitosan-gold complex caused a significant decrease in the electrode's conductivity, compared to the bare electrode, which would lead to the low sensitivity of a sensor. Introducing a layer of gold nanoparticles below the layer of chitosan-gold complex, however, allowed increasing the conductivity of the electrode.

Following this, we demonstrated for the first time that applying OCP to the accumulator IDE significantly improved MB intercalation between dsDNA and therefore allowed a highly sensitive detection. The selectivity of the sensor was confirmed using fluorescently tagged DNA strands and an electrochemical technique. Finally, we established a calibration curve between 100 aM to 1 µM of synthetic target strand, with an experimentally established LOD of 100 aM, and specifically detected chromosomal DNA extracted from overnight bacterial cultures. This work is highly relevant for the development of novel point-of-use devices for rapid pathogens detection without the need for PCR amplification and can be further extended to allow multiplex detection in the future by modifying separate electrodes with different probe sequences. In addition, it demonstrates a novel use of the IDE where one comb can be specifically modified with a biorecognition molecule while the other comb can be used for other applications such as molecule accumulation or electrochemical pH control.

3.5. References

1. S.C. McCarthy, C.M. Burgess, S. Fanning, and G. Duffy, *An Overview of Shiga-Toxin Producing Escherichia coli Carriage and Prevalence in the Ovine Meat Production Chain.* Foodborne Pathogens and Disease, 2021. **18**(3): p. 147-168.
2. G. Duffy, C.M. Burgess, and D.J. Bolton, *A review of factors that affect transmission and survival of verocytotoxigenic Escherichia coli in the European farm to fork beef chain.* Meat science, 2014. **97**(3): p. 375-383.
3. E. McCabe, C.M. Burgess, D. Lawal, P. Whyte, and G. Duffy, *An investigation of shedding and super-shedding of Shiga toxigenic Escherichia coli O157 and E. coli O26 in cattle presented for slaughter in the Republic of Ireland.* Zoonoses and public health, 2019. **66**(1): p. 83-91.
4. L. Beutin and A. Martin, *Outbreak of Shiga toxin–producing Escherichia coli (STEC) O104: H4 infection in Germany causes a paradigm shift with regard to human pathogenicity of STEC strains.* Journal of food protection, 2012. **75**(2): p. 408-418.
5. E.B. Panel, K. Koutsoumanis, A. Allende, A. Alvarez-Ordóñez, S. Bover-Cid, M. Chemaly, et al., *Pathogenicity assessment of Shiga toxin-producing Escherichia coli (STEC) and the public health risk posed by contamination of food with STEC.* EFSA Journal, 2020. **18**(1): p. e05967.
6. P. Kralik and M. Ricchi, *A basic guide to real time PCR in microbial diagnostics: definitions, parameters, and everything.* Frontiers in microbiology, 2017. **8**: p. 108.
7. R. Tavallaie, J. McCarroll, M. Le Grand, N. Ariotti, W. Schuhmann, E. Bakker, et al., *Nucleic acid hybridization on an electrically reconfigurable network of*

gold-coated magnetic nanoparticles enables microRNA detection in blood. Nature nanotechnology, 2018. **13**(11): p. 1066-1071.

8. N. Gupta, S. Augustine, T. Narayan, A. O'Riordan, A. Das, D. Kumar, et al., *Point-of-Care PCR Assays for COVID-19 Detection.* Biosensors, 2021. **11**(5): p. 141.
9. M. Ali, M. Bacchu, M. Setu, S. Akter, M. Hasan, F. Chowdhury, et al., *Development of an advanced DNA biosensor for pathogenic Vibrio cholerae detection in real sample.* Biosensors and Bioelectronics, 2021. **188**: p. 113338.
10. A. Liu, K. Wang, S. Weng, Y. Lei, L. Lin, W. Chen, et al., *Development of electrochemical DNA biosensors.* TrAC Trends in Analytical Chemistry, 2012. **37**: p. 101-111.
11. A.T. Lawal, *Progress in utilisation of graphene for electrochemical biosensors.* Biosensors and Bioelectronics, 2018. **106**: p. 149-178.
12. J.I.A. Rashid and N.A. Yusof, *The strategies of DNA immobilization and hybridization detection mechanism in the construction of electrochemical DNA sensor: A review.* Sensing and bio-sensing research, 2017. **16**: p. 19-31.
13. H.A.M. Faria and V. Zucolotto, *Label-free electrochemical DNA biosensor for zika virus identification.* Biosensors and Bioelectronics, 2019. **131**: p. 149-155.
14. N. Mazlan, M. Ramli, M.M.A.B. Abdullah, D.C. Halin, S.M. Isa, L. Talip, et al. *Interdigitated electrodes as impedance and capacitance biosensors: A review*. in *AIP Conference proceedings*. 2017. AIP Publishing LLC.
15. I. Seymour, B. O'Sullivan, P. Lovera, J.F. Rohan, and A. O'Riordan, *Electrochemical detection of free-chlorine in Water samples facilitated by in-situ pH control using interdigitated microelectrodes.* Sensors and Actuators B: Chemical, 2020. **325**: p. 128774.

16. R. Daly, T. Narayan, H. Shao, A. O'Riordan, and P. Lovera, *Platinum-Based Interdigitated Micro-Electrode Arrays for Reagent-Free Detection of Copper.* Sensors, 2021. **21**(10): p. 3544.

17. L. Wang, M. Veselinovic, L. Yang, B.J. Geiss, D.S. Dandy, and T. Chen, *A sensitive DNA capacitive biosensor using interdigitated electrodes.* Biosensors and Bioelectronics, 2017. **87**: p. 646-653.

18. N.A. Parmin, U. Hashim, S.C. Gopinath, S. Nadzirah, Z. Rejali, A. Afzan, et al., *Voltammetric determination of human papillomavirus 16 DNA by using interdigitated electrodes modified with titanium dioxide nanoparticles.* Microchimica Acta, 2019. **186**(6): p. 336.

19. A.A. Odeh, Y. Al-Douri, C. Voon, R.M. Ayub, S.C. Gopinath, R.A. Odeh, et al., *A needle-like Cu 2 CdSnS 4 alloy nanostructure-based integrated electrochemical biosensor for detecting the DNA of Dengue serotype 2.* Microchimica Acta, 2017. **184**(7): p. 2211-2218.

20. J. Zhang, J. Wang, X. Zhang, and F. He, *Rapid detection of Escherichia coli based on 16S rDNA nanogap network electrochemical biosensor.* Biosensors and Bioelectronics, 2018. **118**: p. 9-15.

21. A. Singh, G. Sinsinbar, M. Choudhary, V. Kumar, R. Pasricha, H. Verma, et al., *Graphene oxide-chitosan nanocomposite based electrochemical DNA biosensor for detection of typhoid.* Sensors and Actuators B: Chemical, 2013. **185**: p. 675-684.

22. A. Ulianas, L.Y. Heng, S.A. Hanifah, and T.L. Ling, *An electrochemical DNA microbiosensor based on succinimide-modified acrylic microspheres.* Sensors, 2012. **12**(5): p. 5445-5460.

23. P. Geng, X. Zhang, Y. Teng, Y. Fu, L. Xu, M. Xu, et al., *A DNA sequence-specific electrochemical biosensor based on alginic acid-coated cobalt magnetic beads for the detection of E. coli.* Biosensors and Bioelectronics, 2011. **26**(7): p. 3325-3330.

24. Y. Jiang and J. Wu, *Recent development in chitosan nanocomposites for surface-based biosensor applications.* Electrophoresis, 2019. **40**(16-17): p. 2084-2097.

25. I. Tiwari, M. Singh, C.M. Pandey, and G. Sumana, *Electrochemical detection of a pathogenic Escherichia coli specific DNA sequence based on a graphene oxide–chitosan composite decorated with nickel ferrite nanoparticles.* RSC advances, 2015. **5**(82): p. 67115-67124.

26. S. Teixeira, N.S. Ferreira, R.S. Conlan, O. Guy, and M.G.F. Sales, *Chitosan/AuNPs modified graphene electrochemical sensor for label-free human chorionic gonadotropin detection.* Electroanalysis, 2014. **26**(12): p. 2591-2598.

27. V.B. Juska and M.E. Pemble, *A dual-enzyme, micro-band array biosensor based on the electrodeposition of carbon nanotubes embedded in chitosan and nanostructured Au-foams on microfabricated gold band electrodes.* Analyst, 2020. **145**(2): p. 402-414.

28. A. Tabasi, A. Noorbakhsh, and E. Sharifi, *Reduced graphene oxide-chitosan-aptamer interface as new platform for ultrasensitive detection of human epidermal growth factor receptor 2.* Biosensors and Bioelectronics, 2017. **95**: p. 117-123.

29. L. Tian, J. Qi, X. Ma, X. Wang, C. Yao, W. Song, et al., *A facile DNA strand displacement reaction sensing strategy of electrochemical biosensor based on*

N-carboxymethyl chitosan/molybdenum carbide nanocomposite for microRNA-21 detection. Biosensors and Bioelectronics, 2018. **122**: p. 43-50.

30. S. Bansal, A. Jyoti, K. Mahato, P. Chandra, and R. Prakash, *Highly sensitive in vitro biosensor for enterotoxigenic escherichia coli detection based on ssDNA anchored on PtNPs-chitosan nanocomposite.* Electroanalysis, 2017. **29**(11): p. 2665-2671.
31. H.-F. Cui, W.-W. Wu, M.-M. Li, X. Song, Y. Lv, and T.-T. Zhang, *A highly stable acetylcholinesterase biosensor based on chitosan-TiO2-graphene nanocomposites for detection of organophosphate pesticides.* Biosensors and Bioelectronics, 2018. **99**: p. 223-229.
32. A.K. Yadav, T.K. Dhiman, G. Lakshmi, A.N. Berlina, and P.R. Solanki, *A highly sensitive label-free amperometric biosensor for norfloxacin detection based on chitosan-yttria nanocomposite.* International journal of biological macromolecules, 2020. **151**: p. 566-575.
33. Y. Du, X.-L. Luo, J.-J. Xu, and H.-Y. Chen, *A simple method to fabricate a chitosan-gold nanoparticles film and its application in glucose biosensor.* Bioelectrochemistry, 2007. **70**(2): p. 342-347.
34. A. Wahl, S. Barry, K. Dawson, J. MacHale, A. Quinn, and A. O'Riordan, *Electroanalysis at ultramicro and nanoscale electrodes: a comparative study.* Journal of The Electrochemical Society, 2013. **161**(2): p. B3055.
35. L.A. Wasiewska, I. Seymour, B. Patella, R. Inguanta, C.M. Burgess, G. Duffy, et al., *Reagent free electrochemical-based detection of silver ions at interdigitated microelectrodes using in-situ pH control.* Sensors and Actuators B: Chemical, 2021. **333**: p. 129531.

36. S. Xu, Y. Zhang, K. Dong, J. Wen, C. Zheng, and S. Zhao, *Electrochemical DNA biosensor based on graphene oxide-chitosan hybrid nanocomposites for detection of Escherichia coli O157: H7.* Int. J. Electrochem. Sci, 2017. **12**: p. 3443-3458.

37. Y. Yang, C. Li, L. Yin, M. Liu, Z. Wang, Y. Shu, et al., *Enhanced charge transfer by gold nanoparticle at DNA modified electrode and its application to label-free DNA detection.* ACS applied materials & interfaces, 2014. **6**(10): p. 7579-7584.

38. L.-Q. Wu, H. Yi, S. Li, G.W. Rubloff, W.E. Bentley, R. Ghodssi, et al., *Spatially selective deposition of a reactive polysaccharide layer onto a patterned template.* Langmuir, 2003. **19**(3): p. 519-524.

39. R.A. Hassan, L.Y. Heng, and L.L. Tan, *Novel DNA biosensor for direct determination of carrageenan.* Scientific reports, 2019. **9**(1): p. 1-9.

40. L.-L. Zhao, H.-Y. Pan, X.-X. Zhang, and Y.-L. Zhou, *Ultrasensitive detection of microRNA based on a homogeneous label-free electrochemical platform using G-triplex/methylene blue as a signal generator.* Analytica chimica acta, 2020. **1116**: p. 62-69.

41. C. Pothipor, N. Aroonyadet, S. Bamrungsap, J. Jakmunee, and K. Ounnunkad, *A highly sensitive electrochemical microRNA-21 biosensor based on intercalating methylene blue signal amplification and a highly dispersed gold nanoparticles/graphene/polypyrrole composite.* Analyst, 2021. **146**(8): p. 2679-2688.

42. W. Yang, M. Ozsoz, D.B. Hibbert, and J.J. Gooding, *Evidence for the direct interaction between methylene blue and guanine bases using DNA-modified carbon paste electrodes.* Electroanalysis: An International Journal Devoted to

Fundamental and Practical Aspects of Electroanalysis, 2002. **14**(18): p. 1299-1302.

43. E. Farjami, L. Clima, K.V. Gothelf, and E.E. Ferapontova, *DNA interactions with a methylene blue redox indicator depend on the DNA length and are sequence specific.* Analyst, 2010. **135**(6): p. 1443-1448.
44. R. Rohs, H. Sklenar, R. Lavery, and B. Röder, *Methylene blue binding to DNA with alternating GC base sequence: a modeling study.* Journal of the American Chemical Society, 2000. **122**(12): p. 2860-2866.
45. P. Vardevanyan, A. Antonyan, M. Parsadanyan, M. Shahinyan, and L. Hambardzumyan, *Mechanisms for binding between methylene blue and DNA.* Journal of Applied Spectroscopy, 2013. **80**(4): p. 595-599.
46. P. Kara, K. Kerman, D. Ozkan, B. Meric, A. Erdem, Z. Ozkan, et al., *Electrochemical genosensor for the detection of interaction between methylene blue and DNA.* Electrochemistry Communications, 2002. **4**(9): p. 705-709.
47. A.I. Munoz, N. Espallargas, and S. Mischler, *Tribocorrosion: Definitions and Relevance*, in *Tribocorrosion*. 2020, Springer. p. 1-6.
48. A. Rabti, R. Zayani, M. Meftah, I. Salhi, and N. Raouafi, *Impedimetric DNA E-biosensor for multiplexed sensing of Escherichia coli and its virulent f17 strains.* Microchimica Acta, 2020. **187**(11): p. 1-9.
49. M.E. Minaei, M. Saadati, M. Najafi, and H. Honari, *Label-free, PCR-free DNA Hybridization Detection of Escherichia coli O157: H7 Based on Electrochemical Nanobiosensor.* Electroanalysis, 2016. **28**(10): p. 2582-2589.
50. C.M. Pandey, I. Tiwari, and G. Sumana, *Hierarchical cystine flower based electrochemical genosensor for detection of Escherichia coli O157: H7.* RSC Advances, 2014. **4**(59): p. 31047-31055.

3.6. Supporting information

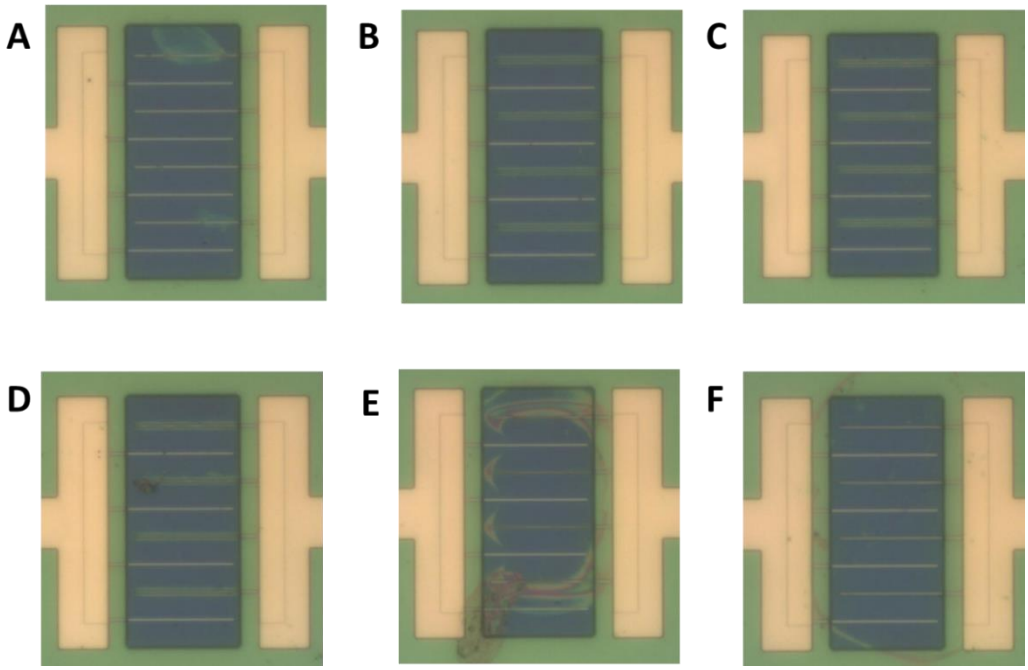

Fig. S3.1 Images under optical microscopy showing IDE modified with Cht/Au at different potential, (A) -1.2 V, (B) -1.4 V, (C) -1.5 V, (D) -1.6 V, (E) -1.8 V, (F) -2 V.

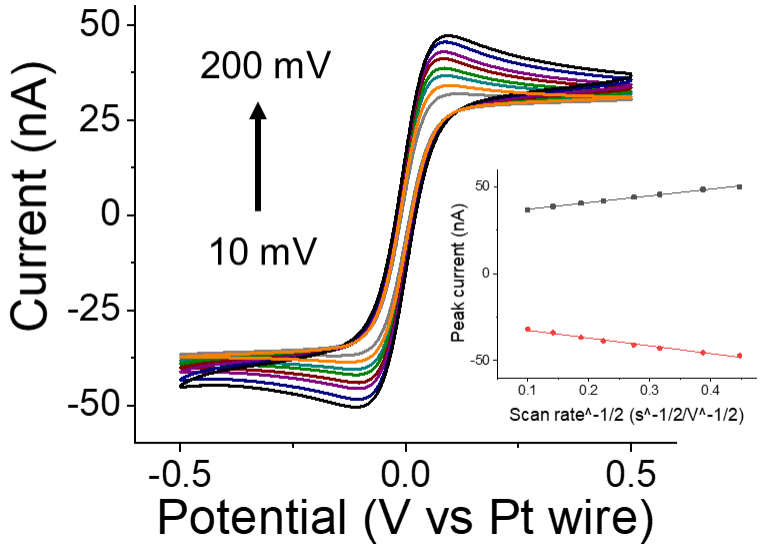

Fig. S3.2 Cyclic voltammograms at AuNPs/Cht-Au modified IDE in 5 mM Fe4-/Fe3−, 0.1 M KCl with a scan rate varying from 10 mV to 200 mV. The inset shows the linear increase between oxidation/reduction peaks and square root scan rate.

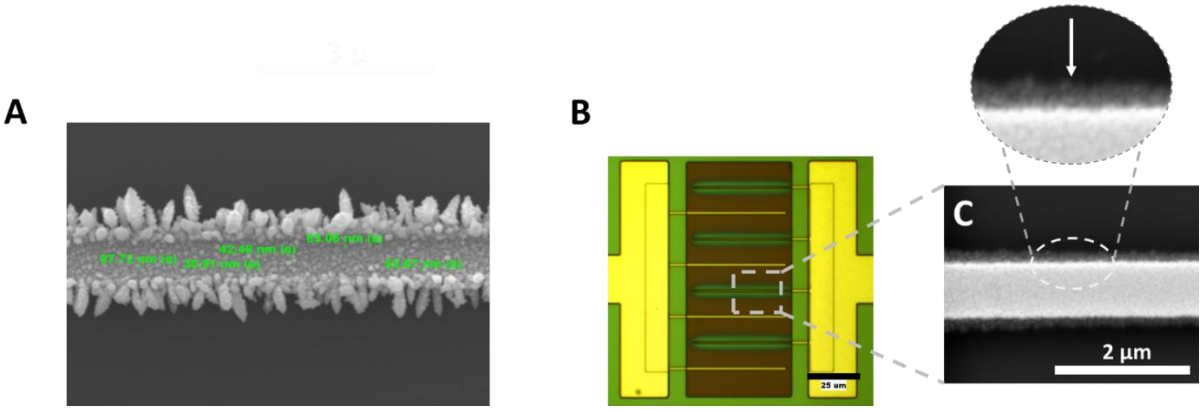

Fig. S3.3 (A) SEM image of the AuNPs surface with NPs size marked. (B) Optical image of the Cht-Au modified IDE. (C) SEM image of the Cht-Au surface.

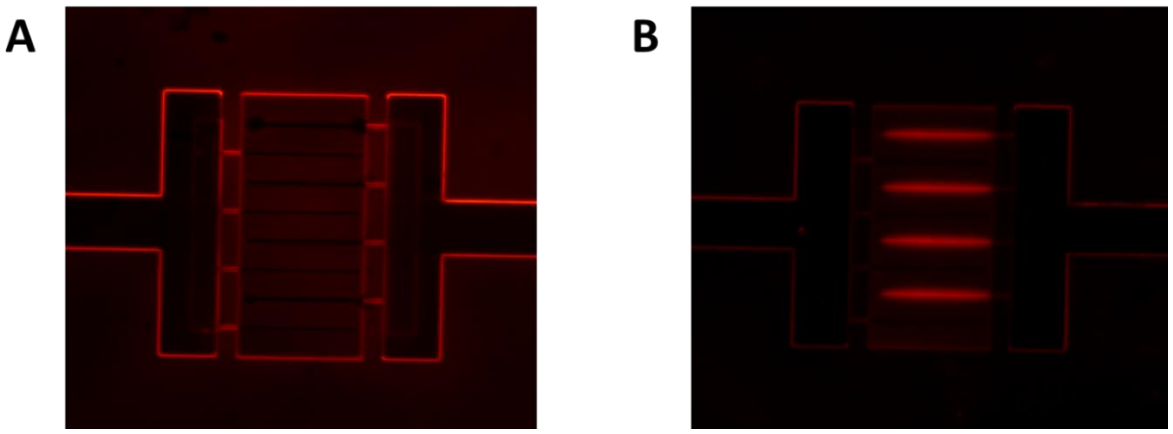

Fig. S3.4 (A) Image under the fluorescent microscope showing the Cht modified sensor IDE after incubation with Atto565 NHS ester dissolved in 0.01 M PBS. (B) Image under the fluorescent microscope showing Cht-Au modified sensor IDE without the fluorescent dye.

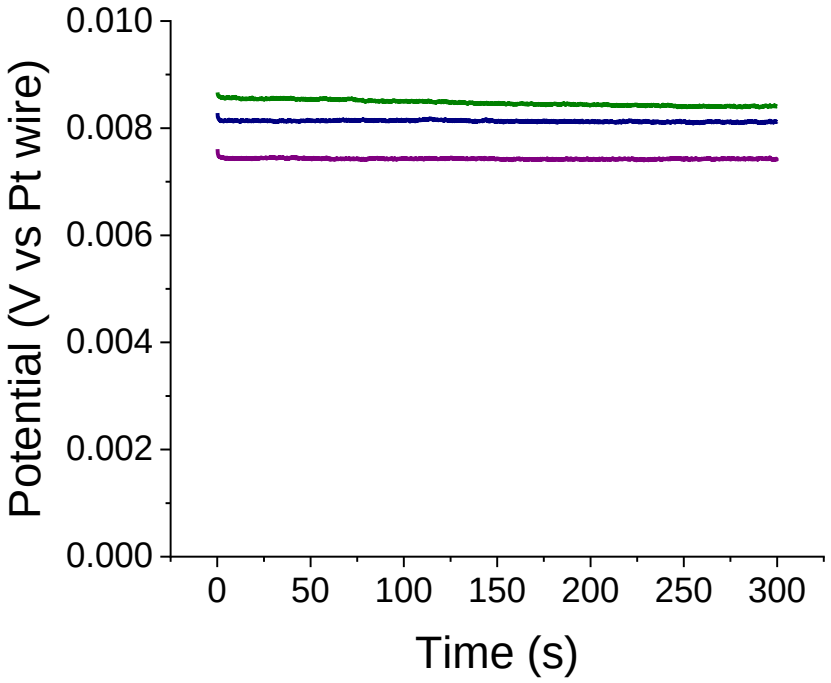

Fig. S3.5 Open circuit potential at three different electrodes during MB accumulation.

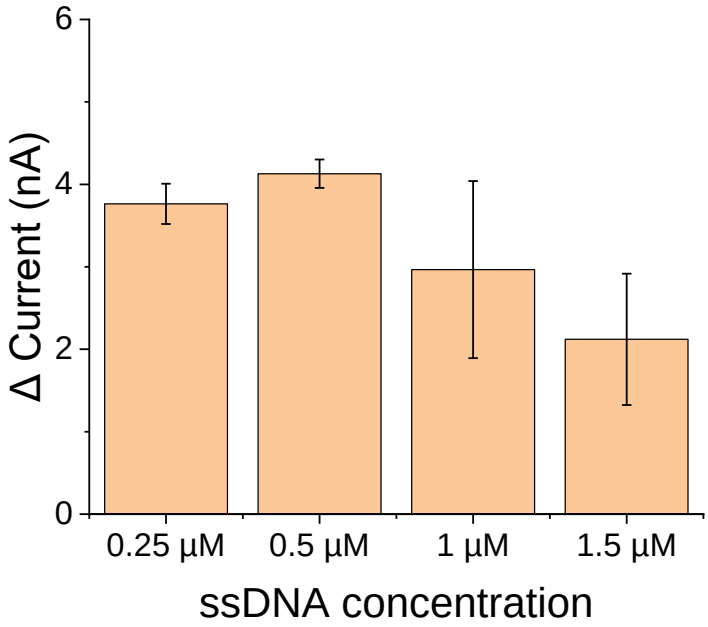

Fig. S3.6 Δ peak current height between MB response at ssDNA and dsDNA when (i) 0.25 µM, (ii) 0.5 µM, (iii) 1 µM and (iv) 1.5 µM ssDNA was immobilised to AuNPs/Cht-Au modified sensors IDE.

Chapter 4. Electrochemical multiplex DNA sensor for simultaneous detection of *stx1* and *stx2* genes of STEC

Submitted to “ACS Applied Materials & Interfaces”

4.1. Introduction

Shiga toxin-producing *E. coli* (STEC) is a food-borne pathogen of significant concern because it can cause severe disease, with symptoms such as bloody diarrhoea, haemorrhagic colitis and life-threatening haemolytic uremic syndrome (HUS) [1]. Their main reservoir is cattle and therefore the primary source of infection is beef meat or dairy products [2, 3]. The rapid detection of STEC along the food chain could significantly decrease the chance of infections [4]. Since the devastating outbreak in Germany in 2011, the approach for the identification of pathogenic strains shifted from using the O antigens on the bacterial cell wall to molecular techniques detecting virulence factor genes [5, 6]. Among several genes responsible for STEC pathogenicity *stx1* and *stx2*, two genes coding for toxin production and *eaeA* responsible for bacterial attachment to the epithelial cells, are considered major virulence factors [7]. It was found, however, that strains containing only *eaeA* rarely caused a serious illness, while strains that contained either *stx2* or *stx1* and *stx2* genes, with or without *eae*A were most likely to cause serious illness, such as haemolytic uraemic syndrome (HUS) [6, 8]. Another study found that a more severe outcome was reported with strains containing both *stx* genes [9].

Usually, STEC detection is undertaken by combining traditional culture and PCR methods to detect the virulence genes. The standard detection protocol (ISO 13136:2012) takes 3 days to obtain results and requires expertise to interpret them and is therefore not suitable for on-site detection on a farm or food-producing company [10]. Recently, electrochemical DNA sensors have gained a lot of attention because of their low cost, while offering a quick and easy way of detecting pathogens [11-13]. The electrochemical devices can easily be miniaturised and operated by non-qualified personnel, allowing for on-site measurement [14, 15]. Several sensors have been

developed for *E. coli* and STEC detection using common electrochemical techniques such as electrochemical impedance spectroscopy (EIS) [16, 17] or differential pulse voltammetry (DPV) [13, 18]. The STEC detection sensors typically focused on a single gene, especially *eae*A, not allowing for real identification of whether the strain could cause disease [19, 20]. Since there are several pathogenicity factors, simultaneous detection of both *stx* genes would be a more suitable approach for quick identification of strains that have a high possibility of causing serious illness [6]. In addition, the developed sensors are usually tested using a synthetic DNA strand or a PCR product without actually testing in more relevant real-world samples [19, 21], which does not allow understanding how the sensor would behave in on-site detection.

For instance, Li et al. [20] developed a sensor for the detection of the *eae*A gene using a glassy carbon electrode modified with graphene oxide and gold nanoparticles (AuNPs). The probe DNA was attached to the AuNPs using thiols, and the detection was performed using DPV. The authors achieved LODs of 10^{-11} M of synthetic DNA and synthetic stool samples were also tested using the standard addition method with synthetic DNA. In other studies reported by Kashish *et al*. [22] and Xu *et al.* [23] the authors used chitosan modified electrodes for covalent attachment of probe DNA and EIS for the detection achieving a low LOD, 3.6 x 10^{-14} M and 3.6 x 10^{-15}, M respectively. However, the complex samples tested by Kashish *et al.* [22] were with the use of PCR amplicons, which means an additional amplification step had to be introduced. In another study, STEC on contaminated chicken samples was directly detected using a sensor developed by *Nadzirah et al.* [24] using interdigitated electrodes (IDEs); which have gained much attention recently [25, 26]. Aluminium IDEs modified with TiO_2 and APTES were used to immobilise probe DNA and the hybridisation event was detected by conductance. The LOD reported was 1×10^{-11} M

of synthetic DNA, which is not sufficient to detect the low levels of STEC at concentrations sufficient to cause disease.

Gold nanoparticles have been shown to significantly increase the sensitivity of electrochemical biosensors because of the increased surface area for probe attachment and the conductivity of the electrode [27]. Our previous work has shown that electrodeposition of AuNPs as an underlying layer to chitosan-gold nanocomposite on interdigitated gold microelectrodes significantly increased the electrode's conductivity and therefore allowed for sensitive DNA detection; see Chapter 3. In that work a sensitive sensor for detection of the *stx1* gene using interdigitated gold microelectrodes was developed, where the probe DNA was selectively immobilised on one comb modified with a gold-chitosan nanocomposite. This method allowed detection of 10^{-16} M of synthetic DNA. In this work, the nanoparticles/chitosan deposition to improve the sensitivity of the previous method is further explored with the aim to develop a multiplex, chip-based sensor for the simultaneous detection of two genes, *stx1* and *stx2*, coding for toxin production. Finally, chromosomal DNA extracted from overnight STEC cultures was tested using a modified sensor to confirm its selectivity.

4.2. Materials and methods

4.2.1. Chemicals

All solutions were prepared by diluting with ultra-pure Milli-Q water (18.2 MΩ.cm, Milli-Q). Chitosan, $HAuCl_4$, N,N-Dimethylformamide (DMF), KCL, PBS, sodium acetate, 50% glutaraldehyde, Atto565 NHS ester, HEPES, synthetic oligonucleotides in dried form were obtained from Sigma Aldrich, Ireland.. Upon arrival, they were diluted with sterile DI water to 100 µM and stored at -20°C. Prior to use, they were diluted in 0.1 M PBS buffer to the desired concentration. The probe sequences for *stx1* and *stx2* detection were selected based on the ISO/TS 13136:2012 standard. The probes were modified with amine groups at the 5' end, enabling attachment to the electrode. For fluorescent confirmation, the target sequence was modified on the 5' end with Atto565 fluorescent dye. The sequences used are detailed in Table 4.1:

Table 4.1 Summary of DNA sequences

Name	Sequence
stx1 probe	5' NH_2 (C6) CTG GAT GAT CTC AGT GGG CGT TCT TAT GTAA 3'
stx1 target	5' TTAC ATA AGA ACG CCC ACT GAG ATC ATC CAG 3'
stx2 probe	5' NH_2 (C6) TCG TCA GGC ACT GTC TGA AAC TGC TCC 3'
stx2 target	5' GGA GCA GTT TCA GAC AGT GCC TGA CGA 3'
stx1 target + Atto565	5' [Atto 565] TTAC ATA AGA ACG CCC ACT GAG ATC ATC CAG 3'
Stx2 target + Atto 565	5' [Atto 565] GGA GCA GTT TCA GAC AGT GCC TGA CGA 3'

Chitosan stock solution (0.2%) was prepared by dissolving 0.1 g of chitosan in 50 mL DI water containing 1% acetic acid. The solution was stirred overnight and filtered using filter paper to remove undissolved polymer. The final pH of the stock solution was ~3. Two gold ions stock solutions were prepared and stored at 4°C. The first stock solution, used for AuNPs electrodeposition, contained 1000 ppm $HAuCl_4$ dissolved in 0.01 M sodium acetate, pH 3, while the second stock solution, used for Cht-Au nanocomposite electrodeposition, contained 1000 ppm of $HAuCl_4$ dissolved in DI water.

4.2.2. Apparatus

Electrochemical measurements, including amperometry (amp), cyclic voltammetry (CV), and square wave voltammetry (SWV) were undertaken using a CHI920 potentiostat while the electrochemical impedance (EIS) measurements for the electrode's characterisation were undertaken using Multi AutoLab M101.

A three-electrode electrochemical setup was used for sensor IDE modification, a gold working electrode, an on-chip gold counter electrode, and an external Ag/AgCl a reference electrode. A modified four-electrode setup was employed for DNA detection: a modified gold IDE was used as a sensor, an unmodified gold IDE was used as an accumulator and on-chip gold and platinum as counter and pseudo reference electrodes, respectively.

White light optical microscopy images and fluorescent microscopy images of the non-modified and modified IDEs were acquired using an Axioskop II (Carl Zeiss Ltd.) microscope equipped with a halogen lamp and a charge-coupled detector camera (CCD; Coolsnap CF, Photometrics). The surface morphology and compositional

analysis of AuNPs and Cht-Au modified IDEs were performed using a field emission scanning electron microscope (FEI QUANTA 650 HRSEM).

4.2.3. Chips fabrication and development of multiplex DNA electrochemical sensor

The silicon chips were fabricated in the same way as described previously in [25] and chapter 3. Prior to electrode modification, the silicon chips were cleaned by sonicating for 10 minutes in ethanol and DI water. Once clean, the chip was dried in a stream of nitrogen, placed in a chip holder and connected to the potentiostat using an SD connector. Fig. 4.1 summarises the steps of multiplex sensor development. Six sensors IDEs were modified at the same time, to avoid variability between the IDEs, by using an SD connector with connected wires. The first step was to electrodeposit gold nanoparticles by applying -0.2 V for 120 s in 500 µL of 400 ppm $HAuCl_4$ in 10 mM sodium acetate, pH 3. The Cht-Au nanocomposite was electrodeposited on the top of the pre-AuNPs modified IDEs by applying -1.4 V for 15 s in 0.03% (v/v) of chitosan diluted with DI water containing 1% acetic acid and 50 ppm of $HAuCl_4$ diluted in DI water. The chitosan solution was adjusted to ~pH 5 using 1 M NaOH. After modification, the sensor chip was immersed in 0.01 M PBS buffer, pH 7, for 10 minutes to stabilise the polymer layer. The amine groups on the Cht modified IDE were activated by incubating the silicon chip in 50 µL of 0.2 % (v/v) glutaraldehyde for two hours. Finally, the activated electrodes were incubated with 0.5 µM amine-modified probe ssDNA diluted in 0.1 M PBS, pH 7.4, also for two hours. The development of the multiplex sensor was achieved by incubating the first three electrodes and the last three electrodes with 10 µL of ssDNA complementary to the *stx1* gene and *stx2* gene, respectively. Electrochemical detection was undertaken using SWV with methylene blue (MB), known to interact with DNA, as a redox molecule.

Before and after hybridisation with the target, the multiplex sensor was incubated in 50 µM MB dissolved in HEPES buffer (0.02 M HEPES, 0.01 KCl, pH 7) for 10 minutes. For the first 5 minutes, OCP was applied to the accumulator IDEs to allow more efficient intercalation of MB between the double-strand DNA (dsDNA), as described in chapter 3. Following this, MB was removed and the chip was washed with the plain HEPES buffer. Finally, the sample holder was filled with HEPES previously degassed using nitrogen, to avoid interference with oxygen, and SWV was performed between 0 and -0.8 V, vs the on-chip platinum pseudo reference electrode (frequency 75 Hz, pulse amplitude 75 mV, increment 15 mV).

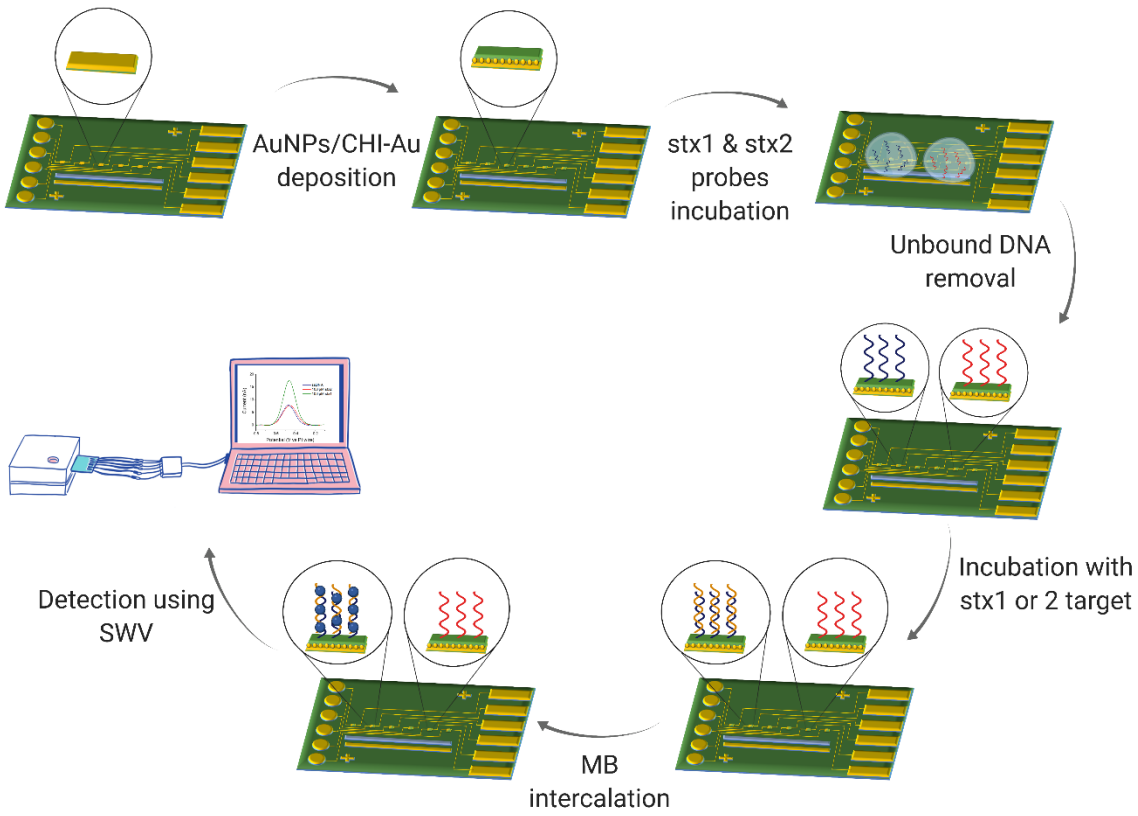

Fig. 4.1 Multiplex sensor development steps, (A) silicon-based chip with non-modified electrodes, (B) electrodeposition of AuNPs and Cht-Au layer, (C) incubation of stx1 and stx2 probes on electrodes 1-3 and 4-6, respectively, (D) developed multiplex sensor for detection of stx1 and stx2 genes, (E) selective hybridisation of stx1 target

on the multiplex sensor, (F) intercalation of MB between dsDNA, (G) selective detection DNA hybridisation using SWV.

4.2.4. Fluorescence characterisation

The density and distribution of amine groups on the AuNPs/Cht-Au modified IDEs were confirmed using a fluorescently labelled succinimidyl ester (Atto565-NHS ester) known to bind to the primary amine groups. The stock solution (500 µL) of the fluorescent label was prepared at a concentration of 2 mg/mL by diluting 1 mg of its powder form in 500 uL DMF and stored for a maximum of two weeks in the freezer. Subsequently, silicon chips with AuNPs/Cht-Au modified IDEs were incubated for 30 minutes at room temperature in 30 mL PBS buffer mixed with 50 µL of the Atto565 stock solution. After the dye was washed away using DI water to remove the unbound dye,the chips were dried under a stream of nitrogen. The modified IDEs were visualised by fluorescent microscopy with Zeiss filter set 15 (excitation 546/12 nm, emission 590 nm).

The fluorescence was also used to confirm the specific hybridisation of only a complementary strand to the multiplex sensor. To this end, two DNA strands, complementary to *stx1* and *stx2*, respectively, modified with Atto565 on 5' end were used. The multiplex sensor was incubated with 10 nM of either *stx1* or *stx2* target for 30 minutes at room temperature. The sensor chip was then washed with DI water and dried under the nitrogen stream. Finally, the sensors were visualised under fluorescent microscopy using the same filter as above.

4.2.5. Culture preparation and target DNA extraction

DNA was extracted from three STEC strains, Salmonella spp. and Listeria inocua. *E. coli* O103 contained the *stx1* gene, *E. coli* O91 contained the *stx2* gene while *E. coli*

O157 contained both *stx1* and *stx2* genes. The cultures were grown up from culture collection stocks (Teagasc Food Research Centre Ashtown) which were stored on protective beads at -80°C. A single bead of each isolate was streaked on Tryptone Soy Agar (Oxoid, Fisher Scientific Ireland) and incubated overnight at 37 °C. An isolated colony was then placed in Tryptone Soy Broth and incubated overnight at 37 °C. DNA was extracted from the overnight culture using a Qiagen DNeasy Blood and Tissue kit (Qiagen, Manchester, UK), and following the manufacturer's instructions. The DNA concentration was measured using a Qubit dsDNA BR Assay Kit (Thermo Fisher Scientific, Ireland) on a Qubit 4.0 fluorometer.

DNA samples were diluted 5 times in 0.1 M PBS buffer, pH 7.2, sonicated for 5 minutes to break the long DNA strand and heated to 95 °C for 2 minutes to denature dsDNA, prior to electrochemical measurements. Afterwards, the samples were cooled down rapidly on ice and 50 µL of the sample was incubated on top of a prepared multiplex sensor for 30 minutes at room temperature. After incubation, the sensor was washed with DI water and electrochemical detection was performed.

4.2.6. Statistical analysis

The data from sensor's optimisation were analysed using a t-test in Excel 2013 (Microsoft). The significance was reported if $p<0.05$.

4.3. Results and discussion

4.3.1. Multiplex sensor optimisation

Fig. 4.2 (A) presents a silicon-based chip, comprising six gold IDEs, gold counter and platinum reference electrodes. The connection pads on both sides of the chip allow an independent connection of two IDE combs, sensor and accumulator. Fig. 4.2 (B) presents the silicon chip in a chip holder that could be directly connected with a PCB mounted microSD port or gold pins to connect the sensor IDEs and to connect the accumulator IDEs.

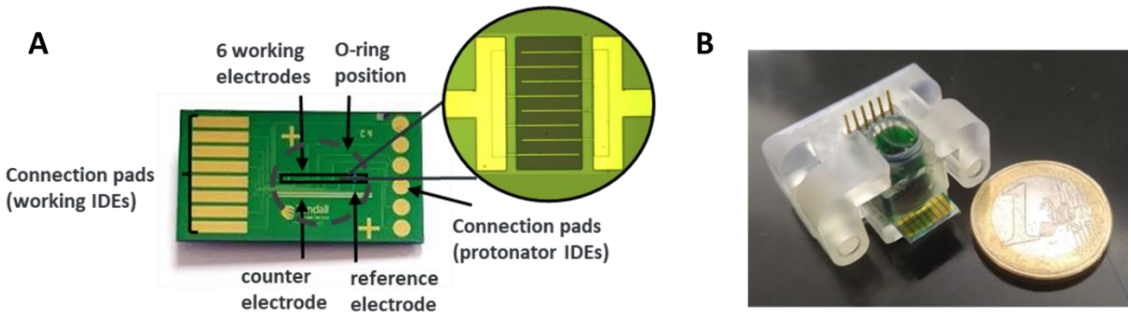

Fig. 4.2 (A) Silicon-based chip comprising six gold IDEs, gold counter and platinum reference electrodes. (B) Silicon chip in a holder.

In the previous chapter, the chitosan modified surface was obtained by its deposition (0.04%) in the presence of gold ions (50 ppm) at -1.5 V for 15 s. Polymer deposition optimisation was performed at the unmodified IDEs using CV and optical microscopy for comparison. After optimisation, the deposition of an underlying layer of AuNPs below the Cht-Au improved the performance of the sensor significantly, but the conditions of Cht-Au deposition were not modified after the layer of AuNPs was introduced. In this chapter, we re-optimised the Cht-Au deposition to improve sensor performance. First, CV at 0.4% and 50 ppm Au was undertaken at the (i) unmodified IDE and (ii) IDE modified with AuNPs, see Fig. 4.3 (A). It can be seen that both voltammograms present a similar shape, however, the current is higher on the pre-

modified IDE and it plateaued at lower potential (~-1.3 V) compared to the unmodified IDE. A set of experiments using a fluorescent dye, Atto565, was done to evaluate the amine group distribution and density on Cht-Au deposited on the AuNPs modified IDE at different potentials. Fig. 4.3 (B-E) shows images under the fluorescent microscopy after electrodeposition of Cht-Au on AuNPs modified IDEs at (i) -1.2 V, (ii) -1.4 V, (iii) -1.5 V and (iv) -1.6 V and incubation with Atto565 for 30 min. Using these conditions, the polymer deposited at -1.2 V, see Fig. 4.3 (B), however, the fluorescence intensity is lower, compared to deposition at -1.4 V and -1.5 V, see Fig 4.3 (C) and (D). This suggests that the amine groups were less dense when deposited at -1.2 V comparing to lower voltage. On the other hand, the current at -1.6 V was too high to allow a selective deposition on sensor IDE and the amine groups were also visible around the passivation layer. The deposition at -1.4 V and -1.5 V resulted in the best visual effect, with -1.4 V being the most optimal, with dense and equally distributed amine groups around the IDE. To this end, Cht-Au nanocomposite was deposited at -1.4 V.

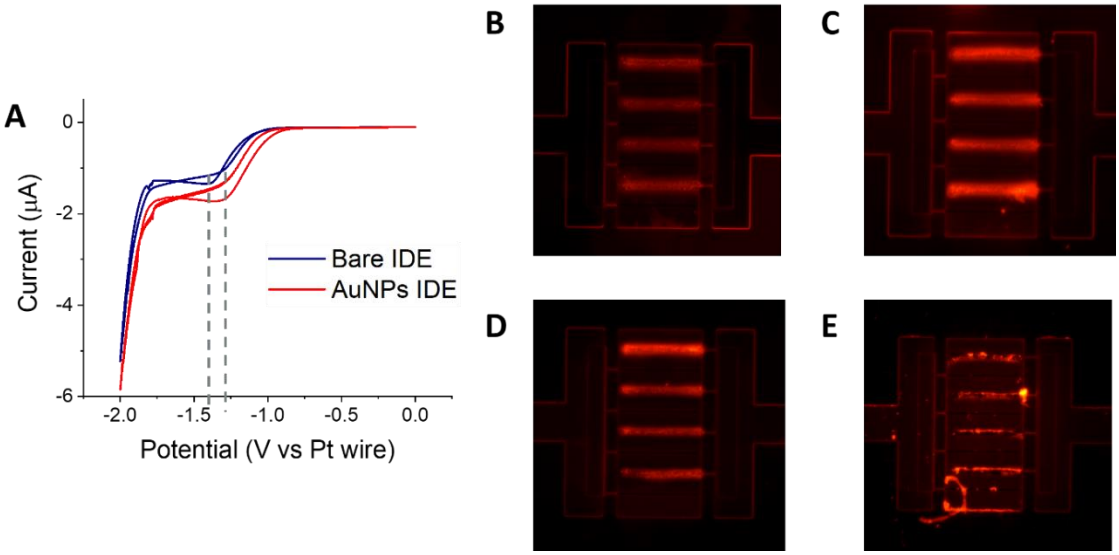

Fig. 4.3 Cht-Au deposition optimisation. (A) Cyclic voltammograms in 0.04 % chitosan, 50 ppm Au pH 5 at the unmodified sensor IDE (blue) and AuNPs modified

sensor IDE (red). Images under the fluorescent microscope showing the AuNPs modified sensor IDE after incubation with Atto565 NHS ester dissolved in 0.01 M PBS after the modification with Cht-Au electrodeposited at (B) -1.2 V, (C) -1.4 V, (D) -1.5 V, and (E) -1.6 V.

In chapter 3, the sensor targeted only a single *stx1* gene, and the probe DNA immobilisation step was done by incubating all six modified electrodes in 50 µM of amine-modified ssDNA complementary to the *stx1* gene. To develop the multiplex sensor, it was necessary to determine the optimal droplet size needed to allow simultaneous incubation of the *stx1* probe on the three first electrodes and the *stx2* probe on the other three electrodes. This is schematically shown in Fig. 4.4 (A). To evaluate the minimum amount of liquid needed for each droplet to achieve the optimal detection, three droplet sizes comprising ssDNA complementary to *stx1* gene were tested, (i) 5 µL, (ii) 10 µL and (iii) 15 µL. It was found that 15 µL was too large and unsuitable as the two droplets merged immediately after pipetting. Fig. 4.4 (B) presents the current difference between ssDNA and dsDNA after incubation with 50 nM of target DNA when 5 µL and 10 µL droplets were used. It can be seen that the detection efficacy was significantly lower with 5 µL, which could be due to not sufficient amount of probe to attach, in addition to the drying of the liquid during the incubation. Using 10 µL we could achieve a similar detection efficacy compared to the previously developed single sensor for the *stx1* gene. To this end, the ssDNA immobilisation on the multiplex sensor was undertaken using 10 µL droplets. The droplet size for DNA immobilisation in other studies typically varies between 5 and 50 uL [28-31]. In the study of Faria and Zucolotto [28], where 5 uL was used, the sensor was incubated in a humid chamber to avoid liquid evaporation which was a problem in this study. However, they did not perform a comparison of whether different droplet sizes could affect improving the sensor's efficacy. A different

approach was taken by Heydarzadeh et al. [32] where 10 uL of probe DNA was left on the sensor's surface until it dried. Such an approach was not effective in our study which could be attributed to the smaller sensor's size and therefore a need for high efficacy DNA immobilisation.

Subsequently, the detection of the *stx2* gene was optimised following electrochemical detection using MB developed in the previous chapter. Even though the DNA immobilisation and detection were the same, the *stx2* sequence used in this work was shorter compared to the *stx1* sequence (27 bases instead of 31), therefore we expected to observe a difference in results. First, the effect of Cht concentration on the detection efficacy was evaluated by electrodepositing three different concentrations of the polymer (i) 0.02 %, (ii) 0.03 %, and (iii) 0.04 %. Fig. 4.4 (C) shows Δ current between ssDNA and dsDNA when 100 pM of target DNA was applied. It can be seen that the current when using 0.04 % of chitosan was significantly lower compared to the *stx1* detection shown in Fig 4.4. (B), with only 1.8 nA (±0.344 nA) increase after target hybridisation. This suggests that the *stx2* probe density may have been too high to achieve efficient hybridisation. Decreasing the chitosan concentration to 0.03 % caused the Δ current increase to 3.2 nA (±0.19 nA) that decreased again to 1.22 nA (±0.08 nA) at 0.02 % suggesting that at this concentration the layer of polymer and therefore the number of amine groups was too low to achieve a sufficient number probe DNA attachment. To this end, 0.03 % of Cht was used. This was a significantly lower concentration compared to other studies where typically 1% Cht solution is used for electrode's modification [32-35]. These studies were done at the macro as well as microelectrodes and the modification was done by either electrodeposition or a drop cast technique where a Cht mixed with nanomaterials such as graphene oxide or gold nanoparticles was pipetted onto the electrode and left until dry. In our study, increasing

Cht concentration for the deposition caused the development of Cht-Au nanocomposite outside of the sensor IDE. This can be attributed to a specific shape of the microarray electrode as well as the high efficacy of gold ions binding with Cht during the electrodeposition.

To further increase the efficacy of the *stx2* detection, different times of AuNPs electrodeposition were explored. Fig. 4.4 (D) presents Δ current between ssDNA and dsDNA after the sensors incubation with 100 pM target DNA when the first layer of AuNPs were electrodeposited from 400 ppm $AuHCl_4$ for (i) 60 s, (ii) 75 s, (iii) 90 s, (iv) 105 s, and (v) 120 s. The detection was similar when AuNPs were electrodeposited for 60 and 75 s, see Fig 4.4 (D). However, the detection efficacy improved significantly when the gold was deposited for 90 s or more, with the highest efficacy recorded after deposition of 120 s. Even though the detection was highest when 120 s deposition was used, there was no statistical difference compared to deposition for 90 and 105 s ($p>0.05$). In addition, it was found that increasing gold deposition even higher could lead to non-specific binding, most likely attributed to gold nanoparticles not covered completely with the Cht-Au layer and therefore being exposed to the DNA from a sample. A gold surface is typically blocked with 6-mercapto-1-hexanol or other aromatic thiols, such as p-toluenethiol to avoid such unspecific binding attributed to interaction with gold [36-38]. In this study, however, the surface was only blocked with glutaraldehyde which binds to the primary amine groups on Cht. Therefore, any exposed AuNPs surface could lead to unspecific binding. In addition, a large layer of AuNPs could cause the subsequent deposition of Cht-Au to occur outside of the sensor IDE, onto the accumulator IDE which we did not intend to modify. To this end, AuNPs were electrodeposited for 120 s.

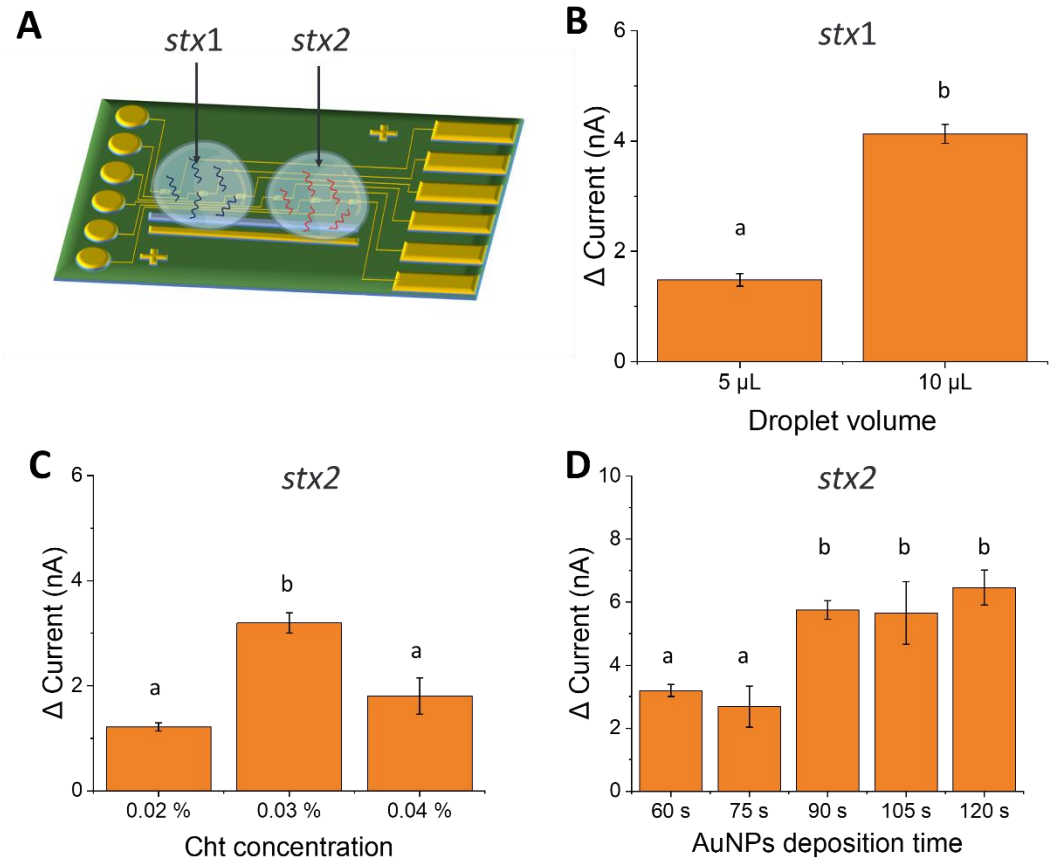

Fig. 4.4 Multiplex sensor optimisation. (A) Scheme of a silicon chip with two separate droplets with stx1 and stx2 probe DNA incubating on top of modified IDEs. (B) Δ current between ssDNA and dsDNA at stx1 detection sensor when (i) 5 µL and (ii) 10 µL of stx1 probe DNA was immobilised. (C) Δ current between ssDNA and dsDNA at stx2 detection sensor when (i) 0.02 %, (ii) 0.03 %, and (iii) 0.04 % of Cht was deposited. (D) Δ current between ssDNA and dsDNA at stx2 detection sensor when the underlying AuNPs layer was deposited for (i) 60 s, (ii) 75 s, (iii) 90 s, (iv) 105 s, and (v) 120s.

4.3.2. Characterisation of IDE modifications

Following the sensor optimisation with MB, the morphology of IDE modification was characterised using optical and electron microscopy (by Dr Sofia Teixeira) and the electrochemical characteristics were evaluated using CV and EIS. These results are summarised in Fig. 4.5 and S4.1. Fig. 4.5 (A) shows an SEM image of the unmodified IDE, presenting a smooth surface of the microarray. The sensor IDE was modified

afterwards with AuNPs for 2 minutes and Fig. S4.1 (A) presents an optical image after the modification. The dark bands around one side of IDE confirm a specific modification of only sensor IDE, further shown in Fig. S4.1 (B), where every second array was modified with gold and every second unmodified. These gold structures were characterised at a higher magnitude using SEM and are presented in Fig. 4.5 (B). Two different gold nanostructures can be distinguished—round NPs with a size <100 nm and larger dendritic particles on the edges with sizes between 500 and 1000 nm. This is in accordance with the findings in chapter 3, where similar structures were shown. In this work, the layer of gold is significantly bigger because of a longer deposition time. Finally, the AuNPs/Cht-Au modified IDE was characterised and its optical image is shown in Fig. S4.1 (C). A defined green colour can be seen around sensor IDE compared to IDE modified with AuNPs only (Fig. S4.1 (A)). The chitosan modification can hardly be seen under SEM in Fig. S4.1 (D), however, under the higher magnification, see Fig. 4.5 (C), a thin layer can be seen around the gold structures, indicated by arrows, which can be attributed to chitosan.

The electrochemical characterisation of the sensor IDE modifications was undertaken using CV and EIS in 5 mM $Fe^{II}(CN)_6^{4-}/Fe^{III}(CN)_6^{3-}$ in 0.1 M KCl as supporting electrolyte (scan rate 100 mV/s) at (i) unmodified IDE, (ii) IDE modified with AuNPs electrodeposited for 120 s, and (iii) IDE modified with AuNPs/Cht-Au. Fig. 4.5 (D) presents the cyclic voltammograms, we can observe that the oxidation current at the unmodified IDE reaches ~26 nA while it increases to ~57 nA and ~58 nA after the modification with AuNPs and AuNPs/Cht-Au. This is in agreement with the findings from Chapter 3, where the current was significantly higher after IDE modification. In this case, the electrodeposition of AuNPs for 120 s instead of 60 s caused the current to increase even more. Fig. 4.5 (E) shows the corresponding EIS measurements that

confirm the findings in agreement with the CV. The charge at the unmodified IDE was ~9 MΩ while it decreased significantly after modification with AuNPs to ~3MΩ and remained at a similar level after the modification with Cht-Au.

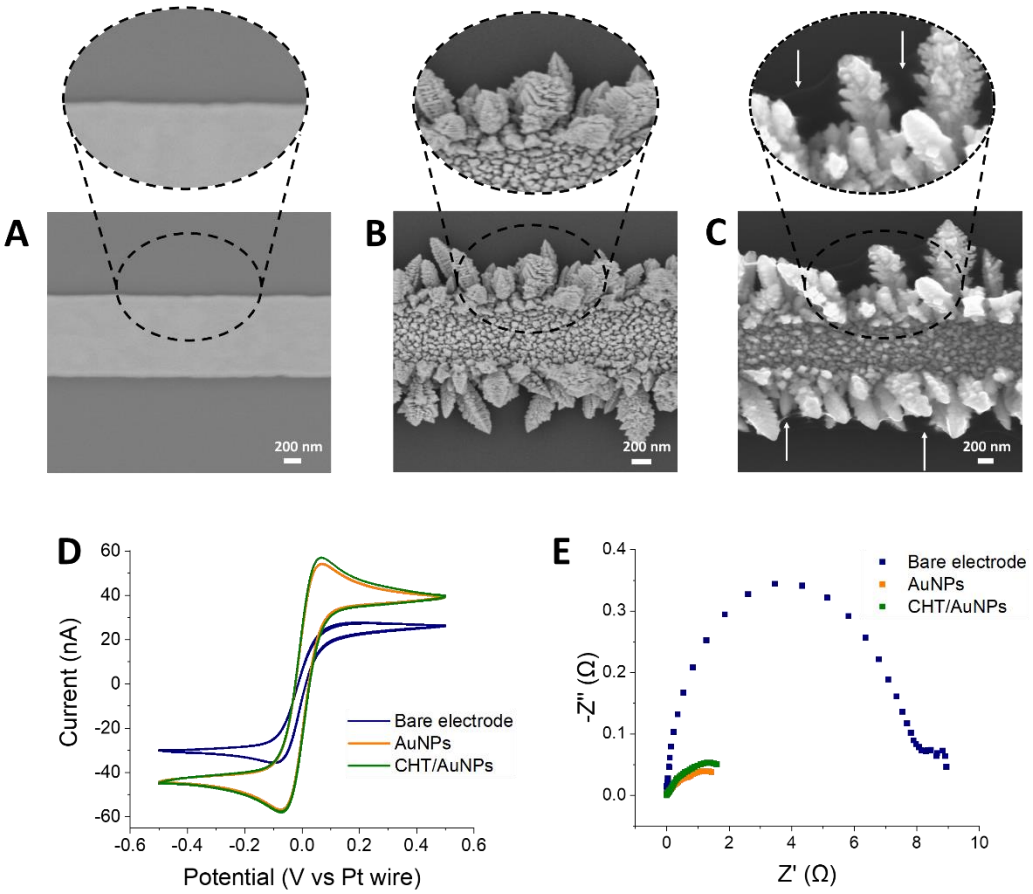

Fig. 4.5 IDE modification characterisation. (A) SEM image of a non-modified IDE; intercept presents a higher magnitude. (B) SEM image of a AuNPs modified IDE; intercept presents a higher magnitude. (C) SEM image of a AuNPs/Cht-Au IDE; intercept presents a higher magnitude. (D) Cyclic voltammograms of electrochemical characterisation of sensor IDE modifications using in a solution of 5 mM Fe^{4-}/Fe^{3-} in 0.1 M KCl as supporting electrolyte (scan rate 100 mV/s). (E) The corresponding EIS measurements in a solution of 5 mM Fe^{4-}/Fe^{3-} in 0.1 M KCl as supporting electrolyte.

4.3.3. Multiplex sensor characterisation

The selectivity of the developed multiplex sensor was first tested using fluorescently tagged DNA targets. Two sensor chips, modified with *stx1* and *stx2* probes, were

prepared using the parameters described above. Subsequently, one chip was incubated in 10 nM *stx1* target DNA modified with Atto565 on the 5' end while the other chip in 10 nM *stx2* target DNA, modified with Atto565 as well. After 30 minutes of incubation, the chips were washed with DI water, dried under a nitrogen stream, and the electrodes were visualised under fluorescent microscopy. Fig. 4.6 (A) presents a schematic representation of a multiplex sensor hybridised with the *stx1* fluorescently tagged target gene. Fig. 4.6 (B) presents a fluorescent image of a sensor IDE modified with the *stx1* probe after the successful hybridisation with the *stx1* target, suggested by the red colour at the sensor IDE. Fig. 4.6 (C) presents a fluorescent image of a sensor IDE modified with the *stx2* probe, where no hybridisation occurred, and therefore, no colouring can be observed at the same light exposure. The scheme presenting the opposite situation is presented in Fig. 4.6 (D) where a multiplex sensor hybridised with target complementary to *stx2*. In this case, as expected, no colour is observed at the sensor IDE modified with *stx1* probe DNA, see Fig. 4.6 (E), while the red colour can be observed at the sensor IDE modified with *stx2* probe DNA, see Fig. 4.6 (F).

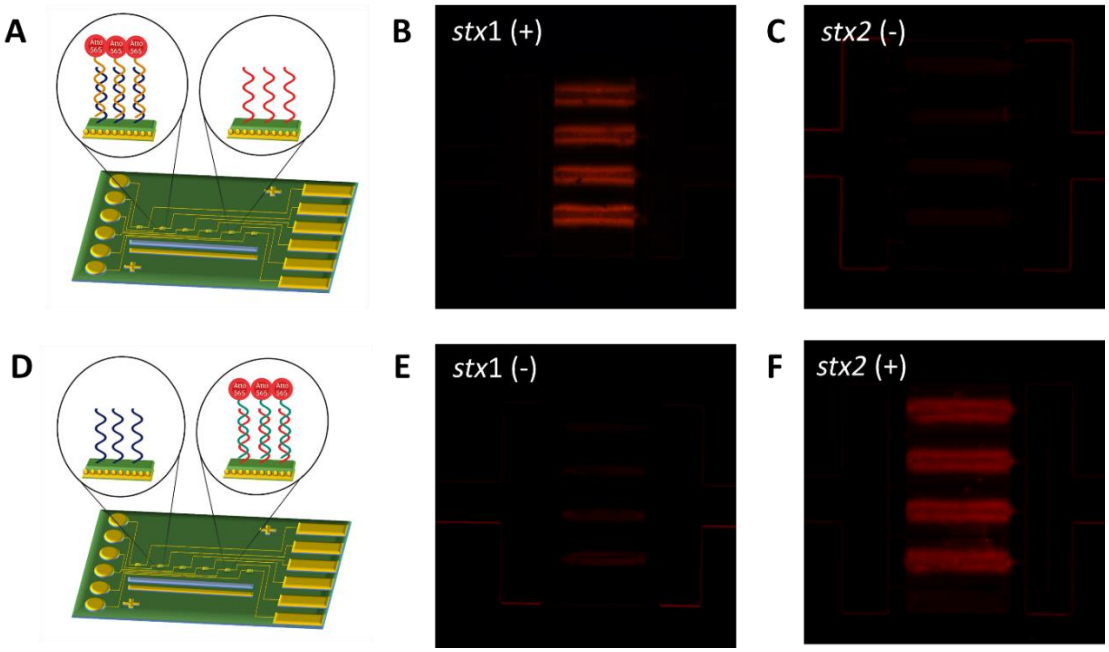

Fig. 4.6 Multiplex sensor's selectivity confirmation using fluorescently labelled targets. (A) Scheme representing a selective hybridisation of stx1 target strand modified with Atto565 onto the multiplex sensor. (B) Image under fluorescence microscopy of an IDE modified with stx1 probe after 30 min incubation with 10 nM of stx1 target. (C) Image under fluorescence microscopy of an IDE modified with stx2 probe after 30 min incubation with 10 nM of stx1 target. (D) Scheme representing a selective hybridisation of stx2 target strand modified with Atto565 onto the multiplex sensor. (E) Image under fluorescence microscopy of an IDE modified with stx2 probe after 30 min incubation with 10 nM of stx2 target. (F) Image under fluorescence microscopy of an IDE modified with stx1 probe after 30 min incubation with 10 nM of stx2 target.

The method used for the electrochemical detection in this work was the same as developed in the previous chapter, where the sensor was incubated in 50 µM MB for ten minutes, with the first five minutes done at OCP applied to the accumulator electrode. To show the selectivity of the multiplex sensor, a set of electrochemical measurements using MB were undertaken before and after incubating the sensor with 1 pM of synthetic target DNA for 20 minutes. First, selective detection of the *stx1* gene was evaluated, which is schematically shown in Fig. 4.7 (A). In brief, the target

gene hybridises specifically with the probe DNA immobilised to the first three IDEs and the MB intercalates between the dsDNA at these IDEs. SWV signal recorded on the sensor incubated with *stx1* target is shown in Fig. 4.7 (B) where, as expected, the peak current increased significantly only for the *stx1* modified IDE, while staying the same for the ssDNA at the *stx2* modified IDE. To evaluate the opposite scenario, the multiplex chip was incubated with the *stx2* target DNA and incubated with MB, schematically presented in Fig. 4.7 (C). In this case, the electrochemical signal increased at the sensor modified with the *stx2* probe while no increase was observed at the sensor modified with the *stx1* probe, see Fig. 4.7 (D).

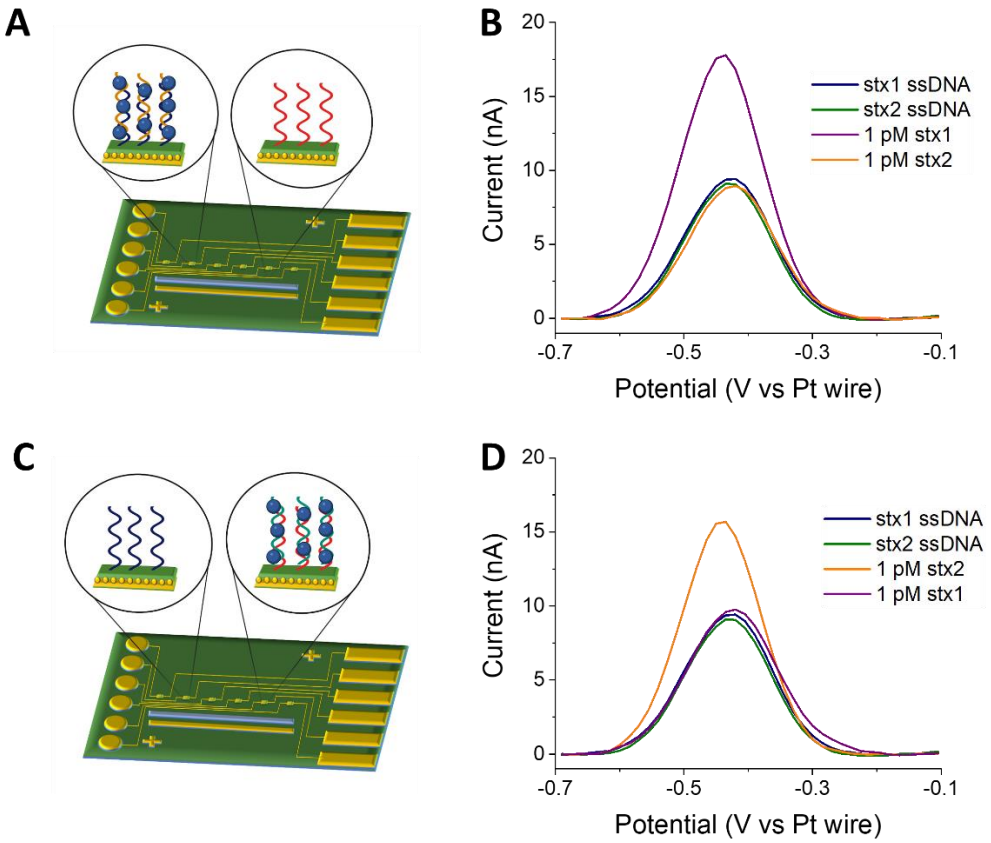

Fig. 4.7 Multiplex sensor's selectivity confirmation using electrochemistry. (A) Scheme representing a selective hybridisation of stx1 target strand onto the multiplex sensor after MB intercalation. (B) Square Wave Voltammograms of MB after incubating the multiplex sensor with stx1 target. (C) Scheme representing a selective hybridisation of stx2 target strand onto the multiplex sensor after MB intercalation.

(D) Square Wave Voltammograms of MB after incubating the multiplex sensor with stx2 target.

To establish the lowest limit of detection (LOD) of the developed sensors for both genes, one sensor was modified only with the *stx1* probe, while the other one was with the *stx2* probe. Both chips were then incubated with an increasing concentration of target DNA between 10^{-19} and 10^{-12} M for 20 min and electrochemical detection was undertaken after each concentration. It was observed that the signal increased for both targets from 10^{-19} M until 10^{-14} for the *stx1* gene and 10^{-13} M for the *stx2* gene. Fig 4.8 (A) and (B) present square wave voltammograms for ssDNA and the increasing target DNA concentrations for *stx1* and *stx2*, respectively. Fig. 4.8 (C) and (D) show the calibration curve for *stx1* and *stx2* genes, respectively, with a log DNA concentration, plotted against the Δ current height. Each data point represents a mean value of three measurements on separate sensors and a standard deviation. Both calibration curves exhibit an excellent linearity with R^2 = 0.991 and R^2 = 0.989 for *stx1* and *stx2*, respectively. The LOD for both targets was 10^{-19} M which is significantly lower compared to similar electrochemical sensors for the detection of nucleic acids developed recently [24, 39-42]. This was also three orders of magnitude lower compared to the sensor developed in chapter 3, where the main difference is the increase in time of AuNPs electrodeposition from 60 s to 120 s in this work.

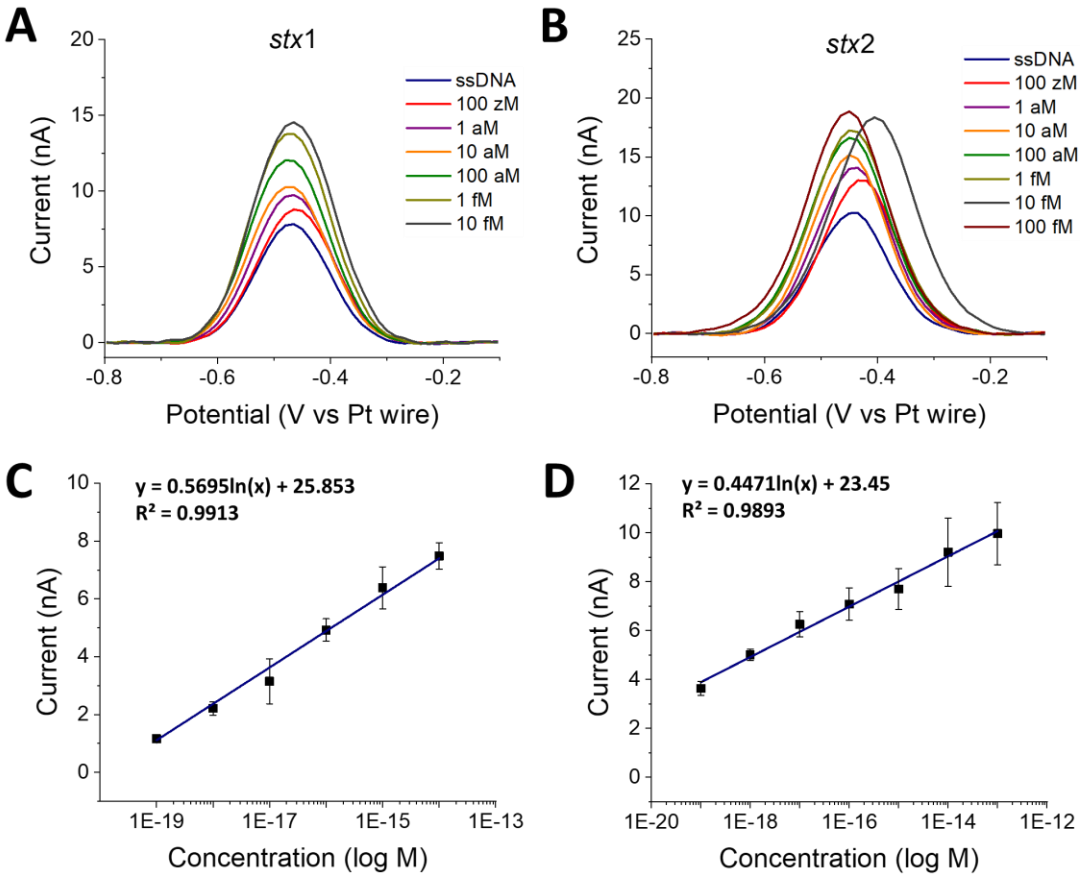

Fig. 4.8 Multiplex sensor's calibration (A) Square wave voltammograms on stx1 sensor after the addition of the increasing concentrations of target DNA. (B) Square wave voltammograms on stx2 sensor after the addition of the increasing concentrations of target DNA. (C) Calibration curve for the stx1 probe. Each data point represents a mean value between three measurements. (D) Calibration curve for the stx2 probe. Each data point represents a mean value between three measurements.

4.3.4. Complex samples analysis

Finally, the developed multiplex sensor was tested using chromosomal DNA extracted from the overnight bacterial cultures to confirm the selectivity of the sensor for more complex samples than PCR products, and the results are summarised in Fig. 4.9. Each data point represents a mean value of four measurements on different sensor IDEs. First, two STEC strains were tested, one of which (STEC O103) contained only the *stx1* gene while the other (STEC O157) contained both toxin coding genes, *stx1* and

stx2. Fig. 4.9 (A) presents the Δ peak current height of MB before and after the sensor's incubation with DNA from STEC O103. It can be observed that the current increased by ~4.5 nA (±0.6) at IDEs modified with *stx1* probe while it only increase by 0.39 nA (±0.39) on the *stx2* modified IDE. This suggests that the chromosomal DNA from STEC O103 was specifically hybridised with the *stx1* probe and it did not attach to the *stx2* probe, showing the selectivity of the sensor IDE. A negative sample showed a slight increase in the current which can be attributed to an additional accumulation of MB on ssDNA. Based on the results obtained we considered a sample to be negative if this increase was below 1 nA compared to measurement on a probe DNA. Results of the sensor incubation with STEC O157, containing both toxin coding genes can be seen in Fig. 4.9 (B). As expected, an increase in current height was observed on sensors modified with both DNA probes. The current height increase was 3.38 nA (±0.26) and 4.4 nA (±0.48) on the *stx1* and *stx2* probe modified sensors, respectively. Subsequently, the developed sensor was tested with non-*E. coli* bacterial species often found in food, *Salmonella spp* and *Listeria incouca* and the results are presented in Fig. 4.9 (C) and (D), respectively. It can be observed that the current in both cases did not increase above 1 nA and the average Δ current height was -0.29 nA (±0.19) for *stx1* and 0.18 (±0.36) for *stx2* while 0.24 nA (±0.25) and 0.09 nA (± 0.38) for *Salmonella* and *Listeria*, respectively.

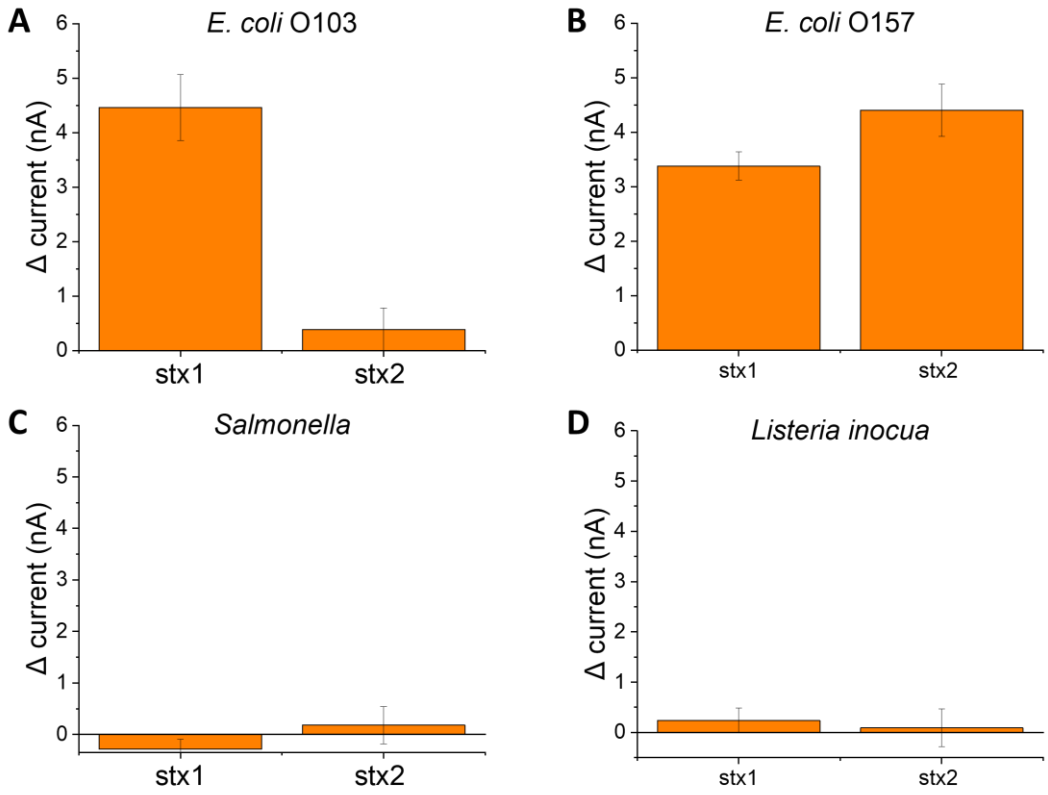

Fig. 4.9 Multiplex detection of chromosomal bacterial DNA. (A) Δ peak current heigh between MB response at stx1 and stx2 probe modified sensor IDEs and after incubation with chromosomal DNA of E. coliO103 (stx1 positive, stx2 negative). (B) Δ peak current height between MB response at stx1 and stx2 probe modified sensor IDEs and after incubation with chromosomal DNA of E. coliO157 (stx1 positive, stx2 positive). (C) Δ peak current height between MB response at stx1 and stx2 probe modified sensor IDEs and after incubation with chromosomal DNA of Salmonella (stx1 negative, stx2 negative). (D) Δ peak current height between MB response at stx1 and stx2 probe modified sensor IDEs and after incubation with chromosomal DNA of Listeria inocua (stx1 negative, stx2 negative).

4.3.5. Comparison to previous work

The data collected for the developed multiplex sensor were compared with the results previously reported in the literature and are summarised in Table 4.2. It can be seen that our multiplex sensor has significantly better sensitivity compared to the previously published work (LOD of 10^{-19} M), including our previous work (LOD 10^{-}

^{16} M). In addition, all other electrochemical DNA sensors for STEC detection focused on a detection of a single virulence gene, usually *stx1* or *eae*A, which is explained above, does not predict if the STEC strain could cause a serious illness. Another important factor when developing an electrochemical DNA sensor is testing its selectivity in more complex samples. Typically, the developed sensors in the literature were tested with synthetic DNA target only, which does not prove the sensor will work with real samples. Other sensors were tested with a PCR product which requires an additional step of DNA multiplication, which increases the time for obtaining the final results. Nadzirah et al. [24] tested chicken samples contaminated with STEC, where their sensor achieved a LOD of 10^{12} M of synthetic DNA. In the present study, we tested the developed sensor with chromosomal DNA extracted from STEC overnight bacterial culture. The sensors achieved excellent selectivity and sensitivity, showing that they might be applied for the detection of real samples. The DNA was, however, extracted from the overnight culture with a high concentration of bacterial cells. The target gene concentration in the real samples would probably be much lower and some kind of amplification or culture enrichment may be needed. Recently, more focus has been placed on fully integrated devices able to both multiply and detect DNA. In that regard, loop-Mediated Isothermal Amplification Assays (LAMP) have gained a lot of attention as a quick multiplication method under isothermal conditions (60 to 65°C) [43]. For instance, Xia et al. [44] used a combination of LAMP and lateral flow sensors for rapid detection of STEC O157, achieving a highly sensitive detection of 1.3 CFU/mL. Integrating LAMP multiplication into our electrochemical sensor would make our sensor even more feasible for on-site detection in the future.

Table 4.2. Comparison to previous work on the development of DNA sensors for STEC detection

Electrode material	Electrode modification	Gene(s) detected	Detection technique	LOD [M]	Complex samples	Author
Al IDE	TiO_2 NPs	Sequence reported	Con	10^{-12}	Chicken	[24]
Au IDE	Thiols	Sequence reported	Amp	$8x10^{-16}$	-	[45]
SPE	PtNPs + chitosan	*stx* gene	EIS	$3.6x10^{-14}$	Surface water (PCR product)	[22]
GCE	GOx + chitosan	Sequence reported	EIS	3.6×10^{-15}	-	[23]
GCE	GOx + AuNPs + thiols	*eae*A gene	DPV	10^{-11}	Synthetic stool samples	[20]
Au IDEs	AuNPs + Cht-Au	*stx1*	SWV	$1x10^{-16}$	Chromosomal DNA	Chapter 3
Au IDEs	**AuNPs + Cht-Au**	***stx1*&2**	**SWV**	**$1x10^{-19}$**	**Chromosomal DNA**	**This work**

SPE - Screen Printed Electrode, **GCE** - Glassy Carbon Electrode, **PtNPs** - Platinum nanoparticles, **GOx** - graphene oxide, **Con** – conductance, **Amp** – amperometry, **EIS** - Electrochemical Impedance Spectroscopy, **DPV** - Differential Pulse Voltammetry

4.4. Conclusions

In this work, we have successfully developed a multiplex electrochemical sensor for the simultaneous detection of *stx1* and *stx2* genes from STEC. First, we have increased the sensitivity of the previously developed method for the detection of the *stx1* gene by three orders of magnitude (from 10^{-16} M to 10^{-19} M). This was achieved by increasing the AuNPs electrodeposition time from 60 s to 120 s and re-optimizing the chitosan deposition parameters. Subsequently, we attached two different probe DNA on a single chip and achieved multiplex detection. This is crucial for the identification of several virulence factors of STEC and predicting if a particular strain can cause serious illness. In the future, more genes should be incorporated, for example, *eae*A, to increase the accuracy of identification of potentially pathogenic strains even more. Such a sensor could be used on a farm or in a food processing company for the detection of the presence of pathogenic STEC strains or in hospital settings for quick identification of genes responsible for causing the disease in patients. In addition, this sensor allows an easy modification of the probe DNA and therefore could be easily modified to the detection of other pathogenic bacteria.

4.5. References

1. U. Naseer, I. Løbersli, M. Hindrum, T. Bruvik, and L.T. Brandal, *Virulence factors of Shiga toxin-producing Escherichia coli and the risk of developing haemolytic uraemic syndrome in Norway, 1992–2013.* European Journal of Clinical Microbiology & Infectious Diseases, 2017. **36**(9): p. 1613-1620.
2. R. Ranjbar, F.S. Dehkordi, M.H.S. Shahreza, and E. Rahimi, *Prevalence, identification of virulence factors, O-serogroups and antibiotic resistance properties of Shiga-toxin producing Escherichia coli strains isolated from raw milk and traditional dairy products.* Antimicrobial Resistance & Infection Control, 2018. **7**(1): p. 1-11.
3. K.S. Anklam, K.S. Kanankege, T.K. Gonzales, C.W. Kaspar, and D. Doepfer, *Rapid and reliable detection of Shiga toxin–producing Escherichia coli by real-time multiplex PCR.* Journal of food protection, 2012. **75**(4): p. 643-650.
4. C.Z. To and A.K. Bhunia, *Three dimensional Vero cell-platform for rapid and sensitive screening of Shiga-toxin producing Escherichia coli.* Frontiers in microbiology, 2019. **10**: p. 949.
5. M.A. Karmali, *Factors in the emergence of serious human infections associated with highly pathogenic strains of shiga toxin-producing Escherichia coli.* International Journal of Medical Microbiology, 2018. **308**(8): p. 1067-1072.
6. E.B. Panel, K. Koutsoumanis, A. Allende, A. Alvarez-Ordóñez, S. Bover-Cid, M. Chemaly, et al., *Pathogenicity assessment of Shiga toxin-producing Escherichia coli (STEC) and the public health risk posed by contamination of food with STEC.* EFSA Journal, 2020. **18**(1): p. e05967.
7. M. Bugarel, L. Beutin, and P. Fach, *Low-Density Macroarray Targeting Non-Locus of Enterocyte Effacement Effectors (nle Genes) and Major Virulence*

Factors of Shiga Toxin-Producing Escherichia coli (STEC): a New Approach for Molecular Risk Assessment of STEC Isolates. Applied and Environmental Microbiology, 2010. **76**(1): p. 203-211.

8. E.F.S. Authority, E.C.f.D. Prevention, and Control, *The European Union One Health 2019 Zoonoses Report.* EFSA Journal, 2021. **19**(2): p. e06406.
9. M. Moeinirad, M. Douraghi, A.R. Foroushani, R. Sanikhani, and M.M.S. Dallal, *Molecular characterization and prevalence of virulence factor genes of Shiga toxin-producing Escherichia coli (STEC) isolated from diarrheic children.* Gene Reports, 2021. **25**.
10. C. Ripolles-Avila, M. Martínez-Garcia, M. Capellas, J. Yuste, D.Y. Fung, and J.J. Rodríguez-Jerez, *From hazard analysis to risk control using rapid methods in microbiology: A practical approach for the food industry.* Comprehensive Reviews in Food Science and Food Safety, 2020. **19**(4): p. 1877-1907.
11. A. Tarasov, D.W. Gray, M.-Y. Tsai, N. Shields, A. Montrose, N. Creedon, et al., *A potentiometric biosensor for rapid on-site disease diagnostics.* Biosensors and Bioelectronics, 2016. **79**: p. 669-678.
12. E. Cesewski and B.N. Johnson, *Electrochemical biosensors for pathogen detection.* Biosensors and Bioelectronics, 2020. **159**: p. 112214.
13. I. Tiwari, M. Singh, C.M. Pandey, and G. Sumana, *Electrochemical genosensor based on graphene oxide modified iron oxide–chitosan hybrid nanocomposite for pathogen detection.* Sensors and Actuators B: Chemical, 2015. **206**: p. 276-283.
14. A. Wahl, S. Barry, K. Dawson, J. MacHale, A. Quinn, and A. O'Riordan, *Electroanalysis at ultramicro and nanoscale electrodes: a comparative study.* Journal of The Electrochemical Society, 2013. **161**(2): p. B3055.

15. K. Dawson, A.l. Wahl, R. Murphy, and A. O'Riordan, *Electroanalysis at single gold nanowire electrodes.* The Journal of Physical Chemistry C, 2012. **116**(27): p. 14665-14673.

16. N. Jaiswal, C.M. Pandey, S. Solanki, I. Tiwari, and B.D. Malhotra, *An impedimetric biosensor based on electrophoretically assembled ZnO nanorods and carboxylated graphene nanoflakes on an indium tin oxide electrode for detection of the DNA of Escherichia coli O157: H7.* Microchimica Acta, 2020. **187**(1): p. 1-8.

17. N. Zainudin, A.R.M. Hairul, M.M. Yusoff, L.L. Tan, and K.F. Chong, *Impedimetric graphene-based biosensor for the detection of Escherichia coli DNA.* Analytical Methods, 2014. **6**(19): p. 7935-7941.

18. I. Tiwari, M. Gupta, C.M. Pandey, and V. Mishra, *Gold nanoparticle decorated graphene sheet-polypyrrole based nanocomposite: its synthesis, characterization and genosensing application.* Dalton Transactions, 2015. **44**(35): p. 15557-15566.

19. A.B. Aissa, J. Jara, R. Sebastián, A. Vallribera, S. Campoy, and M. Pividori, *Comparing nucleic acid lateral flow and electrochemical genosensing for the simultaneous detection of foodborne pathogens.* Biosensors and Bioelectronics, 2017. **88**: p. 265-272.

20. Y. Li, J. Deng, L.C. Fang, K.K. Yu, H. Huang, L.L. Jiang, et al., *A novel electrochemical DNA biosensor based on HRP-mimicking hemin/G-quadruplex wrapped GOx nanocomposites as tag for detection of Escherichia coli O157:H7.* Biosensors & Bioelectronics, 2015. **63**: p. 1-6.

21. Y. Wen, L. Wang, L. Xu, L. Li, S. Ren, C. Cao, et al., *Electrochemical detection of PCR amplicons of Escherichia coli genome based on DNA nanostructural probes and polyHRP enzyme.* Analyst, 2016. **141**(18): p. 5304-5310.

22. Kashish, S. Bansal, A. Jyoti, K. Mahato, P. Chandra, and R. Prakash, *Highly Sensitive in vitro Biosensor for Enterotoxigenic Escherichia coli Detection Based on ssDNA Anchored on PtNPs-Chitosan Nanocomposite.* Electroanalysis, 2017. **29**(11): p. 2665-2671.

23. S.C. Xu, Y.Y. Zhang, K. Dong, J.N. Wen, C.M. Zheng, and S.H. Zhao, *Electrochemical DNA Biosensor Based on Graphene Oxide-Chitosan Hybrid Nanocomposites for Detection of Escherichia Coli O157:H7.* International Journal of Electrochemical Science, 2017. **12**(4): p. 3443-3458.

24. S. Nadzirah, U. Hashim, S.C.B. Gopinath, N.A. Parmin, A.A. Hamzah, H.W. Yu, et al., *Titanium dioxide-mediated resistive nanobiosensor for E. coli O157:H7.* Microchimica Acta, 2020. **187**(4).

25. L.A. Wasiewska, I. Seymour, B. Patella, R. Inguanta, C.M. Burgess, G. Duffy, et al., *Reagent free electrochemical-based detection of silver ions at interdigitated microelectrodes using in-situ pH control.* Sensors and Actuators B: Chemical, 2021. **333**: p. 129531.

26. I. Seymour, B. O'Sullivan, P. Lovera, J.F. Rohan, and A. O'Riordan, *Electrochemical detection of free-chlorine in Water samples facilitated by in-situ pH control using interdigitated microelectrodes.* Sensors and Actuators B: Chemical, 2020. **325**: p. 128774.

27. L. Wang, P.F. Liu, Z.J. Liu, H.X. Cao, S.Y. Ye, K.R. Zhao, et al., *A dual-potential ratiometric electrochemiluminescence biosensor based on Au@CDs nanoflowers, Au@luminol nanoparticles and an enzyme-free DNA*

nanomachine for ultrasensitive p53 DNA detection. Sensors and Actuators B-Chemical, 2021. **327**.

28. H.A.M. Faria and V. Zucolotto, *Label-free electrochemical DNA biosensor for zika virus identification.* Biosensors and Bioelectronics, 2019. **131**: p. 149-155.
29. M. Manzano, S. Viezzi, S. Mazerat, R.S. Marks, and J. Vidic, *Rapid and label-free electrochemical DNA biosensor for detecting hepatitis A virus.* Biosensors and Bioelectronics, 2018. **100**: p. 89-95.
30. H. Ilkhani and S. Farhad, *A novel electrochemical DNA biosensor for Ebola virus detection.* Analytical biochemistry, 2018. **557**: p. 151-155.
31. A. Singh, G. Sinsinbar, M. Choudhary, V. Kumar, R. Pasricha, H. Verma, et al., *Graphene oxide-chitosan nanocomposite based electrochemical DNA biosensor for detection of typhoid.* Sensors and Actuators B: Chemical, 2013. **185**: p. 675-684.
32. S. Heydarzadeh, H. Roshanfekr, H. Peyman, and S. Kashanian, *Modeling of ultrasensitive DNA hybridization detection based on gold nanoparticles/carbon-nanotubes/chitosan-modified electrodes.* Colloids and Surfaces A: Physicochemical and Engineering Aspects, 2020. **587**: p. 124219.
33. S. Majumdar, D. Thakur, and D. Chowdhury, *DNA carbon-nanodots based electrochemical biosensor for detection of mutagenic nitrosamines.* ACS Applied Bio Materials, 2020. **3**(3): p. 1796-1803.
34. F. Zouaoui, S. Bourouina-Bacha, M. Bourouina, I. Abroa-Nemeir, H.B. Halima, J. Gallardo-Gonzalez, et al., *Electrochemical impedance spectroscopy determination of glyphosate using a molecularly imprinted chitosan.* Sensors and Actuators B: Chemical, 2020. **309**: p. 127753.

35. R.P. Shukla and H. Ben-Yoav, *A Chitosan–Carbon Nanotube-Modified Microelectrode for In Situ Detection of Blood Levels of the Antipsychotic Clozapine in a Finger-Pricked Sample Volume.* Advanced healthcare materials, 2019. **8**(15): p. 1900462.

36. A. Banasiak, J. Cassidy, and J. Colleran, *A novel quantitative electrochemical method to monitor DNA double-strand breaks caused by a DNA cleavage agent at a DNA sensor.* Biosensors and Bioelectronics, 2018. **117**: p. 217-223.

37. S. Moura-Melo, R. Miranda-Castro, N. de-Los-Santos-Álvarez, A.J. Miranda-Ordieres, J.R. dos Santos Junior, R.A. da Silva Fonseca, et al., *Targeting helicase-dependent amplification products with an electrochemical genosensor for reliable and sensitive screening of genetically modified organisms.* Analytical chemistry, 2015. **87**(16): p. 8547-8554.

38. S.S. Zarei, S. Soleimanian-Zad, and A.A. Ensafi, *An impedimetric aptasensor for Shigella dysenteriae using a gold nanoparticle-modified glassy carbon electrode.* Microchimica Acta, 2018. **185**(12): p. 1-9.

39. S. Bizid, S. Blili, R. Mlika, A.H. Said, and H. Korri-Youssoufi, *Direct E-DNA sensor of Mycobacterium tuberculosis mutant strain based on new nanocomposite transducer (Fc-ac-OMPA/MWCNTs).* Talanta, 2018. **184**: p. 475-483.

40. D.M. Mills, M.V. Foguel, C.P. Martin, T.T. Trieu, O. Kamar, P. Calvo-Marzal, et al., *Rapid detection of different DNA analytes using a single electrochemical sensor.* Sensors and Actuators B: Chemical, 2019. **293**: p. 11-15.

41. G. Wei, W. Zhang, H. Cui, F. Liao, L. Cheng, G. Ma, et al., *Immobilization-Free Electrochemical DNA Sensor based on signal cascade amplification strategy.* Biotechnology and Applied Biochemistry, 2021.

42. M. Zouari, S. Campuzano, J.M. Pingarrón, and N. Raouafi, *Femtomolar direct voltammetric determination of circulating miRNAs in sera of cancer patients using an enzymeless biosensor.* Analytica chimica acta, 2020. **1104**: p. 188-198.

43. F. Wang, Q. Yang, Y. Qu, J. Meng, and B. Ge, *Evaluation of a loop-mediated isothermal amplification suite for the rapid, reliable, and robust detection of Shiga toxin-producing Escherichia coli in produce.* Applied and environmental microbiology, 2014. **80**(8): p. 2516-2525.

44. X. Xia, B. Zhang, J. Wang, B. Li, K. He, and X. Zhang, *Rapid Detection of Escherichia coli O157: H7 by Loop-Mediated Isothermal Amplification Coupled with a Lateral Flow Assay Targeting the z3276 Genetic Marker.* Food Analytical Methods, 2021: p. 1-9.

45. R. Rajapaksha, U. Hashim, M.N.A. Uda, C.A.N. Fernando, and S.N.T. De Silva, *Target ssDNA detection of E.coli O157:H7 through electrical based DNA biosensor.* Microsystem Technologies-Micro-and Nanosystems-Information Storage and Processing Systems, 2017. **23**(12): p. 5771-5780.

4.6. Supplementary material

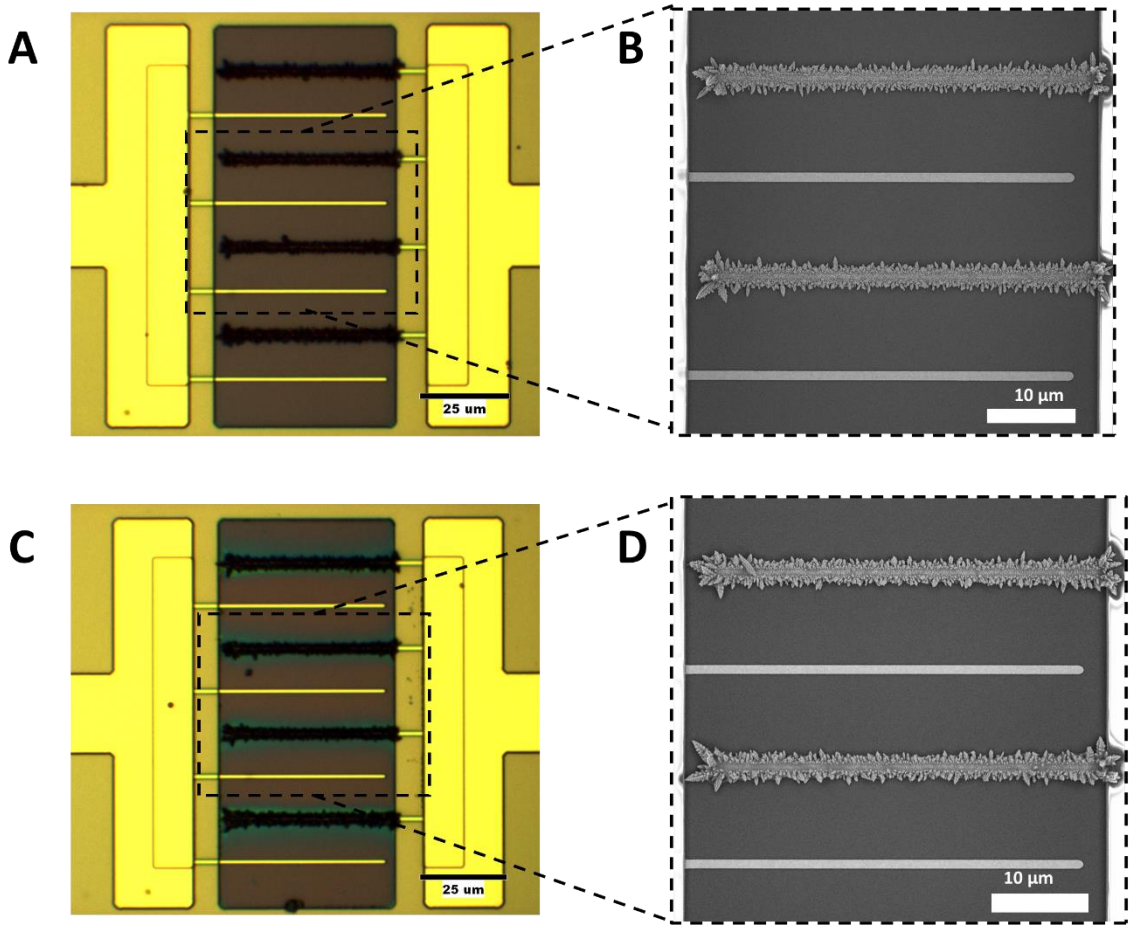

Fig. S4.1 (A) optical image of the AuNPs modified IDE; (B) SEM image of the AuNPs surface; (C) optical image of the AuNPs/Cht-Au modified IDE; (D) SEM image of the AuNPs/Cht-Au surface.

0

Chapter 5. Conclusions and future perspectives

5.1. Conclusions

The body of work presented in this thesis explored the development of a rapid electrochemical sensor for the detection of STEC, targeting the *stx* 1 and 2 genes which encode for Shiga Toxin(s), a key virulence factor which characterises this group of pathogenic *E.coli*. The development of technologies which have the potential to be used as rapid screening tools in agri-food environs is essential to managing this and other groups of pathogens, which are carried in the gut and shed in the faeces of food production animals posing a risk to water and food by direct and indirect contamination. Such a screening tool would allow mitigation strategies to be implemented earlier in the food chain, on farms and at the pre-harvest level rather than at the endpoint.

A rapid screening test must be easy to use and have a very high level of sensitivity. The electrochemical sensor approach described in this thesis meets all these criteria and with further research and validation has real potential for application in an agri-food setting. In particular, the gold IDEs on fully integrated silicon chips are very promising for the future of continuous, point-of-use biosensing.

In the first chapter, the literature regarding STEC and its pathogenicity, common methods of detection, electrochemical techniques and an electrochemical nucleic acid-based sensor developed to date were reviewed. It concluded that the most specific detection of STEC could be achieved by targeting two genes which encode for Shiga toxin production – *stx1* and *stx2*, one or both of which is carried by all STEC strains. In addition, it was found that even though several articles on electrochemical nucleic acid detection of STEC have been published, the researchers generally targeted the *eaeA* gene which encodes for adhesion intimate attachment and microvillus

effacement in the gut, but it is now known not to be present in all STEC strains which can cause serious illness. In addition, the proof of application of the sensors was often to a synthetic DNA strand or PCR product, which is not sufficient to predict how the sensor will behave in more complex samples such as faeces or food.

Chapter 2 presented an easy and quick technique for the electrochemical detection of silver ions using local pH control in a buffer and tap water. This work was an outcome of the original plan for this thesis which was to use silver nanoparticles tagged to DNA that would then be oxidised and effectively the concentration of silver ions would correspond to the concentration of DNA in the sample. Silver detection was undertaken using square wave voltammetry at a working IDA with simultaneous production of hydrogen ions at a generator IDA which allowed the pH to be tailored in the vicinity of the sensor. In addition, the complexation of the silver ions with chlorine present in tap water enabled more sensitive detection and faster time-to-result with no addition of electrolytes. The combination of the complexation of silver ions with chloride and in-situ pH control resulted in a linear calibration range between 0.25 and 2 μM in tap water and a calculated limit of detection of 106 nM without the need to add acid or supporting electrolytes. Even though such a limit of detection was sufficient for the detection of silver ions in tap water, it was not enough to use this technique for DNA detection. Therefore, the original plan of using silver nanoparticles shifted to a focus on methylene blue instead.

In chapter 3, a highly sensitive label-free, electrochemical DNA-based sensor for detection of *stx1* gene using interdigitated gold microelectrodes (IDEs) on fully integrated silicon chips was developed. First, the working IDE was modified with gold nanoparticles (AuNPs) and chitosan gold nanocomposite and an amine-modified probe DNA was immobilised using covalent bonding. The label-free electrochemical

detection was undertaken using methylene blue as a redox molecule, which intercalated into the double-strand DNA after applying an open potential circuit at the generator IDEs and its reduction was recorded using SWV. Using this technique, a highly sensitive sensor with a LOD of 100 aM was achieved and its selectivity was confirmed using chromosomal DNA extracted from STEC and non-STEC strains. This work demonstrated for the first time accumulation of methylene blue around the electrode using the IDEs which increased the sensitivity of the sensor. In addition, such high sensitivity and differentiation of bacterial strains using DNA extracted from wild bacterial strains without the need for PCR amplification is a huge step in developing a simple detection or screening tool feasible for use on a farm or in the food industry.

Finally, in chapter 4, using the same method of detection as in chapter 3, the sensitivity of the sensor was further improved by three orders of magnitude (from 100 aM to 100 zM) by electrodeposition of a thicker layer of gold nanoparticles. Such low LOD is at least four orders of magnitude lower compared to the similar sensors reported in the literature. In addition, two probes targeting both genes coding for toxin production - *stx1* and *stx2* were simultaneously detected using a single chip. This work is a significant improvement to the DNA-based sensors developed for STEC detection described in the literature.

The detection of both genes coding for the toxin production is crucial as STEC strain may carry one or both of the toxin encoding genes. In addition, the high sensitivity of the sensor could allow the detection of STEC even if very low numbers of bacteria are present thus avoiding the need for a liquid enrichment step to increase STEC numbers which is a feature of most commercial methods currently used and renders them unsuited to in-site use. This study is a stepping stone for the future development of

nucleic acid-based sensors with a commercial application for use for instance on-farm or in the food industry to ensure and better manage food safety.

5.2. Future perspectives

The number of published papers in the area of nucleic acid-based sensors is increasing every year. To visualise the number of articles published a search was made using the Web of Science database with the keywords used “DNA or RNA or nucleic acid*” AND “*sensor* or rapid detection or quick detection” in the title AND “bacteria or pathogen*” in the topic. The number of articles found in this search per year since 1980 was plotted in Fig. 5.1. It can be seen that number of articles increased each year from below ten articles per year in the 1980s through around 20 articles a year in the 1990s to the highest number recorded since 2019 with around 160 articles published every year. Even though there is extensive research on the development of nucleic acid-based biosensors undertaken in several laboratories around the world, there is no commercially available nucleic acid-based biosensor for point-of-use detection yet. This section will explore some of the limitations regarding the work presented in this thesis and possible directions for future research to tackle these limitations.

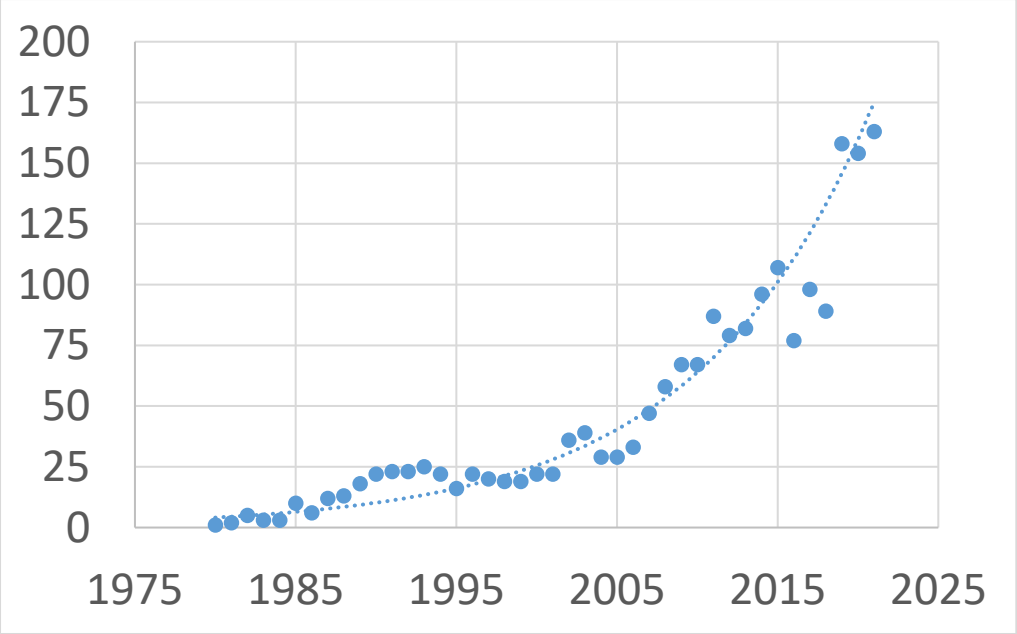

Fig. 5.1. Number of articles published per year regarding the development of nucleic acid-based biosensors since 1980

Firstly, the IDEs developed in this work, electrochemical pH control and MB accumulation offer several possible applications. Another possibility could be to further develop the DNA sensor by recycling it, allowing for applications in continuous monitoring, such as in water treatment plants, to reduce costs and meet sustainability targets. Usually, regeneration of a DNA sensor is achieved by soaking the electrode in NaOH for a certain time to allow breakage of the hydrogen bond in double-stranded DNA, which is known to occur at neutral pH. The complementary strand effectively is washed away and the detection can be repeated while the probe remains active. NaOH is, however, a dangerous chemical and a laboratory environment and protective clothes are required for its use. Being able to use the sensor outside of the laboratory environment – for example, on-farm would require the regeneration to be done without dangerous chemicals. This could be achieved using the interdigitated electrodes which were developed in this thesis. As shown in chapter 2, pH could be locally decreased for more efficient detection of silver by applying a constant positive potential and the generator electrode. Subsequently, in chapter 3 it

was shown that the pH can also be increased by applying constant negative potential which was applied for effective electrodeposition of chitosan on the electrode. Therefore, it would be expected that the DNA sensor could be recycled by applying a sufficiently negative potential to generator/accumulator IDE to break the double bond on a sensor IDE and therefore remove the target DNA so the sensor could be reused several times. This however would need more optimisation to find an optimal potential and the gaps between the electrodes may need to be adjusted. In addition, long-term stability studies would need to be undertaken to prove that the sensor could be reused several times without losing its efficacy.

In addition, this work showed a very high sensitivity for DNA detection by combining probe DNA attachment to the microelectrode modified with chitosan-gold nanoparticles. Increasing the layer of underlying gold nanoparticles improved the sensitivity even further. Even though a very sensitive detection was achieved, gold is an expensive material and alternates are being extensively studied. In future work, other types of nanomaterials could be explored that would allow similar sensitivity while lower cost and more sustainable material. Additionally, in this thesis work, a layer of gold nanoparticles was firstly deposited followed later by a chitosan-gold composite. To simplify the method even further single step deposition of chitosan nanocomposite could be explored to improve the reproducibility of the sensor. For this, a higher concentration of metal/nanoparticles could be used with chitosan.

Subsequently, in chapter 4, a multiplex detection sensor for simultaneous detection of *stx1* and *stx2* genes was developed. The probe immobilisation was done by pipetting two small drops, each containing one probe DNA, and incubating them on top of the chip. This strategy, however, offers great limitations attributed to two drops merging and difficulty in achieving the same conditions each time because of the drops having

various shapes. In addition, the electrodes on the chip are too close together and therefore it is not possible in this scenario to add more probes, allowing for screening for more genes in the same measurement. These limitations could be overcome with the development of a microfluidics device incorporated on top of the silicon chip. Microfluidics is a pattern of micro-channels that could, in our case, allow separating the pathways for each of the six electrodes to specifically modify them with a different probe DNA. An example of how such microchannels would separate the electrodes is presented in Fig. 5.2 where three separate channels were created. After the probes incubation, this microfluidic device would be removed and the detection would be done as described. This would allow the simultaneous detection of more genes at the same time. As described in Chapter 1, there are at least three genes associated w with STEC, *stx1*, *stx2* and *eaeA* which are used as targets in detection assays.

The sensor could also include the gene able to identify *E. coli* species and in the future, other virulence genes or markers for STEC could be added. Having such multiple devices would allow detecting all the genes at once to get an excellent overview of detected strains with the potential to cause serious illness. Furthermore, this type of approach combining an electrochemical sensor with a DNA probe could easily be modified to allow the detection of other pathogens.

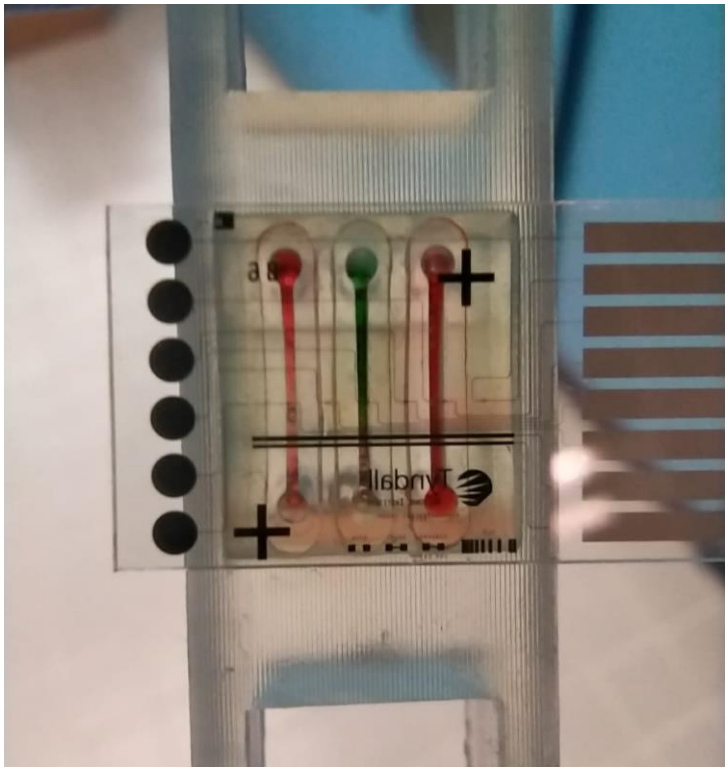

Fig. 5.2 A prototype of a microfluidics device incorporated on the glass chip. The separate channels are highlighted with different colours of liquid.

Finally, as the primary focus of this thesis was placed on the development of a DNA-based detection device there is still much development work to recover and detect STEC from naturally contaminated samples such as faeces, soils, food matrices etc.

The thesis explored the detection of chromosomal DNA directly from the bacterial culture which is a significant step, avoiding the need for DNA amplification. However, even though the sensor showed activity from STEC culture, there are many challenges in detecting STEC in the more complex samples, including a low concentration of STEC compared to very high concentrations of other bacteria. A future development step should therefore explore more complex samples inoculated with known concentrations of STEC to validate its application and sensitivity. Even though adding an amplification step is not desirable, introducing an alternative multiplication step

using isothermal techniques may be beneficial. Recently, the LAMP technique has been applied in such devices, which was described at the end of Chapter 1. Another limitation of using a point-of-use device targeting DNA is the need for effective DNA extraction from the sample, which should be easy, quick and produce DNA of high quality without impurities. Such impurities may cause a false positive signal of the binding to the sensor non-specifically. Designing a fully integrated device that could extract DNA, amplify the desired target and finally detect it would be a stepping stone for getting closer to the real-life application of such devices. This could be solved with the microfluidics device as well which could incorporate DNA extraction, isothermal amplification and multiplex detection using a single chip.

In conclusion, this thesis represents major progress toward the development of an electrochemical sensor for the targeted gene(s) in food pathogens allowed at or near point-of-use, in the agri-food environment.

Appendices

A.1 Peer reviewed, under review or submitted publications

1. **Wasiewska, L. A.**, Seymour, I., Patella, B., Inguanta, R., Burgess, C. M., Duffy, G., & O'Riordan, A. (2021). Reagent-free electrochemical-based detection of silver ions at interdigitated microelectrodes using in-situ pH control. Sensors and Actuators B: Chemical, 333, 129531.
2. **Wasiewska, L. A.**, Diaz, F. G., Shao, H., Burgess, C. M., Duffy, G., & O'Riordan, A. (2022). Highly sensitive electrochemical sensor for the detection of Shiga toxin-producing E. coli (STEC) using interdigitated micro-electrodes selectively modified with a chitosan-gold nanocomposite. Electrochimica Acta, 426, 140748.
3. **Wasiewska, L. A.**, Juska V. B., Burgess C. K., Duffy G., O'Riordan A. (2022) Electrochemical DNA sensors for detection of *E. coli* and Shiga toxin-producing *E. coli* (STEC) – Review of the recent developments.
   Under review in Comprehensive Reviews in Food Science and Food Safety
4. **Wasiewska, L. A.**, Diaz F. G., Teixeira S., Burgess C. K., Duffy G., O'Riordan A. Electrochemical multiplex DNA sensor for simultaneous detection of *stx1* and *stx2* genes of STEC
   Submitted to ACS Applied Materials & Interfaces
5. Yang Y., ***Wasiewska, L. A.***, Burgess, C. M., Duffy G., Lovera P, .O'Riordan A., Detection of *stx2* gene from Shiga toxin-producing *Escherichia coli* (STEC) by SERS using recycled silicon chips
   Under review in Sensors and Actuators B: Chemical

A.2 Publications in preparation

1. *Diaz F. G.,* ***Wasiewska, L. A****., Shao, H. O'Riordan A. Real-time, label-free detection of Potato Virus Y (PVY) in plant sera*

   In preparation for submission to Biosensors & Bioelectronics

A.3 Conferences attended

1. IEEE NANO (Cork, Ireland) 2018 "Reagent-free electrochemical-based detection of silver ions in aqueous solutions using localized pH control" - Poster presentation
2. 69th Annual meeting of the International Society of Electrochemistry (Bologna, Italy) 2018 "Reagent-free electrochemical-based detection of silver ions in aqueous solutions using localized pH control". – Poster presentation
3. ISE student symposium (Limerick, Ireland) 2018 "Reagent-free electrochemical-based detection of silver ions in aqueous solutions using localized pH control" - Oral presentation
4. IAFP European Symposium (Nantes, France) 2019 "Reagent-Free Detection of Silver Ions in Tap Water Using Square Wave Voltammetry and Local pH Control" - Oral presentation
5. One Health Annual Meeting (Dublin, Ireland) 2019 "Reagent-Free Detection of Silver Ions in Tap Water Using Square Wave Voltammetry and Local pH Control" - Poster presentation
6. 31st Anniversary World Congress on Biosensors (online) "Development of ultra-sensitive, on-chip biosensor for detection of *stx1* gene using interdigitated microelectrodes modified with chitosan-gold nanocomposite." – Poster presentation

7. 72nd Annual meeting of International Society of Electrochemistry, September 2021, “Development of an ultra-sensitive, on-chip biosensor for detection of *stx1* gene using interdigitated microelectrodes modified with chitosan-gold nanocomposite.” - Oral presentation (Best oral presentation award)

A.4 Awards

1. Outreach prize in “Present thesis in three minutes…. In French” April 2018, Trinity College, Dublin, Ireland organised by French Embassy in Dublin
2. First prize in Famelab regional heat, February 2019 Cork, Ireland organised by the British Council
3. Best oral presentation at 72nd Annual Meeting of International Society of Electrochemistry sponsored by Bioelectrochemistry division
4. Runner up in 2021 Tyndall Postgraduate Research Publication of the Year

A.5 Travel grant

1. Food Safety Skills Fund, 1200 €, Travel grant to take part in a summer school in micro and nanosensors at DTU in Denmark in August 2019, offered by Safe Food Knowledge Fund, Ireland

A.6 Other public speaking activities

1. “My thesis in Comic strip” 15th Nov 2018, Alliance Française, Dublin, Ireland (see A.7)
2. Famelab Ireland, National Final, April 2019, Dublin, Ireland, “Electrochemistry, a soap opera happing all around us”. 3 minutes long presentation https://www.youtube.com/watch?v=hyxY02dNdX8

3. Hall of Famelab September 2019 Museum of Natural History, London, UK, "Scientists' warning to humanity: microorganisms and climate change". – 3 minutes long presentation
   https://www.youtube.com/watch?v=zDRCGTtqgXk
4. "Biosensor for Bugs, One Health, Horticulture Development"
   The Research Field, Teagasc podcast
   https://soundcloud.com/theresearchfield/episode

A.7 My thesis in Comic strip by Orchimy

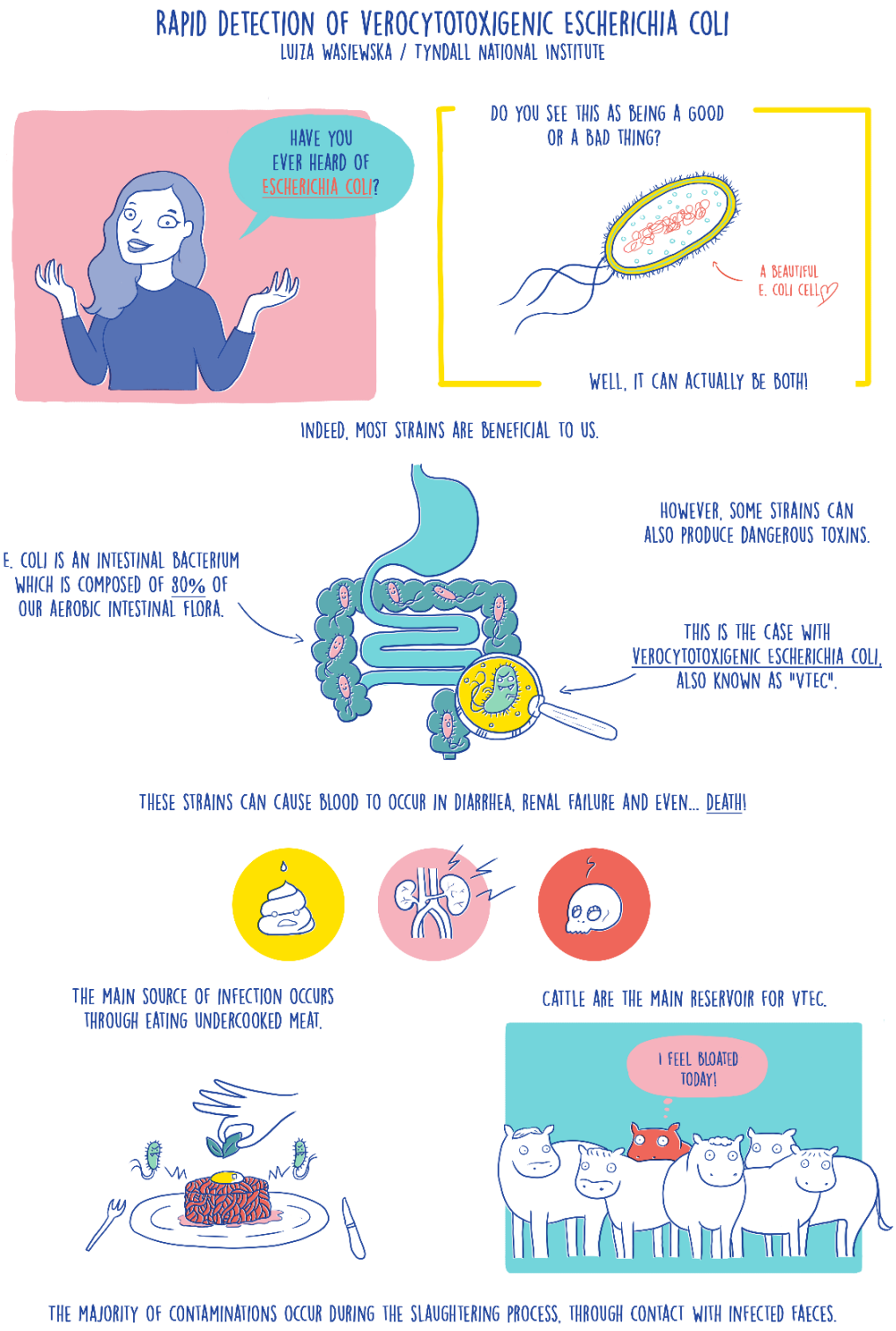

UNFORTUNATELY, IRELAND HAS THE HIGHEST VTEC INFECTION LEVEL IN THE EUROPEAN UNION.

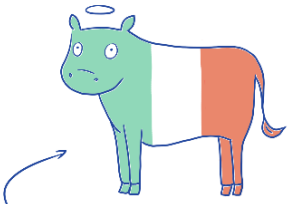

ALMOST 2% OF THE CATTLE HAVE AN ELEVATED VTEC LEVEL IN THEIR FAECES.

TODAY, VTEC DETECTION CAN TAKE UP TO 6 DAYS AND IS DONE IN SPECIALISED LABORATORIES. IT IS THUS IMPOSSIBLE TO TEST ALL THE COWS ON FARMS BEFORE SLAUGHTER.

FINDING A SOLUTION TO RAPIDLY DETECT SERIOUSLY CONTAMINATED COWS, SO AS TO SEPARATE THEM FROM THE REST OF THE GROUP, WOULD ALLOW FOR A REDUCTION IN THE CONTAMINATION LEVEL OF THE MEAT.

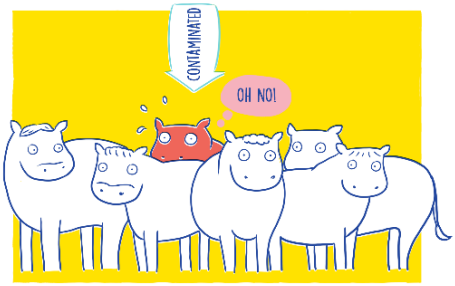

THE AIM OF MY PROJECT IS THUS TO DEVELOP BIOSENSORS IN ORDER TO BE ABLE TO DETECT VTEC IN CATTLE FAECES BEFORE SLAUGHTER.

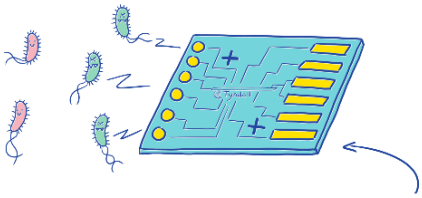

BIOSENSORS' MAIN BENEFITS ARE THAT THEY ARE VERY SPECIFIC AND QUICK TO DETECT CONTAMINATION.

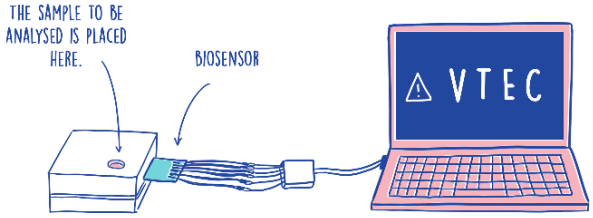

A BIOSENSOR IS AN ANALYTICAL TOOL WHICH USES A BIOLOGICAL ENTITY (ENZYME, ANTIGEN, DNA) TO QUANTIFY A SPECIFIC ANALYTE.

A WELL-KNOWN EXAMPLE OF A BIOSENSOR IS THE PREGNANCY TEST, WHICH USES AN ANTIGEN TO DETECT A SPECIFIC HORMONE PRODUCED DURING PREGNANCY.

MOST E. COLI STRAINS ARE BENEFICIAL FOR THE GUT... THE CHALLENGE IS TO DETECT VTEC AMONG INOFFENSIVE STRAINS!

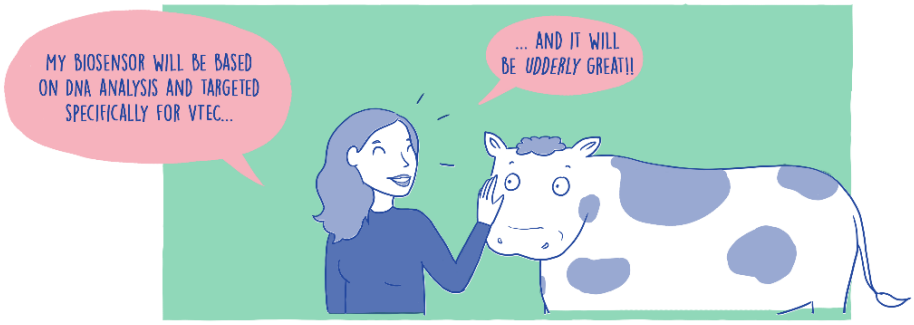

ORCHIMY

MY THESIS IN A COMIC STRIP
DEVELOPED BASED ON AN ORIGINAL IDEA OF THE UNIVERSITÉ DE LORRAINE AND PEB&FOX,
WITH THE SUPPORT OF THE EMBASSY OF FRANCE IN IRELAND AND THE ALLIANCE FRANÇAISE DUBLIN.
RAPID DETECTION OF VEROCYTOTOXIGENIC E. COLI – LUIZA WASIEWSKA
ILLUSTRATION – MÉLODY UNG (ORCHIMY.COM)